ISSN 0021-9673

VOL. 654 NO. 1 NOVEMBER 12, 1993

JOURNAL OF CHROMATOGRAPHY A

INCLUDING ELECTROPHORESIS AND OTHER SEPARATION METHODS

JOURNAL OF CHROMATOGRAPHY A

INCLUDING ELECTROPHORESIS AND OTHER SEPARATION METHODS

Scope. The *Journal of Chromatography A* publishes papers on all aspects of **chromatography, electrophoresis** and related methods. Contributions consist mainly of research papers dealing with chromatographic theory, instrumental developments and their applications. In the *Symposium volumes*, which are under separate editorship, proceedings of symposia on chromatography, electrophoresis and related methods are published. *Journal of Chromatography B: Biomedical Applications* —This journal, which is under separate editorship, deals with the following aspects: developments in and applications of chromatographic and electrophoretic techniques related to clinical diagnosis or alterations during medical treatment; screening and profiling of body fluids or tissues related to the analysis of active substances and to metabolic disorders; drug level monitoring and pharmacokinetic studies; clinical toxicology; forensic medicine; veterinary medicine; occupational medicine; results from basic medical research with direct consequences in clinical practice.

Submission of Papers. The preferred medium of submission is on disk with accompanying manuscript (see *Electronic manuscripts* in the Instructions to Authors, which can be obtained from the publisher, Elsevier Science Publishers B.V., P.O. Box 330, 1000 AH Amsterdam, Netherlands). Manuscripts (in English; *four* copies are required) should be submitted to: Editorial Office of *Journal of Chromatography A*, P.O. Box 681, 1000 AR Amsterdam, Netherlands, Telefax (+31-20) 5862 304, or to: The Editor of *Journal of Chromatography B: Biomedical Applications*, P.O. Box 681, 1000 AR Amsterdam, Netherlands. Review articles are invited or proposed in writing to the Editors who welcome suggestions for subjects. An outline of the proposed review should first be forwarded to the Editors for preliminary discussion prior to preparation. Submission of an article is understood to imply that the article is original and unpublished and is not being considered for publication elsewhere. For copyright regulations, see below.

Publication information. *Journal of Chromatography A* (ISSN 0021-9673): for 1994 Vols. 652–682 are scheduled for publication. *Journal of Chromatography B: Biomedical Applications* (ISSN 0378-4347): for 1994 Vols. 652–662 are scheduled for publication. Subscription prices for *Journal of Chromatography A*, *Journal of Chromatography B: Biomedical Applications* or a combined subscription are available upon request from the publisher. Subscriptions are accepted on a prepaid basis only and are entered on a calendar year basis. Issues are sent by surface mail except to the following countries where air delivery via SAL is ensured: Argentina, Australia, Brazil, Canada, China, Hong Kong, India, Israel, Japan, Malaysia, Mexico, New Zealand, Pakistan, Singapore, South Africa, South Korea, Taiwan, Thailand, USA. For all other countries airmail rates are available upon request. Claims for missing issues must be made within six months of our publication (mailing) date. Please address all your requests regarding orders and subscription queries to: Elsevier Science Publishers, Journal Department, P.O. Box 211, 1000 AE Amsterdam, Netherlands. Tel.: (+31-20) 5803 642; Fax: (+31-20) 5803 598. Customers in the USA and Canada wishing information on this and other Elsevier journals, please contact Journal Information Center, Elsevier Science Publishing Co. Inc., 655 Avenue of the Americas, New York, NY 10010, USA, Tel. (+1-212) 633 3750, Telefax (+1-212) 633 3764.

Abstracts/Contents Lists published in Analytical Abstracts, Biochemical Abstracts, Biological Abstracts, Chemical Abstracts, Chemical Titles, Chromatography Abstracts, Current Awareness in Biological Sciences (CABS), Current Contents/Life Sciences, Current Contents/Physical, Chemical & Earth Sciences, Deep-Sea Research/Part B: Oceanographic Literature Review, Excerpta Medica, Index Medicus, Mass Spectrometry Bulletin, PASCAL-CNRS, Referativnyi Zhurnal, Research Alert and Science Citation Index.

US Mailing Notice. *Journal of Chromatography A* (ISSN 0021-9673) is published weekly (total 52 issues) by Elsevier Science Publishers (Sara Burgerhartstraat 25, P.O. Box 211, 1000 AE Amsterdam, Netherlands). Annual subscription price in the USA US$ 5132.25 (US$ price valid in North, Central and South America only) including air speed delivery. Second class postage paid at Jamaica, NY 11431. **USA POSTMASTERS**: Send address changes to *Journal of Chromatography A*, Publications Expediting, Inc., 200 Meacham Avenue, Elmont, NY 11003. Airfreight and mailing in the USA by Publications Expediting.

See inside back cover for Publication Schedule, Information for Authors and information on Advertisements.

0021-9673/93/$06.00

Printed in the Netherlands

CONTENTS

(Abstracts/Contents Lists published in Analytical Abstracts, Biochemical Abstracts, Biological Abstracts, Chemical Abstracts, Chemical Titles, Chromatography Abstracts, Current Awareness in Biological Sciences (CABS), Current Contents/Life Sciences, Current Contents/Physical, Chemical & Earth Sciences, Deep-Sea Research/Part B: Oceanographic Literature Review, Excerpta Medica, Index Medicus, Mass Spectrometry Bulletin, PASCAL-CNRS, Referativnyi Zhurnal, Research Alert and Science Citation Index)

REGULAR PAPERS

Column Liquid Chromatography

(Continued overleaf)

Contents (continued)

JOURNAL OF CHROMATOGRAPHY A

VOL. 654 (1993)

JOURNAL OF CHROMATOGRAPHY A

INCLUDING ELECTROPHORESIS AND OTHER SEPARATION METHODS

ELSEVIER

AMSTERDAM — LONDON — NEW YORK — TOKYO

0021-9673/93/$06.00

Printed in the Netherlands

Journal of Chromatography A, 654 (1993) 1–16
Elsevier Science Publishers B.V., Amsterdam

CHROM. 25 370

Comparing steady counterflow separation with differential chromatography

Donald K. Roper* and Edwin N. Lightfoot

1415 Johnson Drive, Department of Chemical Engineering, University of Wisconsin-Madison, Madison, WI 53706 (USA)

(First received December 22nd, 1992; revised manuscript received June 9th, 1993)

ABSTRACT

Separation of closely related solutes by steady solid–fluid counterflow is compared with differential separation in a fixed chromatographic bed. Analogous expressions for exit concentration and mean residence time in the two systems are presented. A counterpart to chromatographic resolution is derived for binary steady counterflow separations. Estimated counterflow savings in product-concentration dilution, solvent volume requirement and solid-phase volume requirement obtained with these expressions relative to comparable chromatographic operations are compared with experimental results from adsorptive, simulated moving beds. Analysis of a size-exclusion protein separation suggests counterflow substantially decreases solvent and resin usage relative to conventional, batch operation.

INTRODUCTION

Our purpose in this work is to compare the separation of closely related solutes by steady counterflow of a carrier liquid and an adsorptive solid with the performance expected from comparable fixed-bed chromatography. We are motivated by reports which indicate that reduced solvent and adsorbent volumes are required in experimental simulated-counterflow systems relative to conventional batch adsorption.

Perhaps the most attractive method of achieving steady counterflow without moving a granular bed is to adopt the simulated moving-bed strategy first described by Broughton *et al.* [1] at Universal Oil Products for a continuous paraxylene (PAREX) separation. Movement of solid adsorbent counter to fluid feed and desorbent streams was simulated by intermittently switching feed, extract and raffinate points in the direction of fluid flow using a patented rotary valve. These authors reported simulated-counterflow extraction of 98.5% of one component in a hypothetical binary mix at 99.5% purity decreased adsorbent inventory 25-fold and halved desorbent circulation relative to fixed-bed operation.

This strategy has been adopted in a number of Sorbex-type systems. Recently, Negawa and Shoji [2] reported that to resolve racemic 1-phenylethanol to 99% enantiomeric excess, 87 times less solvent volume per gram of product was required by simulated counterflow than by batch chromatography. The measured adsorbent productivity of counterflow, (calculated as grams of product per hour per liter of bed) was 61 times higher than that of chromatography. Rossiter and Tolbert [3] reported an average ten-fold reduction in adsorbent inventory and roughly 50% reduction in elution volume when simulated-counterflow contacting replaced ion-exchange batch adsorption of amino and carboxylic acids. Relative savings in adsorptive costs upon switching to solid–fluid counterflow were noted by Ernst and McQuigg [4] for recovery of

* Corresponding author.

0021-9673/93/$06.00

citric and lactic acid from crude fermentation broths.

But early comparisons of model countercurrent and chromatographic separations have not anticipated order-of-magnitude decreases in adsorbent volume and substantial reductions in solvent volume which are indicated by these reports. Liapis and Rippin [5] reported a three-fold relative increase in counterflow carbon-adsorbent utilization after numerically simulating non-linear, binary separations in three modes: batch, periodically switched and continuous-countercurrent operation. In their model, orthogonal collocation was used along the particle radii and along the bed axis in a differential model to account for convective axial dispersion, film resistance to mass transfer, and intraparticle diffusion. Ruthven [6] predicted a four-fold adsorbent volume reduction in staged-counterflow relative to batch chromatography for linear systems with equivalent net solute flow-rates and separation factors of 1.1 which yielded 99% fractional purity. The staged-counterflow internal solute reflux in this model was minimized while the fixed-bed production rate was maximized.

Effort has been dedicated in previous modelling of linear and non-linear counterflow systems to obtain and verify intracolumn concentration profiles from underlying equilibrium and mass transfer processes. Lapidus and Amundson [7] calculated analytic expressions for equilibrium stage composition of a single component from an unsteady-state, difference model of two-phase, linear counterflow separation. Miyauchi and Vermeulen [8] derived pointwise concentration profiles from a steady-state, differential description. Subsequent analyses which considered effects of non-linear equilibria, mass-transfer resistances, multicomponent adsorption and periodic switching have been summarized by Ruthven and Ching [9]. Modelling of separations in simulated moving-bed counterflow by Ernst and Hsu [10] and Storti *et al.* [11] and in continuous moving-bed counterflow by Fish *et al.* [12] have recently been reported. In the chromatographic literature, models giving effluent peaks for a range of systems have been detailed by Giddings [13], Aris and Amundson [14], Ruthven [6], Lin *et al.* [15] and others.

Rather than emphasizing concentration profiles, our objective in this work has been to address these practical questions: (i) what is the basis for substantial apparent decreases in solvent and adsorbent usage obtained by simulating counterflow?, (ii) how do the relative gains which have been reported compare with those expected from ideal chromatographic and counterflow systems?, and (iii) is the anticipated increase in performance sufficient to justify replacing a particular chromatographic separation with a simulated-counterflow split?

We begin by comparing reliable descriptions of chromatography and steady counterflow of sufficient detail to analyze reasons for the improved efficiency of simulated moving-bed separations. We then derive general expressions to estimate the volumes of solvent and solid resin required by steady counterflow relative to the corresponding volumes required by differential chromatography for difficult, binary separations of equal resolution. We measure the performance of experimental systems, including separations of solutes whose isotherms are non-linear, using these expressions. We conclude by comparing counterflow and chromatography in a hypothetical separation of two proteins.

SEPARATION IN STEADY COUNTERFLOW AND DIFFERENTIAL CHROMATOGRAPHY

We now summarize analytic relations for exit composition, solute mean residence time and binary resolution in analogous chromatographic and counterflow separations, beginning with chromatography. Other than an equation for separation effectiveness in binary counterflow which we derive in the *Binary counterflow separation* section, these relations have been established by previous investigators and we briefly review pertinent literature as they are introduced. For clarity we define the parameters of the relations in context. We will subsequently use these relations to determine the basis for a steady counterflow advantage and to derive

expressions for the performance of counterflow relative to chromatography.

Differential chromatography

A lumped-parameter, asymptotic solution to one-dimensional, pseudocontinuum equations of differential chromatography in linear systems was obtained by Reis *et al.* [16] for rapid adsorption and later extended by Gibbs and Lightfoot [17] to account for adsorption kinetics and to examine gradient elution. This solution can be extended using the principle of superposition to describe batch adsorption and elution [18]. Athalye *et al.* [19] have recently demonstrated the predictability of protein separations in commercially available size-exclusion systems using this model, together with independent, *a priori* estimates of three transport rate parameters: the convective dispersion coefficient, the intraparticle diffusivity and the fluid-phase mass-transfer coefficient.

Fundamental mass-transport rate processes —convection, diffusion and adsorption— underlie linear systems as well as those in which nonlinearities arise due to concentration-dependence of transport parameters and solute–solute interactions. For this reason, evaluation of steady counterflow efficiency relative to fixed-bed chromatography in linear systems is a useful first step to predicting and optimizing separation performance in more complex operations.

In Table I the fluid-phase solute concentration distribution c_f from a sharp-pulse input of solute mass m_0 which is eluted isocratically in a long column is given as a function of axial coordinate z and time t. The mean solute position, $z_0 \equiv uvt$, is proportional to both the interstitial fluid velocity, v, and the fraction of solute in the moving fluid phase at long times, $u \equiv \alpha\epsilon_b/[\alpha\epsilon_b + (1-\epsilon_b)]$, where ϵ_b is the interparticle or column void fraction. The column cross-sectional area is A. Increases in H, the height of a theoretical chromatographic plate N, with velocity have been estimated using coefficients of physical transport rate processes. Subscripts f and b refer to the moving fluid and stationary bulk phases, respectively. The bulk phase consists of chromatographic packing of porosity ϵ_p, which entrains fluid referred to by subscript p′.

The differential separation of two individual solutes, distinguished by their respective equilibrium and mass transport rate parameters, is

TABLE I

SUMMARY OF ANALOGOUS RELATIONS FOR STEADY COUNTERFLOW AND DIFFERENTIAL CHROMATOGRAPHY

Relation	Differential chromatography	Steady counterflow
Exit Composition	$c_f(z,t) = \frac{m_0 u}{A\epsilon_b\sqrt{2\pi H z_0}} \exp\left[\frac{-(z-z_0)^2}{2Hz_0}\right]$	$y_{N,i} = \frac{y_{e,i}}{\sum_{j=0}^{N} \Gamma_i^{-j}}$
		$x_{1,i} = \frac{y_{e,i}}{\alpha_i \frac{\rho_S}{\rho_U} \sum_{j=0}^{M} \Gamma_i^j}$
Residence time	$\bar{t} = \frac{NH}{uv}$	$\bar{t}_F = \frac{H_{SC}(N_{SC}+1)}{uv_{SC}} \left[\frac{\Gamma}{\Gamma-1} \cdot \frac{\Gamma^{N_{SC}+1}-1}{\Gamma^{N_{SC}+1}+1}\right]$
Resolution	$R = \frac{\delta\sqrt{N}}{4}$	$N_{SC,tot} = 2\left[\frac{2\ln\left(\frac{P_{U,i}}{1-P_{U,i}}\right)}{\delta} - 1\right] + 1$

illustrated in Fig. 1. Observe that only a small fraction of the adsorbent bed actively resolves the overlapping solutes. The remainder acts as expensive storage or is unused (frontal and displacement operations are qualitatively similar). Each solute partitions between fluid and bulk phases thermodynamically as shown by its partition coefficient, $\alpha \equiv c_f/c_b = 1/[\epsilon_{p'} + (1 - \epsilon_{p'})K_{eq}]$, with a constant equilibrium distribution coefficient defined by $K_{eq} \equiv k_{ad}/k_{des} = c_s/c_p$. Subscript s refers to the surface of the porous packing, while k_{ad} and k_{des} are kinetic rate constants for adsorption and desorption, respectively.

The solute mean residence time, $\bar{t}$, given in Table I is the first temporal moment of the fluid-phase solute concentration at the column outlet, $z = L$. The second central temporal moment (variance), $s^2 \equiv \bar{t}H/uv$, is the measured width of a peak in Fig. 1. It is proportional to both the residence time and the chromatographic plate height. Evaluation of temporal moments of c_f is straightforward, because this distribution approaches Gaussian form in time when evaluated at a given coordinate as the number of theoretical chromatographic plates becomes large. Van Deemter [20] obtained equivalent relations for mean residence time and peak width from an equilibrium-plate, continuous-flow description of linear chromatography. Karol [21] derived identical relations from a staged, intermittent-transfer description in which $u_i \rightarrow 0$.

The effective separation of similar components 1 and 2, as illustrated in Fig. 1, has been related to specific thermodynamic and transport rate properties by defining the chromatographic resolution as the ratio of peak separation to the average peak width. In Table I we give a relation for resolution in which the thermodynamic driving force for separation is represented by $\delta \equiv 2|u_1 - u_2|/(u_1 + u_2)$, the fractional difference in migration velocities of 1 and 2. This separation

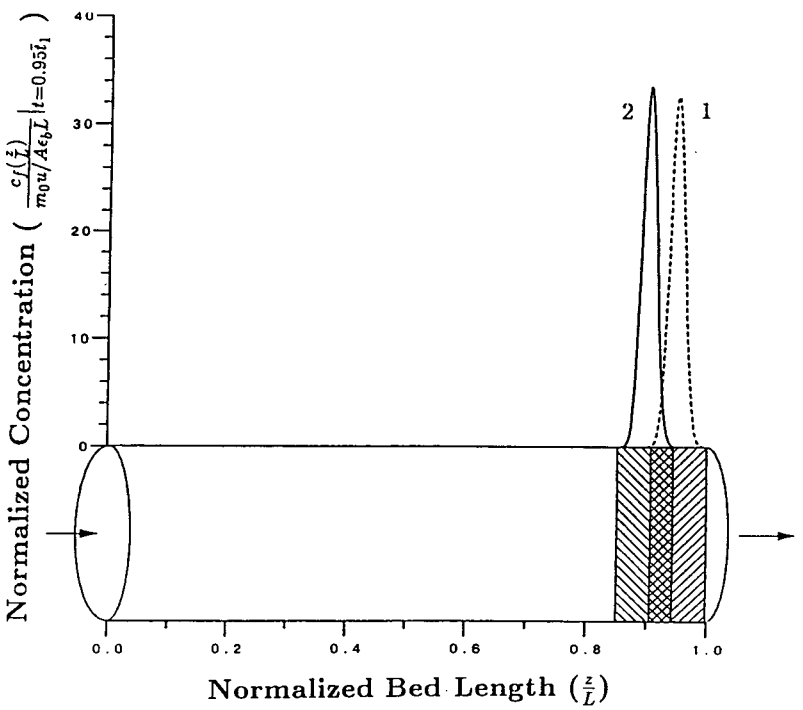

Fig. 1. Underutilization of stationary bed in a binary chromatographic separation. Only 5% of the bed volume (crosshatched) is actively separating component 1 (dashed line) from component 2 (solid line). 9% of the bed volume (hatched) merely retains the eluting species. 86% of the bed is unused. Normalized axial fluid-concentration profiles for 1 and 2 were calculated using the equation for c_f in Table I at $t = 0.95\ \bar{t}_1$. The thermodynamic driving force between 1 and 2 is 0.05. The column illustrated resolves 1 and 2 to unity at $z/L = 1$.

driving force equals the product of relative selectivity and retention factors [22].

We now describe analogous relations from a model of counterflow separation.

Equilibrium-staged counterflow

An equilibrium-stage description of counterflow with constant stage-to-stage phase flow-rates and linear stage-exit equilibrium was introduced by Kremser [23] and Souders and Brown [24] and has been discussed by King [25], Treybal [26] and Henley and Seader [27]. Ruthven [6] showed that an equilibrium-stage approach gives intracolumn profiles which are essentially the same as those from a discrete, one-dimensional, pseudocontinuum description of counterflow. Ching *et al.* [28] and Ruthven and Ching [9] demonstrated qualitative agreement between concentration profiles calculated using the equilibrium-stage description and measurements from four-section simulated moving-bed experiments. Klinkenberg and co-workers [29,30] specialized the Kremser–Souders–Brown equations to model a column with negligible feed flow-rate relative to the flow-rates of initially pure fluid and solid phases.

In Table I the fluid-phase mass fraction of solute i in the stripper product, $y_{N,i}$, and the solid-phase mass fraction in the enricher product, $x_{1,i}$, are related recursively to the mass fraction of i at a central feed stage, $y_{e,i}$. The model counterflow column consisting of a stripping section of N_{SC} hypothetical stages separated by a single feed stage (subscript e) from an enriching section of M hypothetical stages is sketched in Fig. 2. The extraction ratio, $\Gamma_i \equiv (\alpha_i \rho_S/\rho_U)|U/S|$, summarizes the phase-partitioning of component i at steady mass flow-rates of fluid eluent, $U \equiv (1-r)\epsilon_b VT$, and solid adsorbent, $S \equiv -r(1-\epsilon_b)VT$. The volume of one stage is V, T represents the transfer rate of one stage volume, r is the fractional relative motion of the solid phase and ρ_p is the density of phase p. Subscripts U and S refer to the fluid and solid phases, respectively. The fluid-phase mass flow-rate is related to the equivalent countercurrent interstitial liquid velocity, v_{SC}, by $U = A_{SC}\epsilon_b v_{SC}\rho_U$ where A_{SC} is the counterflow-column cross-section.

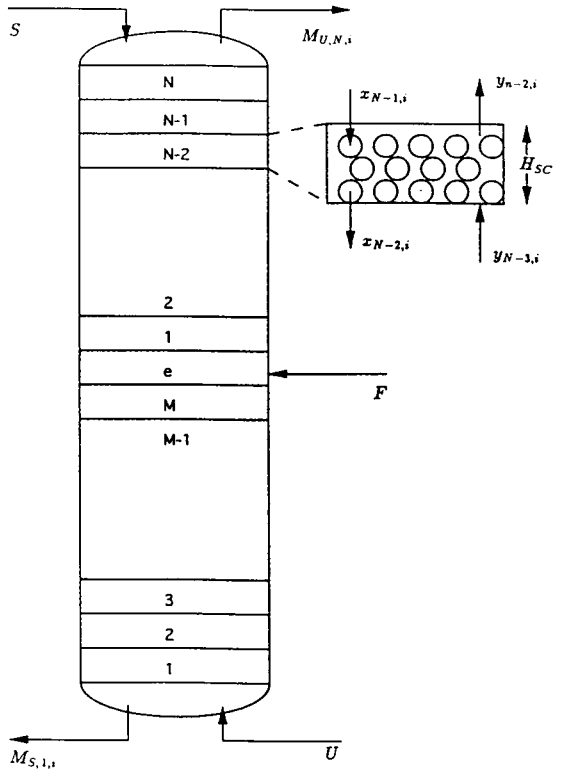

Fig. 2. Equilibrium-stage representation of steady counterflow. The enricher is composed of M stages. N stages comprise the stripper. The feedstream (F) enters stage e. Pure solid (S) and fluid (U) streams enter the stripper and enricher, respectively. The mass flow-rates of component i exiting the column from the stripper ($M_{U,N,i}$) and the enricher ($M_{S,1,i}$) are indicated. Within the column, component i enters and exits a representative stage $j = N-2$ of height H_{SC} with mass fraction values in the lower solid phase (spheres) ($x_{j,i}$) and upper fluid phase ($y_{j,i}$) as shown.

Solutes 1 and 2 enter the column dissolved in liquid eluent at the feed stage and are completely equilibrated on each stage j so that exiting fluid and solid mass fractions are related: $y_{j,i} = \alpha_i x_{j,i}\rho_S/\rho_U$. Ruthven [6] used a pseudocontinuum description of counterflow to relate the height of a steady counterflow stage, H_{SC}, to operating conditions as well as to individual contributions of microscopic, mass-transfer rate processes in difficult separations.

The solute mean residence time in counterflow, $\bar{t}_F$, given in Table I has been evaluated by taking the temporal first moment of the dynamic response to an impulse injection [31]. Subscript F refers to the feedstream. An identical relation

for mean residence time was derived by these authors, following Buffham and Kropholler [32], by calculating the ratio of total solute inventory to throughput in a steady counterflow system.

We now derive the relation for separation effectiveness in steady counterflow given in Table I.

Binary counterflow separation

A compact, analytical equation analogous to chromatographic resolution which relates separation by steady counterflow to specific thermodynamic (δ) and transport rate properties (reflected in H_{SC} or equivalently, in N_{SC}) is not available from the literature. Our derivation of this equation follows. We first relate fractional purity in an optimally operated column to the extraction ratio and the number of equilibrium counterflow stages using the counterflow mass ratio. We then express the extraction ratio in terms of the thermodynamic driving force to obtain the desired relation.

The fractional purity $P_{p,i}$ of species i leaving a counterflow column in phase p may be written in terms of corresponding solute mass flow-rates as

$$P_{p,i} = \frac{M_{p,j,i}}{M_{p,j,i} + M_{p,j,h\neq i}} \tag{1}$$

where the mass flow-rate of solute i leaving stage j in phase p, $M_{p,j,i}$, is the product of a solute mass fraction and its corresponding phase flow-rate *i.e.* $M_{U,j,i} \equiv U y_{j,i}$. For fractional purity in the exiting upper liquid phase, the exit-stage subscript j equals N and the phase subscript p equals U. By way of comparison, fractional purity achieved in differential chromatography can be approximated as

$$P = \int_{(\bar{t}_1+\bar{t}_2)/2}^{\infty} \frac{A\epsilon_b v c_f(t)|_{z=L}}{m_0}\,dt \approx \Phi(2R) \tag{2}$$

where the Gaussian nature of the effluent concentration suggests writing this integral as a cumulative distribution function, Φ, described by Hogg and Ledolter [33]. The argument of this function simplifies to $2R$ since ideal mean residence times and distributional variances of similar solutes are nearly equal. The fractional purity corresponding to a chromatographic resolution, R can be obtained from tabulated values of $\Phi(2R)$.

The species mass flow-rates in eqn. 1 are eliminated in favor of the extraction ratio and stage number using the counterflow mass ratio $M_{U,N,i}/M_{S,1,i} = \Gamma_i^{N_{SC}+1}$ which is obtained for $N_{SC} = M$ from the recursion relations (see Appendix). At operating conditions which produce the maximum binary separation, the mass ratio of one component equals the reciprocal of the other. For optimal operation we rearrange eqn. 1 to obtain

$$N_{SC} + 1 = \frac{\ln M_{F,h\neq i}/M_{F,i} + \ln P_{U,i}/(1-P_{U,i})}{\ln \Gamma_i} \tag{3}$$

where $M_{F,i}$ is the mass flow-rate of solute i in the feedstream.

Now we express the extraction ratio in terms of the thermodynamic separation driving force, δ for difficult, optimized separations to obtain the final form of eqn. 3. In a difficult separation, δ is small and either value of the dimensionless migration velocity, u_i, is close to the average of both, $\bar{u} \equiv 1/2(u_1 + u_2)$. Combining the operating condition for an optimal binary separation, $\Gamma_1\Gamma_2 = 1$ (see Appendix), with the definitions for Γ, u_i and δ yields

$$\Gamma_i^2 = 1 + (-1)^{2/i}\left[\delta + \frac{\bar{u}\delta}{1-\bar{u}} + O(\delta^2)\right] \tag{4}$$

Many bioseparations in particular have large solid-phase capacities for which $\bar{u} \ll 1$, so that a good approximation for the extraction ratio when separating closely related solutes is $\Gamma_i^2 \approx 1 + (-1)^{2/i}\delta$. (The error between this approximation and the "real" value of the extraction ratio relative to the average of the two is, neglecting terms second-order or higher in δ

$$\frac{|\Gamma_i^2 - \Gamma_i^{2\,\text{approx}}|}{\frac{1}{2}(\Gamma_i^2 + \Gamma_i^{2\,\text{approx}})} = \frac{\delta\bar{u}}{1-\bar{u}+(-1)^{2/i}\delta\left[1-\frac{\bar{u}}{2}\right]} \tag{5}$$

which approaches zero rapidly as δ and $\bar{u}$ become small.)

Finally, for a steady counterflow system operated to give maximum separation of similar solutes, we substitute $\Gamma_i^2 \approx 1 + (-1)^{2/i}\delta$ into eqn. 3 to obtain

$$N_{SC,tot} = 2\left[\frac{2\ln\left[\frac{P_{U,i}}{1-P_{U,i}}\right]}{\delta} - 1\right] + 1 \qquad (6)$$

where $N_{SC,tot} \equiv 2N_{SC} + 1$ is the total number of steady counterflow stages in the column. This is the relation we sought.

The equations summarized in Table I relate exit composition, mean residence time and resolution in analogous differential chromatography and steady counterflow systems to column geometry (N and H or N_{SC} and H_{SC}, ϵ_b, ρ_p), equilibrium parameters (α,u) and operating conditions (v or v_{SC}, Γ). For equivalent values of these parameters, separation of two closely related solutes by model chromatographic and counterflow processes can be directly compared.

COMPARING STEADY COUNTERFLOW WITH DIFFERENTIAL CHROMATOGRAPHY

We now examine general expressions to compare optimized counterflow separation of closely related solutes with conventional fixed-bed chromatography. We begin by contrasting the number of stages and processing residence time required by each process to achieve a given resolution. We then estimate the relative volumes of solvent required for two cases: (i) when feedstreams to each system are equally concentrated, and (ii) when mass loading constrains the operation of each system. Finally, we estimate the relative solid-phase requirement in these two cases by comparing columns with identical mass processing rates which produce equally pure products.

Basis of a counterflow advantage

Consider separating two closely related solutes to a predetermined resolution (or fractional purity) by either differential chromatography or steady, solid–liquid counterflow. The equations for resolution in Table I suggest that the number of counterflow stages required to achieve the split increases inversely with the thermodynamic driving force for separation, δ. In contrast, the number of chromatographic plates required increases with the square of the inverse of δ.

Suppose (i) that the same eluent and large-capacity adsorbent are used in both systems so that their equilibrium and transport properties are equal; and (ii) that the systems are operated with equivalent interstitial velocities. Comparing pseudocontinuum formulations of H by Gibbs and Lightfoot [17] and H_{SC} by Ruthven suggests that the height of a counterflow stage is approximately one-half that of a chromatographic plate under these conditions.

In addition to physical requirements, the time necessary to purify solutes by adsorption is a concern. Zhang *et al.* [34] investigated biological separations and reported that protein degradation by proteolysis, denaturation and other known processes [35,36] increased with processing time. The relations for residence time in Table I suggest a relative ratio for solute processing time, $\bar{t}_F/\bar{t}$, of

$$\frac{\bar{t}_F}{\bar{t}} = \frac{uv}{NH}\frac{(N_{SC,tot}+1)^2 H_{SC}}{8uv_{SC}} \qquad (7)$$

since the bracketed term of $\bar{t}_F$ reduces to $(N_{SC}+1)/2$ for closely related solutes. Assuming that identical resolution is obtained in systems which are operated equivalently gives

$$\frac{\bar{t}_F}{\bar{t}} = \left[\frac{\ln\left(\frac{\Phi(2R)}{\Phi(-2R)}\right)}{4R}\right]^2 \qquad (8)$$

This expression suggests that relative solute processing time is approximately equal in differential chromatography and steady counterflow for values of resolution between 0.9 and 1.5.

Three additional observations are in order. First, the number of counterflow stages required in a difficult separation where both solutes tend to partition to the liquid phase ($\bar{u} \sim 1$) increases proportional to $(1-\bar{u})/\delta$. Thus, the equation for steady counterflow resolution in Table I appears adequately cautious in such a case. Second, eqns. 7 and 8 conservatively estimate the relative solute residence time at *steady state* by using the maximum expected value of $\bar{t}_F$ —the counterflow mean residence time. For values of the extraction ratio much greater or less than unity, the bracketed term in the equation for $\bar{t}_F$ in Table I reduces to unity so that smaller processing times

would be anticipated for counterflow relative to chromatography. Lastly, both Lapidus and Amundson [7] and Ching and Ruthven [37] reported that the time required after start-up to approach steady-state in counterflow was significant and increased with the difficulty of the separation. The transient-response time will influence both physical and temporal requirements of counterflow.

Relative solvent requirement

We estimate relative solvent usage by determining the solvent volume per unit mass required in steady counterflow relative to differential chromatography: $[V_{solv}/m]_{SC}/[V_{solv}/m]_{DC}$. Expressions for comparable systems constrained by feedstream concentration or by load limitation are obtained by calculating respective values of the product-concentration dilution. We conclude by examining viscous effects at high loading.

We evaluate the maximum fluid-phase solute concentration in the first and final plates to estimate chromatographic concentration dilution as $(c_f^{max}|_{N=1})/(c_f^{max}|_{N=N}) = \sqrt{N}$. This form is consistent with work by Snyder [38] which shows that product dilution in isocratic elution increases at the same rate as resolution.

Dilution of stripper-product concentration in steady counterflow is the ratio of feedstream concentration to stripper effluent concentration $-M_{F,i}U/M_{U,N,i}F$ at constant density where M_F is the solute mass flow-rate in the feedstream. Substituting the recursion relation for $y_{N,i}$ and making use of the feedstage accumulation (total solute input to the feedstage divided by solute input by the feedstream) obtained by Klinkenberg [29]

$$\frac{M_{U,e,i} + M_{S,e,i}}{M_{F,i}} = \frac{\Gamma_i + 1}{\Gamma_i^{N_{SC}+1} + 1} \cdot \frac{\Gamma_i^{N_{SC}+1} - 1}{\Gamma_i - 1} \tag{9}$$

yields for the product dilution

$$\frac{c_F}{c_N} = \frac{1 + \dfrac{1}{\Gamma^{N_{SC}+1}}}{1 + \dfrac{1}{\Gamma}} \frac{U}{F_{U,e}F} \tag{10}$$

where $F_{U,e}$ is the fraction of i which exits the feed stage in the fluid phase. Enricher-product dilution is obtained analogously.

Dilution in counterflow is relatively independent of stage number and extraction ratio, varying only in proportion to U/F as is consistent with intuition. At optimized operation, dilution decreases slightly from $2U/F$ for closely related solutes to U/F for considerably easier separations. (Because $\Gamma < 1$ identifies a species whose net flow is toward the enricher exit, it is infinite as $\Gamma \to 0$.) The assumption by Klinkenberg that feed flow-rate is negligible appears to have inconsequential affect on our estimates of dilution.

The volume of solvent required by counterflow to separate closely related solutes relative to chromatography corresponds to the ratio of product concentration dilutions:

$$\frac{\left[\dfrac{V_{solv}}{m}\right]_{SC}}{\left[\dfrac{V_{solv}}{m}\right]_{DC}} = \frac{2U}{F\sqrt{N}} \frac{c_f^{max}|_{N=1}}{c_F} \tag{11}$$

We have neglected the void volume of solvent in differential chromatography, supposing that periodic injections are made at a frequency high enough to produce non-overlapping, back-to-back pairs of resolved effluent peaks.

For optimized units whose feedstream concentrations are equal, relative solvent requirement varies with U/F and decreases in direct proportion to square root of the number of chromatographic plates necessary to resolve the solutes. Antia and Horváth [39] and Felinger and Guiochon [40] have shown, however, that separation by differential chromatography in systems with non-linear, multicomponent Langmuir isotherms deteriorates at large solute loadings. Ching *et al.* [41] demonstrated that only diluting a 40:20 (% w/v) monoethanolamine–methanol feedstream could duplicate simulated moving-bed resolution attained at 20:10 (% w/v) due to type-1 non-linearity in the monoethanolamine isotherm.

Suppose that a maximum solute load in chromatography and counterflow is prescribed to avoid degrading the respective separations. Because the largest solute concentration occurs

at the chromatographic inlet and at the counterflow feedstage in our model systems, we obtain for similar solutes

$$\frac{c_f^{max}|_{N=1}}{c_F} = \frac{F}{2U}(N_{SC}+1) \tag{12}$$

since the ratio of feedstage to feedstream concentration equals the product of the feedstage accumulation and $(F_{U,e}F)/U$. Hence, where both columns have been constrained comparably due to non-linearities at high loading

$$\frac{\left[\frac{V_{solv}}{m}\right]_{SC}}{\left[\frac{V_{solv}}{m}\right]_{DC}} = \frac{\ln\left[\frac{\Phi(2R)}{\Phi(-2R)}\right]}{2R} \tag{13}$$

which suggests a relative two-fold increase in counterflow solvent usage for values of resolution between 0.9 and 1.5.

Consider now viscous effects at high sample loading which include viscous fingering observed by Athalye [42] and gross band deformation reported by Yamamoto *et al.* [43] in differential, size-exclusion chromatography. These occur at local concentration gradients where fast-moving, low-viscosity eluent displaces a viscous solute band. We divide the ratio of the peak fluid-phase solute concentration to its value at n standard deviations from the peak ($z = z_0 + ns$) by ns to estimate the local chromatographic concentration change as

$$\frac{1}{ns}\frac{c_f^{max}}{c_f|_{z=ns}} = \frac{\exp\frac{n^2}{2}}{nH\sqrt{N}} \tag{14}$$

The local counterflow concentration change per stage, estimated in the enricher using the stagewise recursion relation, $y_j/y_e = (\Gamma^j - 1)/(\Gamma^{M+1} - 1)$, is

$$\frac{y_{j+1}}{y_j} = \frac{\Gamma^{j+1} - 1}{\Gamma^j - 1} \tag{15}$$

Fig. 3 illustrates the magnitude of local dilution in counterflow for two separations with thermodynamic driving forces of 0.209 and 0.00209, respectively. Although composition changes (see Fig. 4) are large near column exits and the feed stage, local dilution measured by eqn. 15 is

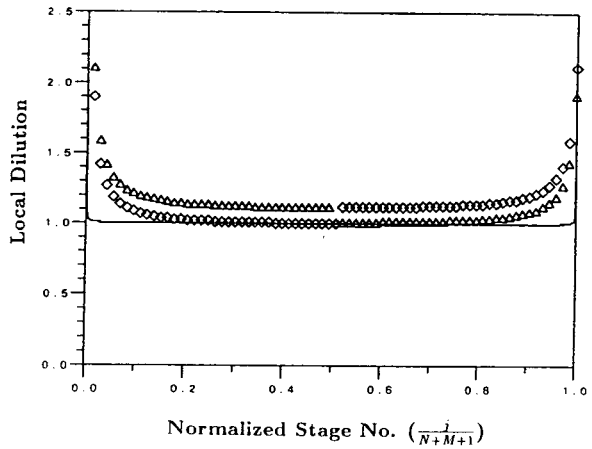

Fig. 3. Local dilution profiles in counterflow for the two separations described in Fig. 4. In the easier separation ($\delta = 0.209$) solute 1 (△) partitions preferentially to the upper fluid phase while solute 2 (◇) tends to the lower solid phase. Similarly, in the more difficult separation ($\delta = 0.00209$) solute 1 is represented by the dashed line and solute 2 by the solid line. In each case, profiles were calculated using stagewise recursion relations for the enricher and stripper with $M = N$ large enough to resolve 1 and 2 to unity ($P_{U,1} = 0.9772$).

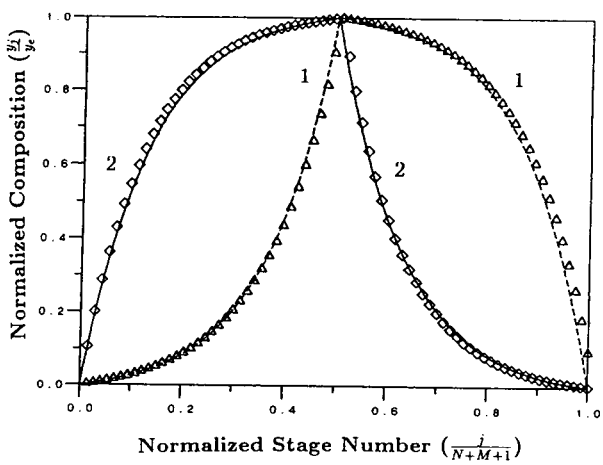

Fig. 4. Relative concentration profiles in counterflow for two separations. In the easier separation ($\delta = 0.209$) solute 1 (△) partitions preferentially to the upper fluid phase while solute 2 (◇) tends to the lower solid phase. Similarly, in the more difficult separation ($\delta = 0.00209$) solute 1 is represented by the dashed line and solute 2 by the solid line. In each case, profiles were calculated using stagewise recursion relations for the enricher and stripper with $M = N$ large enough to resolve 1 and 2 to unity ($P_{U,1} = 0.9772$).

largest in difficult separations for both components near the stripper and enricher exits where relative compositions are relatively small. Dilution values for components 1 and 2 in the larger column are nearly indistinguishable.

Finally, we note that steady counterflow composition profiles (and dilution profiles) plotted for difficult, high-resolution separations using *scaled* variables vary little over two decades of δ, as illustrated in Fig. 4 (and Fig. 3). The appropriate scaling factors —$y_{e,i}$ for stage composition $y_{j,i}$ and $M+1$ for enricher-stage j— were determined by applying the binomial theorem and counterflow mass ratio to the stagewise recursion relation for solute 1 which partitions preferentially to the liquid to obtain

$$\frac{y_{j,1}}{y_{e,1}} = \frac{2j}{M+1} \cdot \frac{(1-P_{U,1})^2}{2P_{U,1}-1} \ln\left[\frac{P_{U,1}}{1-P_{U,1}}\right] \times \left\{1 + \frac{(j-1)\delta}{2}\left[1 + \frac{(j-2)\delta}{3}(1+\cdots)\right]\right\} \tag{16}$$

Relative solid-phase requirement

We estimate relative solid-phase usage by calculating the ratio of counterflow and chromatography column volumes necessary to produce equally pure products at identical mass processing rates, $M_{U,N,i}/P_{U,i} = m_0/\bar{t}$. For simplicity, the rate at which subsequent injections are made is assumed to be $1/\bar{t}$ and both columns are operated to produce equal interstitial velocities. The column volume ratio is computed for equal feedstream concentrations as well as for comparable load limitations.

In high-resolution separations, average chromatographic effluent concentration is approximately $\bar{c}_f|_{z=L} \approx (m_0 u\sqrt{N})/(A\epsilon_b 6L)$ and counterflow exit concentration is very nearly $c_N \approx y_{N,i}\rho_U$ so that at equal processing rates

$$\frac{c_N}{\bar{c}_f|_{z=L}} = \frac{6}{\sqrt{N}} \frac{Av}{A_{SC}v_{SC}} \tag{17}$$

We substitute eqn. 11 and multiply the subsequent ratio of cross-sectional areas by a ratio of required lengths. Then N and N_{SC} are eliminated in favor of δ and R to obtain

$$\frac{(2N_{SC}+1)A_{SC}H_{SC}}{NAH} = \frac{3}{32}\frac{U}{F}\frac{\ln\left[\frac{\Phi(2R)}{\Phi(-2R)}\right]}{R^4}\delta^3 \tag{18}$$

for systems with equal feed concentrations and

$$\frac{(2N_{SC}+1)A_{SC}H_{SC}}{NAH} = \frac{3}{32}\frac{\ln\left[\frac{\Phi(2R)}{\Phi(-2R)}\right]}{R^4}\delta^2 \tag{19}$$

for systems comparably constrained by load limitations.

Eqns. 18 and 19 suggest that the relative solid-phase requirement is larger for separations involving closely related solutes than for easier, low-δ splits. (The comparative advantage is larger for systems with equal feed concentrations.) The physical basis for the decrease in adsorbent requirement is apparent in a comparison of Figs. 1 and 4 in which binary composition profiles are illustrated for a resolution of unity (a 97.72% mutual separation). Five percent of the fixed bed actively separates 1 from 2 while all of the counterflow column actively resolves the two components.

In Table II the expressions for relative mean residence time and relative solvent and solid-phase requirement for counterflow and chromatographic systems with equal feed concentrations are summarized.

RESULTS AND DISCUSSION

Reported values of dilution, solvent requirement and adsorbent requirement from three simulated moving-bed studies in Table III are compared with corresponding steady counterflow estimates in Table IV. Observed values are well within an order of magnitude of expected results. Approximating fixed-bed dilution by $\sqrt{N}$ yielded values about a factor of six lower than reported dilutions. Consequently, the anticipated relative solvent required to purify racemic 1-phenylethanol was about six times higher than observed. In each case, the estimates of counterflow performance relative to chromatography were conservative.

Note that the sugar-fractionation data repre-

TABLE II

SEPARATION BY STEADY COUNTERFLOW RELATIVE TO DIFFERENTIAL CHROMATOGRAPHY

Relative performance	Expression
Mean residence time	$\frac{\bar{t}_F}{\bar{t}} = \left[\frac{\ln\left(\frac{\Phi(2R)}{\Phi(-2R)}\right)}{4R}\right]^2$
Required solvent volume	$\frac{\left[\frac{V_{solv}}{m}\right]_{SC}}{\left[\frac{V_{solv}}{m}\right]_{DC}} = \frac{2U}{F\sqrt{N}}$
Required solid-phase volume	$\frac{(2N_{SC}+1)A_{SC}H_{SC}}{NAH} = \frac{3}{32}\frac{U}{F}\frac{\ln\left[\frac{\Phi(2R)}{\Phi(-2R)}\right]}{R^4}\delta^3$

sent a linear glucose/Duolite adsorption isotherm at the concentrations considered (see Ching *et al.* [28]) while the isotherms of the racemic resolution and lysine recovery were non-linear. The tractable expressions we have derived from counterflow and chromatographic models in which adsorption was presumed linear with a constant equilibrium distribution coefficient approximate the relative performance of both linear and non-linear systems. Previous analyses of non-linear chromatography [15,44] and counterflow [28,41] suggest that more specific comparisons of the relative performance of non-linear systems (other than specialized Langmuir chromatographic adsorptions for which analytic solutions for concentration profiles have been derived by Thomas [45] and Glueckauf [46]) will likely be limited in scope, and that numerical analysis will probably replace analytic expressions such as ours.

Until more general relations are developed, a detailed analysis of linear systems provides a useful starting point to examine relative performance of counterflow and chromatographic separations. Consider resolution of ovalbumin (OA) and bovine serum albumin (BSA) using

TABLE III

EXPERIMENTAL RESULTS: SIMULATED MOVING-BED (SMB) *VS.* DIFFERENTIAL CHROMATOGRAPHY (DC)

	Parameters			Reported performance			
				Dilution		Requirement, SMB/DC	
	$\frac{U}{F}$	H (cm)	δ	SMB	DC	Solvent	Adsorbent
Racemic resolution[a]	31	0.015	nr[d]	11.5	290	0.011	0.016
Sugar fractionation[b]	8.5	10	0.27	8.3	22.0	nr	nr
Lysine recovery[c]	1.2	nr	nr	0.79	0.96	0.5	0.1

[a] Ref. 2. Flow-rate and counterflow dilution ratio calculated from values of flow-rate and concentration reported for *R*-(+)-1-phenylethanol-rich raffinate.

[b] Ref. 52. Flow-rate and counterflow dilution ratio calculated from values of flow-rate and concentration reported for glucose in the post-feed columns of run 4.

[c] Ref. 3. Flow-rate and dilution ratios calculated from arithmatic averages of ranges reported for flow-rates and concentrations.

[d] Not reported.

TABLE IV

CALCULATED RESULTS: STEADY COUNTERFLOW *VS.* DIFFERENTIAL CHROMATOGRAPHY

	Estimated performance			
	Dilution		Requirement, SC/DC	
	SC[a]	DC[b]	Solvent[c]	Adsorbent
Racemic resolution	31	58	0.068	0.017[d]
Sugar fractionation	8.5	3.2	13	0.15[e]
Lysine recovery	1.2	na[f]	na	na

[a] Estimated as U/F since reported concentration profiles suggested $F_{U,e} \sim 1$ in each separation. See *Relative solvent requirement* section.

[b] Estimated as $\sqrt{N}$. See *Relative solvent requirement* section.

[c] Estimated as $U/\sqrt{N}F$. See *Relative solvent requirement* section and footnote a.

[d] Estimated as $(3N_{SC,tot}Uc_f|_{N=1})/(NFc_F)$ with N_{SC} calculated assuming $H \approx 2H_{SC}$ since thermodynamic data for δ were not reported. See *Relative solid-phase requirement* section.

[e] Estimated as $\left(3Uc_f|_{N=1} \ln\left[\frac{\Phi(2R)}{\Phi(-2R)}\right]\delta^3\right)/(64Fc_FR^4)$ with $R = 1$. See *Relative solid-phase requirement* section.

[f] Not available, as measured values of H and δ were not reported.

Toyopearl (TSK gel) HW55F ($d_p = 44\ \mu$m). This separation depends on size exclusion, as do fractionation of dextran by Ca^+ resin and "Molex" processes. Parameter values for this case study including those reported by Yamamoto *et al.* [47] and Germershausen *et al.* [48] are summarized in Table V. The relative error of approximating Γ_1 by $1 + \delta$ is 0.076, as determined using eqn. 5. The calculated measures of relative separation performance are listed in Table VI.

Expected solute mean residence times in the two systems are roughly equal. Solvent usage in counterflow is expected to be less than one quarter of the value required for chromatography, for systems with equal feed concentrations. Due to the low thermodynamic driving force for separation, almost four orders of magnitude less gel filtration resin is required for counterflow relative to fixed-bed separation. In contrast, the anticipated relative solid-phase requirement for less strenuous separations such as fructose/glucose fractionation in Table III is considerably smaller.

Comparing models of counterflow and chromatography suggests that steady counterflow

TABLE V

PARAMETER VALUES FOR SEPARATION OF BOVINE SERUM ALBUMIN (BSA) AND OVALBUMIN (OA) IN TSK HW55F

Parameter	BSA	OA	System
Intraparticle porosity[a], ϵ_p	0.30	0.34	–
Bed void fraction[b], ϵ_b	–	–	0.34
Thermodynamic driving force, δ	–	–	0.048
Required resolution, R	–	–	1.0
Volumetric dilution, U/F	–	–	10

[a] Ref. 47.

[b] Ref. 48.

TABLE VI

SEPARATION OF BOVINE SERUM ALBUMIN AND OVALBUMIN IN TSK HW55F

Steady counterflow *vs.* gel filtration chromatography

Relative performance	Ratio	Value
Required stages	$\frac{N_{SC,tot}}{N}$	$\frac{313}{6975}$
Mean residence time	$\frac{\bar{t}_F}{\bar{t}}$	0.883
Required solvent	$\frac{[V/m_0]_{SC}}{V/m_0]_{DC}}$	0.239
Required solid-phase	$\frac{(2N_{SC}+1)A_{SC}H_{SC}}{NAH}$	0.0004

utilizes stage volumes more efficiently than differential chromatography utilizes plate volumes. For a given resolution, the number of stages required by chromatography to separate close solutes relative to counterflow increases inversely with the thermodynamic driving force for separation. This appears to be the basis for reported order-of-magnitude decreases in adsorbent volume obtained by simulating counterflow in packed beds. Substantial reported reductions in solvent volume may be related to large dilutions observed in chromatography relative to counterflow, whose value is proportional to the square-root of the number of chromatographic stages required to resolve similar products.

Viscous effects such as fingering and gross band deformation are also expected be less problematic in counterflow where local concentration changes are small relative to chromatography. Chromatographic concentration near the inlet changes over an order of magnitude within an axial distance corresponding to one stage, whereas the maximum counterflow change per stage is less than one-fourth that value, as illustrated in Fig. 3. Note that solute composition in counterflow increases in the direction of fluid flow only in the enricher section. So hydrodynamic instabilities reinforced by viscosity differences are not expected to decrease separation efficiency in the stripper.

Simulating counterflow appears particularly advantageous for difficult separations such as resolution of optical isomers or protein variants. In addition to Sorbex-type equipment, the rotating-barrel liquid extractor proposed by Brenner and machines by Ito offer the number of counterflow stages required to separate close solutes. On the other hand, steady operation is limited to binary separations, so equipment must be doubled for ternary systems which are often encountered in present-day chromatography. On balance, progress should be made cautiously, but the potential advantages of counterflow appear attractive enough to deserve a real effort.

SYMBOLS

A	column cross-sectional area (cm^2)
$\bar{c}$	time-averaged fluid-phase solute concentration in chromatography (g/cm^3)
c_f	solute concentration in moving fluid phase in chromatography (g/cm^3)
c_N	solute concentration at the N-stage stripper exit in the upper fluid phase in counterflow (g/cm^3)
$c_{p,i}$	concentration of solute i in phase p in chromatography (g/cm^3)
$D_{p'}$	effective solute diffusivity in pore liquid (cm^2/s)
F	feed mass flow-rate in counterflow (g_U/s)
$F_{p,i}$	fractional recovery of species i in phase p
$F_{p,e}$	fraction of a component exiting the feed stage which leaves in phase p
H	height equivalent to a theoretical chromatographic plate (cm)
H_{SC}	height equivalent to one counterflow stage (cm)
k_{ads}	forward rate constant of adsorption (s^{-1})
k_c	concentration-based fluid-phase mass transfer coefficient (cm/s)
k_{des}	rate constant of desorption (s^{-1})
$K_{eq,i}$	ratio of masses of adsorbed and pore-liquid solutes at equilibrium
L	length of chromatographic column ($=HN$) (cm)
m_0	total solute mass which enters chromatography column in a pulse (g)

M number of stages in the counterflow enricher section
M_F mass flow-rate of species which enters the counterflow column through the feedstream (g/s)
$M_{p,j}$ mass flow-rate of species leaving stage j in phase p (g/s)
$M_{p,j,i}$ mass flow-rate of species i leaving stage j in phase p (g_i/s)
N number of stages
$N_{SC,tot}$ total number of stages in a counterflow system
P purity of species in a chromatographic separation
$P_{p,i}$ fractional purity of species i in phase p
r fractional relative motion of the lower solid phase
R chromatographic resolution
R_b radius of a solid-phase particle (cm)
s^2 variance about the mean (s^2)
s_t standard deviation normalized by the mean residence time
S lower solid-phase mass flow-rate (g_S/s)
t time (s)
$\bar{t}$ mean residence time in chromatography (s)
$\bar{t}_F$ mean residence time in steady counterflow of a component which enters through the feedstream alone
T transfer rate of one stage volume (s^{-1})
u_i equilibrium fraction of species i in the fluid phase
U upper fluid phase mass flow-rate (g_U/s)
v interstitial velocity in chromatography or equivalent countercurrent interstitial velocity in counterflow (cm/s)
V volume of solvent
$x_{j,i}$ fraction of the lower solid phase leaving stage j which is species i (g_i/g_S)
$y_{j,i}$ fraction of the upper fluid phase leaving stage j which is species i (g_i/g_U)
z axial coordinate (cm)
z_0 mean position of a solute peak at a given time, defined as uvt (cm)

Greek letters

α_i partition coefficient of i between fluid and solid phase
δ fractional difference in u for two species: thermodynamic driving force for separation
ϵ convective axial dispersion coefficient (cm^2/s)
ϵ_b interparticle or column void volume
$\epsilon_{p'}$ intraparticle porosity
Γ_i extraction ratio of solute i
Λ selectivity, defined as Γ_1/Γ_2
Φ cumulative distribution function of the standard normal distribution
ρ_U density of upper liquid phase (g_U/m^3)
ρ_S density of lower solid phase (g_S/m^3)
ξ extent of separation

Subscripts and superscripts

1 enricher exit stage
b bulk (stationary) phase in chromatography
e feed stage
f moving fluid phase in chromatography
F feedstream
i species identification subscript
j stage identification subscript
DC differential chromatography
N stripper exit stage
p phase identification subscript
p′ porous fluid entrained in the bulk phase in chromatography
S lower solid phase in counterflow
SC steady counterflow
U upper liquid phase in counterflow

APPENDIX

Here we provide the derivation of the operating condition for optimum binary counterflow separation utilized in the *Binary counterflow separation* section. We have included this derivation which follows a previous analysis by Rony [49] to elucidate the basis of the relation for binary counterflow separation and to clarify our nomenclature, which differs from his.

Binary counterflow separation produces a difference between fractional recoveries of components 1 and 2 from the fluid stripper effluent and the solid enricher extract. This defines the extent of separation ξ as

$$\xi \equiv |F_{U,1} - F_{U,2}| = |F_{S,1} - F_{S,2}| \tag{20}$$

Fractional recovery $F_{p,i}$ of component i from phase p is defined in terms of its flow-rate $M_{p,j,i}$ exiting stage j

$$F_{U,i} \equiv \frac{M_{U,N,i}}{M_{U,N,i} + M_{S,1,i}} \tag{21}$$

$$F_{S,i} \equiv \frac{M_{S,1,i}}{M_{S,1,i} + M_{U,N,i}} \tag{22}$$

Species flow-rates are eliminated from eqns. 21 and 22 in favor of N_{SC} and Γ by defining a mass ratio using the recursion relations in Table I

$$\frac{M_{U,N,i}}{M_{S,1,i}} = \frac{y_{N,i}U}{x_{1,i}S} = \frac{\Gamma_i \sum_{j=0}^{M} \Gamma_i^j}{\sum_{k=0}^{N} \Gamma_i^{-k}} \tag{23}$$

The mass ratio relates exiting compositions without requiring information about the feedstage or feedstream. Using the rule for finite sums of geometric series, $\sum_{j=0}^{n-1} ar^j = [a(1-r^n)/1-r]$, the mass ratio for $N = M$ becomes

$$\frac{M_{U,N,i}}{M_{S,1,i}} = \Gamma_i^{N_{SC}+1} \tag{24}$$

Hence the extraction ratio and the number of counterflow stages completely determine the extent of separation

$$\xi = \left| \frac{1}{1 + \Gamma_1^{-(N_{SC}+1)}} - \frac{1}{1 + \Gamma_2^{-(N_{SC}+1)}} \right| \tag{25}$$

The value of the extraction ratio which optimizes separation is determined by maximizing ξ in eqn. 25 with respect to Γ_1 after assuming constant selectivity, $A \equiv \Gamma_1/\Gamma_2$. This results in

$$\Gamma_{i,opt}^{-1} = A^{\frac{(-1)^i}{2}} \tag{26}$$

which relates the extraction ratio of component i to a constant ratio of the equilibrium partition coefficients for optimized binary separations. This condition can be used to show that fractional recoveries and fractional purities of solutes in their preferred phase are equal.

The maximum value for the extent of separation is then

$$\xi_{max} = \left| \frac{A^{(N_{SC}+1)/2} - 1}{A^{(N_{SC}+1)/2} + 1} \right| \tag{27}$$

and it is seen that

$$\Gamma_1 \Gamma_2 = 1 \tag{28}$$

This is the operating condition for optimal separation of a binary mixture. Using the definition of the extraction ratio, a unique, optimum value for the fractional relative solid motion, r, may be determined.

Rony [50] showed that maximum extent of separation in chromatography with optimum distribution ratio was proportional to $\sqrt{N}$. In staged-counterflow with optimum extraction ratio the maximum extent of separation was proportional to N_{SC}. Adjustments to operating conditions and equipment which increase the performance of ideal counterflow separations have been proposed more recently. Liapis and Rippin [5] observed that increasing the column length and number of subdivisions in a simulated moving bed improved the adsorbent utilization. Storti *et al.* [51] determined countercurrent flow ratios at which solid and desorbent requirement were minimized using characteristic parameters derived from component feed concentrations, then used equilibrium theory to numerically analyze steady, dispersive flow in one- and four-section, non-linear (but constant-selectivity) systems.

ACKNOWLEDGEMENT

We gratefully acknowledge partial financial support for D.K.R. from National Research Service Award 1T32GMO8349 received from the National Institute of General Medical Sciences.

REFERENCES

1 D.B. Broughton, R.W. Neuzil, J.M. Pharis and C.S. Brearley, *Chem. Eng. Prog.*, 66 (1970) 70–75.
2 M. Negawa and F. Shoji, *J. Chromatogr.*, 590 (1992) 113–117.
3 G.J. Rossiter and C.A. Tolbert, presented at the *AIChE Annual Meeting*, Los Angeles, CA, November 17–22, 1991.
4 E.E. Ernst and D.W. McQuigg, presented at the *AIChE Annual Meeting*, Miami Beach, FL, November 1–6, 1992.

5 A.I. Liapis and D.W.T. Rippin, *AIChE J.*, 25 (1979) 455–460.
6 D.M. Ruthven, *Principles of Adsorption and Adsorption Processes*, Wiley Interscience, New York, 1st ed., 1984.
7 L. Lapidus and N.R. Amundson, *Ind. Eng. Chem.*, 42 (1950) 1071–1078.
8 T. Miyauchi and T. Vermeulen, *Ind. Eng. Chem. Fundam.*, 2 (1963) 113–125.
9 D.M. Ruthven and C.B. Ching, *Chem. Eng. Sci.*, 44 (1989) 1011–1038.
10 U.P. Ernst and J.T. Hsu, presented at the *AIChE Annual Meeting*, Los Angeles, CA, November 17–22, 1991.
11 G. Storti, M. Mazzotti, L.T. Furlan, M. Morbidelli and S. Carra, presented at the *AIChE Annual Meeting*, Miami Beach, FL, November 1–6, 1992.
12 B.B. Fish, R.W. Carr and R. Aris, *AIChE J.*, 35 (1989) 737–745.
13 J.C. Giddings, *Dynamics of Chromatography, Part I, Principles and Theory (Chromatographic Science Series*, Vol. 1), Marcel Dekker, New York, 1965.
14 R. Aris and N.R. Amundson, *Mathematical Methods in Chemical Engineering*, Prentice Hall, Englewood Cliffs, NJ, 1973.
15 B. Lin, Z. Ma, S. Golshan-Shirazi and G. Guiochon, *J. Chromatogr.*, 500 (1990) 185–213.
16 J.F.G. Reis, E.N. Lightfoot, P.T. Noble and A.S. Chiang, *Sep. Sci. Technol.*, 14 (1979) 367–394.
17 S.J. Gibbs and E.N. Lightfoot, *Ind. Eng. Chem. Fundam.*, 25 (1986) 490–498.
18 I. Stakgold, *Greens Functions and Boundary Value Problems*, Wiley, New York, 1979.
19 A.M. Athalye, S.J. Gibbs and E.N. Lightfoot, *J. Chromatogr.*, 589 (1992) 71–85.
20 J.J. van Deemter, F.J. Zuiderweg and A. Klinkenberg, *Chem. Eng. Sci.*, 5 (1956) 271–289.
21 P.J. Karol, *Anal. Chem.*, 61 (1989) 1937–1941.
22 J.C. Giddings, *Unified Separation Science*, Wiley, New York, 1991.
23 A. Kremser, *Natl. Pet. News*, 22(21) (1930) 42.
24 M. Souders and G.G. Brown, *Ind. Eng. Chem.*, 24 (1932) 519–522.
25 C.J. King, *Separation Processes*, McGraw-Hill, New York, 2nd ed., 1980.
26 R.E. Treybal, *Mass Transfer Operations*, McGraw-Hill, New York, 3rd ed., 1980.
27 E.J. Henley and J.D. Seader, *Equilibrium-Stage Separation Operations in Chemical Engineering*, Wiley, New York, 1st ed., 1981.
28 C.B. Ching, C. Ho, K. Hidajat and D.M. Ruthven, *Chem. Eng. Sci.*, 42 (1987) 2547–2555.
29 A. Klinkenberg, *Chem. Eng. Sci.*, 1 (1951) 86–92.
30 A. Klinkenberg, H.A. Lauwerier and G.H. Reman, *Chem. Eng. Sci.*, 1 (1951) 93–99.
31 D.K. Roper and E.N. Lightfoot, *Chem. Eng. Sci.*, submitted for publication.
32 B.A. Buffham and H.W. Kropholler, *Chem. Eng. Sci.*, 28 (1973) 1081–1089.
33 R.V. Hogg and J. Ledolter, *Engineering Statistics*, Macmillan, New York, 1st ed., 1987.
34 X. Zhang, R.D. Whitley and N.-H.L. Wang, presented at the *AIChE Annual Meeting*, Los Angeles, CA, November 17–22, 1991.
35 R.K. Scopes, *Protein Purification*, Springer, New York, 1987.
36 W.S. Hancock, S. Wu and J. Frenz, *LC–GC*, 10 (1992) 96–104.
37 C.B. Ching and D.M. Ruthven, *Chem. Eng. Sci.*, 40 (1985) 887–891.
38 L.R. Snyder, in Cs. Horváth (Editor), *High-Performance Liquid Chromatography*, Vol. 1, Academic Press, New York, 1980, pp. 207–316.
39 F.D. Antia and Cs. Horváth, *J. Chromatogr.*, 484 (1989) 1–27.
40 A. Felinger and G. Guiochon, *J. Chromatogr.*, 591 (1992) 31–45.
41 C.B. Ching, C. Ho and D.M. Ruthven, *Chem. Eng. Sci.*, 43 (1988) 703–711.
42 A.M. Athalye, *PhD. Thesis*, University of Wisconsin-Madison, 1993.
43 S. Yamamoto, M. Nomura and Y. Sano, *J. Chem. Eng. Jap.*, 19 (1986) 227–231.
44 T. Gu, G. Tsai and G.T. Tsao, *AIChE J.*, 36 (1990) 784–788.
45 H.C. Thomas, *J. Am. Chem. Soc.*, 66 (1944) 1664.
46 E. Glueckauf, *Proc. R. Soc. London, A*, 186 (1946) 35.
47 S. Yamamoto, M. Nomura and Y. Sano, *J. Chromatogr.*, 394 (1987) 363–387.
48 J. Germershausen, R. Bostedor, R. Liou and J.D. Karkas, *J. Chromatogr.*, 270 (1983) 383–386.
49 P.R. Rony, *Sep. Sci.*, 5 (1970) 1–10.
50 P.R. Rony, *Sep. Sci.*, 5 (1970) 121–135.
51 G. Storti, M. Masi, S. Carra and M. Morbidelli, *Chem. Eng. Sci.*, 44 (1989) 1329–1345.
52 C.B. Ching and D.M. Ruthven, *Chem. Eng. Sci.*, 40 (1985) 877–885.

Journal of Chromatography A, 654 (1993) 17–28
Elsevier Science Publishers B.V., Amsterdam

CHROM. 25 454

Chiral ion-exchange chromatography

Correlation between solute retention and a theoretical ion-exchange model using imprinted polymers

Börje Sellergren[☆] and Kenneth J. Shea*

Department of Chemistry, University of California, Irvine, CA 92717-2025 (USA)

(First received April 29th, 1993; revised manuscript received July 26th, 1993)

ABSTRACT

Mobile phase effects were studied in the separation of D- and L-phenylalanine anilide (D,L-PA) on an imprinted chiral stationary phase (CSP). Using an aqueous-organic mobile phase, an improved column performance was seen, reflected in a two-fold decrease in the reduced plate height and an almost doubling of the resolution as compared to when a pure organic mobile phase was used. A strong dependence of retention (k') and enantiomer selectivity (α) on mobile phase pH was observed. k' reached a maximum at a pH close to the pK_a value of the solute and α was high at low pH value but decreased when pH exceeded the solute pK_a. Potentiometric titration data allowed estimation of the state of protonation of both the carboxylic acid containing CSP and the amino group containing solutes. The data are analyzed using a simple cation-exchange model to allow simulation of the retention as a function of mobile phase pH. The close agreement between the simulated and experimental curves for retention *versus* pH suggests that a simple cation-exchange mechanism controls the retention in this system. Moreover, the slightly lower average pK_a of the imprinted polymer compared to that of a corresponding blank polymer explains the high selectivity seen at low pH values. Based on these findings, a model describing the events controlling binding and selectivity as a function of pH is proposed.

INTRODUCTION

During the last years several examples of the use of imprinted polymers for specific molecular recognition have been reported [1–12]. In one case [4–9] (Fig. 1) a chiral template molecule (L-phenylalanine anilide = L-PA) was used to preorganize functionalized monomers (methacrylic acid = MAA) in solution. Copolymerization of the template assemblies with a cross-linking monomer (ethylene glycol dimethacrylate = EDMA) gave a network polymer which was freed from template by extraction. After crushing and sieving a selective chromatographic stationary phase was obtained.

With this technique resolutions of a variety of racemates have been successfully achieved [12]. Recently the technique has also been used to prepare affinity matrices for the DNA-bases [10] and as antibody mimics in a drug assay [11].

For the user of chiral stationary phases (CSPs) it is desirable that *predictable* separations of enantiomers as well as achiral compounds from several classes can be performed on a single column [13]. Although the imprinted CSPs usually have a high substrate selectivity, the similarity in composition between these CSPs and meth-

* Corresponding author.
☆ Present address: Bioherb Inc., Bifrostgatan 40, 25362 Helsingborg, Sweden.

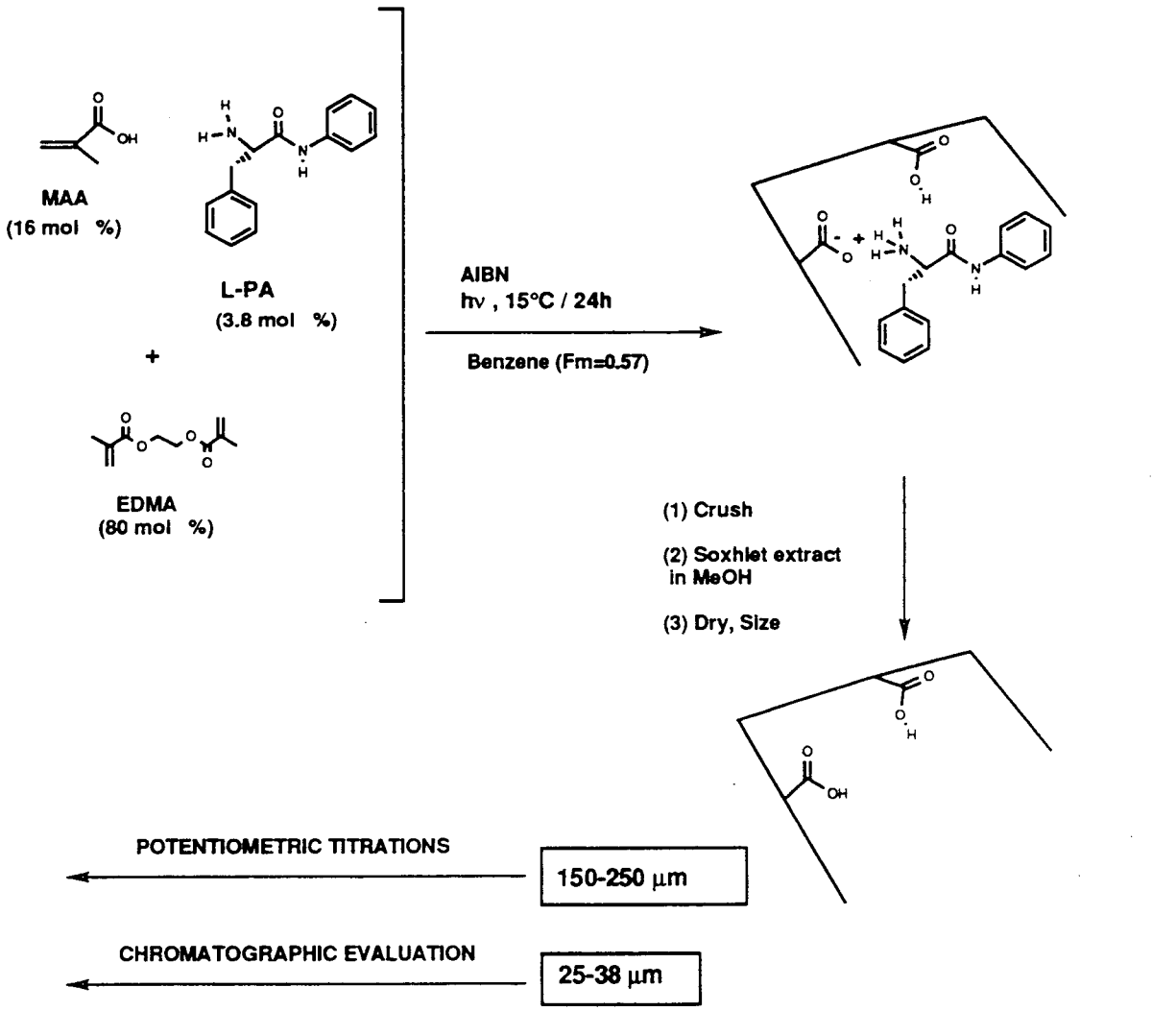

Fig. 1. Schematic of the synthesis, processing and evaluation of imprinted polymers as chiral stationary phases. Fm refers to the volume fraction of polymerisable monomers to benzene solvent.

acrylate-based weak cation-exchange resins [14–16] suggests that they may be applied in simple cation-exchange separations as well. This therefore led us to investigate whether ion exchange is the main process controlling retention on these CSPs.

EXPERIMENTAL

General procedures

D- and L-PA were synthesized as described elsewhere [5,6]. The methacrylate monomers were obtained from Aldrich. EDMA was purified by extraction with 10% NaOH, brine, drying over anhydrous magnesium sulfate followed by distillation. MAA was purified by drying over anhydrous magnesium sulfate followed by distillation. The porogens were all distilled under a positive nitrogen atmosphere prior to use and all other reagents purified according to standard procedures. The pH was monitored with a standard pH electrode connected to a pH meter (Fischer Scientific, Accumet 910) standardized at pH 4, 7 and 10 using

buffer solutions. All chromatographic evaluations was done using a Waters 484 UV detector, Waters 501 pump equipped with a U6K injector and a Hewlett-Packard integrating recorder.

Polymerizations

The polymers were prepared as follows: The monomer mixture consisted of EDMA (3.8 ml, 20 mmol) and MAA (0.34 ml, 4 mmol) in benzene (5.6 ml) to which was added template and the initiator azo-bis-isobutyronitrile (AIBN; 40 mg, 0.25 mmol). The templates were L-PA (240 mg, 1 mmol) giving polymer P-L-PA or benzylamine (BA) (107 mg, 1 mmol) giving polymer PBA. No addition of template gave the blank polymer (PBL). The mixture was transferred to a 50-ml thick-walled glass tube. This was freeze thaw degassed three times and sealed under vacuum. The tubes were symmetrically placed at *ca.* 10 cm distance from a standard UV light source in a waterbath thermostatted at 15°C and turned at regular intervals for a symmetric exposure. After 24 h the tubes were broken and the polymers separated then ground in a mortar followed by Soxhlet extraction in methanol for 12 h. The polymers were dried overnight under vacuum at 50°C and then sieved to a 150–250 μm and a 25–38 μm particle size.

Chromatographic evaluation

The polymers with a 25–38 μm particle size were slurry packed into 100-mm stainless-steel columns [5 mm I.D. containing *ca.* 0.5 g (dry mass) of polymer after packing] using acetonitrile–water–acetic acid (92.5:2.5:5, v/v/v) as mobile phase. After passing *ca.* 50 ml at a flow-rate of 10 ml/min the column was equilibrated at 1 ml/min until a stable baseline was reached. The flow rate was 1 ml/min, the volume of injected solute 10 μl and the detection wavelength 260 nm unless otherwise stated. The capacity factor was calculated as $(t_R - t_0)/t_0$ where t_R is the peak maxima retention time of the solute and t_0 the retention time of a non-retained void marker ($NaNO_3$). The separation factor (α) measures the relative retention between the enantiomers ($\alpha = k'_L/k'_D$) and h the reduced plate height from the number of theoretical plates (N) as $h = L/(d_p N)$ where L = column length (=10 cm), d_p = average particle diameter (=31.5 μm) and $N = 5.55\ (t_R/t_{1/2})^2$ where $t_{1/2}$ is the peak width at half height. The resolution factor R_s [3] and the asymmetry factor A_s [17] were obtained graphically as described elsewhere.

Potentiometric pH titrations

Conditioning. The polymers were initially converted to the acid form. Polymer (0.6 g, 150–250 μm) was washed by shaking with 2 × 25 ml 0.1 *M* HCl for 1 h each. After sedimentation the supernatant was removed with Pasteur pipette followed by several wash cycles with water until no change in pH was observed (pH *ca.* 4). In the second cycle the polymer was stirred by shaking for 1 h.

Titration. Polymer (0.5 g) was suspended in 20 ml of a CO_2-free 0.1 *M* NaCl solution by magnetic stirring. Titrations were performed under nitrogen atmosphere by addition of 25-μl increments of 0.5 *M* NaOH allowing *ca.* 30 min equilibration between additions. After titration of the polymers a blank solution (in absence of polymer) was titrated in presence and absence of an amount of acetic acid corresponding to the theoretical amount of carboxylic acid groups in the polymer. Following the above procedure another titration was done in acetonitrile–0.1 *M* NaCl (7:3, v/v). Standardization was again performed against the aqueous buffers [18,19]. During titration some mechanical breakdown of the polymer particles occurred due to the mechanical stirring. This caused the response time to decrease during the titration. Homogeneous titrations were carried out on L-PA and BA in the same solvent system. This resulted in apparent pK_a values of 6.4 and 8.6, respectively.

Calculations

The degree of ionization (α^*) was obtained from a combination of mass and charge balance equations as described by Dubin and Brant [18] in the reduced equation:

$$\alpha^* = [V + V_a - V_b]/V_{eq} \quad (1)$$

where V = volume added base titrant to achieve a certain pH, V_a and V_b = volume of added acid

and base titrant to the blank solution to achieve the same pH. V_{eq} = volume of added titrant at the equivalence point. V_{eq} in the aqueous and organic–aqueous systems were determined from the maximum in the plot of dpH/dV. Since a correct determination of the equivalence point may be critical for the resulting shape of the graph $V_{eq} \pm 0.1$ ml was also used in the α^* calculations. This did not change the general shape of the curve. The pK_a was then determined at each pH from the equation $pK_a = pH - \log[\alpha^*/(1-\alpha^*)]$ and the average pK_a (p$\overline{K_a}$) from the y-intercept of a plot of pH *versus* $\log[\alpha^*/(1-\alpha^*)]$ according to the equation $\log[\alpha^*/(1-\alpha^*)] = pH - pK_a$.

RESULTS AND DISCUSSION

Mobile phase effects

One of the drawbacks to the routine use of imprinted polymers in chromatography has been the extensive peak broadening and asymmetry. Although clear improvements were seen by either increasing the column temperature (up to 90°C) [6] or by using polymers prepared at lower temperature [20], the column efficiency was still poor compared to that of commercially available chiral stationary phases. A mobile phase containing acetic acid as additive was routinely used. In view of the unusual isotherms, broad peaks and peak splitting associated with this mobile phase, we suspected that the poor performance was mobile phase related. Other mobile phases were therefore tried (see Table I).

By increasing the aqueous content of the mobile phase retention decreases, possibly due to the extensive solvation of ammonium ions by water [21]. In the absence of acetic acid a remarkably large retention is seen. The retention volume seems to be strongly dependent on the acetic acid concentration since by adding 1% acetic acid a low k' is again observed. This suggests that both retention and selectivity can be modulated by controlling the mobile phase pH. Thus, by using the same organic-aqueous volume ratio but adding potassium phosphate buffer salts, a clear dependence of k' and α on pH was seen with strong retention and high selectivity at low pH and weak retention and low selectivity at high pH. With interest we noted that these changes improved chromatographic performance. This can be seen in the almost *50% reduction in the reduced plate heights (h) of the retained solutes in the buffered system compared to those observed using the original acetic*

TABLE I

STEPWISE MOBILE PHASE OPTIMIZATION IN THE CHROMATOGRAPHIC ENANTIOMER SEPARATION OF D,L-PA ON POLYMER P-L-PA

At a flow-rate of 1 ml/min 10 μmol of D,L-PA in 10 μl was injected. MeCN = Acetonitrile; HOAc = acetic acid; KP = potassium phosphate. ND = Not determined; VB = very broad; NR = no enantiomeric resolution. h_D, h_L and h_0 are the reduced plate heights for the D and L enantiomers of PA and for a weakly retained compound (acetone), respectively.

Mobile phase	k'_L	α	h_D	h_L	h_0	R_s
MeCN–H_2O–HOAc (92.5:2.5:5, v/v/v)	14	5.4	118	397	6	1.1
MeCN–5% HOAc (7:3, v/v)	0.8	3.2	ND	ND	ND	<1
MeCN–H_2O (7:3, v/v)	64	13	167	VB	ND	ND
MeCN–1% HOAc (7:3, v/v)	3.6	4.1	53	244	ND	1.3
MeCN–0.05 *M* KP, pH 3.5 (7:3, v/v)	9.3	5.4	75	167	6	2.0
MeCN–0.05 *M* KP, pH 9 (7:3, v/v)	0.4	NR	11		ND	NR
MeCN–0.05 *M* KP, pH 3 (3:7, v/v)	10	2.8	70	1060	42	1.0
MeCN–0.05 *M* KP, pH 9 (3:7, v/v)	87	2.1	50	VB		53

acid containing system. In addition, there was a parallel increase in resolution (R_s) for a constant separation factor (α) (see elution profiles in Fig. 2). The column efficiency on the other hand does not change with the mobile phase as seen from the reduced plate height (h_0) for a weakly retained compound such as acetone. This suggests that the use of organic–acetic acid mobile phases results in slow mobile phase equilibria. When further increasing the aqueous content using the buffered mobile phases, k' increases while α decreases. The pH interval for separation is now extended to higher pH while the column efficiency, reflected in the reduced plate height (h_0), is considerably poorer (see Fig. 2). Since both k' and α appeared to respond to pH changes, information about the protonation state of the polymer and the solute in organic aqueous solvent systems is of primary interest. Potentiometric titrations were therefore carried out.

Potentiometric titration of the acid groups of the polymers

Potentiometric pH titrations on linear polymers containing carboxylic acid groups has provided information about conformational changes as well as estimates of the related energy barriers and electrostatic free energies [18,19]. Titrations of highly cross-linked carboxylic acid containing polymers (*i.e.* weak cation exchangers) are mostly used in order to determine ion-exchange capacity buffering range and the average pK_a of the polymer [14–16]. Fig. 3 shows pH-titration profiles in aqueous and organic–aqueous systems of imprinted and blank polymers. The ionic strength was kept constant by addition of 0.1 *M* NaCl. Obviously most of the carboxylic acid groups originally added as monomers have been titrated, indicating that they are accessible. A lower accessibility, 60–70%, is seen in the titration in the aqueous system compared to the aqueous–organic system, 75–85%. This may be related to the lower swelling observed in water [9] leading to a more compact structure and a lower accessibility. The accuracy of the titrations was checked by titrating an amount of acetic acid corresponding to one equivalent of carboxylic

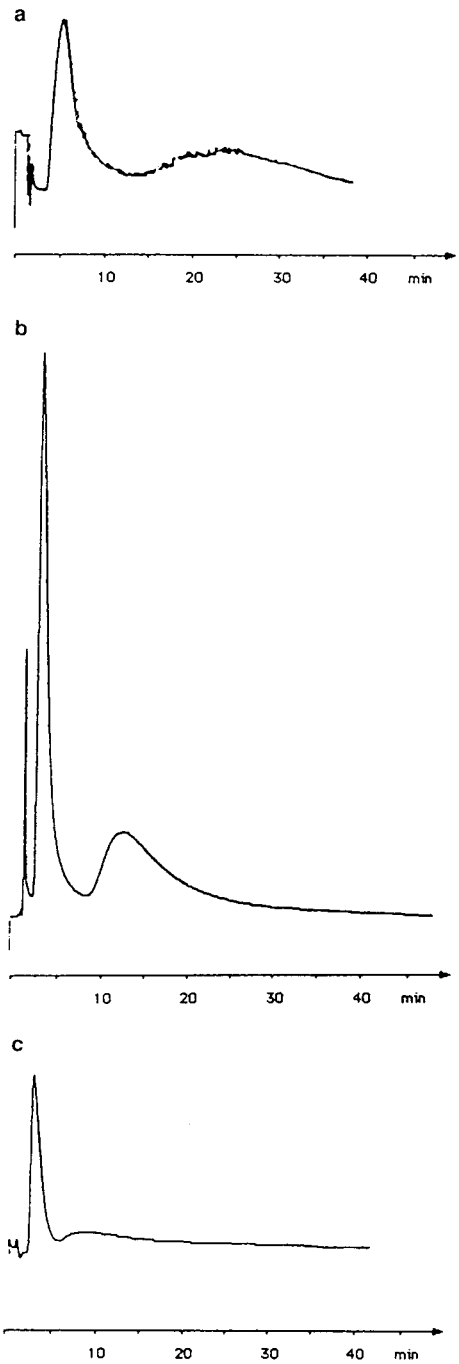

Fig. 2. Elution profiles from the experiment described in Table I using as mobile phase (a) MeCN–H_2O–HOAc (92.5:2.5:5, v/v/v), (b) MeCN–0.05 *M* potassium phosphate, pH 3.5 (7:3, v/v) and (c) MeCN–0.05 *M* potassium phosphate, pH 3 (3:7, v/v).

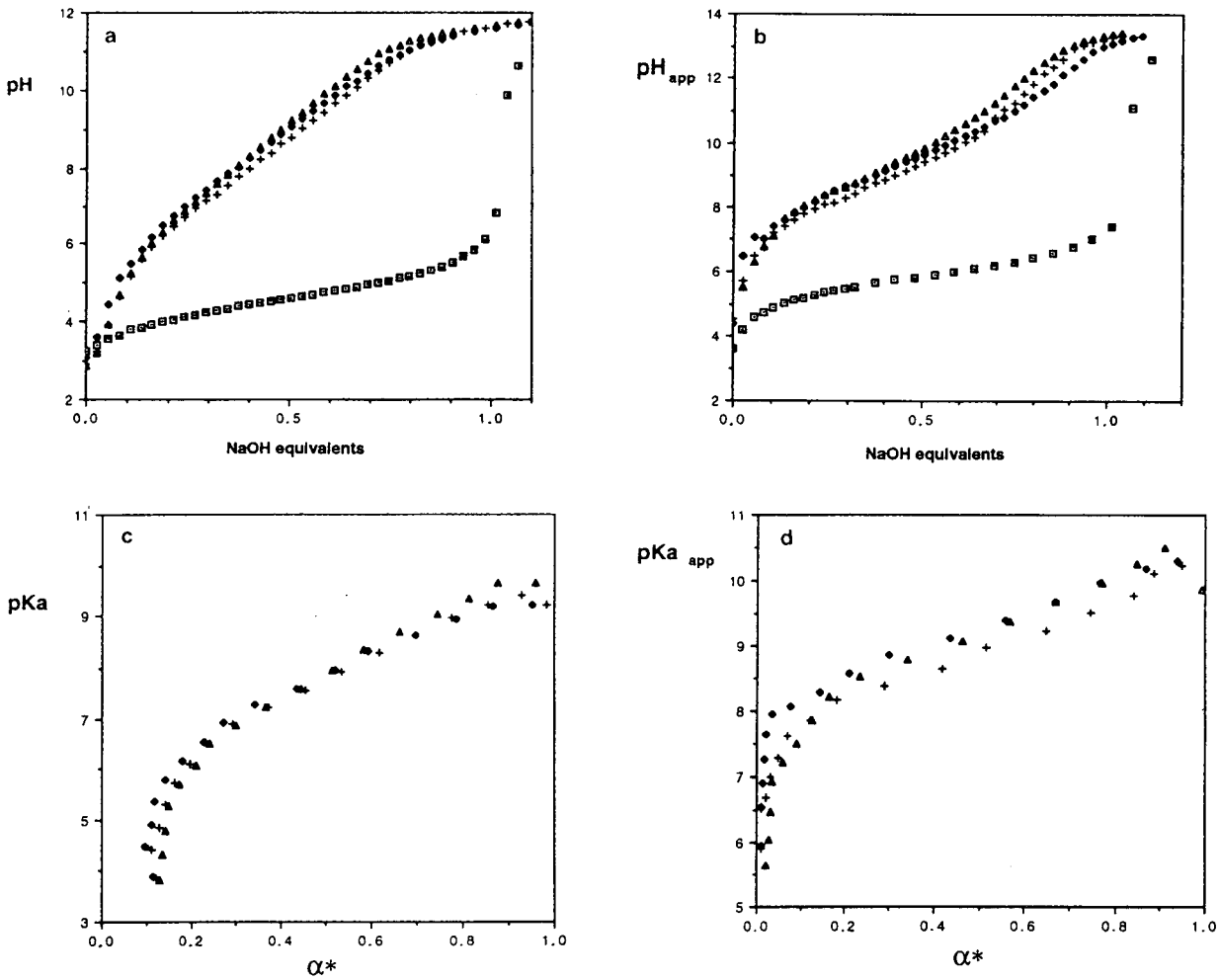

Fig. 3. Potentiometric titration curves on P-L-PA (+), PBA (▲), PBL (◆) and acetic acid (□) in (a) 0.1 *M* NaCl and (b) MeCN–0.1 *M* NaCl (7:3, v/v). The NaOH equivalents (*x*-axis) are calculated based on the theoretical amount of carboxylic acid groups present in the polymer. In (c) and (d) are seen the calculated pK_a distribution as a function of the degree of ionization (α^*). (c) $\overline{pK_a} = 8.0$ (P-L-PA), 8.1 (PBA), 8.2 (PBL); (d) $\overline{pK_a} = 8.9$ (P-L-PA), 9.2 (PBA), 9.3 (PBL). The polymer swelling [9] (ml/ml) in this solvent system was constant in the pH interval 3–12 and was for P-L-PA: 1.32 and for PBL: 1.26.

acid groups in the polymer. The polymers have a buffer capacity over a wide pH range and in the organic–aqueous system this range is found at a higher pH than in the aqueous system. The physical meaning of this difference is not clear since the method used to standardize the pH meter gives only apparent pH values.

In the titration of polyelectrolytes, neighboring group effects are a significant influence on the pH-titration profile [22]. For instance, in polyacrylic acid the ionization of the most acidic group may be facilitated by hydrogen bonding to a neighboring carboxylic acid group. However at higher levels of ionization the net increase in negative charge of the polymer will make it more difficult to ionize the remaining carboxylic acid group. It has been shown that the apparent pK_a increases with the degree of ionization (α^*) may be represented by:

$$pK_a = pH - \log[\alpha^*/(1 - \alpha^*)] \quad (2)$$

A plot of pK_a as a function of α^* can therefore

be regarded as a measure of the ease of proton removal from the polyion at a given degree of ionization. The average apparent pK_a was higher in the organic aqueous system but this may be due to the standardization procedure discussed above. However the differences exhibited by the polymers in the shape of the pK_a *versus* α^* plot is more interesting. Similar titrations of weak cation exchangers commonly exhibits buffering capacity at a lower pH [14,15]. The difference may reflect the influence of different charge densities. The more weakly cross-linked cation exchange resins exhibits higher swelling and can thus expand and reduce the buildup of electrostatic repulsion, leading to a titration curve that approaches that of the free acid. Swelling as a function of pH was measured in the organic aqueous system. *As seen in the legend to Fig. 3 the L-PA imprinted polymer P-L-PA showed significantly larger swelling than the corresponding blank non-imprinted polymer PBL. However no change in swelling was observed when the pH was varied.* In the organic–aqueous system the difference between the titration curves of PBL and P-L-PA can therefore be explained by their different swelling. Contribution from the structural organization of the carboxylic acid groups in the polymer is also possible (which *per se* may be the reason for the difference in swelling). In PBL the absence of template during polymerization will leave the carboxylic acid groups to interact mainly with themselves forming acid dimers. However in the presence of template, the acid groups will interact also with the template molecule. After freeing the polymers from template the acid groups in PBL will still have other acid groups to interact with while in P-L-PA the acid groups have lost their hydrogen bond partner and are thus in a more isolated environment. Such an arrangement would result in a lower pK_a for the more isolated acid groups compared to the pK_a of the associated groups. *Indeed the pK_a of P-L-PA is lower than that of PBL.* It should be noted however that the polymers exhibited very similar Fourier transform IR spectra [9], indicating that no large detectable difference exists in the extent of hydrogen bonding between the carboxylic acid groups of the polymers. However as discussed below the chromatographic data support the above explanation for the observed pK_a difference between the polymers.

Mobile phase pH dependence

Using polymer P-L-PA and PBA as stationary phases 10 and 100 nmol amounts of D,L-PA and BA were injected at different mobile phase apparent pH values (pH_{app}) ranging from 3.5 to 10 (measured on the total mobile phase) at 0.5 pH unit intervals. In Fig. 4a and b the resulting pH–retention graphs are shown. For reasons of comparison the given pH is that of the net mobile phase mixture (measured and standardized as described for the potentiometric titrations in the Experimental section) and not that of the aqueous buffer. The reproducibility was confirmed by repeating the experiment at intervals of one pH unit. Moreover similar pH dependence was observed using other L-selective polymers. It should be noted that due to the weak retention at low and high pH values the α determination is highly dependent on an accurate determination of the void retention time. When increasing the aqueous content in the mobile phase the solvent peak (MeCN) eluted at a 20% shorter time while acetone, used as a void marker in the organic–acetic acid mobile phases, still eluted at the original void retention time. However sodium nitrate, a commonly used void marker in aqueous systems [23], coeluted with the solvent peak and was therefore used as void marker in this system. The possibility of a Donnan exclusion effect at high pH did not result in any significant change in the retention time. When further increasing the aqueous content (see Table I) a lower t_0 was observed. These effects may be related to the lower swelling observed in the aqueous solvents [9].

As seen in Fig. 4a and b maxima in retention occur at pH values corresponding to the apparent pK_a values of the solutes, measured potentiometrically in the same solvent system (Note that the salt concentration of the aqueous portion in the titrations was 0.1 *M* while in the LC experiments the buffer concentration was constant at 0.05 *M*. For solubility reasons no extra salt was added here. Although titration curves can be strongly dependent on ionic strength it is

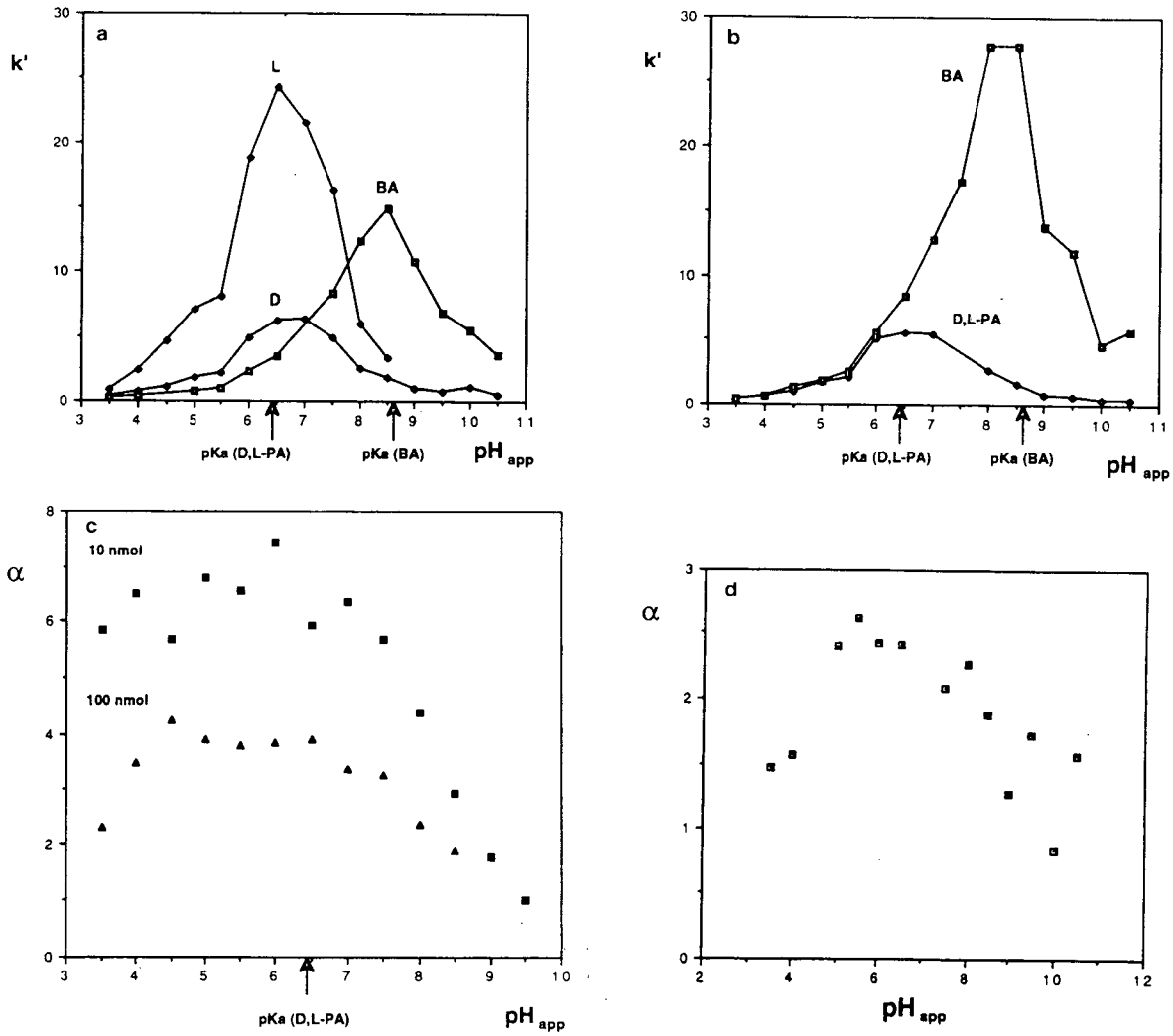

Fig. 4. Retention (k') of D- and L-PA and BA on (a) P-L-PA and (b) PBA injecting 100 nmol solute *versus* mobile phase pH_{app}. (c) and (d) show the corresponding separation factors (α) obtained at two different sample loads. The separation factor of D,L-PA (c) was calculated as $\alpha = k'_L/k'_D$ and of benzylamine (100 nmol) (d) as $\alpha = k'_{BA}$ (on PBA)$/k'_{BA}$ (on P-L-PA).

unlikely that this difference will have a major influence on the position and relative height of the maxima in Fig. 4). Moreover Fig. 4c and d shows that each polymer binds preferentially the compound used as template. Thus the α *versus* pH plots of D,L-PA on P-L-PA show a stable high selectivity in the low pH region both at 10 and 100 nmol sample load. When pH_{app} exceeds pK_a of the solute, α drops off to approximately 1 at pH_{app} 9.5. The selectivity factor of BA on PBA was estimated as an α value calculated from the ratio of k' on PBA to k' on P-L-PA[a]. This graph also shows a trend of decreasing α with increasing pH although here the falloff is observed over a larger pH range. *The fact that maximum retention is observed at a pH_{app} corresponding to the apparent pK_a of the solute suggested to us that*

[a] In this treatment P-L-PA has been taken as a blank polymer to BA. The absence of selective interaction of P-L-PA with BA is seen in the weak retention at low pH where L-PA is strongly retained.

the retention was controlled by a simple ion-exchange process. Thus the amino group containing solute B (D,L-PA or BA) is bound to the polymer containing carboxylic acid groups (HA) forming ion-pairs BH^+A^-. The capacity factor can now be expressed as:

$$k'_B = \phi[B]_b/[B]_f = \phi[BH^+A^-]/([B] + [B^+]) \quad (3)$$

where b and f indicates bound and free solute respectively and ϕ = phase volume ratio. Since potassium ions (K^+) are the counterions in the buffered system the following equilibria should be considered [24].

$$HA + K^+ \overset{K_a^A}{\rightleftharpoons} A^-K^+ + H^+$$

(acid dissociation equilibria) (4)

$$BH^+ \overset{K_a^B}{\rightleftharpoons} B + H^+$$

(base dissociation equilibria) (5)

$$A^-K^+ + BH^+ \overset{K_e}{\rightleftharpoons} BH^+A^- + K^+$$

(ion-exchange equilibria) (6)

Eqn. 3 can now be rewritten as:

$$k'_B = \frac{\phi K_e[BH^+][A^-K^+]}{[K^+]([B] + [BH^+])}$$

$$= \phi(1/[K^+])K_e\alpha^*_B\alpha^*_A[A]_{tot} \quad (7)$$

where α^*_A and α^*_B are the degree of ionization of the acid (A) and the base (B) respectively, K_e = the ion-exchange equilibrium constant and $[A]_{tot}$ = the total concentration of A. Eqn. 7 can be even further simplified:

$$k'_B = K\alpha'_B\alpha^*_A \quad (8)$$

where K is a constant for a given column and ionic strength. In order to test this model α^*_A and α^*_B need to be determined as a function of pH_{app}. In Fig. 5 values for α^* for L-PA, BA and the polymer have been plotted *versus* pH_{app} and in Fig. 6 the product $\alpha^*_B\alpha^*_A$. *The agreement with the experimental chromatographic data, both in the pH region where the maxima are found and in the relative retention of the solutes at these maxima is striking*. Similar behavior is often observed for weak bases on weak cation exchangers

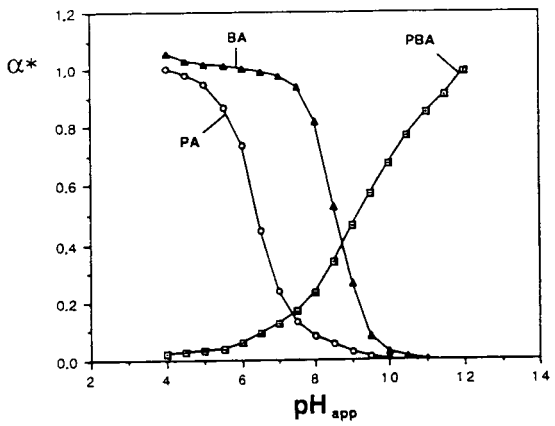

Fig. 5. Degree of ionization (α^*) as a function of mobile phase pH_{app} for the solutes BA and D,L-PA and for PBA. α^* was calculated from the corresponding potentiometric titration data as described in the experimental section.

[24]. It can therefore be concluded that cation exchange is the process controlling retention in this system. What about the selectivity? According to the retention model (eqn. 8) α can be expressed as:

$$\alpha = k'_L/k'_D = k_L\alpha^*_L\alpha^*_A/K_D\alpha^*_D\alpha^*_A = K_L/K_D \quad (9)$$

where K_L and K_D are the average ion-exchange equilibrium constants to the imprinted sites for the L and the D form respectively. Eqn. 9 follows from the fact that the degree of ionization of the D and the L form are the same at a given pH. In

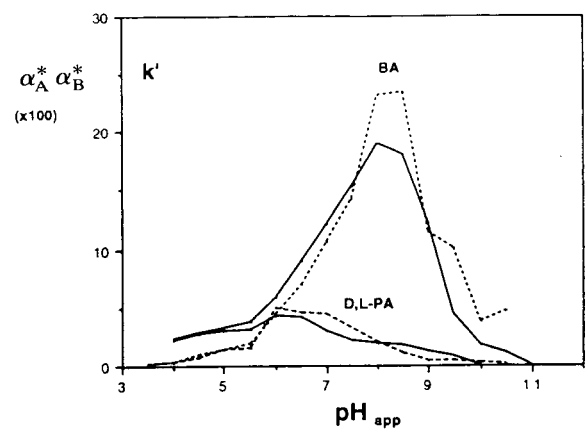

Fig. 6. Product of the degree of ionization of the solute (α^*_B) and the polymer PBA (α^*_A) (×100) *versus* mobile phase pH_{app} (solid line). Overlayed are the experimental data from Fig. 4b (dashed line).

other words, α does not change with the protonation state of either the polymer or the solute as long as these changes affect K_L and K_D to the same degree [25]. This would be the case if the binding involved just one electrostatic interaction. We propose that the decrease in enantioselectivity upon an increase in mobile phase pH is due to either: (a) deprotonation of a second group in the site, leading to a loss of an enantioselective hydrogen bond interaction, or (b) deprotonation of additional non-selective sites. If K_{ns} in case (b) represents the average ion-exchange equilibrium constant to the non-selective sites (ns) α can here be expressed as:

$$\alpha = \frac{K_L \alpha_L^* \alpha_s^* + K_{ns} \alpha_L^* \alpha_{ns}^*}{K_D \alpha_D^* \alpha_s^* + K_{ns} \alpha_D^* \alpha_{ns}^*} \quad (10)$$

Since the second term in both the numerator and the denominator are identical an increase in α_{ns}^* will obviously lead to a decrease in α. An argument for this explanation is the sharp increase in non-specific binding above pH_{app} 6. This is clearly seen in the plot of k' *versus* pH_{app} for BA on P-L-PA (Fig. 4) and in the parallel increase in α^* for the latter (Fig. 5). This can also be seen from the plot of the estimated separation factor of benzylamine (α_{BA}) *versus* pH_{app} (Fig. 4d) where α is highest at low pH values [below pK_a(BA)] and decreases over a large pH interval. Furthermore the potentiometric titrations showed that P-L-PA had a lower average pK_a than PBL (see Fig. 3). *This strongly suggests that the carboxylic acid groups of the selective sites have a lower average pK_a than those of the non-selective sites*. It could be argued that nonionic sorption could contribute to the observed retention. However such a process seems to be negligible in view of the parallel decrease in the degree of ionization and the retention of PA and BA. For instance k_L' decreases from 25 to less than 1 upon neutralization.

In Fig. 7 a model is presented, showing how the protonation states of D,L-PA and the polymer (P-L-PA) can account for the observed retention and selectivity. At pH_{app} 4 the solute D- and L-PA (two-dimensional representation) are protonated and bind differentially to enantioselective sites. At pH_{app} 5.5 the solute is partly deprotonated while a larger amount of selective sites are available. This will result in an increase in k' whereas α remains constant. At pH_{app} 6.5 (*ca.* pK_a for D,L-PA) half of the solute is protonated and non-selective sites are becoming deprotonated resulting in stronger non-selective interactions and a net increase in binding. At pH_{app} 8 the solute is only partly protonated while the negative charge of the polymer increases mainly

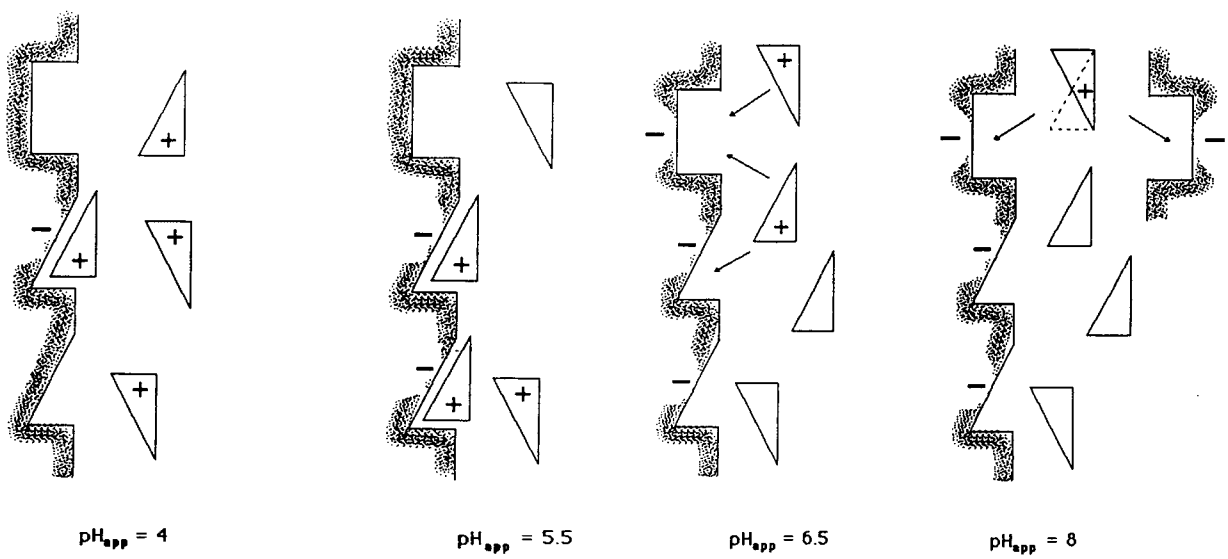

Fig. 7. Proposed model for the influence of pH on the retention volume.

as non-selective sites are deprotonated. Thus the chance of non-selective binding increases while retention as a whole decreases.

As noted in the first proposed explanation (a) for the change in enantioselectivity, an increase in pH may *per se* lead to a decrease in the enantioselectivity of the imprinted sites. Contribution from this effect cannot be estimated and thus it cannot be excluded. Therefore it is not possible at this stage to draw any conclusions about the origin of the enantioselectivity at a molecular level.

CONCLUSIONS

During mobile phase optimization using imprinted CSPs a buffered aqueous–organic mobile phase was found to give a clear improvement in column performance. Since both enantiomer retention and selectivity were sensitive to mobile phase pH a study of the protonation state of both solute and polymer in the same solvent system was carried out. A potentiometric titration of the polymers revealed a high accessibility of the carboxylic acid groups and a buffering capacity on the basic side with an average pK_a in water of around 8. A slightly lower pK_a was observed for the imprinted polymers compared to the blank polymers prepared in the absence of template. A molecular level explanation was given based on the difference in the state of hydrogen bonding in the imprinted and the blank polymer respectively. This explanation was supported by the high selectivity found at low pH and a close correlation observed between the chromatographic experimental data and a weak cation exchange model.

The combination of the weak cation-exchange properties and the predictable enantioselectivity of the phase may have interesting applications in the separation of basic drugs containing stereogenic centers. For instance pH control may be used to switch chiral separation on and off or to speed up separations using pH gradient elutions. Furthermore, advantage may be taken of the difference in pK_a between the selective and the non-selective sites for selective inhibition of non-specific binding sites. This may lead to an improved column performance. In this context it should be mentioned that heat-treated polymers run at elevated column temperatures (Fig. 8) have been found to give resolutions and reduced plate heights in the same order as those observed for some commercially available CSPs [9].

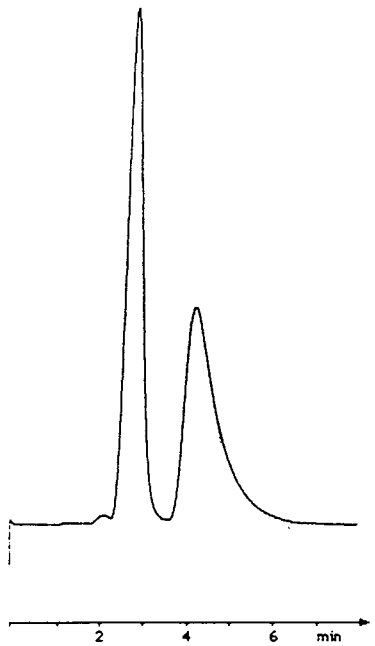

Fig. 8. Elution profile of D,L-PA (10 nmol) applied on a heat treated L-PA selective polymer. Mobile phase: MeCN–0.05 *M* KP, pH 4 (7:3, v/v). Flow-rate: 1 ml/min. Column temperature: 80°C. Reduced plate heights: $h_D = 9$, $h_L = 18$.

ACKNOWLEDGEMENTS

The authors wish to thank Professor David Brant (University of California, Irvine) for valuable discussions. The financial support of the National Science Foundation (Division of Materials Research), the National Institutes of Health, and the Swedish Natural Science Research Council (to B.S.) is also gratefully acknowledged.

REFERENCES

1 G. Wulff, in W.T. Ford (Editor), *Polymeric Reagents and Catalysts* (*ACS Symposium Series*, No. 308), American Chemical Society, Washington, DC, 1986, pp. 186–230.

2 G. Wulff, in M. Zief and L.J. Crane (Editors), *Chromatographic Chiral Separations*, Marcel Dekker, New York, 1988, pp. 15–49.
3 G. Wulff, H.-G. Poll and M. Minarik, *J. Liq. Chromatogr.*, 9 (1986) 385.
4 L. Andersson, B. Sellergren and K. Mosbach, *Tetrahedron Lett.*, 25 (1984) 5211–5214.
5 B. Sellergren, B. Ekberg and K. Mosbach, *J. Chromatogr.*, 347 (1985) 1–10.
6 B. Sellergren, M. Lepistö and K. Mosbach, *J. Am. Chem. Soc.*, 110 (1988) 5853.
7 B. Sellergren, *Chirality*, 1 (1989) 63.
8 M. Lepistö and B. Sellergren, *J. Org. Chem.*, 54 (1989) 6010.
9 B. Sellergren and K.J. Shea, *J. Chromatogr.*, 635 (1993) 31–49.
10 K.J. Shea, D.A. Spivak and B. Sellergren, *J. Am. Chem. Soc.*, 115 (1993) 3368.
11 G. Vlatakis, L.I. Andersson, R. Muller and K. Mosbach, *Nature*, 361 (1993) 645.
12 B. Sellergren, in G. Subramanian (Editor), *Chiral Separations by Liquid Chromatography*, VCH, Weinheim, in press.
13 M. Zief and L.J. Crane (Editors), *Chromatographic Chiral Separations*, Marcel Dekker, New York, 1988.
14 F. Helfferich, *Ion Exchange*, McGraw-Hill, New York, 1962.
15 D.J. Pietrzyk, in K.K. Unger (Editor), *Packings and Stationary Phases in Chromatographic Techniques*, Marcel Dekker, New York, 1990, p. 585.
16 O. Mikeš, P. Štrop, M. Smrž and J. Čoupek, *J. Chromatogr.*, 192 (1980) 159.
17 G.S. Weber and P.W. Carr, in P.R. Brown and R.A. Hartwick (Editors), *High Performance Liquid Chromatography*, Wiley, New York, 1989.
18 P.L. Dubin and D.A. Brant, *Macromolecules*, 8 (1975) 831.
19 E.P. Serjeant, *Potentiometry and Potentiometric Titrations*, Wiley, New York, 1984.
20 D.J. O'Shannessy, B. Ekberg and K. Mosbach, *Anal. Biochem.*, 177 (1989) 144.
21 M. Meot-Ner, in J.F. Liebman and A. Greenberg (Editors), *Molecular Structure and Energetics*, Vol. 4, VCH, Weinheim, 1987.
22 P. Molyneux, *Water-Soluble Synthetic Polymers: Properties and Behaviour*, Vol. II, CRC Press, 1984.
23 C.F. Simpson (Editor), *Techniques in Liquid Chromatography*, Wiley–Heyden, Chichester, 1982.
24 P.J. Schoenmakers, *Optimization of Chromatographic Selectivity*, Elsevier, Amsterdam, 1986.
25 W.H. Pirkle and C.J.J. Welch, *J. Chromatogr.*, 589 (1992) 45–51.

Journal of Chromatography A, 654 (1993) 29–41
Elsevier Science Publishers B.V., Amsterdam

CHROM. 25 472

Characterization and application of strong ion-exchange membrane adsorbers as stationary phases in high-performance liquid chromatography of proteins

Oscar-W. Reif and Ruth Freitag*

Institut für Technische Chemie (Prof. K. Schügerl), Universität Hannover, Callinstrasse 3, 30167 Hannover (Germany)

(First received April 29th, 1993; revised manuscript received July 23rd, 1993)

ABSTRACT

Filtration membranes carrying strong cation- or anion-exchange groups on their surface were evaluated for their potential as membrane adsorber stationary phases in the high-performance liquid chromatography of proteins. The membranes are commercially available and can be obtained inserted into ready-to-use filter holders. Owing to their thinness (170–190 μm), the pressure drop of the membranes is extremely low. Flow-rates of up to 65 ml min^{-1} per unit became thus possible. The low pressure drop of a single membrane layer also permitted an effortless scaling up, as a stack of several membranes or filter units could be used, if necessary. Sample distribution, protein binding capacity, elution conditions, separation efficiency and recovery were investigated as a function of the flow-rate. The time required for the separation of certain protein mixtures could be reduced to less than 1 min. Appropriate conditions were defined for the separation of human serum and for the isolation of subtilisin Carlsberg and β-galactosidase from cell culture supernatants.

INTRODUCTION

In recent years, two types of stationary phase design have been introduced for the chromatographic separation of biopolymers, which offer advantages over the columns packed with porous particles generally used for that purpose. One design is based on the well known hollow-fibre filtration modules, but employs hollow fibres with selectively interactive surfaces. The other is based on compact, several millimetre thick, porous polymer or silica discs [1–4]. Another design consists of layers of porous polymer membranes incorporating sub-micron silica particles [5,6]. A laboratory-made module containing a stack of thin nylon membranes separated by gaskets has also been introduced [7]. In addition, thin membranes have been used in affinity-based separations, *i.e.*, for the selective removal of a specific component following the all-or-nothing principle. All of these systems are grouped together under the generic term membrane adsorbers (MA). In MA phases, the mass transport of biomolecules to the adsorptive surface occurs largely by convection and is hardly diffusion limited [8,9]. Faster adsorption kinetics can therefore be attained [10]. Furthermore, efficient HPLC columns cause high back-pressures and the maximum flow-rate applicable is therefore limited to *ca.* 5 ml min^{-1} [11]. Membrane adsorbers, on the other hand, cause less back-pressure and therefore higher operating flow-rates can be employed [12,13]. According to the pertinent literature, however, even in MA-based chromatographic systems flow-rates of only 10 ml min^{-1} per unit at the most are used.

Although a number of weak ion-exchanger MAs have been used in protein chromatography,

* Corresponding author.

0021-9673/93/$06.00

affinity MA chromatography clearly dominates the field at present. Plasma proteins [14], antibodies [15], recombinant interleukin [16,17] and TPA (tissue plasminogen activator) [18], for example, have been separated on affinity MAs. γ-Globulins were isolated using an MA containing hydrophobic amino acids as ligands [19]. Protein A membranes were used for the efficient isolation of fibrinogen and immunoglobulin G (IgG) [20,21]. Cibacron Blue membranes were used in the separation of microbial enzymes [22,23]. Another protein separation scheme combined affinity or ion-exchange chromatography with size-dependent cross-flow filtration in a hollow-fibre module, separating various enzymes from crude protein mixtures such as crude horse serum [24]. Experiments showed that MA supports were comparable to established fast protein LC (FPLC) and HPLC columns in terms of separation power [22,25–28].

In this work, a new type of ion-exchange MA was characterized and employed for rapid and efficient protein separations; it offers several advantages from an application point of view over the systems described so far. The materials are functionalized with strong rather than weak ion-exchange groups. To the best of our knowledge, this is the first time that a strong anion-exchange MA has been used in high-performance membrane chromatography (HPMC). A single reference to a strong cation exchanger was found [29]; however, the purpose of that work was the optimization of a preparative cross-flow filtration MA. As many protein separations, *e.g.*, in biotechnology, involve complex sample mixtures, the character of which changes with process time, the limitation in the experimental variables found with strong ion exchangers will speed up the optimization of the chromatographic procedure considerably. Moreover, the MAs introduced here are extremely thin, in the micrometre rather than the millimetre range, and therefore significantly higher flow-rates can be used, which leads to faster separations. Single membrane sheets rather than stacks were appraised for standard protein separations. However, stacks of up to ten membranes can be used without surpassing the pressure limit of the system. Scale-up is therefore possible. Further, no laboratory-made device is necessary for the integration of the MA into the chromatographic system, as the MAs are already inserted into HPLC/FPLC-compatible filter holders.

EXPERIMENTAL

Chemicals

Human IgG (h-IgG), lysozyme, α-chymotrypsinogen, soybean trypsin inhibitor, human serum albumin (HSA), bovine serum albumin (BSA) and β-galactosidase were purchased from Sigma and bulk chemicals from Fluka or Merck. Human serum was kindly donated by the Red Cross (Blutbank Springe, Germany). Buffers and sample solutions were prepared with deionized water and prefiltered, using a 0.2-μm filter (Sartorius, Göttingen, Germany). Cell culture supernatants containing recombinant proteins were donated by various members of the biotechnology group at the Institut für Technische Chemie, Universität Hannover. All supernatants were stored at −4°C until used. β-Galactosidase was produced by an insect cell line (*Spodoptera fungiperda*) after infection by a genetically modified *Baculovirus* as described in ref. 30. The protease subtilisin Calsberg was produced extracellularly during cultivations of *Bacillus licheniformis* as described in ref. 31.

Protein analysis

The protein samples were analysed by sodium dodecyl sulphate polyacrylamide gel electrophoresis (SDS-PAGE) according to the method of Laemmli [32] with a laboratory-made electrophoresis apparatus. The determination of the protein concentration was carried out according to the procedures of Bradford [33] and Lowry *et al.* [34] or by immunodiffusion [35] using BSA and h-IgG as respective standard proteins. The activities of β-galactosidase and subtilisin Carlsberg were determined as described in refs. 36 and 31, respectively. The determination of proteins by free zone capillary electrophoresis (FZCE) was carried out on a Beckman P/ACE 2000 system, controlled by P/ACE system software. The fused-silica capillaries (CS-Service, Darmstadt, Germany) were pretreated with 1 *M* NaOH for 15 min and washed with deionized

water for 3 min. The analysis was performed in capillaries of 37 cm × 50 μm I.D. at a detection wavelength of 200 nm (0.05 a.u.f.s.). Electrophoresis was carried out at 15 kV with an electrophoresis buffer of 40 m*M* tris–borate (pH 10.5). The samples were injected by pressure (5 s) without further pretreatment.

Instrumentation

The FPLC system (Pharmacia, Uppsala, Sweden) consisted of two P 500 pumps, a Model 2141 UV detector, a Superrac fraction collector and an MV7 injection valve, all controlled by an LCC 500 controller. The data were analysed by the FPLC software on a PS/2 computer. The HPLC system consisted of a preparative pump (Model 64, Knauer, Berlin, Germany), an injection valve (Valco, Houston, TX, USA), and a UV detector (Model 7215, Erma, Tokyo, Japan). The ternary gradient was controlled by an Autochrom (Milford, MA, USA) System 300 and an Autochrom valve box. A CIM box (ERC, Alteglofsheim, Germany) was used for data collection. Data analysis was carried out on a PC using APEX software (ERC). The FPLC system was used for the application studies and all other studies were performed on the HPLC system. Depending on the system used, data were obtained as absorbance units full-scale (a.u.f.s; FPLC system) or in mV (HPLC system).

Strong ion-exchange membrane adsorber

Experiments were performed with quaternary ammonium anion-exchange membrane adsorbers (Sartobind Q, SM 17871 B; Sartorius) and with sulphonic acid cation-exchange membrane adsorbers (Sartobind S, SM 17873 B; Sartorius). Both types of MA were made of a synthetic copolymer with a thickness of 170–190 μm and an average pore size of 0.45 μm. In one option the MAs were obtained in ready-to-use filter holders made of Cyrolite containing one membrane layer with an effective filtration area of 5.4 cm^2. This unit had a given operating pressure maximum of 400–600 kPa. In another option, an SM 16517 reusable syringe prefilter holder (Sartorius) was used to integrate the MA into the chromatographic system. These filter holders were made of polycarbonate. The effective filtration area was 3.5 cm^2 per membrane layer and the maximum operating pressure given by the manufacturer was 700 kPa. This option offered the additional advantage that several membrane layers could be put simultaneously into one holder. Both filter holders were coupled to the FPLC/HPLC tubing by a female Luer lock at the inlet and a male Luer slip (both from Upchurch Scientific, Oak Harbor WA, USA) at the outlet. All membranes including the ready-to-use units were kindly donated by Sartorius.

New MAs were stored under dry conditions at room temperature. Between use the MAs were kept in the appropriate equilibration buffer containing 0.002% chlorhexidine and 0.5% chloroacetone added as bacteriostatic agents for anion-exchange and cation-exchange MAs, respectively. When blocking or a significant decrease in capacity was observed, regeneration by washing with 1 *M* NaOH and 1 *M* HCl or by rinsing with 0.5 *M* NaOH for 30 min at 50°C was carried out.

Methods

For the investigation of the irreversible binding of ions to the cation- and anion-exchange MAs, radiolabelled $^{45}Ca^{2+}$ ions (Calcium chloride; Sigma) and $^{125}I^-$ ions (sodium iodide; Sigma) were loaded on to the MAs until saturation. The MAs were repeatedly washed with a buffer solution that contained no radiolabelled ions and dissolved in scintillation cocktail (Sigma). The radioisotopes that were retained by the MA were measured in a scintillation counter (Beckman Scinter; Beckman, Fullerton, CA, USA). The flow distribution of the sample on the surface of the MAs was examined by loading the membranes with ferritin (Sigma) dissolved in the appropriate buffer. The distribution and homogeneity of loading on the membrane as a function of the flow-rate and the sample concentration could be determined visually as ferritin is coloured. To determine the dependence of the binding capacity on the flow-rate, HSA (0.5 mg ml^{-1}) was loaded on to the MA at the given flow-rate until saturation, *i.e.*, until the protein concentration in the effluent was constant again. After washing, the retained protein was eluted and determined. The adsorption and elution conditions for proteins on the MAs were adapted

from established procedures [37,38]. All chromatographic experiments were repeated three times.

RESULTS AND DISCUSSION

The MA used in the experiments should, according to the manufacturer's information, fulfil the major prerequisites for a chromatographic stationary phase for protein separation, *e.g.*, hydrophilicity, little unspecific protein adsorption, high chemical and physical resistance and narrow pore-size distribution. Their actual usefulness for the purpose was demonstrated in the following experiments.

Characterization of strong ion-exchange membrane adsorbers

An important advantage of MAs over conventional LC columns is their more efficient mass transfer characteristics [8–10]. The resulting faster adsorption kinetics putatively allow the use of much higher flow-rates and shorter contact times without impeding the separation efficiency. However, at present only flow-rates of up to 10 ml min^{-1} have been used in HPMC. Owing to the low back-pressure and good mechanical stability of the MAs introduced here, much higher flow-rates became possible. A close investigation of the effect of flow-rate on the sample distribution, the protein binding capacity, the elution conditions, the peak shape and the separation efficiency was therefore carried out.

The flow distribution over the MA depending on the flow-rate constitutes a major problem, because a liquid emerging at comparatively high speed from the narrow-inlet tubing has to be distributed over the entire membrane sheet. The ready-to-use filter holders employed in this work were constructed in such a way that the liquids were pumped through thin porous distribution channels over the membrane. In our experience, operating pressures of up to 100 kPa could be used with this construction. According to results achieved after loading with Ferritin, the sample distribution is optimum for flow-rates of up to 5 ml min^{-1} per unit. At higher flow-rates there is a distinct breakthrough in the centre of the membrane, while little or no adsorption takes place at the outer regions of the MA.

The protein binding capacities of the MAs were investigated using human serum albumin (HSA). The binding and elution conditions for this protein with respect to pH, type and salt concentration of the buffer were adapted from those published for similar HPLC and FPLC methods [37,38]. As shown in Fig. 1, the protein binding capacity of a given MA decreases non-linearly with increasing flow-rate. The capacity decreases steadily by about 10% when the flow-rate is increased from 0.2 to 10 ml min^{-1} per unit. Only insignificant changes in the capacity are observed for flow-rates between 10 and 35 ml min^{-1} per unit. If the flow-rate is increased further, an adverse effect on the flow-rate is found again. However, even at a flow-rate of 65 ml min^{-1} per unit, the capacity is 80% of that determined for the lowest flow-rates possible with our system, *i.e.*, 0.2 ml min^{-1} per unit. As the above experiments suggest that only the centre area of the MA is active at higher flow-rates, a decrease in total binding capacity with increasing flow-rate was to be expected. The problem of decreasing capacity can be overcome by using several membranes in one filter holder or by using several ready-to-use filter holders in a row. At all flow-rates investigated, the capacity increased linearly with increasing number of ready-to-use filter holders employed. The pressure resistance also increased, but kept well below the maximum operating pressure if not more than ten units were used.

Even at low flow-rates the MAs showed a decrease in the protein binding capacity of *ca.* 6% after the first run. After the second run, no further decline in binding capacity could be observed over several hundred cycles. The protein recovery was better than 90% in these experiments. Experiments with radiolabelled ions were carried out to elucidate the phenomenon. It was found that a certain amount of these ions could not be removed even with repeated washing and equilibration procedures if the ion containing sample was loaded on to a fresh membrane. These results suggest that during the first run sample components may be trapped in dead end zone of the membranes,

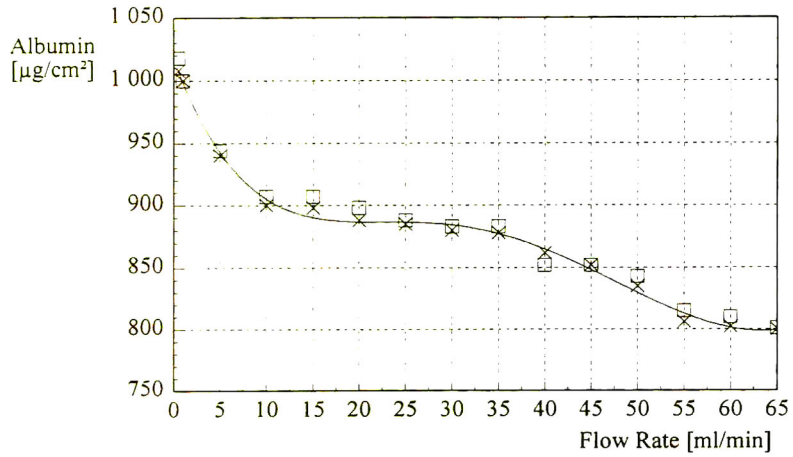

Fig. 1. Protein binding capacity as a function of flow-rate. The MA was loaded with HSA until saturation. After washing, the bound protein was eluted. Protein concentration, 0.5 mg/ml in loading buffer; buffer for anion-exchange MA, 10 m*M* Tris–HCl (pH 9.0) (loading, washing), 10 m*M* Tris–HCl + 1 *M* KCl (pH 9.0) (elution); buffer for cation-exchange MA, 10 m*M* sodium acetate/citric acid (pH 4.0) (loading, washing), 10 m*M* sodium acetate/citric acid + 1 *M* KCl (pH 4.0) (elution). × = Anion exchanger; □ = cation exchanger; solid line = regression.

thus blocking adsorption sites and concomitantly decreasing the binding capacity. Nevertheless, the decline is slow and can usually be ignored in further experiments or day-to-day laboratory routine.

The flow-rate does not influence the peak shape, as shown in Fig. 2. Even at a flow-rate of 20 ml min^{-1} per unit the elution profile is identical with that found at 1 ml min^{-1} per unit. More than 90% of the bound protein is eluted in the first 1.5 ml, while the remaining protein appears in the following 2.5 ml. The pronounced tailing of the signals could be due to, *e.g.*, overloading, problems caused by poor flow dis-

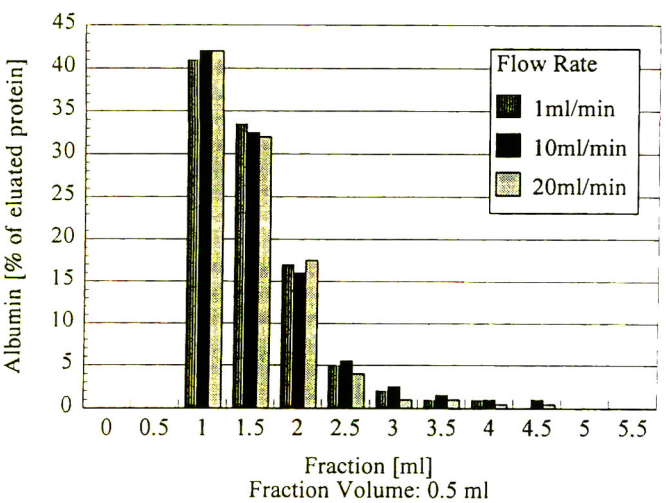

Fig. 2. Influence of flow-rate on peak shape. An anion-exchange MA was loaded with HSA until saturation. After washing, the protein was eluted and 0.5-ml fractions were collected. Buffers, 10 m*M* Tris–HCl (pH 9.0) (loading, washing), 10 m*M* Tris–HCl + 1 *M* KCl (pH 9.0) (elution); total amount of eluted protein at 1 ml min^{-1} per unit, 5.35 mg, at 10 ml min^{-1} per unit, 5.2 mg, at 20 ml min^{-1} per unit, 5.28 mg.

tribution within the MA or pronounced extra-"column" band broadening. For the ready-to-use MA units employed here, the latter seems to apply, with the large dead volume at the Luer slip outlet acting as a continuous mixer. As the MA filter holder was originally intended for application as a syringe prefilter for sterile filtration, no attention was paid to the consequences of the outlet design for chromatographic purposes. To improve the performance, the outlet design was modified by decreasing the outlet volume, concomitantly suppressing the dispersion. In Fig. 3, peak shapes obtained for three different types of outlet can be compared: the unmodified cartridge (Fig. 3a), a cartridge where the outlet volume was reduced by halving the Luer slip (Fig. 3b) and a cartridge where the outlet was removed totally and the tubing leading to the detector was fixed next to the membrane, thus nearly eliminating the dead volume (Fig. 3c). As expected, the peak shape was improved by decreasing the outlet volume. However, in order to investigate the commercially available units as a chromatographic tool, the following experiments were performed with the unmodified cartridges.

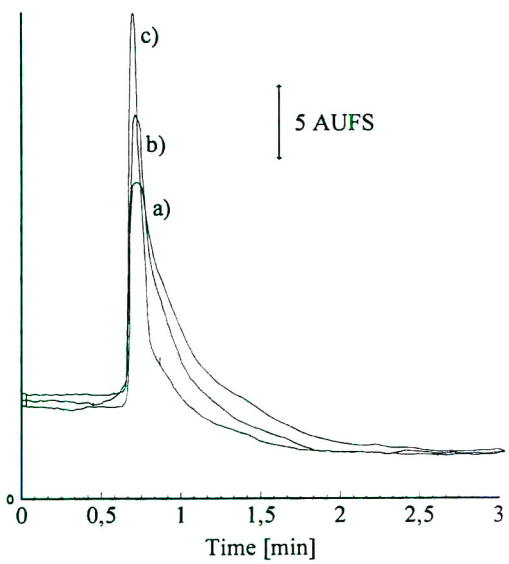

Fig. 3. Effect of modification of the prefilter membrane cartridge outlet on peak shape. The anion-exchange MA was loaded with HSA until saturation. After washing, the protein was eluted in a single step gradient (100% buffer B). Flow-rate, 2 ml min^{-1} per unit; buffers, 10 m*M* Tris–HCl (pH 9.0) (loading, washing), 10 m*M* Tris–HCl + 1 *M* KCl (pH 9.0) (elution). (a) Unmodified cartridge outlet; (b) outlet volume reduced by half; (c) minimized cartridge outlet volume.

Protein separations on strong ion-exchange membrane adsorbers

The results of experiments on the influence of flow-rate on the separation attainable with the investigated MAs are shown in Fig. 4. The separation of the three proteins (trypsin inhibitor, α-chymotrypsinogen and lysozyme) were achieved in less than 15 min at a flow-rate of 1 ml min^{-1} per unit using a pH step gradient (Fig. 4a). By increasing the flow-rate to 30 ml min^{-1} per unit, the proteins were separated within 1 min, without any apparent decrease in resolution (Fig. 4c). Flow-rates of more than 20 ml min^{-1} per unit, however, entail some difficulties. Whereas the MA itself poses only a negligible resistance to the flow, a certain amount of back-pressure is built up by the tubing and by the flow cell of the detector, where in fact often the main pressure drop of the system occurs. The danger of damaging the flow cell of an analytical detector is always present at high flow-rates. With regard to these technical problems, the maximum flow-rate was limited to 20 ml min^{-1} per unit in routine applications. By using preparative detector cells and tubing of a larger inner diameter, however, flow-rates of up to 65 ml min^{-1} per unit could be applied.

As mentioned before, the MA capacity decreases if the flow-rate is increased. The use of a stack of several membranes rather than a single membrane was suggested to relieve this problem. In Fig. 5, the influence on the peak shape of such an increase in the number of membranes inserted into the reusable filter holder is shown. The total amounts of trypsin inhibitor, α-chymotrypsinogen and lysozyme separated could be increased from 0.25 to 1.2 mg ml^{-1} of each if the number of membranes was increased from one to six. As the gradient was chosen such that the retention times of the proteins remained the same, the resolution was lower in the latter instance because the higher protein concentrations caused broader signals. However, the three protein peaks are still well resolved. Conse-

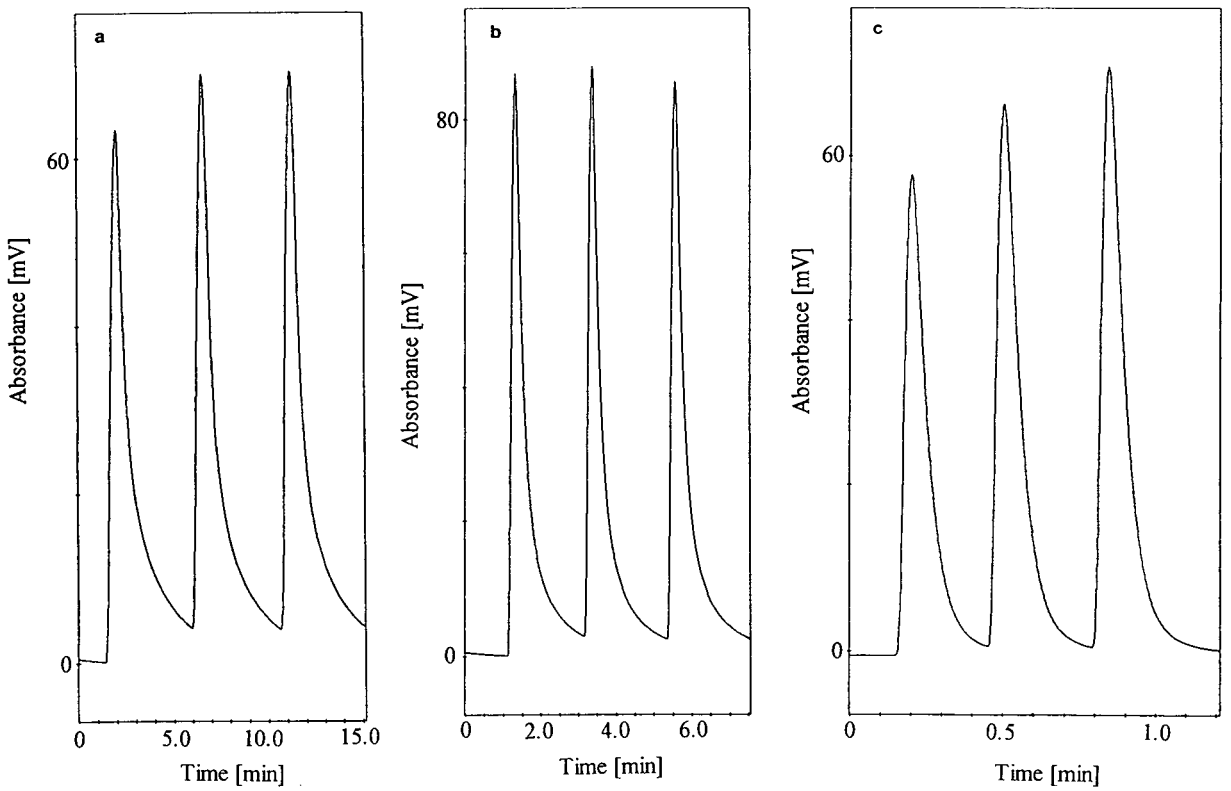

Fig. 4. Separation of three standard proteins (0.25 mg ml^{-1} each of trypsin inhibitor, α-chymotrypsinogen and lysozyme) as a function of flow-rate. The first peak contains lysozyme, followed by α-chymotrypsinogen and trypsin inhibitor. A stack of three anion-exchange MAs was used. Flow-rate: (a) 1; (b) 15; (c) 30 ml min^{-1} per unit. Detection wavelength, 280 nm; sample volume, 1 ml; buffer A, 10 m*M* sodium borate/NaOH (pH 10.2); buffer B, 10 m*M* sodium acetate/citric acid (pH 4.0); step gradient: 1st step, 0% buffer B; 2nd step, 20% buffer B (*ca.* pH 8.0); 3rd step, 100% buffer B.

quently, an easy scale-up can be achieved by simply using more membranes. Alternatively, stacks of ready-to-use filter holders can also be used (data not shown).

Many of the protein separations prevalent in the biosciences involve the removal of a minor component from the bulk protein. Such separations can also be achieved using the MAs, as shown in Fig. 6a. A mixture of h-IgG and lysozyme (both in low concentrations) was applied to a cation-exchange MA in the presence of an excess of BSA. The conditions were chosen such that BSA was not adsorbed on the MA, whereas the other proteins were retained. Both the h-IgG and the lysozyme were separated in a salt concentration step gradient and obtained free of any BSA. This was demonstrated by free zone capillary electrophoresis of the respective fractions (Fig. 6b and c). At the same time, no trace of either substance could be detected by the same method in the collected BSA fractions (Fig. 6d). The recovery after elution was better than 80%. This demonstrates the possibility of separating even very diluted proteins in the presence of an excess of another protein. The high flow-rates and short process times achievable in such separations constitute an important advantage of the MAs.

Applications

In an application study, biological samples such as human serum proteins and proteins from cell culture supernatants were separated on the MAs. Protein recovery and, if possible, the biological activity of the recovered proteins were

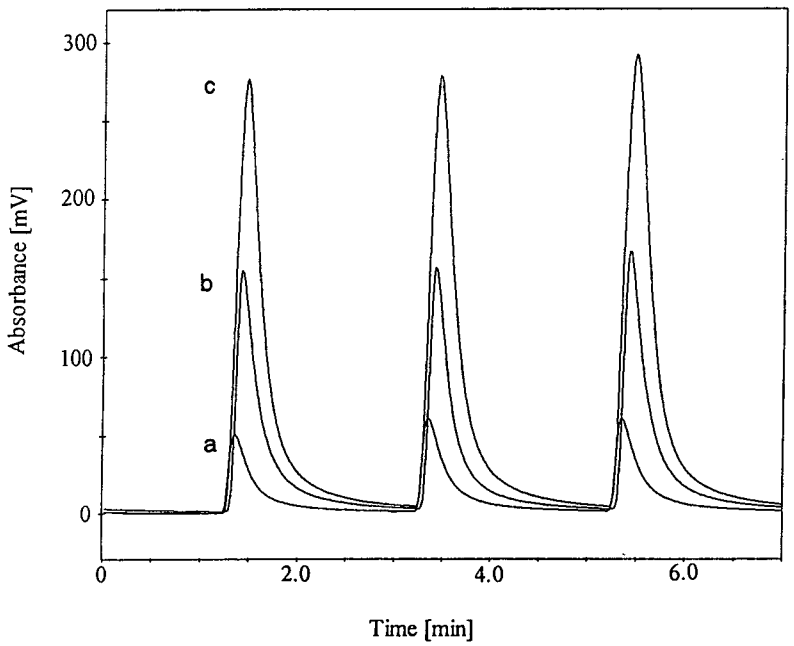

Fig. 5. Separation of standard proteins on anion-exchange MAs. The first peak contains lysozyme, followed by α-chymotrypsinogen and trypsin inhibitor. (a) One membrane; (b) three membranes; (c) six membranes. Detection wavelength, 280 nm; flow-rate 12 ml min^{-1} per unit; sample (1 ml), trypsin inhibitor, α-chymotrypsinogen and lysozyme, (a) 0.25, (b) 0.6 and (c) 1.2 mg ml^{-1} each; buffer A, 10 m*M* sodium borate/NaOH (pH 10.2); buffer B, 10 m*M* sodium acetate/citric acid (pH 4.0); step gradient: 1st step, 0% buffer B; 2nd step, 20% buffer B (*ca.* pH 8.0); 3rd step, 100% buffer B.

determined. The separation of human serum proteins on the strong anion-exchange MA at a flow-rate of 2 ml min^{-1} per unit (Fig. 7a) shows a similar pattern to those achieved on comparable strong anion-exchange FPLC columns. The main fractions were determined by SDS-PAGE to consist of IgG [fraction 1,(2)], transferrin [fraction (2),3] and albumin [fractions 6,7,(8)] (fractions that contain only traces of a substance are given in parentheses). As shown in Fig. 7b, no decrease in performance was observed when the flow-rate was increased to 10 ml min^{-1} per unit, which, on the other hand, reduced the separation time to less than 5 min.

An important difference between membrane and column chromatography is the general suitability of step *versus* linear gradients. Whereas linear gradients are preferred in column chromatography, as they have a sharpening effect on the signals, they often generate poor peak shapes if used in membrane chromatography. In contrast, the resolution and peak shape are usually enhanced if the proteins are eluted by step gradients [25–28]. This was also observed in our studies, *i.e.*, with thin MAs. Again, step gradients of the eluent pH and/or its salt concentration proved to be superior to linear gradients in terms of resolution and peak shape. Using a combination of pH and salt step gradients, human serum could be separated into nine fractions, as shown in Fig. 8. As only one membrane layer was used, the MA was overloaded and the first fraction is the breakthrough. Apart from the first fraction, all fractions were analysed by SDS-PAGE. IgG is found in fraction 2, fractions 3 and 4 contain mainly transferrin and albumin is found mainly in fractions 5–7. The purity of the serum proteins was higher than that obtained with a linear gradient, but most fractions did still contain small amounts of albumin. This is to be expected, as this protein not only constitutes the main serum protein, but is

also known to aggregate with other serum proteins. If necessary, the aggregation of albumin to other proteins could be prevented by addition of a detergent such as Triton X-100 [25].

In Fig. 9, the isolation of subtilisin Carlsberg, produced extracellularly during a cultivation of *Bacillus licheniformis*, using an anion-exchange MA is shown. Subtilisin activity is found only in

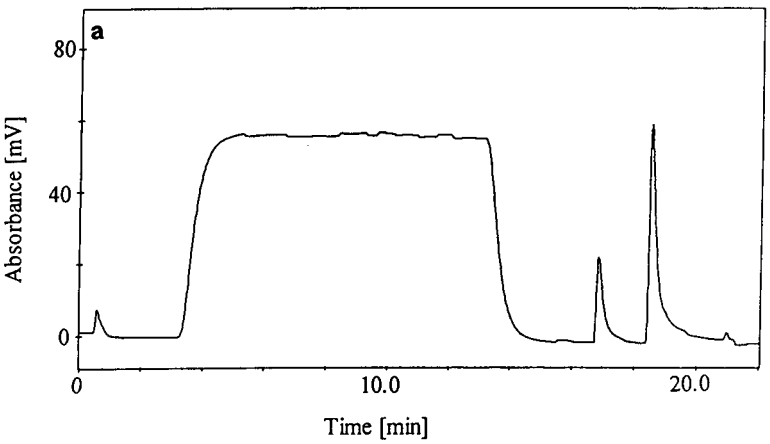

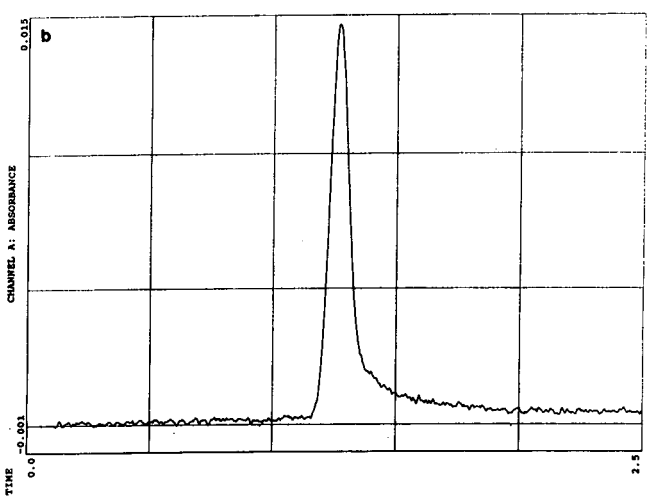

Fig. 6.

(*Continued on p. 38*)

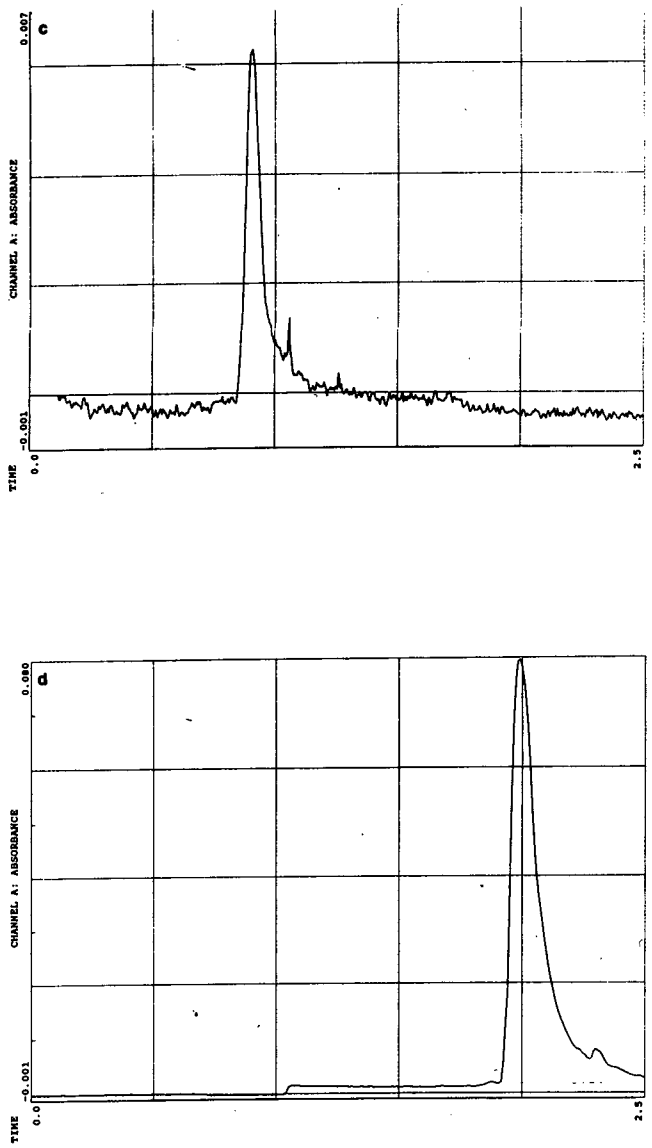

Fig. 6. (a) Separation of h-IgG and lysozyme in the presence of an excess of BSA on a cation-exchange MA. Detection wavelength, 280 nm; flow-rate, 5 ml min^{-1} per unit; sample volume, 50 ml (in buffer A); sample content, BSA 0.5 mg ml^{-1}, h-IgG 5 μg ml^{-1}, lysozyme 10 μg ml^{-1}; buffer A, 10 m*M* phosphate (pH 5.0); buffer B, 10 m*M* phosphate–1 *M* KCl (pH 5.0); step gradient, 10 ml 0% buffer B, 10 ml 15% buffer B, 10 ml 40% buffer B. (b)–(d) Analysis of the protein fractions by FZCE: (b) peak after 17.01 min (h-IgG); (c) peak after 18.78 min (lysozyme); (d) breakthrough 3.5–12 min (BSA).

the indicated fraction. According to the analysis by SDS-PAGE, this fraction is contaminated by small amounts of two other proteins, which we were not able to identify. The total enzymatic activity of the protease prior and after the separation was nearly the same, indicating high recovery and low stress caused by the adsorption on the MA.

The possibility of using MAs for rapid bioprocess control was demonstrated in a so-called

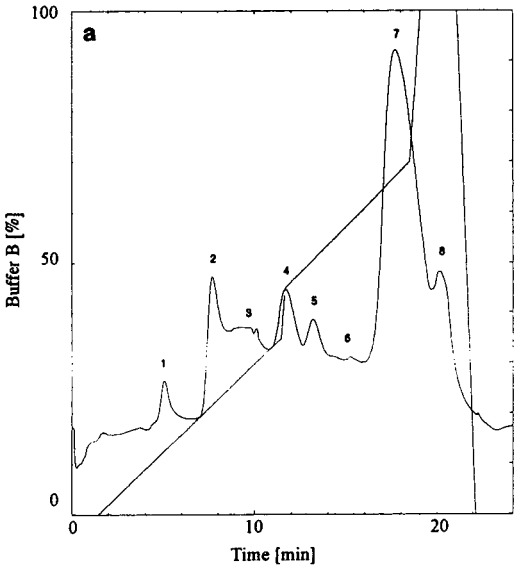

Fig. 7. (a) Separation of human serum proteins on anion-exchange MAs (eight membranes) using a linear gradient. Flow-rate, 2 ml min^{-1} per unit; detection wavelength, 280 nm; sample, 1 ml of human serum (protein content 3 mg ml^{-1}); buffer A, 10 m*M* Tris–HCl (pH 9.5); buffer B, 10 m*M* Tris–HCl + 0.4 *M* KCl (pH 9.5). (b) Conditions as given in (a), with the exception of the flow-rates.

"simulated fermentation" [39], taking the production of β-galactosidase by *Spodoptera frugiperda* cells as an example. In a simulated fermentation an on-line or quasi-on-line analytical system is used to monitor gradients run

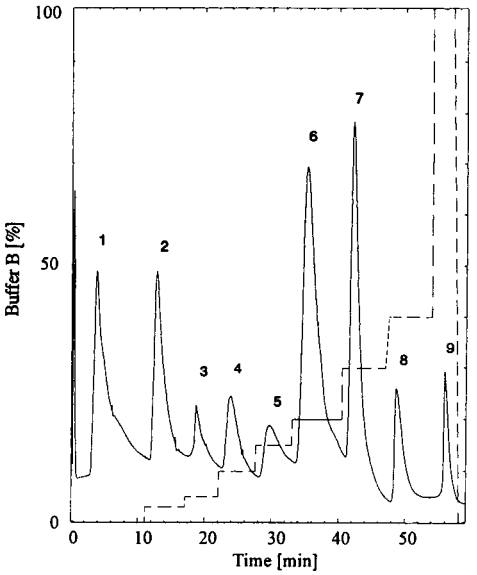

Fig. 8. Separation of human serum proteins on an anion-exchange MA with a pH/salt concentration step gradient. Flow-rate, 1 ml min^{-1} per unit; detection wavelength, 280 nm; sample, 1 ml of human serum (protein content 0.5 mg ml^{-1}); buffer A, 10 m*M* Tris–borate (pH 8.7); buffer B, 10 m*M* Tris–borate + 1 *M* KCl (pH 6.0).

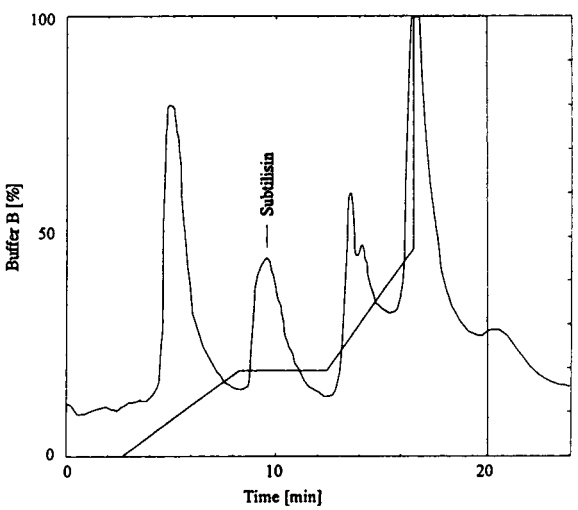

Fig. 9. Separation of subtilisin Carlsberg from culture supernatants of *Bacillus licheniformis* on an anion-exchange MA. Flow-rate, 2 ml min^{-1} per unit; detection wavelength, 280 nm; sample, 200 μl of subtilisin containing culture supernatant of a *Bacillus licheniformis* culture in 300 μl of buffer A; Buffer A, 15 m*M* Tris–HCl (pH 9.0); buffer B, 15 m*M* Tris–HCl + 0.8 *M* KCl (pH 9.0).

from 100% fresh culture medium to 100% of a culture supernatant containing the analyte in addition to all the products, by-products, metabolites, cell debris, etc., that are produced during the cultivation. The method allows the testing and optimization of an analytical system under realistic conditions, while taking considerably less time than an actual bioprocess. The results obtained with an anion exchange MA are shown in Fig. 10. β-Galactosidase activity is found only in the indicated fraction. The peak area, although not its height, increased linearly with increasing enzyme concentration in the culture supernatant. The relative deviation of the peak area was less than 2%, even at flow-rates of 10 ml min^{-1} per unit and more. The high speed, the good reproducibility and the low cost of the MAs used make HPMC an attractive option in bioprocess control.

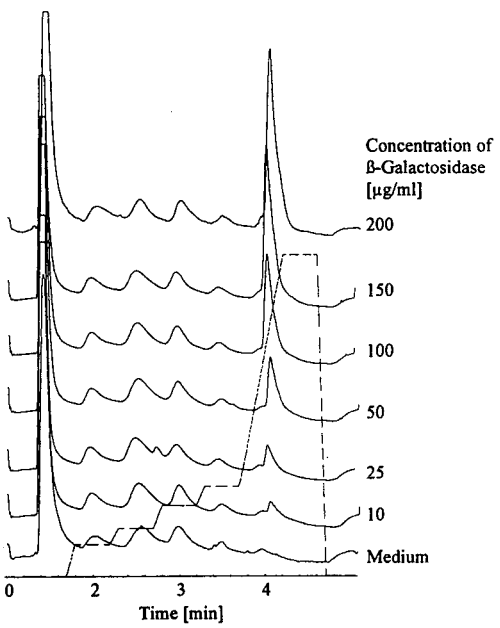

Fig. 10. Determination of β-galactosidase in culture supernatants with an anion-exchange MA. Flow-rate, 10 ml min^{-1} per unit; detection wavelength, 280 nm; sample, 1 ml of cultivation medium in buffer A (1:1, v/v); buffer A, 5 m*M* Tris–HCl (pH 5.8); buffer B, 5 m*M* Tris–HCl + 0.6 *M* NaCl (pH 6.8).

CONCLUSIONS

Two types of commercially available, strong ion-exchange MAs integrated in syringe filter holders were shown to be cheap and efficient substitutes for conventional HPLC and FPLC columns for protein separations. Standard proteins, human serum proteins and even cell culture supernatants could be separated and analysed. The low pressure drop of the membranes allows high flow-rates, resulting in separation times of less than 1 min with a performance as good as those achieved with equivalent columns. The cartridges used as membrane holders are commercially available and simple to handle. No packing or maintenance of a column is necessary and a scale-up can be performed easily. The physical and chemical properties of the membrane adsorbers were stable over a period of at least 1 month of constant use. The field of application of HPMC can thus be expected to expand in the near future.

REFERENCES

1 S. Brandt, R.A. Goffe, S.B. Kessler, J.L. O'Conner and S.E. Zale, *Bio/Technology*, 6 (1988) 779.
2 L.J. Cummings, D.L. Hardy and A. Stevens, *Int. Lab.*, No. 9/10 (1990) 40.
3 C.A. Heath and G. Belfort, *Adv. Biochem. Eng.*, 47 (1992) 45.
4 V.K. Garg, S.E. Zale, A.R.M. Azad and O.D. Holton, in P. Todd, S.K. Sikdar and M. Bier (Editors), *Frontiers in Bioprocessing II*, American Chemical Society, Washington, DC, 1992, p. 321.
5 J.J. Piotrowski and M.H. Scholla, *BioChromatography*, 3 (1988) 161.
6 D.D. Frey, R. van de Water and B. Zhang, *J. Chromatogr.*, 603 (1992) 43.
7 K.-G. Briefs and M.-R. Kula, *Chem. Eng. Sci.*, 47 (1992) 141.
8 F. Svec and T.B. Tennikova, *J. Bioact. Compat. Polym.*, 6 (1991) 393.
9 T.B. Tennikova, B.G. Belenkii and F. Svec, *J. Liq. Chromatogr.*, 13 (1990) 63.
10 M. Unarska, P.A. Davies, M.P. Esnouf and B.J. Bellhouse, *J. Chromatogr.*, 519 (1990) 53.
11 K. Kalghatgi and C. Horvath, *J. Chromatogr.*, 398 (1987) 335.
12 T.B. Tennikova, M. Bleha, F. Svec, T.V. Almazova and B.G. Belenkii, *J. Chromatogr.*, 555 (1991) 97.
13 J.A. Gerstner, R. Hamilton, S.M. Cramer, *J. Chromatogr.*, 596 (1992) 173.

14 D. Josic, F. Bal, H. Schwinn, *J. Chromatogr.*, 632 (1993) 1.
15 A. Jungbauer, F. Unterluggauer, K. Uhl, A. Buchacher, F. Steindl, D. Pettauer and E. Wenisch, *Biotechmnol. Bioeng.*, 32 (1988) 326.
16 Y. Kikumoto, Y.-M. Hong, T. Nishida, S. Nakai, Y. Masui and Y. Hirai, *Biochem. Biophys. Res. Commun.*, 147 (1987) 315.
17 M. Nachman, A.R.M. Azad and P. Bailon, *J. Chromatogr.*, 597 (1992) 155.
18 A. Upshall, A.A. Kumar, M.C. Bailey, M.D. Parker, M.A. Favreau, K.P. Lewison, M.L. Joseph, J.M. Maragnora and G.L. McKnight, *Bio/Technology*, 5 (1987) 1301.
19 M. Kim, K. Saito, S. Furusaki, T. Sato, T. Sugo and I. Ishigaki, *J. Chromatogr.*, 585 (1991) 45.
20 R.M. Mandaro, S. Roy and K.C. Hou, *Bio/Technology*, 5 (1987) 928.
21 P. Langlotz and K.H. Kroner, *J. Chromatogr.*, 591 (1992) 107.
22 S. Krause, K.H. Kroner and W.-D. Deckwer, *Biotechnol. Tech.*, 5 (1991) 199.
23 B. Champluvier G. Briefs and M.-R. Kula, in C. Christiansen, L. Munck and J. Villadsen (Editors), *Proceedings of the 5th European Congress on Biotechnology, Copenhagen, July 8–13, 1990,* Vol. I, Munksgaard, Copenhagen, 1990, p. 525.
24 R. Molinari, J.L. Torres, A.S. Michaels, P.K. Kilpatrick and R.G. Carbonell, *Biotechnol. Bioeng.*, 36 (1990) 572,
25 D. Josic, J. Reusch, K. Löster, O. Baum and W. Reutter, *J. Chromatogr.*, 590 (1992) 59.
26 B. Champluvier and M.-R. Kula, *J. Chromatogr.*, 539 (1991) 315.
27 D. Josic, K. Zeilinger, Y.-P. Lim, M. Raps, W. Hofman and W. Reutter, *J. Chromatogr.*, 484 (1989) 327.
28 H. Abou-Rebyeh, F. Körber, K. Schubert-Rehberg, J. Reusch and D. Josic, *J. Chromatogr.*, 566 (1991) 341.
29 D. Lütkemeyer, S. Siwiora, H. Büntemeyer, J. Lehmann, *BioEngineering*, 2 (1992) 34.
30 R. Akhnoukh, G. Kretzmer and K. Schügerl, *Bioprocess Eng.*, 8 (1993) 229.
31 U. Hübner, *Doctoral Thesis*, University of Hannover, Hannover, 1991.
32 U.K. Laemmli, *Nature*, 227 (1970) 680.
33 M. Bradford, *Anal. Biochem.*, 72 (1976) 248.
34 O.H. Lowry, N.J. Rosebrough, A.L. Farr and R.J. Randall, *J. Biol. Chem.*, 193 (1951) 265.
35 G.S. Bailey, in J.M. Walker (Editor), *Methods in Molecular Biology, Vol. 1 (Proteins)*, Humana Press, Clifton, NJ, 1984, p. 301.
36 J.H. Miller, *Experiments in Molecular Genetics* (*Cold Spring Harbor Monograph Series*), Cold Spring Harbor Laboratory, Cold Spring Harbor, NY, 1972.
37 P.G. Stanton, R.J. Simpson, F. Lambrou and M.T.W. Hearn, *J. Chromatogr.*, 266 (1983) 273.
38 W. Kopaciewicz, M.A. Rounds, J. Fausnaugh and F.E. Regnier, *J. Chromatogr.*, 266 (1983) 3.
39 R. Freitag, Th. Scheper and K. Schügerl, *Enzyme Microb. Technol.*, 13 (1991) 969.

Journal of Chromatography A, 654 (1993) 43–52
Elsevier Science Publishers B.V., Amsterdam

CHROM. 25 468

Use of reversed-phase high-performance liquid chromatography in lipophilicity studies of 9*H*-xanthene and 9*H*-thioxanthene derivatives containing an aminoalkanamide or a nitrosoureido group

Comparison between capacity factors and calculated octanol–water partition coefficients

Anna Tsantili-Kakoulidou*, Evangelos Filippatos, Ourania Todoulou and Aspasia Papadaki-Valiraki

Department of Pharmacy, Division of Pharmaceutical Chemistry, University of Athens, Panepistimiopolis, Zografou, Athens 157 71 (Greece)

(First received May 10th, 1993; revised manuscript received July 30th, 1993)

ABSTRACT

The lipophilicity of 9*H*-xanthene and 9*H*-thioxanthene derivatives, containing either a basic alkanamide or a nitrosoureido group, was studied by means of reversed-phase high-performance liquid chromatography using an octadecylsilane stationary phase, methanol as organic modifier and *n*-decylamine as a masking agent. Correlation of the extrapolated capacity factors with log *P* values calculated according to Rekker's fragmental system showed an excellent parallelism between HPLC and the octanol–water partition system and permitted the generation of a hydrophobic fragmental constant for the nitrosoureido group. Tetrahydrofuran was also tried as an organic modifier but without satisfactory results.

INTRODUCTION

The lipophilic character of drugs is a parameter of major importance in quantitative structure–activity (QSAR) studies and has attracted considerable interest [1–3]. Octanol–water partition coefficients, the most widely accepted lipophilicity index, are measured mainly by means of the shaking flask method, which presents a number of practical disadvantages and is limited to compounds with a log *P* range between −2 and +4 [3,4]. Calculation procedures based on the additive–constitutive character of the logarithm of partition coefficients have also been developed [5,6]. However, hydrophobic fragmental constants are not available for every structural characteristic, so log *P* predictions are not always possible. In recent years, partition chromatography, especially RP-HPLC, has become a popular alternative for measuring lipophilicity. Under suitable conditions the logarithms of the capacity factors show good linear correlations with log *P* [7,8]. Moreover, extrapolated log k_w values which correspond to a mobile phase consisting of pure water are in

* Corresponding author.

0021-9673/93/$06.00

many instances and under suitable chromatographic conditions very close to octanol–water partition data [9]. Thus, Collander-type equations ($\log P = a \log k_w + b$) with a regression coefficient close to 1 and an intercept close to zero have often been reported [10–12].

Theoretically, $\log k_w$ values should be independent of the organic modifier that usually must be added to the mobile phase in order to facilitate the elution of solutes. However, it has been shown that the effect of the organic modifier is not fully suppressed by the extrapolation and this is reflected in the significant deviations that may be observed among $\log k_w$ values obtained using different solvents. Bechalany *et al.* [10], who studied the effects of three different organic modifiers on $\log k_w$, suggested that methanol should be the solvent of choice. Moreover, when an ODS column is used as the stationary phase, *n*-decylamine should be added in order to suppress the silanophilic interactions that arise between the solutes and the free silanol groups [11,13]. Tetrahydrofuran (THF), which has been used for the analysis of more lipophilic solutes in order to reduce retention times [14], may also be suitable for the determination of the lipophilicity of compounds containing polar functional groups, especially strong hydrogen bond acceptors, provided that the measurements are restricted only to volume fractions rich in water. In this case the addition of a masking agent is not necessary [10]. However, such studies concern model series that include compounds with low or moderate lipophilicity. For highly lipophilic compounds, limitations in the performance of the experiments impede analogous investigations.

The aim of this study was to apply HPLC in order to determine lipophilicity indices for some novel highly lipophilic 9*H*-xanthene and 9*H*-thioxanthene derivatives and to compare them with calculated octanol–water partition coefficients. The compounds under study were designed and synthesized as potential anticancer agents and include derivatives with a side-chain that bears either an aminoalkanamide group (type I) or a nitrosoureido moiety (type II) (Tables I and II). For the latter a hydrophobic fragmental constant in the octanol–water system

TABLE I

AMINOALKANAMIDES **I.1–I.11**

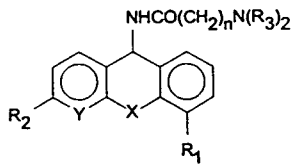

Compound	R_1	R_2	R_3	X	Y	*n*
I.1	H	H	C_2H_5	O	CH	1
I.2	CH_3	H	CH_3	O	CH	1
I.3	CH_3	H	C_2H_5	O	CH	1
I.4	CH_3	H	CH_3	O	CH	2
I.5	CH_3	H	C_2H_5	O	CH	2
I.6	CH_3	Cl	CH_3	O	CH	1
I.7	CH_3	H	CH_3	S	CH	1
I.8	CH_3	H	C_2H_5	S	CH	1
I.9	CH_3	H	CH_3	S	CH	2
I.10	CH_3	H	C_2H_5	S	CH	2
I.11	CH_3	H	CH_3	O	N	1

TABLE II

NITROSOUREAS **II.1–II.13**

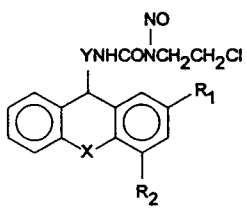

Compound	R_1	R_2	X	Y
II.1	H	H	O	–
II.2	CH_3	H	O	–
II.3	H	CH_3	O	–
II.4	CH_3	CH_3	O	–
II.5	OCH_3	H	O	–
II.6	OC_2H_5	H	O	–
II.7	H	OCH_3	O	–
II.8	H	H	S	–
II.9	CH_3	H	S	–
II.10	H	CH_3	S	–
II.11	H	H	O	SCH_2CH_2
II.12	H	H	S	SCH_2CH_2
II.13	H	H	O	CH_2

is not available and part of this study was focused on evaluating the contribution of that fragment to the overall lipophilicity. The choice of the organic modifier with respect to the practical limitations and the establishment of suitable partitioning conditions is also discussed.

EXPERIMENTAL

All compounds (Tables I and II) were synthesized in our laboratory and identifier by ^{1}H NMR spectroscopy and elemental analysis, the results of which have been reported elsewhere [15,16].

Capacity factors were determined using a Waters HPLC instrument equipped with a UV detector operating at 254 nm. An ODS column (25 cm × 4 mm I.D.) prepacked with LiChrosorb RP-18 (particle size 10 μm) stationary phase was used. Mobile phases were made up volumetrically using different concentrations of methanol with 0.02 *M* 3-morpholinopropanesulphonic acid buffer (pH 7.4) in the presence of *n*-decylamine (0.2%) as a masking agent. Compounds of type II were measured also using different mixtures of THF and water as the mobile phase in the absence of a masking agent. All solutions were purified and degassed by filtration using a Millipore Milli-Q system. Retention times were measured at ambient temperature. The flow-rate was adjusted at 2.5 ml/min and the column dead time was determined using the organic modifier as the non-retained compound. Isocratic capacity factors, log k_i, defined as $\log[(t_r - t_0)/t_0]$ were determined at three different proportions of methanol in the range 70–60% and five different proportions of THF in the range 60–40% and extrapolated to 100% water as the mobile phase to yield log k_w and log k_{wTHF} values, respectively.

RESULTS AND DISCUSSION

Use of methanol as organic modifier

The use of methanol in the mobile phase led to long retention times so that measurements were limited to a small range of organic modifier concentrations. However, the excellent linearity observed between capacity factors and volume fractions of methanol permitted the derivation of reliable extrapolated capacity factors, log k_w (Table III). For compounds of type I suitable corrections for ionization were applied using the equation

$$\log k_w = \log k_w(\text{pH } 7.4) + \log(1 + 10^{pK_a - pH}) \quad (1)$$

pK_a values were calculated as suggested by Perrin [17], starting from the pK_a value of a tertiary amine and taking into account the presence of the amide group attached one or two carbon atoms away from the basic centre and also the number of methyl groups directly attached to the basic centre. According to this procedure, pK_a values around 7.30 and 7.70 were assigned to the dimethylamino and diethylamino derivatives, respectively, when $n = 1$. When $n = 2$ the base-weakening effect of the amide group is lower and the corresponding pK_a values were calculated to be around 8.40 and 8.80, respectively. The corrected log k_w values are presented in Table IV.

In a preliminary study [18], a relationship was established between the chromatographic data and calculated octanol–water log *P* values, expressed by the equation

$$\log P = 0.768(\pm 0.021) \log k_w + 2.115(\pm 0.115) I_N + 0.415(\pm 0.095) I_S \quad (2)$$

$n = 24$; $r = 0.985$; $s = 0.260$; $F = 302$

Log *P* values were calculated according to Rekker's system [6] as a summation of fragmental constants and correction terms expressed as multiples of the magic constant ($c_M = 0.289$). For the –NHCOCH$_2$N– group the fragmental value −2.729 proposed by Le Therizien *et al.* [19] was used. For compounds of type II the expression log $P - f_{[-NHCON(NO)-]}$ was considered in place of log *P*, as a fragmental constant for the –NHCON(NO)– group is not available. The presence of the –NHCON(NO)– fragment was expressed by the indicator parameter I_N on the right-hand side of eqn. 2. The regression coefficient of I_N with opposite sign then represents the contribution of that fragment to the lipophilicity. In eqn. 2, a second indicator I_S was necessary to account for the presence or absence of a sulphur

TABLE III

ISOCRATIC AND EXTRAPOLATED CAPACITY FACTORS DETERMINED USING METHANOL AS ORGANIC MODIFIER AND *n*-DECYLAMINE AS A MASKING AGENT

Compound	Log k_{60}	Log k_{65}	Log k_{70}	Log k_w [a]	S	r
I.1	0.87	0.60	0.43	3.49(±0.38)	4.4	0.992
I.2	0.95	0.72	0.52	3.53(±0.11)	4.3	0.999
I.3	1.15	0.85	0.62	4.32(±0.26)	5.3	0.997
I.4	0.85	0.77	0.56	2.61(±0.49)	2.9	0.968
I.5	0.71	0.56	0.34	2.94(±0.26)	3.7	0.994
I.6	1.47	1.24	1.00	4.29(±0.04)	4.7	1.000
I.7	0.95	0.72	0.52	3.53(±0.11)	4.3	0.999
I.8	1.20	0.89	0.69	4.24(±0.41)	5.1	0.992
I.9	0.83	0.78	0.53	2.66(±0.75)	3.0	0.933
I.10	0.71	0.58	0.36	2.83(±0.34)	3.5	0.989
I.11	0.39	0.25	0.09	2.19(±0.07)	3.0	0.999
II.1	1.10	0.89	0.59	4.17(±0.34)	5.1	0.995
II.2	1.34	1.09	0.79	4.65(±0.19)	5.5	0.999
II.3	1.40	1.16	0.84	4.77(±0.30)	5.6	0.997
II.4	1.64	1.38	1.05	5.19(±0.26)	5.9	0.998
II.5	1.18	0.91	0.63	4.48(±0.04)	5.5	1.000
II.6	1.38	1.09	0.80	4.86(±0.01)	5.8	1.000
II.7	0.92	0.70	0.46	3.68(±0.07)	4.6	0.999
II.8	1.27	1.04	0.72	4.59(±0.34)	5.5	0.996
II.9	1.52	1.25	0.94	5.01(±0.15)	5.8	0.999
II.10	1.54	1.28	0.96	5.03(±0.23)	5.8	0.998
II.11	1.34	1.04	0.73	5.00(±0.04)	6.1	1.000
II.12	1.31	1.02	0.70	4.98(±0.11)	6.1	0.999
II.13	1.12	0.89	0.62	4.13(±0.15)	5.0	0.999

[a] Capacity factors linearly extrapolated to 100% water according to the equation $\log k = \log k_w - S\varphi$ (φ = fraction of methanol).

atom in the molecule. All data used in eqn. 2 are reported in Table IV.

Eqn. 2 however, although highly significant, represents a rough analysis of the data and further investigation is necessary in order to draw final conclusions. A drawback of eqn. 2 is the low regression coefficient of log k_w. Under analogous chromatographic conditions a regression coefficient of log k_w close to 1 and an intercept close to zero has been reported [10,12]. Closer examination of the data reveals that compounds **II.7** and **II.13**, although not outliers, show deviating behaviour, their lipophilicity being much lower than predicted. For compound **II.7** the reason may lie in the steric *ortho* effect of the methoxy group with respect to the ring oxygen. For compound **II.13** the decrease in lipophilicity can be attributed to the presence of a methylene bridge between the xanthene moiety and the polar nitrosoureido function. Omission of compounds **II.7** and **II.13** from the statistical analysis leads to the following equation with a higher correlation coefficient and a regression coefficient of log k_w almost equal to 1 but with a large negative intercept:

$$\log P = 1.012(\pm 0.071) \log k_w + 1.819(\pm 0.087) I_N + 0.433(\pm 0.060) I_S - 0.983(\pm 0.284) \quad (3)$$

$n = 22$; $r = 0.995$; $s = 0.159$; $F = 636$

Separate analysis of the aminoalkanamide derivatives leads to the following equation, in good agreement with eqn. 3:

$$\log P = 1.004(\pm 0.092) \log k_w + 0.536(\pm 0.121) I_S - 0.989(\pm 0.370) \quad (4)$$

$n = 11$; $r = 0.968$; $s = 0.191$; $F = 77$

The large negative intercept generated by

TABLE IV

DATA USED IN REGRESSION EQNS. 2–10

Compound	Log k_w [a]	Log P [b]	Log P_c [c]	Log P_{rev} [d]	I_N	I_S
I.1	3.97	3.214	4.081	4.385	0	0
I.2	3.78	2.695	3.562	3.866	0	0
I.3	4.80	3.733	4.600	4.904	0	0
I.4	3.65	2.509	3.376	3.728	0	0
I.5	4.36	3.547	4.414	4.766	0	0
I.6	4.54	3.437	4.304	4.595	0	0
I.7	3.78	3.244	4.111	3.980	0	1
I.8	4.72	4.282	5.149	5.018	0	1
I.9	3.70	3.058	3.925	3.842	0	1
I.10	4.24	4.096	4.963	4.880	0	1
I.11	2.44	1.557	2.424	2.497	0	0
II.1	4.17	5.176	6.043	6.325	1	0
II.2	4.65	5.695	6.562	6.844	1	0
II.3	4.77	5.695	6.562	6.844	1	0
II.4	5.19	6.214	7.081	7.363	1	0
II.5	4.48	5.256	6.123	6.394	1	0
II.6	4.86	5.775	6.642	6.913	1	0
II.7	3.68	5.256	5.545	5.737	1	0
II.8	4.59	5.725	6.592	6.437	1	1
II.9	5.01	6.244	7.111	6.956	1	1
II.10	5.03	6.244	7.111	6.956	1	1
II.11	5.00	6.282	6.860	7.026	1	1([e])
II.12	4.98	6.831	7.409	7.140	1	2([e])
II.13	4.13	5.695	5.695	6.187	1	0

[a] For compounds of type I the log k_w values are corrected for ionization according to eqn. 1.
[b] For compounds of type II the values in this column correspond to log $P - f_{[NHCON(NO)]}$.
[c] For compounds of type II the values in this column correspond to log $P_c - f_{[NHCON(NO)]}$.
[d] For compounds of type II the values in this column correspond to log $P_{rev} - f_{[NHCON(NO)]}$.
[e] The values in parentheses correspond to those used in eqn. 8 (only ring sulphur is taken into account).

eqns. 3 and 4 reflects an underestimation of lipophilicity, indicating that special attention should be paid in the calculation procedure to the direct attachment of polar groups to the bulky tricyclic system. Such a direct attachment may lead to a decrease in the hydration of the polar groups and consequently to an increase in lipophilicity. This assumption is further supported by the bad fit of compound **II.13**, already mentioned. In this respect, and as evaluated from the magnitude of the intercept in eqn. 4, a correction equal to 3 c_M should be considered for the direct attachment of the –NHCO– group to the ring system. Correlation of the corrected log P_c of the aminoalkanamide derivatives and the corresponding log k_w values leads to the equation

$$\log P_c = 1.004(\pm 0.092) \log k_w + 0.536(\pm 0.120) I_S - 0.122(\pm 0.370) \quad (5)$$

$n = 11$; $r = 0.968$; $s = 0.191$; $F = 77$

In eqn. 5, the intercept is no longer significant and after forcing through the origin the following equation is obtained:

$$\log P_c = 0.974(\pm 0.017) \log k_w + 0.536(\pm 0.114) I_S \quad (5')$$

Eqn. 5′ can be further refined by omission of compound **I.9**. Compound **I.9** has an inacurrate log k_w value with a standard error that substantially exceeds twice the standard deviation of eqn. 5 (Table III). Eqn. 6′, derived from eqn. 6

after forcing through the origin, includes only good-quality data and may serve as a reference equation.

$$\log P_c = 0.976(\pm 0.091) \log k_w + 0.612(\pm 0.129) I_S - 0.015(\pm 0.363) \quad (6)$$

$n = 10$; $r = 0.974$; $s = 0.182$; $F = 84$

$$\log P_c = 0.973(\pm 0.016) \log k_w + 0.613(\pm 0.120) I_S \quad (6')$$

For the direct attachment of the nitrosoureido and sulphur group, corrections of 3 and 2 c_M, respectively, were incorporated in the expression $\log P - f_{[\text{-NHCON(NO)-}]}$. The following equation includes all compounds except **I.9** and **II.7**:

$$\log P_c = 1.016(\pm 0.077) \log k_w + 1.749(\pm 0.091) I_N + 0.377(\pm 0.068) I_S - 0.104(\pm 0.308) \quad (7)$$

$n = 22$; $r = 0.993$; $s = 0.173$; $F = 476$

After forcing through the origin, the following, equation is obtained

$$\log P_c = 0.990(\pm 0.014) \log k_w + 1.763(\pm 0.079) I_N + 0.382(\pm 0.064) I_S \quad (7')$$

If the indicator I_S is assigned only to the sulphur present in the ring, eqn. 8′ is obtained, which does not differ in statistics but with a higher regressor of I_S, which is in better accordance with the value generated by eqn. 6′.

$$\log P_c = 1.030(\pm 0.074) \log k_w + 1.799(\pm 0.089) I_N + 0.461(\pm 0.080) I_S - 0.186(\pm 0.298) \quad (8)$$

$n = 22$; $r = 0.993$; $s = 0.169$; $F = 509$

After forcing through the origin, the following equation is obtained:

$$\log P_c = 0.985(\pm 0.014) \log k_w + 1.825(\pm 0.078) I_D + 0.470(\pm 0.078) I_S \quad (8')$$

Using the value −1.825 for the nitrosoureido fragment, the partition coefficients of compounds of type II were calculated and are reported in Table V. Log P values estimated according to reference eqn. 6′ are also reported. For compound **II.7** $\log P_{est} = 3.580$. Comparison of that value with the value of 4.298 obtained by the calculation procedure reveals a correction of $-2\ c_M$ to be necessary for the *ortho* steric effect.

Calculation of partition coefficients according to Rekker's revised system

Rekker recently revised his fragmental system [20]. In the revised system, much attention has been paid to heteroaromatics. Heteroaromatics should not be further fragmented and the revised system includes several fragments concerning whole structures. Molecules such as diphenyl ether and diphenyl sulphide, although they do not strictly belong to that class of compounds, need extra correction terms which are equal to 4 and 2 times the magic constant c_M (in the revised system $c_M = 0.219$), respectively. Hence both structures are more lipophilic than expected and at the same time sulphur and oxygen appear to be almost isolipophilic. This behaviour is in accordance with the lack of differentiation between the xanthene and thioxanthene derivatives observed also in the HPLC partition system.

Partition coefficients were therefore recalculated using the revised fragmental constants and considering the diphenyl ether or diphenyl sulphide moieties as the starting structures. For the $-NHCOCH_2N-$ group a fragmental constant was calculated for the revised system using Le Therizien's data and procedure [19]. A value of −2.895 is proposed which includes 5 c_M for the proximity effect. Moreover, corrections of 3, 3 and 2 c_M were considered for the direct attachment of –NHCO–, –NHCON(NO) and –S– to the ring system, respectively. Log P_{rev} values (Table IV) show an excellent parallelism with the corresponding log k_w data, in accordance with the results obtained so far by studying model series of compounds [10,12]. As revealed by eqns. 9 and 10, the introduction of an indicator variable for the presence of sulphur in the ring system is not necessary, while the slope and intercept remain close to 1 and 0, respectively.

TABLE V

CALCULATED AND ESTIMATED PARTITION COEFFICIENTS OF COMPOUNDS OF TYPE II

Compound	Log P [a]	Log P_{est} [b]	Log P_{rev} [c]	Log P_{est} [d]
II.1	4.218	4.057	4.557	4.411
II.2	4.737	4.524	5.076	4.920
II.3	4.737	4.641	5.076	5.047
II.4	5.256	5.050	5.595	5.491
II.5	4.298	4.359	4.626	4.740
II.6	4.817	4.728	5.145	5.142
II.7	3.431[e]	3.580	3.969[f]	3.893
II.8	4.767	5.079	4.669	4.856
II.9	5.286	5.487	5.188	5.300
II.10	5.286	5.506	5.188	5.321
II.11	5.035	4.865	5.258	5.290
II.12	5.584	5.457	5.372	5.267
II.13	3.870	4.018	4.419	5.369

[a] Calculated according to Rekker's original system.
[b] Estimated according to eqn. 6′.
[c] Calculated according to Rekker's revised system.
[d] Estimated according to eqn. 9′.
[e] An extra correction equal to $-2 \cdot 0.289$ is included to account for the *ortho* effect.
[f] An extra correction equal to $-3 \cdot 0.219$ is included to account for the *ortho* effect.

$$\log P_{rev} = 1.087(\pm 0.096) \log k_w - 0.116(+0.393) \quad (9)$$

$n = 10$; $r = 0.966$; $s = 0.199$; $F = 124$

$$\log P_{rev} = 1.066(\pm 0.067) \log k_w + 1.763(\pm 0.082) I_N - 0.036(\pm 0.273) \quad (10)$$

$n = 22$; $r = 0.994$; $s = 0.157$; $F = 825.86$

Eqns. 9 and 10 do not include compound **I.9** and compounds **I.9** and **II.13**, respectively, for the same reasons as already mentioned for eqns. 6 and 7.

After forcing through the origin, the following equations are obtained

$$\log P_{rev} = 1.058(\pm 0.014) \log k_w \quad (9')$$

$$\log P_{rev} = 1.058(\pm 0.012) \log k_w + 1.768(\pm 0.071) I_N \quad (10')$$

According to eqn. 10′, the value −1.768 represents the hydrophobic fragmental constant of –NHCON(NO)– for the revised system and was used to calculate the partition coefficients of the nitrosoureido derivatives. Calculated log P values and log P values obtained using the reference eqn. 9′ are reported in Table V. For compound **II.7** log $P_{est} = 3.969$. This value indicates that in the revised system a correction of $-3\ c_M$ is required to account for the *ortho* effect.

Use of tetrahydrofuran as organic modifier

In efforts to overcome the experimental limitations that arise from the use of methanol, measurements for compounds of type II were also performed using THF as organic modifier. THF is a more hydrophobic solvent and leads to shorter retention times. A second reason for the choice of THF was to check its merits when a polar group such as –NHCON(NO)– is attached to a highly lipophilic skeleton. As already mentioned, studies on model series suggest that this solvent may be suitable for the assessment of the lipophilicity of compounds that contain polar groups and especially hydrogen bond acceptors [10]. Moreover, this solvent drags enough water on to the stationary phase to mask the free

silanol groups, so the addition of a hydrophobic amine as a masking agent may not be necessary. On the other hand, THF disturbs the water network to a greater extent than methanol and may therefore exhibit a selective effect on solute retention [10,21]. For this reason, large percentages of THF in the mobile phase should be avoided. A mobile phase containing 60% THF was considered to be the upper limit of the concentration range used in the experiments while a lower limit of 40% THF could be reached. This concentration range, although wider than that achieved with methanol, is not satisfactory because a quadratic relationship is usually expected between isocratic capacity factors and the percentage of THF [10]. Therefore, more data should be available for the extrapolation procedure. If only the linear part of the relationship is considered, then data restricted to those obtained with mobile phases rich in water should be used. In the concentration range used in this study, linear extrapolation was possible but as the percentage of THF was fairly high, its effect is reflected in the log k_{wTHF} values, which are much lower than those derived from methanol (Table VI). Straightforward correlation between the two sets of log k_w values leads to the following equation with poor statistics:

$$\log k_w = 1.274(\pm 0.245) \log k_{wTHF} + 0.396(\pm 0.818) \quad (11)$$

$n = 12$; $r = 0.838$; $s = 0.245$; $F = 26$

The regression equation is improved when an indicator parameter I_S for the presence or absence of sulphur in the molecule is introduced:

$$\log k_w = 1.276(\pm 0.120) \log k_{wTHF} + 0.419(\pm 0.074) I_S + 0.247(\pm 0.403) \quad (12)$$

$n = 12$; $r = 0.963$; $s = 0.120$; $F = 68$

After forcing through the origin, the following equation is obtained:

$$\log k_w = 1.349(\pm 0.013) \log k_{wTHF} + 0.426(\pm 0.073) I_S \quad (12')$$

Similar results, expressed by eqns. 13 and 14, are obtained when log k_{60} and log k_{40THF} values, which represent the limits of the organic modifier concentration range, are compared:

$$\log k_{60} = 1.349(\pm 0.242) \log k_{40THF} - 0.371(\pm 0.303) \quad (13)$$

$n = 12$; $r = 0.855$; $s = 0.107$; $F = 31$

TABLE VI

ISOCRATIC AND EXTRAPOLATED CAPACITY FACTORS DETERMINED USING TETRAHYDROFURAN AS ORGANIC MODIFIER

Compound	Log k_{60}	Log k_{55}	Log k_{50}	Log k_{45}	Log k_{40}	Log k_{wTHF} [a]	S	r
II.1	0.18	0.39	0.65	0.81	1.22	3.15(±0.22)	5.0	0.9897
II.2	0.23	0.50	0.73	0.97	1.32	3.40(±0.12)	5.3	0.997
II.3	0.24	0.48	0.76	0.99	1.36	3.51(±0.13)	5.5	0.996
II.4	0.19	0.52	0.85	1.04	1.50	3.96(±0.21)	6.3	0.999
II.5	0.11	0.39	0.69	0.80	1.18	3.18(±0.21)	5.1	0.990
II.6	0.20	0.43	0.71	0.95	1.32	3.48(±0.14)	5.5	0.996
II.7	0.00	0.22	0.44	0.62	0.95	2.75(±0.17)	4.6	0.995
II.8	0.19	0.39	0.61	0.81	1.18	3.04(±0.19)	4.8	0.988
II.9	0.18	0.45	0.68	0.92	1.27	3.35(±0.12)	5.3	0.997
II.10	0.16	0.41	0.67	0.93	1.30	3.49(±0.13)	5.6	0.997
II.11	0.11	0.37	0.63	0.93	1.21	3.41(±0.05)	5.5	0.999
II.13	0.11	0.37	0.59	0.80	1.17	3.16(±0.16)	5.1	0.994

[a] Capacity factors linearly extrapolated to 100% water according to the equation $\log k = \log k_{wTHF} - S\varphi$ (φ = fraction of THF).

$$\log k_{60} = 1.379(\pm 0.138) \log k_{40\text{THF}} + 0.174(\pm 0.037) I_S - 0.467(\pm 0.174) \quad (14)$$

$n = 12$; $r = 0.956$; $s = 0.061$; $F = 59$

Correlation between the calculated log P values and log k_{wTHF} leads to eqn. 15, which, after forcing through the origin, gives eqn. 15′:

$$\log P_{\text{rev}} = 1.398(\pm 0.107) \log k_{\text{wTHF}} + 0.271(\pm 0.065) I_S + 0.157(\pm 0.356) \quad (15)$$

$n = 12$; $r = 0.972$; $s = 0.106$; $F = 87$

$$\log P_{\text{rev}} = 1.445(\pm 0.010) \log k_{\text{wTHF}} + 0.273(\pm 0.062) I_S \quad (15')$$

The regressors of log k_{wTHF} in eqns. 12′ and 15′ indicate a hypodiscriminative power of the HPLC partition system obtained with THF as organic modifier compared with the corresponding system obtained with methanol and with the octanol–water system. Moreover, with THF as organic modifier, the sulphur appears to be less lipophilic than in the two other systems.

CONCLUSIONS

Despite the experimental limitations, and HPLC partition system formed using an ODS stationary phase, methanol as organic modifier and *n*-decylamine as a masking agent, proved to be suitable for the assessment of the partitioning behaviour of compounds with log P values above 4. It may be concluded that if good linear relationships are found between capacity factors and the percentage of methanol, the extrapolated capacity factors can be regarded as reliable substitutes for octanol–water log P values even if the concentration range of the organic modifier is narrow and limited data points are available for the extrapolation procedure. The good parallelism between octanol–water and the HPLC system described above, as revealed by the proper description of the structural characteristics in the calculated partition coefficients, permitted the generation of a hydrophobic fragmental constant for the –NHCON(NO)– group, which may be used for the calculation of the log P values of other compounds containing a nitrosoureido function. In this respect, the advantage of Rekker's revised system mainly consists in the better description of oxygen and sulphur in the 9*H*-xanthene and 9*H*-thioxanthene moieties.

The use of THF for the study of highly lipophilic compounds is not recommended as its merits (lower retention times) are offset by restrictions in the extrapolation procedure and by its higher selective effect towards special structural characteristics (the presence of sulphur in the case studied).

REFERENCES

1 H. Kubinyi, *Prog. Drug. Res.*, 23 (1979) 97.
2 H. van de Waterbeemd and B. Testa, *Adv. Drug. Res.*, 16 (1987) 85.
3 H. Walter, D.E. Brooks and D. Fisher, *Partitioning in Aqueous Two Phase Systems*, Academic Press, London, 1985.
4 A. Leo, *J. Pharm. Sci.*, 76 (1987) 166.
5 C. Hansch and A. Leo, *Substituent Constants for Correlation Analysis in Chemistry and Biology*, Wiley, New York, 1979.
6 R.F. Rekker and H.M. De Kort, *Eur. J. Med. Chem.*, 14 (1979) 479.
7 S.H. Unger and G.H. Chiang, *J. Med. Chem.*, 24 (1982) 257.
8 D.J. Minnick, J.H. Frenz, M.A. Patrick and D.A. Brent, *J. Med. Chem.*, 31 (1988) 1923.
9 Th. Braumann, *J. Chromatogr.*, 373 (1987) 191.
10 A. Bechalany, A. Tsantili-Kakoulidou, N. El Tayar and B. Testa, *J. Chromatogr.*, 541 (1991) 221.
11 N. El Tayar, H. van de Waterbeemd and B. Testa, *J. Chromatogr.*, 320 (1985) 293.
12 A. Tsantili-Kakoulidou, N. El Tayar, H. van de Waterbeemd and B. Testa, *J. Chromatogr.*, 389 (1987) 33.
13 E. Bayer and A. Paulus, *J. Chromatogr.*, 400 (1987) 1.
14 C. Horvath and W. Melander, *J. Chromatogr. Sci.*, 15 (1977) 393.
15 E. Filippatos, A. Papadaki-Valiraki, C. Roussakis and J.-F. Verbist, *Arch. Pharm. (Weinheim, Ger.)*, 326 (1993) 451.
16 A. Filippatos, A. Papadaki-Valiraki, O. Todoulou and J. Sablon, *Arch. Pharm. (Weinheim, Ger.)*, in press.

17 D.D. Perrin, in S. Yalkowsky, A. Sinkula and S. Valvani (Editors), *Physical Chemical Properties of Drugs*, Marcel Dekker, New York, 1980, pp. 1–48.
18 E. Filippatos, A. Tsantili-Kakoulidou, A. Papadaki-Valiraki, presented at the *9th European Symposium on Structure–Activity Relationships: QSAR and Molecular Modeling, Strasbourg, September 7–11, 1992.*
19 L. Le Therizien, F. Heymans, C. Redeuilh, J.J. Godfroid and N. Bush, *Eur. J. Med. Chem.*, 15 (1980) 311.
20 R.F. Rekker and R. Mannhold, *Calculation of Drug Lipophilicity*, VCH, Weinheim, 1992.
21 E.D. Katz, K. Ogan and R.P.W. Scott, *J. Chromatogr.*, 352 (1986) 67.

Journal of Chromatography A, 654 (1993) 53–64
Elsevier Science Publishers B.V., Amsterdam

CHROM. 25 373

Resolution of chiral cannabinoids on amylose tris(3,5-dimethylphenylcarbamate) chiral stationary phase: effects of structural features and mobile phase additives

Shulamit Levin* and Saleh Abu-Lafi

Pharmaceutical Chemistry Department, School of Pharmacy, The Hebrew University of Jerusalem, P.O. Box 12065, Jerusalem 91120 (Israel)

Jamal Zahalka and Raphael Mechoulam

Department of Natural Products, School of Pharmacy, The Hebrew University of Jerusalem, P.O. Box 12065, Jerusalem 91120 (Israel)

(First received April 6th, 1993; revised manuscript received June 17th, 1993)

ABSTRACT

The separation of six pairs of chiral cannabinoids was achieved using a dimethylphenylcarbamate derivative of amylose, immobilized on silica gel (ChiralPak AD, Daicel), using 2-propanol and ethanol as the modifiers of *n*-hexane in the mobile phase. Good separation was achieved for most of the solutes in both solvent systems under various conditions. The chromatographic parameters of various cannabinoids in the two solvent systems were determined. The pairs differ from each other in small structural features such as the degree of saturation, position of a double bond and closure of a pyran ring. Therefore, a comparative study could give some clues regarding the mechanism of discrimination between the enantiomeric pairs on the chiral stationary phase. Preliminary measurements of limit of determination showed that it was possible to assess 99.9% enantiomeric purity of the cannabinoids, owing to the high efficiency of the separation. Enantiomers of two monoterpenes, used as intermediates or as starting materials in the chiral synthesis of cannabinoids, were also separated, hence the described procedure is capable of assessing whether the chiral centres in the molecules were sustained throughout the synthetic procedures.

INTRODUCTION

The increased interest in and importance of problems related to the stereoselectivity of drug action [1] have made the development of procedures of enantioselective analysis by chromatographic methods a focus of intensive research [2,3]. Chiral stationary phases, which serve as chiral discriminators during the chromatographic process, are of central importance. The stationary phase is prepared by derivatization and immobilization of chiral compounds on the surface of the support material, generally silica gel.

An effective group of chiral stationary phases are derivatized polysaccharides immobilized on silica [4–9]. Polysaccharides such as cellulose and amylose consist of linked D-glucose units, forming natural polymers with a highly ordered structure. Differential access to the helical backbone or to the glucose chiral cavities can affect discrimination between enantiomers. While resolution can sometimes be achieved using the natural cellulose as the stationary phase, the immobilized version with ester or phenylcarbamate derivatives has shown far better performance. Numerous compounds of pharmaceutical

* Corresponding author.

0021-9673/93/$06.00

importance have been separated using polysaccharide-based stationary phases [2–9].

Understanding the mechanism of discrimination of enantiomers in a chiral stationary phase can facilitate a rational approach to the optimization of their resolution. Studies on the separation of enantiomeric amides, using cellulose tribenzoate stationary phases [7–9], suggested that the formation of transient diastereomeric complexes between enantiomeric solutes and the chiral binding sites on the stationary phase is based on a combination of hydrogen bonding, $\pi-\pi$ and dipole interactions with the aromatic amide. Once the solutes have been bound by these interactions, chiral recognition is based on the fit of the asymmetric portion of the solute into a chiral cavity of the chiral discrimination site. This fit has rigid steric requirements.

Optimization of the resolution is based on the type and proportion of the mobile phase modifier. Solvent effects on the chromatographic parameters in several stationary phases have been systematically studied. Zief *et al.* [10] examined the effect of a series of alcoholic mobile phase modifiers on the chromatographic parameters of 2,2,2-trifluoro-1-(9-anthryl)ethanol using a Pirkle-type stationary phase. It was concluded that an increase in the bulk of alcohol increased the ability of the enantiomers to displace it from the stationary phase. Another study of solvent effects on the resolution of enantiomers in cellulose triacetate [11], using methanol, ethanol and 2-propanol as mobile phase modifiers, suggested that the polarity of the modifier may not be the key to its elution performance. If the elution involves access into a chiral cavity on the stationary phase, the effectiveness of the resolution may be determined by the steric size of the alcoholic modifier, rather than its polarity. A study of the effect of the steric bulk of an alcoholic mobile phase modifier on k' and α, using cellulose tribenzoate as the stationary phase, similarly indicated that the alcoholic modifier competes for both chiral and achiral binding sites on the stationary phase [12]. It was suggested that, as in cellulose triacetate described above, the mobile phase modifier may bind to sites near (or at) the chiral cavities of the stationary phase, changing their steric environment and, presumably, their stereoselectivity.

Numerous cannabinoids [13,14], including Δ^1-tetrahydrocannabinol (Δ^1-THC), the major psychoactive constituent of *Cannabis sativa* and its preparations (marijuana, hashish, etc.), have shown therapeutic activities [15] in addition to their psychotropic properties. This group of compounds has regained attention recently with the discovery of a cannabinoid receptor in the brain [16], its cloning [17] and the isolation from the brain of the endogenous substrate [18] that binds to the receptor. A new field of research can evolve from these findings and open the way for new therapeutic compounds.

The plant-derived cannabinoids are usually optically pure; Δ^1-THC has a 3*R*,4*R* stereochemistry. Synthetic procedures for the preparation of both enantiomers of most cannabinoids have been developed [13,19]. Most of the procedures are based on commercial chiral starting materials of various enantiomeric purity. Unless chiral purification has been done at some stage of the synthesis, the end products may not be of very high optical purity, owing to the variability of the commercial products.

The therapeutic properties of the cannabinoids have led numerous groups to investigate the possibility of the separation of their undesirable psychotropic effects from the desirable effects by chemical modification. A major advancement in this field was the establishment that some of the unnatural (3*S*,4*S*)-cannabinoid enantiomers are antiemetic [20] and exhibit functional NMDA antagonism [21] without producing THC-like psychotropic effects. The most thoroughly investigated compound in this series is the (3*S*,4*S*)-7-hydroxy Δ^6-THC-dimethylheptyl homologue (HU-211). Its 3*R*,4*R* enantiomer (HU-210) is one of the most potent psychotropically active cannabinoids [22]. Hence any future development of (3*S*,4*S*)-cannabinoids as therapeutic agents will depend to a large extent on the stereochemical efficiency of the enantiomeric synthesis. The products of such syntheses will have to be monitored by analytical procedures capable of separating enantiomeric mixtures, in which the undesirable enantiomer may be present in minute amounts. In the case of HU-211 the optical purity [enantiomeric excess (e.e.)] required, in order to prevent psychotropic effects, would be >99.8 e.e.

This paper describes the resolution of enantiomeric pairs of cannabinoids, using a commercial Daicel ChiralPak-AD column, which is based on amylose tris(3,5-dimethylphenylcarbamate) (ADMPC) supported on macroporous silica gel (Fig. 1). This chromatographic system fulfils the above requirements for enantiomeric excess of the cannabinoids. Understanding of the mechanism of chiral recognition by this polymeric chiral stationary phase is a complex task in the absence of the exact structural features of the immobilized polymeric backbone and the chiral sites. Nevertheless, some suggestions, made by Okamoto and co-workers [4–6] and Wainer and co-workers [7,12], may give preliminary guidance for the design of the appropriate chromatographic separation system. As a rule, chirality is a property of the molecule as a whole, hence all the possible chiral and achiral interactions between the solute and the chiral stationary phase should be accounted for. It has been proposed that the main chiral adsorbing sites are the carbamate polar functional groups, which interact with the solute via hydrogen bonding (through NH and CO groups) and dipole–dipole interactions on CO. The $\pi-\pi$ interactions of the dimethylphenyl groups, with the aromatic groups of the solute, are also important. The presence of the dimethyl groups on the phenylcarbamate moiety probably increases the electron density at the carbonyl oxygen group, which in turn intensifies its hydrogen bonding with hydroxyl groups in the solutes. The two methyl groups on the phenylcarbamate can also play a role in controlling the steric fit of the solute into the chiral cavity on the stationary phase. A comparative study is presented here, aimed at further understanding the mechanism of chiral discrimination in polysaccharide-based stationary phases.

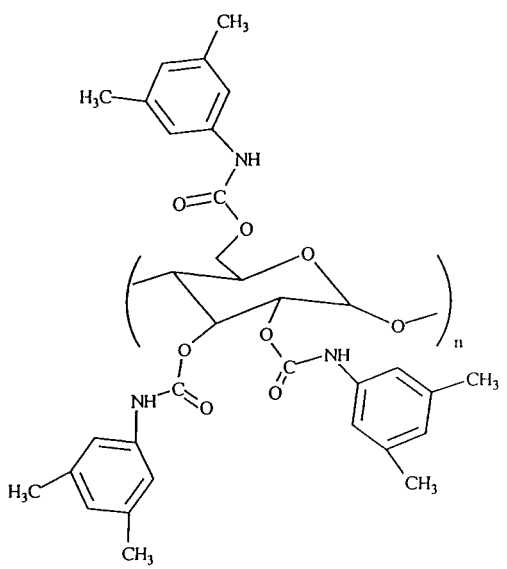

Fig. 1. An adsorption site in the chiral stationary phase used in this study.

EXPERIMENTAL

Instrumentation

The HPLC system was an HP1050 (Hewlett-Packard, Palo Alto, CA, USA) with a diode-array UV detector and an HPCHEM data station, with a ThinkJet printer, and a Rheodyne (Cotati, CA, USA) injection valve equipped with a 20-μl loop. The chiral column (250 mm × 4.6 mm I.D.) was a ChiralPak AD column (10 μm) (Daicel Chemical Industries, Tokyo, Japan).

Materials

HPLC-grade solvents were all purchased from Merck (Darmstadt, Germany). Six pairs of enantiomeric cannabinoids and two pairs of enantiomeric monoterpenes were subjected to the enantiomeric analysis.

Pair 1. (−)-(3*R*,4*R*)-Δ^1-THC, $[\alpha]_D$ −175° ($CHCl_3$), was isolated from hashish or prepared by partial synthesis from natural cannabidiol (CBD) as described previously [23]. (+)-(3*S*,4*S*)-Δ^1-THC, $[\alpha]_D$ +176° ($CHCl_3$), was prepared according to a published procedure [24]. In order to obtain a high enantiomeric excess, an intermediate in its synthesis, (+)-verbenol, was recrystallized to a constant m.p. 72°C and a constant rotation $[\alpha]_D$ +9.9° ($CHCl_3$).

Pair 2. (−)-(3*R*,4*R*)-Δ^6-THC, $[\alpha]_D$ −252° ($CHCl_3$), was prepared from CBD [23]. (+)-(3*S*,4*S*)-Δ^6-THC, $[\alpha]_D$ +252° ($CHCl_3$), was prepared according to a published procedure [24]. The intermediate (+)-verbenol was prepared as described for pair 1.

Pair 3. (−)-(3*S*,4*R*)-CBD, m.p. 66°C, $[\alpha]_D$ −79° ($CHCl_3$) and −129° (EtOH), was isolated

from hashish [23,25]. (+)-(3*R*,4*S*)-CBD, m.p. 65°C, $[\alpha]_D$ +79° ($CHCl_3$) and +128° (EtOH), was prepared according to a published procedure [26].

Pair 4. (−)-(3*R*,4*R*)-7-Hydroxy-Δ^6-THC, dimethylheptyl homologue (HU-210), m.p. 141–142°C, $[\alpha]_D$ −277° ($CHCl_3$), and (+)-(3*S*,4*S*)-7-hydroxy-Δ^6-THC, dimethylheptyl homologue (HU-211), m.p. 141–142°C, $[\alpha]_D$ +227° ($CHCl_3$), were prepared as described previously [19].

Pair 5. (−)-(1*R*,3*R*,4*R*)-7-Hydroxyhexahydrocannabinol, dimethylheptyl homologue, (HU-243), m.p. 80–82°C, $[\alpha]_D$ −92° ($CHCl_3$), and (+)-(1*S*,3*S*,4*S*)-7-hydroxyhexahydrocannabinol ($CHCl_3$), dimethylheptyl homologue (HU-251), m.p. 80–82°C, $[\alpha]_D$ +92° ($CHCl_3$), were prepared by reduction of HU-210 and HU-211, respectively, as derived previously [27].

Pair 6. The tetracyclic HU-249, m.p. 156–158°C, $[\alpha]_D$ +178° ($CHCl_3$), and HU-250, m.p. 156–158°C, $[\alpha]_D$ −178° ($CHCl_3$), were prepared as described previously [28].

Pair 7. (−)-4-Oxomyrtenyl pivalate, m.p. 42–43°C, $[\alpha]_D$ −165° ($CHCl_3$), and (+)-4-oxomyrtenyl pivalate, m.p. 42–43°C, $[\alpha]_D$ +165° ($CHCl_3$), were prepared as described previously [19].

Pair 8. (−)-*cis*-Verbenol and (+)-*cis*-verbenol were purchased from Aldrich (Milwaukee, WI, USA).

Procedure

The mobile phase consisted of various mixtures of *n*-hexane with ethanol or 2-propanol (1–20%, v/v). A flow-rate of 1 ml/min was used in all the experiments at room temperature. Each run was monitored at two wavelengths simultaneously; one of them was either 260 or 270 nm, depending on the cannabinoid, and the other was 220 nm. In each instance, *ca.* 0.1 mg of analyte was dissolved in 1 ml of the appropriate solvent (mixture of 2-propanol or ethanol with *n*-hexane, according to the composition of the mobile phase) and injected both individually and as a racemic mixture. The day-to-day reproducibility was high; the R.S.D. was <1% for capacity factors and <2% for selectivity factors.

RESULTS AND DISCUSSION

Six pairs of cannabinoids were studied, using various proportions of either ethanol or 2-propanol as alcoholic additives to *n*-hexane in the mobile phase. The six pairs are shown in Fig. 2. The group consisted of members that differed from each other in small structural features. The parameters studied were the retention factor, k', which combines the extent of selective and non-selective retention of the enantiomers, the selectivity factor, α, which expresses the degree of discrimination between the two enantiomers, the resolution, R_s, which indicates the efficiency of the separation, and elution order, which indicates the type of stereoselective fit into the binding site.

Optimization of the separation of the six enantiomeric pairs of cannabinoids was performed, using various compositions of *n*-hexane with a modifier, either ethanol or 2-propanol, in the mobile phase. Results for the k', α and R_s using 1–20% ethanol are summarized in Table I and using 2–20% 2-propanol in Table II.

The chromatographic system operated very well in terms of discrimination and efficiency of the enantiomeric resolution, judging from the α and R_s values in Tables I and II. Apart from the two enantiomers of Δ^6-THC, all the enantiomeric pairs could be easily separated using various percentages of 2-propanol or ethanol in the mobile phase. Values of $\alpha \geq 1.2$ were easily obtained at relatively high resolution values. The system operated in the normal-phase mode in terms of average retention of the enantiomeric pairs. Fig. 3 shows two chromatograms of the (+)- and (−)-enantiomers of Δ^6-THC, obtained using *n*-hexane–2-propanol (98:2, v/v) and *n*-hexane–ethanol (98:2, v/v). Shorter retention times were obtained when ethanol was the modifier. Also typical was the decrease in retention parameters with increase in the percentage of modifier in the mobile phase.

Detection limits and enantiomeric purity

The stereoselectivity of the pharmacological activity of chiral medicinal compounds cannot be established quantitatively unless a sensitive method for the determination of enantiomeric

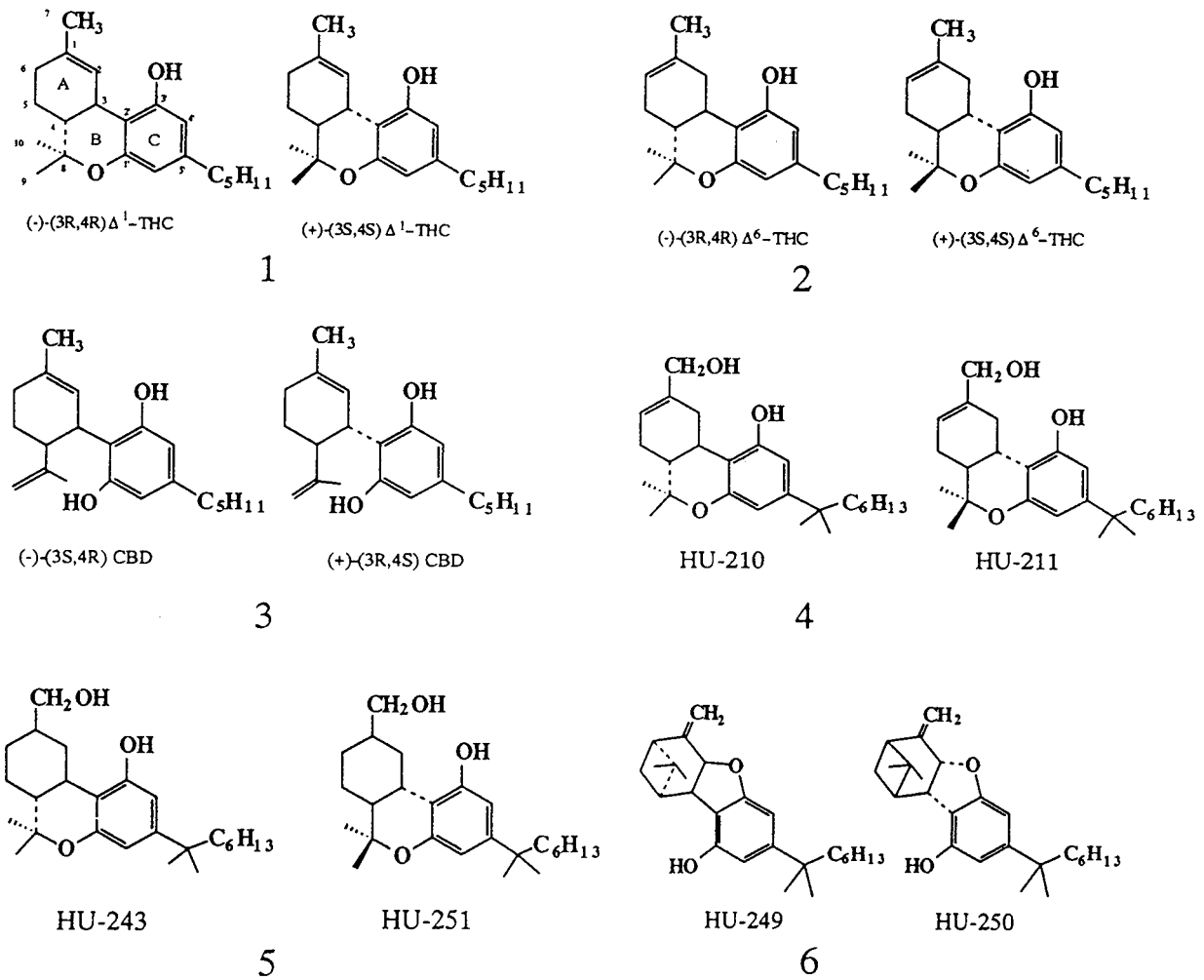

Fig. 2. Structures of the six pairs of cannabinoids studied.

purity is available. Research aimed at the development of therapeutic derivatives of cannabinoids devoid of psychotropic side-effects should include the determination of optical purity. The quantitative criterion of the minimum degree of optical purity of the therapeutic enantiomer is dictated by the pharmacological potency of the contamination. The higher the psychotropic activity of the enantiomer, the stricter is the requirement for optical purity. An extreme example is the enantiomeric pair HU-211 and HU-210, in which the very high undesirable psychotropic effects of HU-210 require that HU-211 should be at least 99.8% optically pure.

A full quantitative study of the limits of detection and determination that constrain the maximum optical purity that can be measured with the ChiralPak column for cannabinoids is currently under study. Preliminary studies involved calibration graphs for the (+)- and (−)-enantiomers of 4-oxomyrtenyl pivalate, the precursors of HU-210 and HU-211. Typical correlation coefficients were above 0.999 and the limits of determination were *ca.* $1 \cdot 10^{-5}$ mol/l (*ca.* 60

TABLE I

CHROMATOGRAPHIC PARAMETERS OF THE SIX PAIRS OF CANNABINOIDS IN FIG. 2 USING VARIOUS ETHANOL CONCENTRATIONS (1–20%, v/v) IN THE MOBILE PHASE

Pair No.	1%				2%				5%				10%				15%				20%			
	k'_+ [a]	k'_- [a]	α [b]	R_s [c]	k'_+	k'_-	α	R_s	k'_+	k'_-	α	R_s	k'_+	k'_-	α	R_s	k'_+	k'_-	α	R_s	k'_+	k'_-	α	R_s
1					3.21	5.93	1.85	9.58	1.13	2.14	1.89	5.08	0.56	1.19	2.10	3.18	0.38	0.86	2.26	2.41				
2	4.01	3.79	1.06	0.85	3.15	2.96	1.06	0.57	1.04	1.04	1.00	0												
3					6.12	8.59	1.40	14.7	1.99	2.84	1.42	2.00	0.83	1.15	1.38	0.42	0.51	0.67	1.30	0.15	0.40	0.49	1.23	0.09
4					4.50	6.85	1.52	44.0	1.07	1.61	1.50	1.05	0.39	0.59	1.51	0.27	0.27	0.42	1.57	0.13	0.17	0.29	1.63	0.11
5					4.52	8.78	1.94	32.6	1.08	1.95	1.79	1.92	0.54	0.80	1.48	0.27	0.26	0.50	1.89	0.19	0.20	0.32	1.63	0.16
6					2.00	7.95	3.96	44.0	0.70	2.68	3.80	6.30	0.38	1.39	3.60	1.75	0.22	0.91	4.00	1.01	0.16	0.71	4.29	0.71

[a] $k' = (t_R - t_0)/t_0$, where t_R is the retention time and t_0 is the void time.
[b] $\alpha = k'_-/k'_+$.
[c] $R_s = 2(t_{R-} - t_{R+})/(w_- + w_+)$, where w is the peak width at the base.

TABLE II

CHROMATOGRAPHIC PARAMETERS OF THE SIX PAIRS OF CANNABINOIDS IN FIG. 2 USING VARIOUS 2-PROPANOL CONCENTRATIONS (2–20%, v/v) IN THE MOBILE PHASE

Pair No.	2%				5%				10%				15%				20%			
	k'_+	k'_-	α	R_s	k'_+	k'_-	α	R_s	k'_+	k'_-	α	R_s	k'_+	k'_-	α	R_s	k'_+	k'_-	α	R_s
1	7.32	11.3	15.4	18.4	2.34	6.73	2.87	14.5	1.06	2.78	2.62	7.92	0.65	1.70	2.60	4.80	0.47	1.24	2.63	3.01
2	6.19	7.79	1.26	9.07	2.01	2.62	1.30	1.40	0.93	1.21	1.30	0.38	0.61	0.78	1.29	0.38	0.38	0.50	1.31	0.11
3	12.9	13.3	1.08	7.77	3.35	3.64	1.09	0.83	1.36	1.48	1.09	0.18	0.76	0.82	1.08	0.07				
4	11.6	21.5	1.84	11.3	3.34	5.14	1.54	7.08	1.07	1.56	1.46	0.86	0.54	0.77	1.42	0.26	0.32	0.45	1.43	0.13
5	9.63	13.5	1.40	9.64	5.29	6.60	1.25	7.64	1.87	2.03	1.08	0.35	0.94	0.95	1.01	0.08				
6	4.93	25.4	5.15	226	1.37	6.45	4.72	19.7	0.62	2.73	4.42	3.8	0.40	1.70	4.22	1.74	0.30	1.23	4.0	1.02

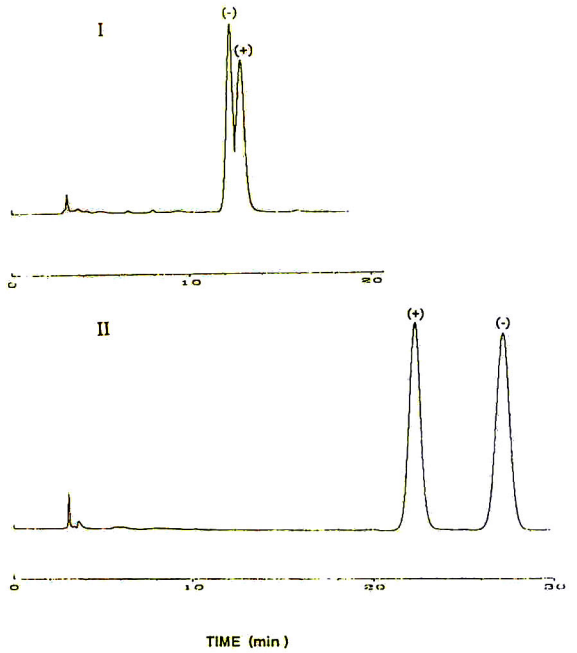

Fig. 3. Chromatograms showing the separation of (+)- and (−)-Δ^6-THC in ethanol and 2-propanol as mobile phase modifiers. Mobile phase: (I) *n*-hexane–ethanol (98:2, v/v); (II) *n*-hexane–2-propanol (98:2, v/v).

ng). Identical calibration graphs were obtained for the individual and the mixed enantiomers owing to the high selectivity and resolution values obtainable in this system. With such limits of determination an enantiomeric purity of 99.9% could be easily assessed. Preliminary studies of Δ^6-THC and Δ^1-THC have shown similar limits of determination. Enantiomeric purities ≥99.9% of all the enantiomers used in the present study could be easily determined.

Sustaining the chiral centre during synthesis

Optically pure cannabinoids can be prepared from chiral starting materials if the chirality is sustained throughout the entire synthesis. It is essential to begin the synthesis with optically pure compounds, and a sensitive enantioselective analysis is required for every stage of the synthesis. For example, (+)-Δ^6-THC can be prepared from (+)-verbenol whereas HU-211 and HU-210 can be prepared from the corresponding (+)- or (−) 4-oxomyrtenyl pivalate. The starting material should be optically pure, otherwise it may yield products of poor enantiomeric purity. Therefore, enantioselective analysis is currently being developed for the complete set of starting materials, intermediates and final products in the synthesis of cannabinoids. Two examples are presented here, the separation of enantiomers of *cis*-verbenol and 4-oxomyrtenyl pivalate in Figs. 4 and 5, respectively. Good separation and sensitivity were observed in both instances.

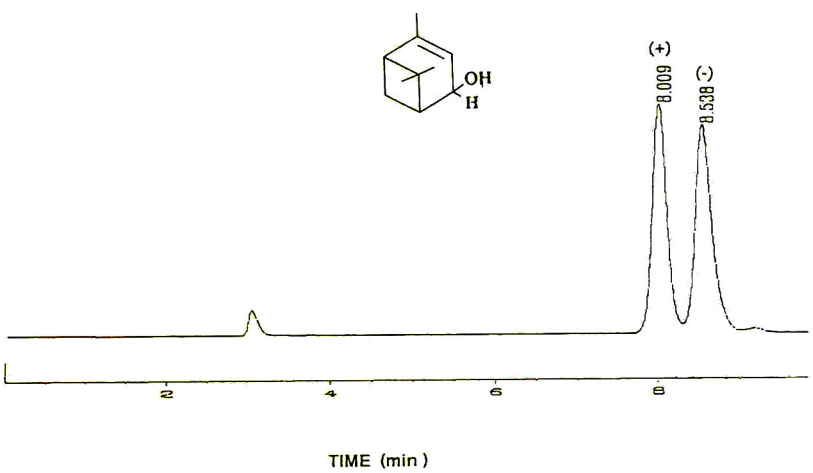

Fig. 4. Chromatogram showing the separation of (+)- and (−)-*cis*-verbenol. Mobile phase, *n*-hexane–ethanol (98:2, v/v); wavelength of detection, 210 nm.

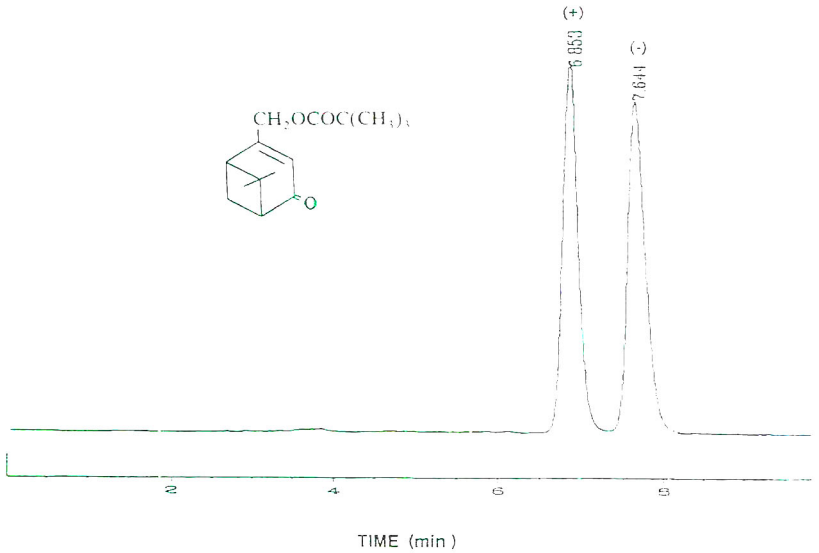

Fig. 5. Chromatogram showing the separation of (+)- and (−)-4-oxomyrtenyl pivalate. Mobile phase, *n*-hexane–2-propanol (95:5, v/v); wavelength of detection, 220 nm.

Selective solvent effects and structural features

The influence of the type and composition of the modifier in the mobile phase on solute retention, elution order, selectivity and resolution was studied with reference to previous observations on other types of polysaccharide-based stationary phases. Values of α and R_s obtained using 2% and 5% of the two modifiers (see Tables I and II) are presented in Figs. 6 and 7. This type of illustration serves as a quick reference to the chromatographic parameters during examination of the structural effects.

The availability of several enantiomeric pairs of cannabinoid compounds made possible preliminary comparative studies of chiral recognition by the chiral sites of the dimethylphenylcarbamate derivatives of amylose. The features, common to all these solutes, are the aromatic moiety and at least one hydroxyl group near the chiral centres. The pairs, shown in Fig. 2, vary from each other in small structural features: position of a double bond on ring A (pairs 1 and 2); open and closed ring B (pairs 1 and 3); and non-saturated and saturated ring A (pairs 4 and 5). These aspects are considered below.

Position of the double bond: Δ^1-THC vs. Δ^9-

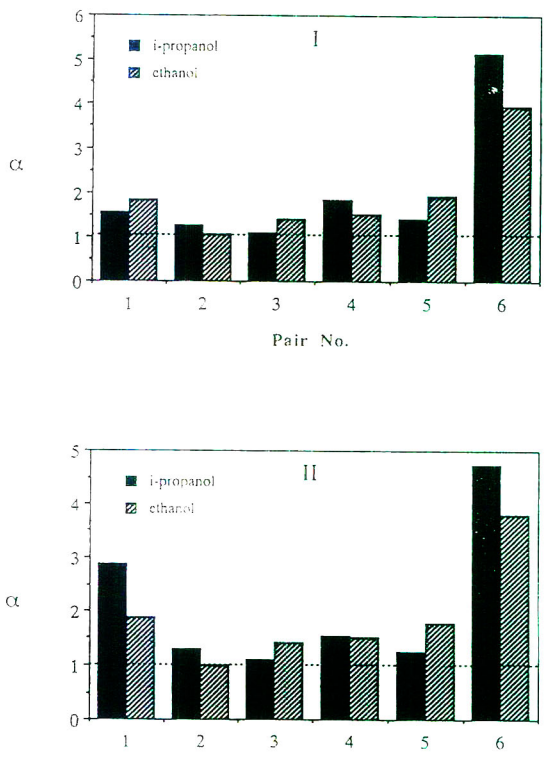

Fig. 6. Selectivity factor of the enantiomeric pairs of the cannabinoids using (I) 2% and (II) 5% (v/v) 2-propanol and ethanol in the mobile phase.

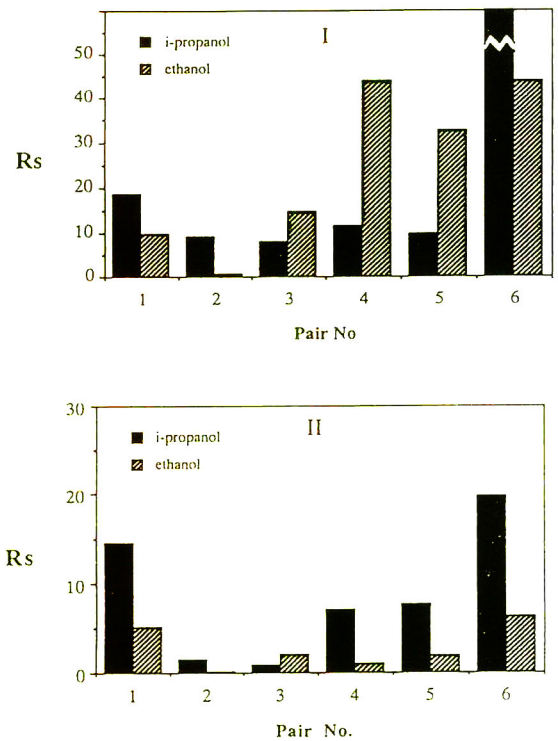

Fig. 7. Resolution between the enantiomeric pairs of the cannabinoids using (I) 2% and (II) 5% (v/v) 2-propanol and ethanol in the mobile phase.

THC. Pair 1 are the natural active cannabinoid (−)-(3*R*,4*R*)-Δ^1-THC and the synthetic (+)-(3*S*,4*S*)-Δ^1-THC enantiomer; pair 2 are the natural (−)-(3*R*,4*R*)-Δ^6-THC and the synthetic (+)-(3*S*,4*S*)-Δ^6-THC enantiomer. The structural difference between the two pairs is the position of the double bond on ring A. The different position of the double bond affected the chromatographic behaviour of the two pairs of enantiomers considerably, the following effects being observed.

The two enantiomers of Δ^1-THC were generally retained longer than the two Δ^6-THC enantiomers, using either modifier, in spite of the presumably subtle difference in polarity between them (see Tables I and II). Apparently, the position of the double bond in ring A dictates the differences in capacity factors of the two enantiomeric pairs of THC.

The selectivity factors and resolution values were generally better for the enantiomers of Δ^1-THC in both solvent systems. Therefore, better selectivity and efficiency, combined with the higher capacity factor of the Δ^1-THC enantiomers compared with Δ^6-THC, indicate a better steric fit with the chiral adsorption sites on the stationary phase.

According to the α and R_s values in Figs. 6 and 7, 2-propanol was the preferred solvent for both the Δ^6-THC and Δ^1-THC pairs. Moreover, the Δ^6-THC enantiomers could not be separated at all using ethanol at concentrations above 2% in the mobile phase. Examination of the efficiency of the resolution revealed that although selectivity factors observed for the (+)- and (−)-Δ^1-THC enantiomers using 2-propanol were comparable to those using ethanol, the resolution was significantly better with 2-propanol. The different efficiency of the separation between ethanol and 2-propanol suggests that the kinetics of the chromatographic process (efficiency of the distribution) in the chiral column are also affected by the solvent.

The elution order was (+)- and then (−)-enantiomers for all the pairs except (+)- and (−)-Δ^6-THC. An unusual reversal of the elution order of (+)- and (−)-Δ^6-THC was observed when the solvent was changed from 2-propanol to ethanol, as shown in Fig. 3. Although the average k' behaved as expected for an achiral normal-phase mode of retention, the elution order of the two enantiomers was changed. The k' values of the two (+)- and (−)-Δ^6-THC enantiomers decreased as the percentage of modifier in the mobile phase increased, keeping the reversed elution order, the (+)-enantiomer being first to elute when 2-propanol was used whereas the (−)-enantiomer was first to elute when ethanol was used.

In contrast to Δ^6-THC, the closely related Δ^1-THC enantiomers showed regular normal-phase retention behaviour with an elution order similar to those for the other enantiomeric pairs in this study.

The reversal of the elution order of the (+)- and (−)-enantiomers of Δ^6-THC indicates that it is sensitive to the steric environment at the chiral binding site. Wainer and co-workers [7,12] suggested that the mobile phase modifier, which is

constantly present at the binding site, plays a role in the chiral discrimination at that site. Either it may alter the steric environment or it has to be displaced from the binding site for a better fit of the solute to the chiral site. The displacement of the modifier molecules from the chiral site can be non-selective, and is common to all the other enantiomers. However, the reversal of the elution order of the (+)- and (−)-enantiomers of Δ^6-THC indicates that there was also an alteration of the shape of the chiral site by ethanol. This suggestion seems to explain the considerable difference between the elution properties of the two alcohol modifiers in the carbamate amylose stationary phase.

In conclusion, the two pairs behaved very differently in the given chromatographic system in spite of the subtle conformational differences between them. Preliminary molecular mechanics calculations on the two isomers (−)-Δ^6-THC and (−)-Δ^1-THC were carried out using the Insight II/Discover 2.0.0 software package of BIOSYM Technologies (San Diego, CA, USA). Superimposition of the two structures gave rise to a very small root mean square difference in the x, y, z coordinates of the heavy atoms, indicating that they have very similar structures. Therefore, the unequal chiral discrimination of the two THC enantiomeric pairs in the chiral binding site obviously cannot be explained by the structural differences between them alone. The position of the double bond in terms of intramolecular distances rather than total conformational changes seems to have a considerable effect on the enantioselective fit of these analytes to the chiral sites on the stationary phase. This assumption is currently being studied, using molecular modelling techniques, to provide new insights into the mechanism of chiral recognition in the amylose-based stationary phase and to explain the differences in the chromatographic behaviour.

Open and closed ring B. Δ^1-THC has a completely different conformation from that of CBD, hence the differences in their chromatographic behaviour are understandable. Δ^1-THC has three rings, A, B and C, with one free phenolic group; CBD has no ring B, and two phenolic groups, with the two A and C rings being almost perpendicular to each other.

The capacity factors observed for the two pairs (see Tables I and II) showed that CBD is retained longer than Δ^1-THC over the entire range of percentages of either ethanol or 2-propanol modifier in the mobile phase. This is a typical behaviour in the normal-phase mode of retention, where an additional hydroxyl group enhances the interaction with the stationary phase. In spite of the longer retention times of CBD, the selectivity factor and resolution were both better for the two enantiomers of Δ^1-THC using both ethanol and 2-propanol. Apparently, the opening of ring B reduced the extent of discrimination between the two CBD enantiomers by the chiral stationary phase.

The selectivity factors and resolution between the two pairs showed that the preferable solvent for the CBD enantiomers was ethanol, in contrast to Δ^1-THC (and Δ^6-THC). Both the selectivity and efficiency of the separation between the CBD enantiomers were better using ethanol. Apparently, the modification of the chiral site by ethanol in the mobile phase (indicated in the previous section) improved the steric fit of CBD enantiomers into the chiral cavity, in contrast to the two THC pairs.

Saturated and non-saturated ring A. Pair 4 (7-OH-DMH-Δ^6-THC) and pair 5 (7-OH-DMH-HHC) have a hydroxyl group on atom 7 attached to ring A. The difference between them is the degree of saturation of ring A. Compounds with unsaturated rings are expected to be retained longer than homologous compounds with saturated rings in the achiral normal-phase retention mode. According to the retention data in Tables I and II, the two enantiomers of HHC (saturated ring A) were retained longer in all instances but one, *viz.*, with *n*-hexane–2-propanol (98:2, v/v). Under these conditions selectivity between the two 7-OH-DMH-Δ^6-THC enantiomers (non saturated ring A) sharply increased, indicating domination of selective interactions.

Examination of the chromatographic parameters of the two pairs in the two solvent systems (Tables I and II, Figs. 6 and 7) reveals that selectivity factors in both solvent systems were comparable, with a slight better discrimination between (+)- and (−)-7-OH-DMH-Δ^6-THC enantiomers. Also, an increase in the percentage of

modifier affected both solutes similarly in all their chromatographic parameters.

Fig. 7 highlights the observation that the two alcoholic modifiers were interchangeable at low percentages for both enantiomeric pairs. 2-Propanol was the preferred modifier at *n*-hexane–modifier (95:5, v/v), whereas ethanol was preferred at *n*-hexane–modifier (98:2, v/v).

It was surprising that the position of the double bond of ring A contributed more to the chromatographic resolution than the saturation of the same ring. It is interesting also that the chromatographic parameters of all three pairs 1, 4 and 5 (Δ^1-THC, 7-OH-DMH-Δ^6-THC and 7-OH-DMH-HHC) were similar in terms of selectivity, efficiency and elution order. Apparently, neither the addition of a bulky alkyl group on ring C nor the hydroxyl attached to atom 7 had a dramatic effect on the capability of the stationary phase to discriminate between the enantiomers.

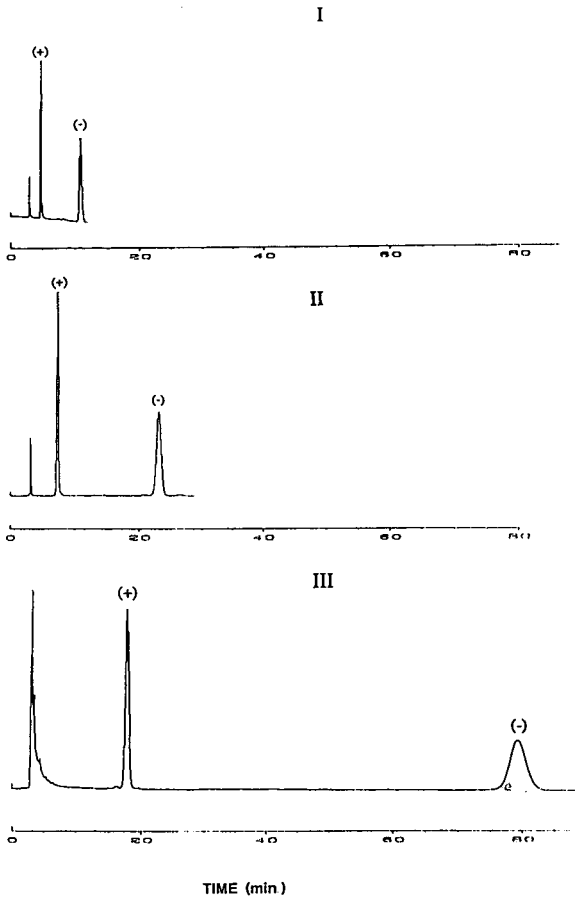

Fig. 8. Chromatograms showing the separation of the tetracyclic HU-249 and HU-250 using the following mixtures of *n*-hexane–2-propanol in the mobile phase: (I) 90:10; (II) 95:5; (III) 98:2 (v/v). Wavelength of detection, 260 nm.

Change of both ring A and ring B. Pair 6, the tetracyclic HU-249 and HU-250, are different from the other cannabinoids in rings A and B; ring C is the same as in pairs 4 and 5. The carbamate derivative of amylose showed an extraordinary capability to discriminate between this two enantiomers under all conditions, even at relatively high percentages of the alcoholic modifiers in the mobile phase, as shown in Fig. 8, where three chromatograms of the two enantiomers, using 2%, 5% and 10% 2-propanol in the mobile phase, are presented. This unusually high degree of discrimination and efficiency of the separation, relative to the other enantiomeric pairs of the cannabinoids studied, supports the suggestion that the conformations of rings A and B, next to the chiral centres, play a key role in the steric fit with the chiral adsorption site.

CONCLUSIONS

The resolution of six enantiomeric pairs of cannabinoids and two pairs of monoterpenes was achieved using an amylose tris(3,5-dimethylphenylcarbamate) stationary phase. The chromatographic system described is capable of assessment of enantiomeric excesses of the cannabinoids $\geq$99.9%. A comparative study of the various pairs indicated that the conformations of rings A and B next to the chiral centres in the cannabinoids are features of major importance in the chiral discrimination by the stationary phase. 2-Propanol and ethanol were not interchangeable in the separation of some of the enantiomeric pairs studied, and their polarity was not the determining factor in their elution properties. These findings supported indications from previous studies on polysaccharide stationary phases that the solvent modifiers participate in the process of chiral discrimination. Molecular modelling of all the solutes that were studied and their steric fit into the chiral sites on the stationary phase is currently being explored in order to understand better the mechanism of chiral discrimination in the present chromatographic system.

ACKNOWLEDGEMENTS

Financial support of this work by the Israel Ministry of Health is gratefully acknowledged. We thank Noa Sobe for her technical help.

REFERENCES

1 J.D.E. Lee and K.M. Williams, *Clin. Pharmacokinet.*, 18 (1990) 339–345.
2 D.R. Taylor and K. Maher, *J. Chromatogr. Sci.*, 30 (1992) 67–85.
3 G. Gubitz, *Chromatographia*, 30 (1990) 555–564.
4 Y. Okamoto, M. Kawashima and K. Hatada, *J. Chromatogr.*, 363 (1986) 173.
5 Y. Okamoto, R. Aburatani, T. Fukumoto and K. Hatada, *Chem. Lett.*, (1987) 1857.
6 Y. Okamoto, R. Aburatani, K. Hatano and K. Hatada, *J. Liq. Chromatogr.*, 11 (1988) 2147–2163.
7 I.W. Wainer, R.M. Stiffin and T. Shibata, *J. Chromatogr.*, 411 (1987) 139.
8 M.H. Gaffney, R.M. Stiffin and I.W. Wainer, *Chromatographia*, 27 (1989) 15.
9 I.W. Wainer and M.C. Alembik, *J. Chromatogr.*, 358 (1986) 85.
10 M. Zief, L.J. Crane and J. Horvath, *J. Liq. Chromatogr.*, 7 (1984) 709.
11 H. Koller, K.-H. Rimbock and Mannschreck, *J. Chromatogr.*, 282 (1983) 89.
12 I.W. Wainer, M.C. Alembik and E. Smith, *J. Chromatogr.*, 388 (1987) 65–74.
13 R.K. Razdan, *Pharmacol. Rev.*, 38 (1986) 75.
14 B.R. Martin, *Pharmacol. Rev.*, 34 (1986) 45.
15 R. Mechoulam (Editor), *Cannabinoids as Therapeutic Agents*, CRC Press, Boca Raton, FL, 1986.
16 W.A. Devane, F.A. Dysarz, III, M.R. Johnson, L.S. Melvin and A.C. Howlett, *Mol. Pharmacol.*, 34 (1988) 605–613.
17 L.A. Matsuda, S.J. Lolait, M.J. Brownstein, A.C. Young and T.I. Bonner, *Nature*, 346 (1990) 561–564.
18 W.A. Devane, L. Hanus, A. Breuer, R.G. Pertwee, L.A. Stevenson, G. Griffin, D. Gibson, A. Mandelbaum, A. Etinger and R. Mechoulam, *Science*, 258 (1992) 1946–1949.
19 R. Mechoulam, N. Lander, A. Breuer and J. Zahalka, *Tetrahedron: Asymmetry*, 1 (1990) 315–318.
20 J.J. Feigenbaum, S.A. Richmond, Y. Weissman and R. Mechoulam, *Eur. J. Pharmacol.*, 169 (1989) 159–165.
21 J.J. Feigenbaum, F. Bergmann, S.A. Richmond, R. Mechoulam, V. Nadler, Y. Kloog and M. Sokolovsky, *Proc. Natl. Acad. Sci. U.S.A.*, 86 (1989) 9584–9587.
22 R. Mechoulam, W.A. Devane and R. Glaser, in L. Murphy and A. Bartke (Editors), *Marijuana/Cannabinoids: Neurobiology and Neurophysiology*, CRC Press, Boca Raton, FL, 1992, pp. 1–33.
23 Y. Gaoni and R. Mechoulam, *J. Am. Chem. Soc.*, 93 (1971) 217.
24 R. Mechoulam, P. Braun and Y. Gaoni, *J. Am. Chem. Soc.*, 94 (1972) 6159.
25 R. Mechoulam and Y. Shvo, *Tetrahedron*, 19 (1963) 2073.
26 J.R. Leite, E.A. Carlini, N. Lander and R. Mechoulam, *Pharmacology*, 24 (1982) 141–146.
27 W.A. Devane, A. Breuer, T. Sheskin, T.U.C. Jarbe, M. Eisen and R. Mechoulam, *J. Med. Chem.*, 35 (1992) 2065–2069.
28 R. Mechoulam, A. Breuer, T.U.C. Jarbe, A.J. Hiltunen and R. Glaser, *J. Med. Chem.*, 33 (1990) 1037–1043.

Journal of Chromatography A, 654 (1993) 65–77
Elsevier Science Publishers B.V., Amsterdam

CHROM. 25 424

Coupling of ion-pair liquid chromatography and thermospray mass spectrometry via phase-system switching with a polymeric trapping column

R.J. Vreeken*, R.T. Ghijsen, R.W. Frei☆, G.J. de Jong☆☆ and U.A.Th. Brinkman

Department of Analytical Chemistry, Free University, De Boelelaan 1083, 1081 HV Amsterdam (Netherlands)

(First received April 15th, 1993; revised manuscript received July 12th, 1993)

ABSTRACT

A trapping column packed with polymeric material (PLRP-S) was used to couple ion-pair liquid chromatography on-line with thermospray mass spectrometry by phase-system switching. Phase-system switching was used to remove non-volatiles from the eluent before it entered the mass spectrometer. The total analytical system was optimized for chlorinated phenoxy acids, which were separated as ion pairs with cetyltrimethylammonium bromide as ion-pair reagent. Parameters such as percentage of modifier and concentrations of ion-pairing reagent and buffer affected the sorption of the ion-pair on the trapping column. Desorption was effected by protonation of the acids with, *e.g.*, trifluoroacetic acid or an ion-pair switch with, *e.g.*, ammonium formate. The influence of pH and modifier concentration during desorption was examined. In addition to target-compound analysis, group-selective analysis was also demonstrated. As an example, the system was used to identify chlorinated phenoxy acids in river Rhine water.

INTRODUCTION

In recent years, the on-line combination of liquid chromatography and mass spectrometry (LC–MS) has developed rapidly [1–3]. The currently popular thermospray (TSP) and particle beam (PB) interfaces are now available from several manufacturers. The choice of the interface depends strongly on the characteristics of the analytes and the information desired; it also limits the range of LC methods available, because all current interfaces have problems with non-volatiles, such as buffer salts, ion-pairing reagents and complexing agents.

So far, research in LC–MS has mainly focused on interface design and MS compatibility. Today, especially with LC–TSP-MS [3], much attention is devoted to the LC part of the system and to topics such as the introduction of on-line preconcentration techniques [4,5] or derivatization procedures [6,7]. The incompatibility of complex LC systems with MS can be solved by eliminating the non-volatiles from the LC eluent [8–25]. In addition to the substitution of volatile additives for non-volatiles [21,23–25], which may affect the selectivity of the LC system, post-column removal of the non-volatiles should be considered. Suppressor membranes [17–20] and postcolumn segmented ion-pair extraction, with subsequent phase separation [15,16,22], have been reported. Several workers have reported the use of valve-switching techniques, *i.e.*, so-called phase-system switching (PSS), to overcome some of the problems [8–14]. Via heart cutting, the analyte is transferred from the LC column to a trapping column (TC), placed at the

* Corresponding author.
☆ Author deceased.
☆☆ Present address: Solvay Duphar B.V., P.O. Box 900, 1380 DA Weesp, Netherlands.

0021-9673/93/$06.00

LC column outlet. Here the analyte is retained and, after removal of the non-volatile constituents, it is desorbed to the MS system using a solvent compatible with the interface and the mass spectrometer. PSS can also be used to change the flow-rate or the modifier concentration or to change the complete solvent system, *e.g.*, from reversed-phase to normal-phase [26]. Flow-rate and modifier concentration certainly affect peak shape after desorption [8,27]. Especially with a mass-flow sensitive detector, *i.e.*, a mass spectrometer, these parameters can improve analyte detectability.

So far, PSS using hydrophobic alkyl-bonded silica or polymeric packing materials as the stationary phase in the trapping column has been used to couple LC with mobile phases containing non-volatile buffers or using eluents with extremely high or low modifier contents to both TSP [10], moving-belt [8,9] and continuous-flow fast atom bombardment (CF-FAB) [11,14] interfaces. In previous work [27], we used an ion-exchange trapping column in LC–PSS–TSP-MS. A benzenesulphonic acid-type cation-exchange column was used to determine quaternary ammonium compounds separated from nasal drops by RPLC with a mobile phase containing 0.1 *M* phosphate.

Nowadays, there is distinct interest in using LC–MS for the determination of ionogenic compounds [1,2,28,29]. Ion-pair LC (IPLC) is a technique used to separate ionogenic compounds that has found many applications in recent years [30]. In IPLC, non-volatile buffers and ion-pairing agents are generally used, which makes on-line coupling with MS virtually impossible. However, on the basis of the above experience, there appears to be a reasonable chance that PSS can help solve this problem.

In this paper, the use of a trapping column packed with a hydrophobic polymer for the on-line coupling of an IPLC procedure involving the use of a non-volatile ion-pairing agent and a buffer with TSP-MS via PSS will be reported. Chlorinated phenoxy acids (pK_a 2.5–3.0) [31] were used as test compounds. They are normally determined by GC–MS after derivatization [32,33], but recently LC [31,34–36] and LC–MS methods [16,23,28,29,37] have been reported. At high pH and with a suitable counter ion, these acids can be separated by IPLC. The hydrophobicity of the trapping column packing should enable one to trap the ion pairs quantitatively and eliminate the non-volatiles present in the LC eluent. After flushing of the trapping column, the compounds of interest can be desorbed and, by using valve-switching techniques, directed to the MS system. The system was studied with regard to the LC modifier concentration and the nature and concentrations of the buffer and ion-pair reagent. The nature of the desorption solution, *i.e.*, the displacer and its concentration, modifier concentration and pH, was also studied.

EXPERIMENTAL

Chemicals

2-Methoxy-4-chlorophenoxyacetic acid (mecoprop), 2,4-dichlorophenoxyacetic acid (2,4-D), 2,4-dichlorophenoxypropionic acid (2,4-DP), 2,4,5-trichlorophenoxyacetic acid (2,4,5-T) and 2,4,5-trichlorophenoxypropionic acid (Silvex), all of 98% purity, were obtained from Sandoz (Basle, Switzerland). Acetonitrile (gradient grade), ammonia solution (25%), formic acid (98%), potassium monohydrogenphosphate and potassium dihydrogenphosphate were obtained from J.T. Baker (Deventer, Netherlands). Ammonium formate (AmFo) solutions were prepared from concentrated formic acid, which was diluted with water and adjusted to the desired pH with ammonia solution. Doubly distilled, demineralized water was used throughout. Tetrahexylammonium bromide ($THxA^+B^-$) and tetraheptylammonium bromide ($THpA^+B^-$) were obtained from Aldrich (Milwaukee, WI, USA), tetramethylammonium bromide (TMA^+B^-) and cetyltrimethylammonium bromide (CTA^+B^-) from Baker and tetrabutylammonium bromide (TBA^+B^-) and iodide (TBA^+I^-) and tetrapentylammonium iodide (TPA^+I^-) from Eastman Kodak (Rochester, NY, USA). Trifluoroacetic acid was purchased from Merck (Darmstadt, Germany). All chemicals were of analytical-reagent grade and were used as received.

Water samples were collected at Lobith (river Rhine) and were obtained from RIZA (Lelystad, Netherlands). Prior to use, they were filtered

through a 0.45-μm BA membrane (Schleicher & Schüll, Dassel, Germany).

Liquid chromatography

The LC system (see Fig. 1) consisted of two Gilson (Villiers-le-Bel, France) Model 302 LC pumps (P1 and P2, flow-rates 0.5 and 1 ml/min, respectively) and one Applied Biosystems (Foster City, CA, USA) Model 400 LC pump (P3, flow-rate 1 ml/min), with laboratory-made pulse dampers. Four six-port valves (Model 7010) were obtained from Rheodyne (Berkeley, CA, USA). Valves 1 and 3 were equipped with a 20- and a 70-μl loop, respectively. A 150 mm × 4.6 mm I.D. analytical column (AC) packed with 5-μm, 90-Å cyano-bonded silica (Chemie Uetikon, Eke, Belgium) and a trapping column consisting of a preconcentration column holder (Chrompack, Middelburg, Netherlands) containing a 10 mm × 4.0 mm I.D. precolumn manually filled with 15–25-μm, 100-Å PLRP-S copolymer material (Polymer Labs, Church Stretton, Shropshire, UK) were used. A Perkin-Elmer (Norwalk, CT, USA) LC-75 UV detector operated at 280 nm was used together with a Kipp & Zonen (Delft, Netherlands) BD 40 recorder.

Mass spectrometry

A Finnigan Model 4500 quadrupole mass spectrometer (Finnigan MAT, San Jose, CA, USA) which was adapted for LC–TSP-MS with a Finnigan TSP interface was used. A typical source temperature was 200°C. The vaporizer temperature was set between 90 and 120°C. The discharge voltage was set at 1000 V; at higher voltages no gain in sensitivity was observed. The repeller voltage was optimized with every new eluent used and was set at a voltage where the background intensity was stable and not all of the clusters were yet dissociated. The voltage generally was in the range −100 to −150 V. All three modes of operation (filament-off, filament-on and discharge ionization) were used. Normally only the negative-ion (NI) mode was used. In addition to full-scan (100–550 u/s) data, selected ion monitoring (SIM) data were also acquired. SIM data were recorded on two ions per compound, *i.e.*, the $[M-H]^-$ and the $[M+HCOO]^-$ ions. The ions were scanned with a mass window of 4 u, *i.e.*, from $[X-1]^-$ up to $[X+2]^-$ (X being the $[M-H]^-$ or the $[M+HCOO]^-$ ion). This was done to determine the noise level ($[X-1]^-$ ion) and to check the isotope ratio ($[X+2]^-$ ion). Typical sampling times were 0.1 s per ion window (4 u wide).

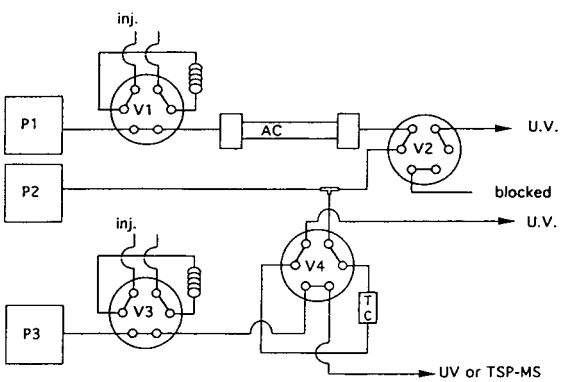

Fig. 1. Set-up of the analytical system used to study sorption, desorption and on-line IPLC–PSS–UV or IPLC–PSS–TSP-MS. P1, P2 and P3, LC pumps delivering a flow of 0.5 ml/min of mobile phase (P1) or 1 ml/min of water (P2 and P3); AC, analytical column; TC, trapping column; V1 and V3, six-port switching valves with 20- and 70-μl loops, respectively; V2 and V4, six-port switching valves.

PSS procedure

For PSS the analytical system depicted in Fig. 1 was used. During optimization of the PSS parameters (sorption, cleaning and desorption) the analytical column was removed. Table I shows the positions of the four valves during the various stages of the optimization procedure performed with flow-injection analysis (FIA). A brief explanation of the procedure is given below. With on-line LC–PSS–TSP-MS, *i.e.*, with the analytical column inserted, the time at which conditioning and sorption (steps 1 and 3, respectively) started depended on the retention time of the analyte; injection of the sample was at time $t = 0$.

In order to condition the trapping column with CTA^+B^- (step 1) after the previous run, valve V2 is switched at $t = 0$. After 2.5 min the analyte is injected into the carrier stream via valve V1 (step 2). After sorption of the analyte on the trapping column (step 3), valve V2 is switched in order to flush the capillaries and the trapping column with water (step 4). By switching valve

TABLE I

VALVE-SWITCHING SCHEDULE FOR THE PSS PROCEDURE

Step	Event	Time (min)	Valve position[a]			
			V1	V2	V3	V4
1	Conditioning of TC with LC eluent	0–2.5	B	B	B	B
2	Injection of analyte	2.5	A	B	B	B
3	Sorption of analyte on TC	2.5–5	A	B	B	B
4	Flushing of capillaries and TC with water	5–7.5	A	A	B	B
5	Changing flow direction of water through TC and making connection with UV or TSP-MS system	7.5–8	A	A	B	A
6	Desorption of analyte by triplicate injection of desorption solvent	8–10	A	A	A	A
7	Cleaning of TC by injection of several loop volumes of cleaning solvent	10–12	A	A	A	A

[a] A =  ; B = 

V4 (step 5) after 7.5 min, the direction of the flow through the trapping column is reversed, for backflush desorption, and the trapping column is switched on-line with the UV detector or the TSP-MS system. After another 30 s of flushing the trapping column in order to remove residual buffer, desorption is achieved by multiple injections of 70 μl of the desorption solvent, via valve V3, in the carrier stream, water (step 6). In order to clean the column completely, valve V3 is used for the injection of several loop volumes of cleaning solvent (step 7). The composition of the sorption, desorption and cleaning solvents will be discussed below.

RESULTS AND DISCUSSION

IPLC is not directly compatible with TSP-MS, because of the presence of non-volatiles in the eluent. PSS [3,8,9] seems to be a simple and straightforward solution to this problem, but designing an IPLC–PSS–TSP-MS system made us realise that many parameters are involved and that this optimization may well lead to mutually conflicting results (see Table II). For example, efficient trapping of the ion pairs on the trapping column requires narrow and well separated peaks eluting from the IPLC column, which have a high capacity factor on the trapping column. However, in IPLC such peaks are obtained after rapid analysis, *i.e.*, using a low concentration of counter ion, a high percentage of modifier and a low ionic strength. Adequate trapping on the trapping column, on the other hand, requires a solution with a low percentage of modifier, a high concentration of counter ion and a high ionic strength. Therefore, in order to optimize the total IPLC–PSS–TSP-MS system, the IPLC separation of the analytes and the PSS procedure using the trapping column were studied separately, taking into account the criteria set by the other steps in the procedure. Finally, the total system was assembled and its overall performance evaluated.

Ion-pair chromatography of phenoxy acids

Chlorinated phenoxy acids can be separated by means of IPLC with various counter ions such as TMA^+, TBA^+ and CTA^+ [31,34–36]. In our study, a reagent was desired that forms an ion pair with a high capacity factor on the trapping column (see Table II), but a much smaller capacity factor on the analytical column (see above). An analytical column containing a

TABLE II

REQUIREMENTS AND PARAMETERS INVOLVED IN DESIGNING AND OPTIMIZING AN IPLC–PSS–TSP-MS SYSTEM

Part of system	Requirements	Aspects
LC	Analyte in ionized form	Buffer mobile phase at $pH > pK_a + 2$
	Counter ion	Counter ion $R_4N^+X^-$ ($R = C_1$–C_{16})
	Stationary phase	RP-type material
Trapping	Narrow peaks (low k' for ion pairs in LC)	High % modifier, low counter ion concentration and low ionic strength
	Preconditioned TC	Loading time and concentration of counter ion
	High k' for ion pairs on TC	Low % modifier, high counter ion concentration, high ionic strength and hydrophobic stationary phase
Flushing	High k' for ion pairs on TC	No or low % modifier, hydrophobic stationary phase
Desorption	Low k' for analyte on TC	$pH \leq pK_a - 2$, high displacer concentration and high % modifier
	Extremely high k' for counter ion on TC	High displacer concentration and low % modifier
Detection with SP-MS	TSP-MS-compatible solvent	No counter ion and low % modifier
	Volatile additives	Low additives concentration

cyano-bonded silica and a trapping column packed with a polymer such as PLRP-S provide a large difference in hydrophobicity. With this combination, different tetraalkylammonium salts (concentration 1 m*M*), with alkyl groups from methyl up to hexyl, and CTA^+B^- were tested as ion-pair agents. As expected, the higher the hydrophobicity of the ion-pair agent and the lower the modifier percentage, the higher is the retention. CTA^+, a popular cationic counter ion in IPLC [38,39], appears to be a good choice in the present instance also. However, it will certainly clog the vaporizer of the TSP-MS unit unless it is completely removed beforehand.

With 10 m*M* sodium phosphate buffer (pH 7)–acetonitrile (90:10, v/v) as the LC eluent, the concentration of CTA^+B^- was varied from 0.1 to 10 m*M*. Although the retention times of the phenoxy acids increased rapidly with increasing CTA^+B^- concentration, *i.e.*, up to 65 min [29], the resolution increased only slightly. A compromise between analysis time and resolution was found at a CTA^+B^- concentration of 1 m*M*, resulting in two sets of peaks. Fig. 2 shows the IPLC–UV traces for each of the compounds with an aqueous 1 m*M* CTA^+B^-, 10 m*M* sodium phosphate (pH 7)–acetonitrile (70:30, v/v) eluent. One group consists of mecoprop, 2,4-D and 2,4-DP ($k' = 1.8$–2.2) and the other of 2,4,5-T and 2,4,5-TP ($k' = 3.3$–3.4). In fact, the in-

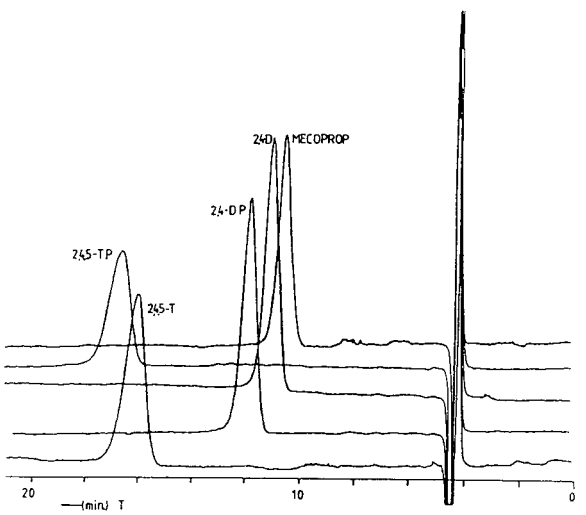

Fig. 2. IPLC–UV traces for the five test compounds (mecoprop, 2,4-D, 2,4-DP, 2,4,5-T and 2,4,5-TP; concentration 10^{-5} *M*) injected separately on a cyano-bonded silica (5-μm, 90-Å) column. Eluent, water (1 m*M* CTA^+B^-, 10 m*M* sodium phosphate buffer, pH 7)–acetonitrile (70:30, v/v); injection volume, 20 μl; flow-rate, 0.5 ml/min; UV detection at 280 nm.

complete separation is interesting, because simultaneous trapping and desorption of several compounds at the same time can now be studied.

PSS

Using a PSS procedure for on-line IPLC–TSP-MS is complicated (see Table II). For example, in order to have sufficient retention, the capacity factors of the test compounds on the trapping column should at least be equal to $(6\sigma_{v,AC}/V_{0,TC}) - 1$ ($\sigma_{v,AC}$ is the peak standard deviation of the analytical column and $V_{0,TC}$ the void volume of the trapping column [3,9]). Further, if instead of selective packing materials such as an anion or a cation exchanger [27] a non-selective stationary phase is used, one should be aware of the fact that, in addition to the counter ion–analyte ion pair, also the ion-pair reagent itself will be trapped. Third, a solvent must be found that effects rapid desorption of the phenoxy acids from the trapping column and is suitable for direct introduction into the TSP-MS system. Finally, a cleaning step will be necessary, especially after selective analyte desorption leaving the ion-pairing reagent on the trapping column.

Several parameters will influence the recovery of the analytes during each of the steps in the PSS procedure. Therefore, each step was optimized separately. The analyte recovery was determined as the ratio of the summed peak areas (TSP-MS) or peak heights (UV) of the desorbed compound after multiple desorptions (see below) and the peak area or height in FIA.

Sorption. In order to check the capacity of the 10 mm × 3.0 mm I.D. trapping column packed with 15–25-μm, 100-Å PLRP-S, breakthrough volumes (V_b) of 2,4-D and 2,4,5-T (concentration 10^{-4} *M*), were determined using various eluents. Without CTA^+B^- added to the eluent (water), the phenoxy acids showed breakthrough volumes of less than 1 ml. Adding CTA^+B^- and adjusting the pH to 7, to ensure dissociation of the acids, gave a marked increase to values of over 100 ml (Table III). The addition of acetonitrile, of course, caused the breakthrough volumes to decrease rapidly. Quantitative trapping was still possible, however, with an eluent containing *ca.* 20% of acetonitrile. Although, theoretically, breakthrough volumes of 1.5–2.5 ml are large enough to trap the phenoxy acids, in practice they are too small, especially when flushing of the trapping column, to remove non-volatiles, is considered. In other words, the acetonitrile concentration should be lower than 15%.

TABLE III

BREAKTHROUGH VOLUMES OF 2,4-D AND 2,4,5-T (10^{-4} *M*) ON A TC (PLRP-S) IN WATER (1 m*M* CTA^+B^-, 10 m*M* PHOSPHATE BUFFER, pH 7) CONTAINING 0–30% OF ACETONITRILE

Concentration of acetonitrile (%, v/v)	Breakthrough volume (ml)	
	2,4-D	2,4,5-T
0	>100	>100
10	50	75
15	4	5
20	1.5	2.5
25	0.5	1.5
30	–	0.5

Subsequently, preloading of the trapping column with CTA^+ was examined to achieve higher breakthrough volumes, which could result in higher allowable modifier concentrations during IPLC. Loading the trapping column with CTA^+B^- by passing 1 ml of water (1 m*M* CTA^+B^-, 10 m*M* phosphate buffer, pH 7)–acetonitrile (75:25, v/v) over it at 1 ml/min caused a 2–3-fold increase of the breakthrough volumes of the test compounds compared with a non-loaded trapping column. No further gain was observed with longer preconditioning times.

In summary, when using water (1 m*M* CTA^+B^-, 10 m*M* phosphate buffer pH 7)–acetonitrile (85:15, v/v) as eluent and a CTA^+B^--loaded trapping column, the breakthrough volumes will be sufficiently large to prevent breakthrough of the phenoxy acids during sorption and flushing (see below).

Finally, the ionic strength of the sorption eluent was examined. Changing the concentration of the sodium phosphate buffer (pH 7) from 1 to 100 m*M* in an aqueous 1 m*M* CTA^+B^-–acetonitrile (85:15, v/v) solution gave no signifi-

cant changes in the breakthrough volumes. A 10 m*M* buffer was used in all further experiments.

Flushing. Prior to desorption of the analytes, the PSS unit, *i.e.*, the connecting capillaries and the trapping column, must be flushed to remove the ion-pairing reagent and the phosphate buffer in order to avoid contamination of the mass spectrometer. Avoiding contamination of the MS, the system was flushed with 2.5 ml of water at 1 ml/min, *i.e.*, 50 times the void volume. With UV detection no breakthrough of the test compounds was observed during this washing step.

Desorption. Once the counter ion–analyte ion pair has been trapped, desorption can be performed, either by desorption of the ion pair or by selective desorption of the analyte itself. If the ion pair is sufficiently volatile not to block the vaporizer, *e.g.*, with tetramethyl- and tetraethylammonium ion pairs [40], the intact ion pair can easily be desorbed to the mass spectrometer by increasing the modifier concentration. However, in the case of a non-volatile ion pair, *e.g.*, CTA^+ ion pairs, selective desorption should be used.

In this study, *i.e.*, using CTA^+–phenoxy acid ion pairs, desorption can be accomplished by breaking up the ion-pair via protonation of the acid or by forming a volatile ion pair with a volatile counter ion via an ion-pair switch.

First, the effect of the modifier concentration (range tested 0–80%) on the desorption of the ion-pairing reagent and analyte was studied to determine the maximum allowable modifier percentage that still retains the ion-pairing reagent on the trapping column. Quantitative desorption of the analyte could be accomplished with an aqueous desorption solvent containing at least 40% of acetonitrile. However, as was confirmed by the decrease in breakthrough volumes after desorption, the analyte is then desorbed as a CTA^+ ion pair. In fact, more than 90% of the CTA^+X^- (X being the phenoxy acid or bromide) is desorbed. In order to prevent CTA^+ desorption completely, the acetonitrile content of the desorption solvent should be less than 25%.

Desorption by protonation. Protonation of the phenoxy acids at low pH was studied by adding trifluoroacetic acid (TFA) to the desorption solvent. As the phenoxy acids have pK_a values of 2.5–3.0, quantitative protonation only occurs at $pH < 1$. However, at these pH values the PLRP-S material in the trapping column slowly dissolves. When, on the other hand, desorption is carried out by plugs of a strongly acidic solution, injected via a loop mounted on valve V3 (see Fig. 1), into the carrier stream, the polymer material will be less affected. In most instances, 3–5 plugs of aqueous TFA solution were injected. Varying the TFA concentration (range tested 0.06–6 *M*) showed a shallow optimum at 3 *M* TFA (pH 0.1; 80–90% recovery for 2,4-D and 2,4,5-T). However, even using small loop volumes (10–15-μl plugs), the trapping column deteriorated rapidly. After fifteen analyses the breakthrough volumes had dramatically decreased and the trapping column had to be repacked. Therefore, as an alternative, the TFA concentration was decreased (to 0.25 *M*) and simultaneously acetonitrile was added to the solution (25%, v/v is allowed; see above). Further, the loop volume was increased to 70 μl (no deterioration of the trapping column was observed), because this will decrease the number of plugs necessary for complete desorption. Three plugs of aqueous 0.25 *M* TFA (pH 0.85)–acetonitrile (75:25, v/v) resulted in 80–85% recoveries of the phenoxy acids without any desorption of CTA^+.

TFA also served as a displacer for the phenoxy acids from the trapped ion pair. This was concluded from the fact that the first cleaning step with water–acetonitrile (17:83, v/v) (see *Cleaning*) showed an intense peak (not observed when no TFA was used) when UV detection was used. This signal is obviously caused by desorption of the CTA^+–TFA^- ion pair.

Desorption by ion-pair switching. Several quaternary ammonium compounds [ammonium acetate, formate (AmFo) and oxalate, tetramethyl- and tetrabutylammonium salts such as iodides, fluorides, bromides, hydroxides and nitrates] dissolved in water and in water–acetonitrile were tested with regard to their desorption efficiency. Using 70-μl plugs of 0.1 *M* salt solutions in water–acetonitrile (75:25, v/v), AmFo and the ammonium bromide and iodide salts effected desorption of the phenoxy acids from the trapping column (30–60% for 2,4-D

with a single 70-μl plug, compared with less than 15% with 0.1 *M* salt solutions in pure water). The desorption efficiencies of the iodide salts were higher than those obtained with the corresponding bromides. This is due to the larger ionic radius of the iodides [41], resulting in better ion-pair formation.

As tetramethylammonium iodide is of low volatility and will clog the vaporizer, AmFo is the only compound suitable for desorption. Optimization of the AmFo concentration (range tested 0.05–2 *M*) in water–acetonitrile (75:25, v/v) resulted in desorption efficiencies of 80–90% for 2,4-D and 2,4,5-T (three 70-μl injections; 60% after the first injection) with 0.5 *M* AmFo. At higher AmFo concentrations, the analyte recovery did not increase any further; in fact, it even decreased slightly, possibly because of salting-out of the analyte.

These first experiments were carried out at pH 5. Optimization with respect to the pH was performed with 2,4-D as test solute. Fig. 3 indicates that analyte recovery is essentially quantitative at pH 5.7–7.6 with one injection of 70 μl (the relatively good result at pH 2.6 can be attributed to protonation of the phenoxy acid). This can be explained by the formation of a volatile ion pair between the ammonium ions, present in large excess, and the deprotonated phenoxy acid, with the formate ion occupying the vacant position on the CTA^+-loaded stationary phase. Similar high recoveries (90–100%) were obtained for all other test solutes. Measuring the breakthrough volume of 2,4-D directly after desorption, with water (0.5 *M* AmFo, pH 7.6)–acetonitrile (75:25, v/v), confirmed that no CTA^+X^- (X being the phenoxy acid or bromide) is desorbed.

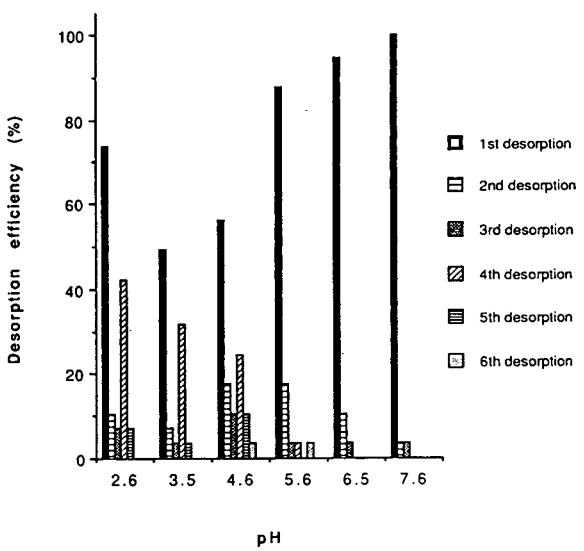

Fig. 3. Influence of the pH of the desorption solvent [70-μl plugs of aqueous 0.5 *M* AmFo–acetonitrile (75:25, v/v)] injected into the carrier stream (water) on the desorption efficiency of 2,4-D ($n = 5$, R.S.D. 10%). Analyte concentration, $5 \cdot 10^{-6}$ *M*; injection volume, 20 μl; flow-rate, 1 ml/min; UV detection at 280 nm.

Cleaning. After each run, the trapping column was cleaned with several loop volumes (70 μl) of water–acetonitrile (17:83, v/v). It became clear, by measuring the breakthrough volumes of 2,4-D on the trapping column directly after this cleaning step, that five loop volumes were necessary to clean the trapping column effectively (2–3-fold reduction of the breakthrough volume; see above).

IPLC–PSS–UV coupling

Separation and trapping of the phenoxy acids require different percentages of acetonitrile in the LC eluent, *viz.*, *ca.* 30% *versus* 10–15%. By using a flow-rate of 0.5 ml/min for the LC eluent and postcolumn addition of water at 1 ml/min, both criteria can be met. Although the reduced flow-rate increased the retention times, the separation of the phenoxy acids was still achieved within 20 min (see Fig. 2). In addition, the preloading time for the trapping column had to be adjusted, *i.e.*, up to 2.5 min, because of the lower concentration of CTA^+B^- (0.33 m*M* instead of 1 m*M*) in the mobile phase entering the trapping column.

Desorption was carried out with both water (0.25 *M* TFA, pH 0.85)–acetonitrile (75:25, v/v), and water (0.5 *M* AmFo, pH 7.6)–acetonitrile (75:25, v/v). After performing the whole procedure, *i.e.*, separation, trapping, flushing and desorption, the summed peak areas of three desorptions were compared with the peak areas measured by the UV detector at the outlet of the analytical column. The recoveries were 80–95% for all analytes with both desorption solutions. The method showed linear calibration graphs,

i.e., $r^2 = 0.981–0.993$, over two orders of magnitude of concentration (range $10^{-4}–10^{-6}$ *M*). For higher concentrations, the recovery decreased because of incomplete desorption, *i.e.*, a too low concentration of TFA or AmFo, or breakthrough of the compounds. Increasing the concentration of TFA or AmFo will cause problems with the PLRP-S material (TFA) or faster contamination of the ion source (AmFo). Under the present conditions, the limits of detection (LODs) of the phenoxy acids ranged from $5 \cdot 10^{-7}$ to $1 \cdot 10^{-6}$ *M* (20 μl injected).

During desorption of the test compounds from the trapping column, peak compression can be obtained or, in other words, the concentration of the analyte in the peak maximum, C_{max}, can be increased [9,13]. Increasing the flow-rate has the same effect (square root [13]), but the main gain stems from a proper choice of the trapping column material and the solvents used during sorption and desorption. They determine the capacity factors during trapping (k'_{in}) and desorption (k'_{out}). The above can be expressed by the following equation, which was adapted from Verhey [13]:

$$C_{max} = \frac{m}{(1 + k'_{out})} \sqrt{\frac{(1 + k'_{in})}{(2\pi A_{TC} H_{TC} 3\sigma_{AC})}}$$

where m is the mass of analyte injected, A_{TC} and H_{TC} the column area and plate height of the trapping column, respectively, and σ_{AC} the peak standard deviation.

The capacity factors, k'_{in}, can easily be increased by adding water to the column effluent. As the breakthrough volume is directly related to the capacity factor, the attainable peak compression can be roughly estimated from the data given in Table III. Decreasing the acetonitrile content from 30 to 10% causes an increase in C_{max} of $50^{0.5}$ and $75^{0.5}$ for 2,4-D and 2,4,5-T, respectively. Peak compression factors, determined by comparing peak widths directly after elution from the analytical column and after desorption, were 6.5 for mecoprop, 2,4-D and 2,4-DP and 8.5 for the later eluting 2,4,5-T and 2,4,5-TP. These data agree well with the predicted values, especially when the decrease in flow-rate (see above) and the extra band broadening in the connecting capillaries and valves are considered.

IPLC–PSS–TSP-MS coupling

Analyte detectability in LC–TSP-MS is influenced by factors such as ionization technique, percentage of modifier, vaporizer temperature and flow-rate stability. As regards the last aspect, Walhagen *et al.* [10] observed a background signal at all masses during desorption of the analyte which originated from the valve switching necessary to resume liquid introduction into the interface. We circumvented this problem by using an extra valve (valve V3 in Fig. 1). The TSP-MS system was now operated at a continuous flow of 1 ml/min of water, which led to a stable signal. Because water is used, desorption will not take place after on-line switching of the trapping column and the TSP-MS system. Desorption is carried out by injection(s) of (a) desorption plug(s) into the carrier stream.

When aqueous 0.25 *M* TFA (pH 0.85)–acetonitrile (75:25, v/v) was used for desorption of the analytes, many large signals of TFA-containing clusters (up to m/z 500) were observed in the mass spectrum. Because of the high electron-capturing ability of TFA, the ionization efficiency of the analytes was negatively influenced, and clusters between TFA and the phenoxy acids, expected on the basis of the gas-phase acidities [42], were not observed. Further experiments with this desorbent were considered to be superfluous.

With aqueous 0.5 *M* AmFo (pH 7.6)–acetonitrile (75:25, v/v) as desorbent, a high background signal was also observed during the first desorption. The mass spectrum was dominated by bromide ions and clusters containing bromide ions which originate from the CTA^+B^- used as ion-pairing agent. As these ions also influence the ionization efficiency, they must be removed before desorption of the analyte. A single clean-up desorption with aqueous 0.25 *M* AmFo (pH 5.2) was found to be sufficient to remove the bromide-containing ions from the trapping column. This is shown in Fig. 4, where the ion current traces (full-scan acquisition) of the deprotonated molecular ion and the formate adduct of mecoprop and one of the bromide-

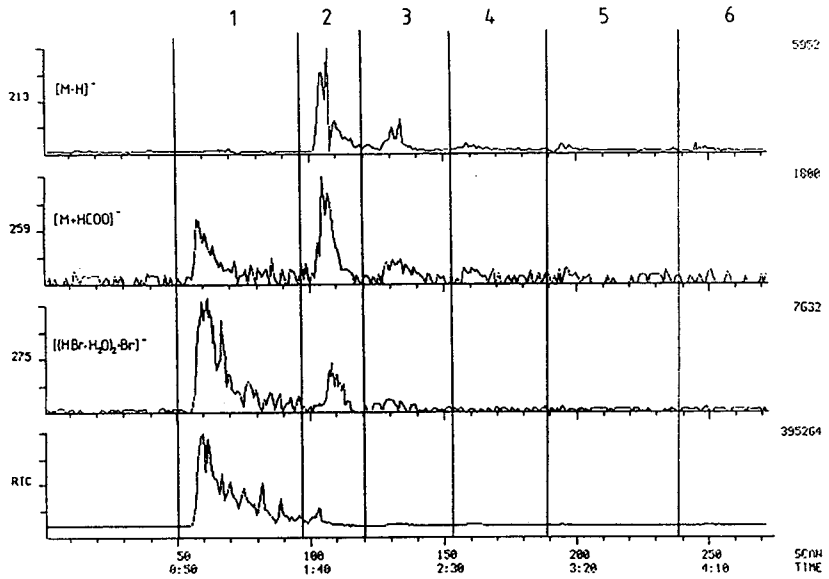

Fig. 4. Reconstructed ion current of the IPLC–PSS–TSP-MS (full-scan) analysis of mecoprop (concentration 10^{-5} *M*). Ions at *m/z* 213, 259 and 275 correspond to $[M-H]^-$, $[M+HCOO]^-$ and $[(HBr \cdot H_2O)_2 \cdot Br]^-$, respectively. Desorption No. 1: cleaning of the TC to remove the bromide with 70 μl of 250 m*M* AmFo (pH 5.2) in water. Analyte desorptions 2–6: five injections of 70 μl of aqueous 0.5 *M* AmFo (pH 7.6)–acetonitrile (75:25, v/v) into a carrier stream of water (flow-rate 1 ml/min). Time in min:s.

containing ions at *m/z* 213, 259 and 275, respectively, are shown. The clean-up desorption (desorption No. 1) clearly releases most of the bromide-containing ions. Next, the analyte is desorbed using injections of water (0.5 *M* AmFo, pH 7.6)–acetonitrile (75:25, v/v) into the carrier stream (water) (desorptions 2–6), as was described in the previous section. It is clear that analyte desorption is complete (>95%) after three desorptions (desorptions 2–4). A further optimization of the loop volume, *i.e.*, 70 μl (valve 3; Fig. 1), to reduce the number of desorptions was not carried out because otherwise it would have been necessary to optimize the AmFo concentration and the percentage of acetonitrile again.

Finally, the signal at *m/z* 259 suggests analyte release during the clean-up desorption (desorption 1); however, full-scan mass spectra showed that this signal can be attributed to the isotope peak of the $[(HBr)_2 \cdot H_2O \cdot Br]^-$ ion at *m/z* 257. Using the positive-ion mode it was confirmed that no CTA^+ desorption took place during the above sequence. This is in agreement with the results obtained above.

Fig. 5 shows the full-scan mass spectra of 10^{-5} *M* solutions of mecoprop and 2,4,5-TP after on-line IPLC–PSS–TSP-MS, using discharge ionization in the negative-ion mode. The $[M-H]^-$ ion was the base peak for all test compounds. The $[M+HCOO]^-$ ion was present in all instances with intensities up to 100%. Although the $[M+HCOO]^-$ ion was more abundant with filament-off and filament-on ionization, higher signal-to-noise ratios were obtained with discharge ionization. Therefore, discharge ionization was used in all further experiments.

Using the complete on-line system, good-quality full-scan mass spectra were obtained for the test compounds at levels down to 10 ng injected into the system, *i.e.*, 20 μl of $2 \cdot 10^{-6}$ *M* solutions. With SIM, on two ions per compound, the LODs were 0.1–1 ng for all five test compounds. Linear calibration graphs ($r^2 = 0.925$–0.973, seven data points, $n = 5$) were obtained over three orders of magnitude of concentration (range 10^{-7}–10^{-4} *M*) with the complete system.

As an example of group-selective analysis, mecoprop, 2,4-D and 2,4-DP were trapped simultaneously (elution window 9–13 min). The results were identical with those found for the individual compounds. However, at high concen-

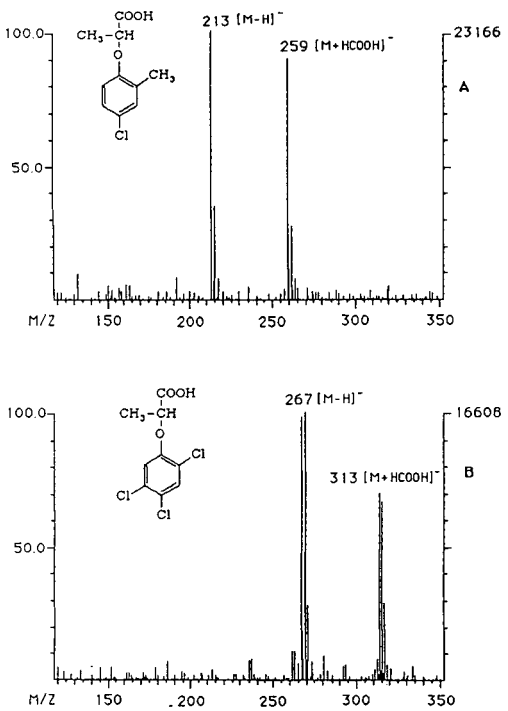

Fig. 5. Full-scan mass spectra of (A) mecoprop and (B) 2,4,5-TP after on-line IPLC–PSS–TSP-MS, using discharge ionization. Desorption solvent, 70 μl of water (0.5 *M* AmFo, PH 7.6)–acetonitrile (75:25, v/v) injected into the carrier stream (water, flow-rate 1 ml/min). Analyte concentration, 10^{-5} *M*.

trations, *i.e.*, above *ca.* $5 \cdot 10^{-5}$ *M*, the analyte recovery decreased because of early breakthrough.

In a first attempt to study a real sample, 100 μl of river Rhine water were analysed without any trace enrichment or sample clean-up (apart from membrane filtration). The test compounds (spiking level 20 μg/l) were separated, trapped on the PLRP-S column, desorbed and subsequently detected by TSP-MS. Although at this level, which was close to the LODs (amount injected 2 ng per analyte), reliable quantification could not be achieved, the SIM signals confirmed the presence of the phenoxy acids in the sample by their correct isotope ratios. In other words, even a modest degree of analyte trace enrichment (*e.g.*, *ca.* 50-ml volumes [5]) will be sufficient for the analysis of surface water samples containing phenoxy acids and related contaminants at or below the so-called alert level of 1 μg/l (amount then injected *ca.* 50 ng of each analyte).

CONCLUSIONS

The on-line coupling of IPLC and TSP-MS via PSS has been demonstrated for the first time. A non-selective hydrophobic polymer was used as the stationary phase in the trapping column. Designing an IPLC–PSS–TSP-MS system turned out to be very complicated because of the many experimental aspects involved (see Table II). The system described here, which uses CTA^+ as the counter ion, is in principle applicable to a wide variety of acidic compounds. In principle, although with another counter ion, it is also applicable to basic compounds, *e.g.*, secondary and tertiary amines, which can be separated by IPLC with sulphonates or sulphates as counter ions.

Optimum sorption of the phenoxy acids was achieved, after preloading the trapping column with CTA^+B^-, using water (1 m*M* CTA^+B^-, 10 m*M* phosphate buffer, pH 7)–acetonitrile (90:10, v/v). Desorption of the analytes was accomplished by three 70-μl injections of water (0.5 *M* AmFo, pH 7.6)–acetonitrile (75:25, v/v) into the carrier stream (water). Postcolumn addition of water proved to be a simple way to increase the capacity factor of the ion pair on the trapping column, *i.e.*, obtaining peak compression.

Desorption by means of plugs injected into a carrier stream, instead of desorption by flushing with an eluent, proved advantageous as many eluents suitable for desorption could be screened in a relatively short time. Further, the desorption solvent need not be the optimum solvent for the interface used. Nevertheless, desorption with high concentrations of the electronegative TFA is not advisable in this instance because of its adverse effect on the ionization.

On injecting standard solutions of the phenoxy acids into the IPLC–PSS–TSP-MS system, the recoveries were at least 90% for all five analytes tested. Recording full-scan mass spectra required an injected mass of at least 10 ng; the LODs using SIM were between 0.1 and 1 ng. First experiments with surface water samples showed

distinctly higher background signals and increased noise. However, even under these conditions, the phenoxy acids could be detected at the low-nanogram level. Therefore, using on-line trace enrichment of a sample volume of about 50 ml (see refs. 5, 43, 44 and 45 for its successful use in LC–UV and LC–MS), application to environmental analysis at contamination levels of, typically, 0.5 μg/l should pose no problems.

ACKNOWLEDGEMENTS

We thank G. Bakker, J. Brakenhoff and W.D. van Dongen for their experimental contributions to this work. The investigations were supported by the Netherlands Foundation for Chemical Research (SON) with financial aid from the Netherlands Organization for the Advancement of Scientific Research (NWO), grant No. 700.344.006.

REFERENCES

1 A.L. Yergey, G.E. Edmonds, I.A.S. Lewis and M.L. Vestal (Editors), *Liquid Chromatography/Mass Spectrometry. Techniques and Applications*, Plenum Press, New York, 1990.
2 M.A. Brown (Editor), *Liquid Chromatography/Mass Spectrometry. Applications in Agriculture, Pharmaceutical, and Environmental Chemistry (ACS Symposium Series*, No. 420), American Chemical Society, Washington, DC, 1990.
3 J. van der Greef, W.M.A. Niessen and U.R. Tjaden, *J. Chromatogr.*, 474 (1989) 5.
4 R.J. Vreeken, H. Bagheri, R.T. Ghijsen and U.A.Th. Brinkman, in preparation.
5 H. Bagheri, E.R. Brouwer, R.T. Ghijsen and U.A.Th. Brinkman, *Analysis*, 8 (1992) 475.
6 R.J. Vreeken, M. Honing, R.T. Ghijsen, G.J. de Jong and U.A.Th. Brinkman, *Biol. Mass Spectrom.*, in press.
7 J. Paulson and C. Lindberg, *J. Chromatogr.*, 554 (1991) 149.
8 E.R. Verhey, H.J.E.M. Reeuwijk, W.M.A. Niessen, U.R. Tjaden and J. van der Greef, *Biomed. Environ. Mass Spectrom.*, 16 (1988) 393.
9 J. van der Greef, W.M.A. Niessen and U.R. Tjaden, *J. Pharm. Biomed. Anal.*, 6 (1989) 565.
10 A. Walhagen, L.E. Edholm, C.E.M. Heeremans, R.A.M. van der Hoeven, W.A.M. Niessen, U.R. Tjaden and J. van der Greef, *J. Chromatogr.*, 474 (1989) 257.
11 P.S. Kokkonen, W.M.A. Niessen and U.R. Tjaden, *J. Chromatogr.*, 565 (1991) 265.
12 W. Luyten, G. Damien and J. Capart, *J. Chromatogr.*, 474 (1989) 265.
13 E.R. Verhey, *Ph.D. Thesis*, Leiden University, Leiden, 1993, pp. 71–81.
14 N. Asakawa, H. Ohe, M. Tsimo, Y. Nezu, Y. Yoshida and T. Sato, *J. Chromatogr.*, 541 (1991) 231.
15 D. Barceló, G. Durand, R.J. Vreeken, G.J. de Jong and U.A.Th. Brinkman, *Anal. Chem.*, 62 (1990) 1696.
16 D. Barceló, G. Durand, R.J. Vreeken, G.J. de Jong, H. Lingeman and U.A.Th. Brinkman, *J. Chromatogr.*, 553 (1991) 311.
17 R.C. Simpson, C.C. Fenselau, M.R. Hardy, R.R. Townsend, Y.C. Lee and R.J. Cotter, *Anal. Chem.*, 62 (1990) 248.
18 J.J. Conboy, J.D. Henion, M.W. Martin and J.A. Zweigenbaum, *Anal. Chem.*, 62 (1990) 800.
19 J. Hsu, *Anal. Chem.*, 64 (1992) 434.
20 W.M.A. Niessen, R.A.M. van der Hoeven, J. van der Greef, J. Schols, G. Lucas-Lokhorst, A.G.J. Voragen and C. Bruggink, *Rapid Commun. Mass Spectrom.*, 6 (1992) 474.
21 R.D. Voyksner and C.A. Haney, *Anal. Chem.*, 57 (1985) 991.
22 P. Vouros, E.P. Lankmayr, M.J. Hayes and B.L. Karger, *J. Chromatogr.*, 251 (1982) 175.
23 D. Barceló, *Org. Mass Spectrom.*, 24 (1989) 219.
24 R.E.A. Escott and D.W. Chandler, *J. Chromatogr. Sci.*, 27 (1989) 134.
25 A.L.L. Duchateau, R.G.J. van Leuken and G.T.C. Kwakkenbos, *J. Chromatogr.*, 552 (1991) 605.
26 E. Noroozian, F.A. Maris, R.B. Geerdink, R.W. Frei, G.J. de Jong and U.A.Th. Brinkman, *J. High Resolut. Chromatogr. Chromatogr. Commun.*, 10 (1987) 35.
27 R.J. Vreeken, W.D. van Dongen, R.T. Ghijsen, G.J. de Jong, U.A.Th. Brinkman, R.G.J. van Leuken, G.T.C. Kwakkenbos and R.S. Deelder, *Biol. Mass Spectrom.*, 21 (1992) 305.
28 M.J. Incorvia Mattina, *J. Chromatogr.*, 542 (1991) 385.
29 I.S. Kim, F.I. Sasinos, R.D. Stephens, J. Wang and M.A. Brown, *Anal. Chem.*, 63 (1991) 819.
30 M.T.W. Hearn (Editor), *Ion-Pair Chromatography, Theory and Biological and Pharmaceutical Applications (Chromatographic Science Series*, Vol. 31), Marcel Dekker, New York, 1985.
31 R.B. Geerdink, C. van Balkom and H.J. Brouwer, *J. Chromatogr.*, 481 (1989) 287.
32 V. Lopez-Avila, P. Hirata, S. Kraska and J.H. Taylor, *J. Agric. Food Chem.*, 34 (1986) 530.
33 R. Infante and C. Perez, in R.M. Caprioli (Editor), *Proceedings of the 38th ASMS Conference on Mass Spectrometry and Allied Topics, Tucson, AZ, June 3–8, 1990*, American Society for Mass Spectrometry, East Lansing, MI, 1990, p. 645.
34 R.B. Geerdink, A.M.B.C. Graumans and J. Viveen, *J. Chromatogr.*, 547 (1991) 478.
35 A. Di Corcia, M. Marchetti and R. Samperi, *Anal. Chem.*, 61 (1989) 1363.
36 C. de Ruiter, W. Minnaard, H. Lingeman, E. Kirk, U.A.Th. Brinkman and R.T. Otten, *Int. J. Environ. Anal. Chem.*, 43 (1991) 79.
37 R.J. Vreeken, U.A.Th. Brinkman, G.J. de Jong and D. Barceló, *Biomed. Environ. Mass Spectrom.*, 19 (1990) 481.

38 W.L. Hinze, H.N. Singh, Y. Baba and N.G. Harvey, *Trends Anal. Chem.*, 3 (1984) 193.
39 D.W. Armstrong and G.Y. Stine, *J. Am. Chem. Soc.*, 105 (1983) 6220.
40 E.R.J. Wils and A.G. Hulst, *J. Chromatogr.*, 454 (1988) 155.
41 R.C. Weast (Editor), *Handbook of Chemistry and Physics*, CRC Press, Boca Raton, FL, 67th ed., 1986.
42 A.G. Harrison, *Chemical Ionization Mass Spectrometry*, CRC Press, Boca Raton, FL, 1983.
43 H. Bagheri, E.R. Brouwer, R.T. Ghijsen and U.A.Th. Brinkman, *J. Chromatogr.*, 647 (1993) 121.
44 I. Liska, E.R. Brouwer, A.G.L. Ostheimer, H. Lingeman, U.A.Th. Brinkman, R.B. Geerdink and W.H. Mulder, *Int. J. Environ. Anal. Chem.*, 47 (1992) 267.
45 E.R. Brouwer, I. Liska, R.B. Geerdink, P.C.M. Frintrop, W.H. Mulder, H. Lingeman and U.A.Th. Brinkman, *Chromatographia*, 32 (1991) 445.

Journal of Chromatography A, 654 (1993) 79–86
Elsevier Science Publishers B.V., Amsterdam

CHROM. 25 457

Sensitive and selective liquid chromatographic postcolumn reaction detection system for biotin and biocytin using a homogeneous fluorophore-linked assay

Andrzej Przyjazny[☆], Nathaniel G. Hentz and Leonidas G. Bachas*

Department of Chemistry, University of Kentucky, Lexington, KY 40506-0055 (USA)

(First received April 14th, 1993; revised manuscript received July 27th, 1993)

ABSTRACT

A homogeneous fluorophore-linked assay was used to develop a postcolumn reaction detection system for high-performance liquid chromatography (HPLC). Biotin and biocytin were chosen as the model analytes. The effluent from the HPLC column was merged with a reagent stream containing avidin that was labeled with fluorescein isothiocyanate (avidin-FITC). The binding of the separated analytes by the labeled avidin was accompanied by an enhancement of the fluorescence intensity at 520 nm. This increase in fluorescence was proportional to the concentration of the analytes and constituted the analytical signal. The procedure was optimized with respect to the reagent concentration and the flow-rate of the reagent solution. Analytical characteristics of the method were determined. The procedure was highly selective for biotin and its derivatives. The detection limits for biotin and biocytin were 89 and 94 pg, respectively, for 20-μl injections. The developed postcolumn reaction detection system was validated by determining biotin in a liquid vitamin preparation and a horse-feed supplement.

INTRODUCTION

High-performance liquid chromatography (HPLC) has become a valuable tool for the study of complex mixtures. The range of separations available makes it an excellent choice for the characterization of biological samples. At present, UV–Vis absorbance, fluorescence, and electrochemical detectors are the most commonly used HPLC detectors. The applicability of these detectors can be further expanded by using suitable derivatization techniques to convert the analytes into compounds that can be detected with high sensitivity and selectivity. Indeed, coupling chemical reactions to compound-detection following chromatographic separation (*i.e.*, postcolumn) has become an acceptable and widely used means of analysis [1–5].

This article presents a novel postcolumn-reaction detection system based on principles of homogeneous fluorophore-linked assays (a general term that includes homogeneous fluoroimmunoassays). Although the use of these assays in bioanalytical chemistry has been growing because of their specificity and detection limits [6–9], their practical application has been hindered by the many fluorescing compounds, such as proteins and pigments (*e.g.*, bilirubin) that are present in biological samples. Consequently, the coupling of homogeneous fluorophore-linked assays to separation techniques, such as HPLC, should solve the problem of interferences caused by components of the sample matrix, and at the same time, provide highly selective and sensitive detection systems for biologically important compounds.

* Corresponding author.
☆ Present address: GMI Engineering & Management Institute, Science and Mathematics Department, 1700 West 3rd Avenue, Flint, MI 48504, USA.

0021-9673/93/$06.00

In this study, the feasibility of using homogeneous fluorophore-linked assays as a means of reaction detection in HPLC was evaluated by using biotin and biocytin as model analytes. Biotin and biocytin were selected because of their biological significance [10–12]. In addition, the two compounds have very similar properties and, therefore, a separation step is required in their determination [13,14]. Although HPLC seems to be the method of choice for determining biotin and biocytin in complex natural matrices, the absence of strong chromophores or fluorophores in these analytes has precluded their sensitive detection by common HPLC detectors. Consequently, the HPLC methods of separation and determination of these analytes described in the literature [14–16] make use of UV detection in the 205–230 nm range. Attempts have been made to improve the detectability of biotin and its analogues via precolumn derivatization techniques that produce UV-absorbing [17] or fluorescent [17–19] species. Although derivatization has resulted in appreciably improved detection limits, the procedures were time-consuming and did not lend themselves readily to automation.

Recently, two postcolumn reaction detection systems for the HPLC determination of biotin and biocytin based on the competitive-binding principle have been developed [20,21]. One of these systems [20] took advantage of the displacement of the dye 2-(4′-hydroxyphenylazo)benzoic acid (HABA) from its complex with avidin by the analytes, which was monitored by a UV detector at 345 nm. The second system [21] employed a similar displacement reaction using a fluorescent probe, 2-anilinonaphthalene-6-sulfonic acid, and fluorometric detection at 438 nm.

In this article, a postcolumn reaction detection system was designed and evaluated based on a homogeneous fluorophore-linked assay. The system made use of the approximately two-fold enhancement of the fluorescence intensity of fluorescein-labeled avidin upon the binding of biotin or its derivatives [22,23]. Other binding characteristics of the fluorescein-labeled avidin can be found in ref. 22. Because in this case there is no competition between a labeled and an unlabeled ligand for the binding protein, this system is a direct fluorophore-linked assay, rather than the more common competitive binding fluorophore-linked assay. It was anticipated that the application of this assay as a reaction detection system for the HPLC determination of biotin and biocytin should result in further improvement in the detection limits and selectivity of the procedure.

EXPERIMENTAL

Apparatus

The experimental setup used in this work is shown in Fig. 1. It consisted of a Rainin (Woburn, MA, USA) HPLC system interfaced with a Macintosh Plus computer (Apple Computer, Cupertino, CA, USA). The system included a Rainin Rabbit solvent-delivery system, a Rheodyne Model 7125 injector with a 20-μl sample loop (Berkeley, CA, USA), and a Knauer Model 87 variable-wavelength UV–Vis detector set at 220 nm. Reversed-phase separations were achieved by using a 5-μm Microsorb C_{18} column (250 × 4.6 mm I.D.) (Rainin) operated at ambient temperature, which was preceded by a 5-μm Microsorb C_{18} guard column (15 × 4.6 mm) (Rainin).

The effluent stream from the HPLC column was mixed with the reagent stream containing the avidin labeled with fluorescein isothiocyanate (avidin-FITC). The binding of the analytes to the labeled avidin resulted in an enhancement of the fluorescence intensity. The reagent solution, pumped by an ISCO Model LC-2600 syringe pump (Lincoln, NE, USA), was added to the column effluent through a tee-connector followed by a 10.0-m knitted open-tubular (KOT) reactor made from PTFE tubing (0.5 mm I.D., 14 mm helix diameter) prepared after Krull (KOT2 from ref. 24). The choice of this reactor was based on a previous work [20]. Unless otherwise stated, postcolumn reaction detection was carried out by using a Perkin-Elmer Model LS 50 luminescence spectrometer (Norwalk, CT, USA) with a μ-fluorescence flow cell (20-μl cell volume, NSG Precision Cells, Farmingdale, NY, USA). For the postcolumn reaction system employing the avidin-FITC reagent, the excitation

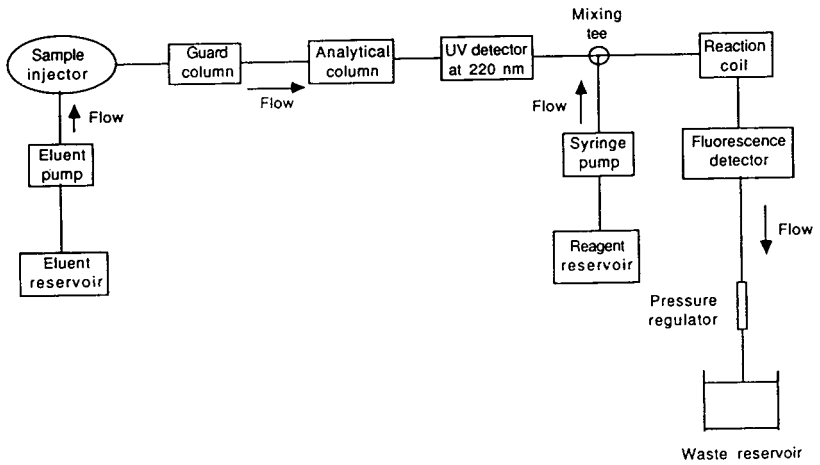

Fig. 1. Schematic diagram of an HPLC postcolumn reaction system for the fluorometric detection of biotin and biocytin employing a homogeneous fluorophore-linked assay.

was at 490 nm and the emission was monitored at 520 nm; the excitation and emission slits were set at 5 and 20 nm, respectively. The fluorescence intensity was recorded in arbitrary units.

Postcolumn reaction detection was also carried out by a Fluorolog-2 spectrofluorometer (SPEX Industries, Edison, NJ, USA) with the same μ-fluorescence flow cell. Fluorescence detection employed the same excitation and emission wavelengths as the previous LS 50 spectrometer. However, the respective slitwidths were set at 2 mm for the SPEX spectrofluorometer. With both fluorometers, a back-pressure regulator was placed at the detector outlet to eliminate outgassing problems.

Solvent system

The solvent system for the separation of biotin and biocytin consisted of aqueous 0.100 *M* phosphate buffer, pH 6.0 (solvent A), and 0.200 *M* phosphate buffer (pH 6.0)–methanol (50:50, v/v) (solvent B). Solvents were filtered through a 0.4-μm membrane filter (Nuclepore, Pleasanton, CA, USA) before use. A 54:46 (solvent A–solvent B) ratio of the two solvents was used to provide baseline resolution of biotin and biocytin in an isocratic mode. A mobile phase flow-rate of 0.40 ml/min was used in all the experiments.

Reagents

Biotin, biocytin, monobasic sodium phosphate (reagent grade) and avidin-FITC (with 3.9 fluoresceins attached per avidin molecule) were purchased from Sigma (St. Louis, MO, USA). N,N-Dimethylformamide (DMF) (ACS reagent grade) and acetone (spectrophotometric grade) were obtained from Aldrich (Milwaukee, WI, USA). Methanol (HPLC reagent grade) and methyl ethyl ketone (MEK) (certified) were purchased from Fisher Scientific (Fair Lawn, NJ, USA). Deionized (Milli-Q water purification system; Millipore, Bedford, MA, USA) distilled water was used to prepare all solutions.

Biotin and biocytin stock solutions ($4.0 \cdot 10^{-4}$ *M*) were prepared by dissolving the compounds in the mobile phase. Standard solutions were made by further dilutions with the mobile phase. A stock solution of avidin-FITC (50 mg/l, which corresponds to $7.5 \cdot 10^{-7}$ *M*) was prepared in 0.100 *M* phosphate buffer, pH 7.0, and stored refrigerated in an amber bottle. Unless otherwise specified, fresh working solutions of this reagent were prepared daily from the stock solution by dilution with the same buffer.

Characterization of the avidin-FITC reagent

A standard 1×1 cm quartz cuvette was used in all batch mode fluorescence experiments. A

$5 \cdot 10^{-5}$ *M* solution of biotin was added to a cuvette containing 2.0 mg/ml avidin-FITC and the enhancement of fluorescence intensity as a function of reaction time was measured with the LS 50 spectrometer. These data were used to determine the time required for equilibrium to be attained (represented by maximum fluorescence emission intensity).

Characterization of the postcolumn reaction detection system

The developed system was optimized in terms of the detection sensitivity by varying the avidin-FITC concentration, the flow-rate of the reagent solution, and the fraction of organic modifier in the reagent solution. Sensitivity, detection limits, linearity of response, precision, and selectivity of the postcolumn reaction system were determined and compared to direct UV detection of biotin and biocytin at 220 nm. A comparison between two different fluorescence detectors (one of them operating in a photon-counting mode) was made. The stability of the avidin-FITC reagent and the cost per analysis of the developed system were also estimated.

Real sample analyses

The postcolumn reaction detection system was validated by determining the biotin content of a liquid vitamin preparation and a horse-feed supplement. Specifically, a 50-μl volume of ABDEC liquid multi-vitamin supplement for infants and children under 4 years of age (Parke-Davis, Morris Plains, NJ, USA), containing 0.05 mg/ml biotin, was diluted to 2.00 ml with the mobile phase. Filtered volumes of 20 μl of the resulting solution were analyzed by HPLC using the simultaneous direct UV detection at 220 nm and the developed postcolumn reaction system with the fluorometric detection. The two detectors were connected in series, as indicated in Fig. 1. The biotin content in the sample was determined from the calibration curve based on injections of 20-μl volumes of standard biotin solutions.

In addition, biotin was extracted from two weighed samples (around 0.10 g) of a horse-feed supplement (Gen-a-Hoof from Nickers International, Staten Island, NY, USA) with 10.0 ml of 1.0 *M* NaOH. The pH of 6.00-ml aliquots of these solutions was adjusted to between 6 and 7 with 1.0 *M* HCl. The solutions were further diluted to 100.0 ml with the pH 6.0 phosphate buffer (0.100 *M*), and 20-μl volumes of the resulting solutions were analyzed after filtration by the procedure described for the liquid vitamin preparation analysis.

RESULTS AND DISCUSSION

The described postcolumn reaction detection system is based on the natural ability of avidin to bind biotin. When biotin and its analogues associate with avidin labeled with fluorescein, the fluorescence emission signal is enhanced [22].

Isocratic elution with the mobile phase described in the experimental section provided a baseline resolution of biotin and biocytin. A typical chromatogram representing postcolumn reaction detection of 0.10 nmol of the analytes using the avidin-FITC reagent is shown in Fig. 2. This chromatogram indicates that a homogeneous fluorophore-linked assay approach can indeed be used for the sensitive detection of biotin and biocytin.

The dependence of the detector response on

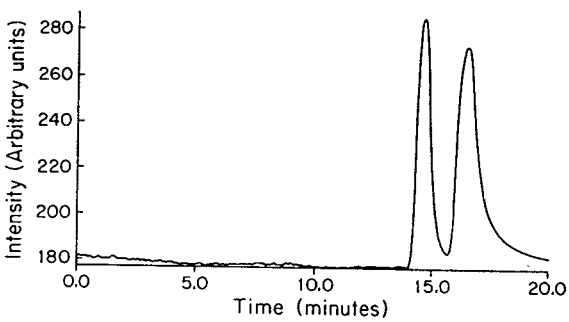

Fig. 2. Typical chromatogram of 20 μl of a solution containing $5.0 \cdot 10^{-6}$ *M* biotin (first peak) and $5.0 \cdot 10^{-6}$ *M* biocytin (second peak) using the postcolumn reaction system with fluorometric detection. Mobile phase: solvent A–solvent B (54:46); solvent A: 0.100 *M* phosphate buffer, pH 6.0; solvent B: 0.100 *M* phosphate buffer, pH 6.0, in water–methanol (50:50, v/v). Mobile phase flow-rate: 0.40 ml/min. Postcolumn reagent: 2.0 mg/l avidin-FITC in 0.100 *M* phosphate buffer, pH 7.0. Reagent flow-rate: 1.00 ml/min. A 10.0-m KOT reactor was used for postcolumn reaction detection. The remaining conditions are described in the Experimental section.

the concentration of the avidin-FITC was studied at three concentration levels of the reagent solution: 1.0, 2.0 and 3.0 mg/l avidin-FITC. In this experiment, the flow-rate of the reagent solution was 1.00 ml/min and the concentration of the analytes was kept constant at $5.0 \cdot 10^{-6}$ *M*. It was found that an increase in the reagent concentration from 1.0 to 2.0 mg/l avidin-FITC resulted in an enhancement of the response of the fluorometric detector by 80 and 64% for biotin and biocytin, respectively. In contrast, a further increase in the reagent concentration from 2.0 to 3.0 mg/l avidin-FITC caused only a small enhancement of the detector response, not exceeding 20%. On the basis of these data, a reagent concentration of 2.0 mg/l avidin-FITC was selected for further experiments, this value being a compromise between detector response and reagent consumption (*i.e.*, cost of analysis).

The effect of the flow-rate of the reagent solution on the detector response was examined by varying the reagent flow-rate in the 0.40–1.20 ml/min range, while keeping constant the amount of biotin and biocytin injected (0.10 nmol), the mobile phase flow-rate (0.40 ml/min), as well as the other chromatographic conditions. This dependence is shown in Fig. 3. The presence of a maximum can be accounted for as follows: an initial increase of the detector response with the flow-rate is consistent with the law of mass action, *i.e.*, the supply of the reagent available for the binding of the analytes increases

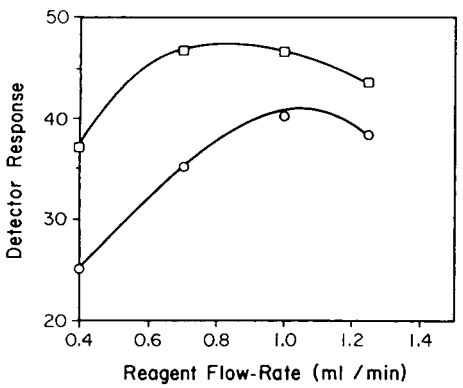

Fig. 3. Dependence of the detector response (expressed as peak height) for 0.10 nmol of biotin (□) and biocytin (○) on the reagent flow-rate. Reagent concentration: 2.0 mg/l avidin-FITC. For the remaining conditions, see Fig. 2.

with the flow-rate. A decrease in the detector response at high flow-rates (over 1.00 ml/min) is presumably due to the dilution of the column effluent stream, which in turn lowers the analyte concentration at the detector, and to insufficient reaction time. Indeed, batch mode experiments (measuring the change in fluorescence intensity as a function of time upon addition of biotin/biocytin to avidin-FITC) indicated that binding reactions were complete within 3 min. However, at higher flow-rates the reaction time in the postcolumn reaction detection system was in the order of 1 min. To maximize the detector response, the flow-rate of the reagent used throughout the remaining experiments was kept at 1.00 ml/min. The cost of the reagent per analysis estimated for these chromatographic conditions was under US$ 0.50.

The type and content of organic modifier are known to influence the fluorescence properties of fluorophores. Therefore, the effect of the methanol content on the detector response was examined by separating 0.10 nmol of biotin and biocytin using the optimum conditions for postcolumn reaction detection, but the reagent solution in this experiment was prepared in 0.100 *M* phosphate, pH 7.0 buffer–methanol (50:50, v/v). The resulting chromatograms exhibited a lower fluorescence background compared to the ones obtained by using the aqueous reagent solution (the remaining chromatographic conditions were the same), and no detector response for the analytes was observed. This effect was presumably due to denaturation of avidin by methanol and/or to fluorescence quenching. Consequently, the reagent solution used in the remaining studies was aqueous.

The repeatability of the results was examined by determining the relative standard deviation (R.S.D.) of the detector response that corresponds to 20-μl injections of $5.0 \cdot 10^{-6}$ *M* biotin and biocytin. In the case of retention times, the R.S.D. was 0.25%, whereas for the peak heights it ranged from 2.8 to 3.1% ($n = 8$). These results indicate that the developed procedure has the typical precision of chromatographic determinations.

The developed reaction detection system was evaluated in terms of its selectivity properties by

analyzing a series of solutions containing 0.10 nmol of the analytes and increasing amounts of three other organic compounds: DMF, acetone and MEK. Under the chromatographic conditions used in the present study, these compounds have similar retention times as biotin and biocytin, and their molecules contain chromophores absorbing at 220 nm. It was established that when the proposed reaction detection scheme was used, concentrations of DMF, acetone and MEK as high as $7 \cdot 10^{-2}$ *M* did not affect the detector response. In contrast, the direct absorptiometric detection at 220 nm suffered from severe interference by these compounds due to peak overlapping, which precluded correct determination of either of the two analytes. Therefore, it may be concluded that the selectivity of the developed procedure is primarily controlled by the binding characteristics of the binding protein employed (avidin).

The developed procedure was further characterized by constructing calibration curves for biotin and biocytin that were based on the chromatographic peak heights and peak areas. The data for these curves were obtained under the optimum conditions for the reaction detection. For the LS 50 detector, the curves for the two analytes were linear from $5 \cdot 10^{-7}$ to $1 \cdot 10^{-5}$ *M* (*i.e.*, 0.01 to 0.2 nmol for a 20-μl sampling loop). An increase in the concentration of the analytes over $1.0 \cdot 10^{-5}$ *M* was accompanied by an appreciable peak broadening and deteriorated resolution, and above $2.0 \cdot 10^{-5}$ *M* the calibration curves leveled off. A photon-counting spectrofluorometer was also evaluated as a detector in this system. In this case, the calibration curves were linear from $4 \cdot 10^{-8}$ *M* to $6 \cdot 10^{-7}$ *M*. In addition, it was determined that the introduction of the KOT reactor did not result in appreciable band broadening. Typically, the peak width increase due to the KOT reactor was about 15%. Further, the resolution of the postcolumn HPLC system toward biotin and biocytin did not change significantly.

The detection limits were estimated by analyzing a series of biotin and biocytin solutions of decreasing concentrations, until a signal-to-noise ratio (S/N) of 3 was obtained. Using the LS 50, the detection limits for both analytes were found to be $1.4 \cdot 10^{-7}$ *M*, which corresponds to 0.66 ng biotin and 1.0 ng biocytin for a 20-μl sample volume. The detection limits when using the photon-counting detector were estimated to be 89 and 94 pg for biotin and biocytin, respectively. These values were almost an order of magnitude lower than those obtained from the LS 50. The better detection limits were attributed to the photon-counting mode of detection. This constitutes an improvement with respect to the UV detection at 220 nm by a factor of 67 and $2.6 \cdot 10^{2}$ for biotin and biocytin, respectively.

The analytical utility and the accuracy of the proposed procedure were examined by determining the biotin content in a commercial liquid vitamin preparation and in a horse-feed supplement. The amount of biotin found in the liquid vitamin supplement ABDEC was 0.051 mg/ml (average from two determinations), which is in good agreement with the amount claimed by the manufacturer (0.05 mg/ml). The composition of 1 ml of ABDEC is: 1500 international units (I.U.) of vitamin A, 400 I.U. of vitamin D, 5 I.U. of vitamin E, 35 mg of vitamin C, 0.5 mg of thiamine, 0.6 mg of riboflavin, 8 mg of niacin, 0.4 mg of vitamin B_6, 2 μg of vitamin B_{12}, 0.05 mg of biotin, and 3 mg of pantothenic acid.

The selectivity of the postcolumn reaction detection system for biotin over the other ten vitamins present in the ABDEC preparation was excellent. This can be perceived by comparing two chromatograms of the vitamin solution obtained with the direct UV detection at 220 nm (Fig. 4A) and by employing the postcolumn reaction system with the fluorometric detection (Fig. 4B). It is evident that the interference from the other sample components precludes a correct quantitative determination of biotin when using the direct detection at 220 nm, whereas no interference is observed for the developed postcolumn reaction detection system. The difference in retention times for biotin between the chromatograms in Fig. 4A and B is a result of the additional time required for the eluent to pass through the 10.0-m KOT reactor.

Likewise, a horse-feed supplement was analyzed that contained, in addition to biotin (231 mg/kg), zinc methionine, maltodextrin, and ground rice hulls. Two samples of the supple-

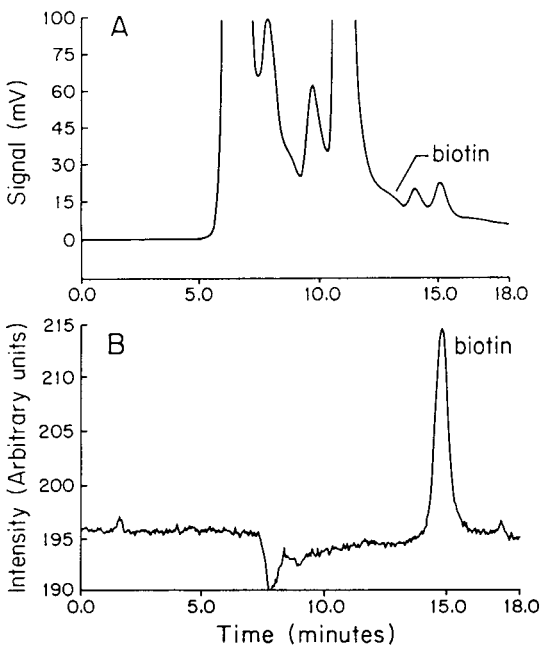

Fig. 4. Chromatograms of 20 μl of a diluted solution (1:40, v/v) of the liquid vitamin preparation ABDEC: (A) absorbance detection at 220 nm, (B) postcolumn reaction with fluorometric detection. For the chromatographic conditions, see Fig. 2.

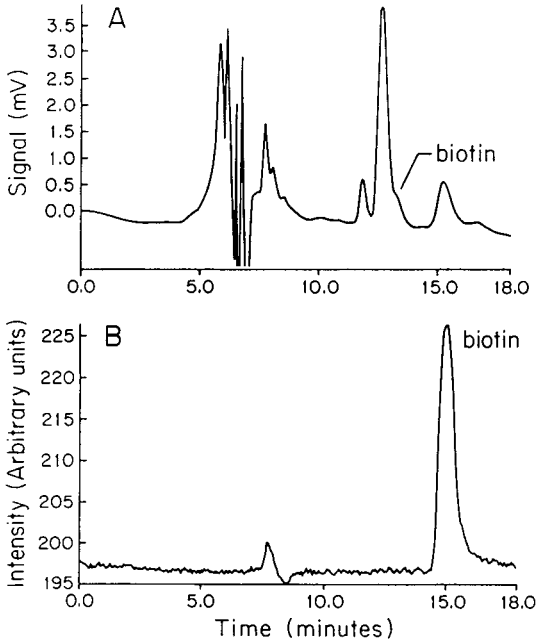

Fig. 5. Chromatograms of 20 μl of the extract of a horse-feed supplement: (A) direct UV detection at 220 nm, (B) postcolumn reaction with fluorometric detection. For the chromatographic conditions, see Fig. 2.

ment were extracted and analyzed for the biotin content by following the procedure outlined in the experimental section. As shown in Fig. 5, the UV detection at 220 nm suffered from severe interferences, while the chromatogram obtained by using the developed reaction system revealed the presence of only the biotin peak. The quantitative determination of biotin in the two samples yielded the following results: 240 and 236 mg/kg. The average value, 238 mg/kg, is in good agreement with the biotin content claimed by the manufacturer (the difference amounting to 3%).

The stability of the postcolumn reagent was evaluated by filling the syringe pump with 2.0 mg/l avidin-FITC and using it repetitively to analyze a test solution containing fixed amounts of biotin and biocytin. It was found that the reagent solution was sufficiently stable for at least eight hours as revealed by the unchanged peak heights of biotin and biocytin. However, after 24 h no chromatographic peaks corresponding to the analytes were observed. Apparently, this is due to adsorption of avidin-FITC (present at very low concentration of $3 \cdot 10^{-8}$ M) on the walls of the syringe pump. In contrast, the stock avidin-FITC solution was stable for at least two weeks when stored refrigerated in amber vials. As a result, fresh working solutions of avidin-FITC were prepared daily from the stock solution.

CONCLUSIONS

This study has demonstrated the feasibility of a postcolumn reaction detection system for biotin and biocytin based on a homogeneous fluorophore-linked assay. The developed procedure has an improved selectivity over the direct UV detection at 220 nm. The detection limits were 89 and 94 pg for biotin and biocytin, respectively. The high sensitivity of the described system is a result of the high quantum efficiency of fluorescein. Further, because fluorometric detection is performed at a wavelength in the visible region, the majority of compounds present in natural samples do not interfere. Indeed

the developed method was used to determine the biotin content in real samples with minimum pretreatment. The high selectivity of the described system is a combination of the binding selectivity of avidin (*i.e.*, ability to discriminate between compounds that contain the biotin moiety and those that do not) and the separation process itself (to separate biotin and its analogues).

The applicability of the proposed system is more general and can be extended to postcolumn reaction detection of other analytes as long as there exist fluorophore-labeled biological binders (*e.g.*, antibodies, binding proteins, receptors, and lectins) that undergo spectral changes as a function of the concentration of the analytes. Work in this direction is currently underway in our laboratory.

ACKNOWLEDGEMENT

This research was supported by grants from the National Institutes of Health (Grant GM 40510) and American Cyanamid.

REFERENCES

1 R.W. Frei, H. Jansen and U.A.Th. Brinkman, *Anal. Chem.*, 57 (1985) 1529A.
2 J.J. Rusik and J.C. Gluckman, *Chromatography*, 2(4) (1987) 29.
3 I.S. Krull, *Reaction Detection in Liquid Chromatography*, Marcel Dekker, New York, 1986.
4 C.X. Gao and I.S. Krull, *Biochromatography*, 4 (1989) 222.
5 U.A.Th. Brinkman, R.W. Frei and H. Lingeman, *J. Chromatogr.*, 492 (1989) 251.
6 I. Hemmilä, *Clin. Chem.*, 31 (1985) 359.
7 E. Soini and E. Hemmilä, *Clin. Chem.*, 25 (1979) 353.
8 R.M. Nakamura, in R.M. Nakamura, Y. Kasahara and G.A. Rechnitz (Editors), *Immunochemical Assays and Biosensor Technology for the 1990s*, American Society for Microbiology, Washington, DC, 1992, pp. 205–227.
9 H.T. Karnes, J.S. O'Neal and S.G. Schulman, in S.G. Schulman (Editor), *Molecular Luminescence Spectroscopy —Methods and Applications*, Part I, Wiley, New York, 1985, pp. 717–779.
10 R.S. Harris, P. György and B.W. Langer, in W.H. Sebrell and R.S. Harris (Editors), *The Vitamins*, Vol. II, Academic Press, New York, 1968, pp. 261–359.
11 J.P. Bonjour, J. Bausch, T. Suormala and E.R. Baumgartner, *Int. J. Vit. Nutr. Res.*, 54 (1984) 223.
12 E.R. Baumgartner, T.M. Suormala, H. Wick, J. Bausch and J.P. Bonjour, *Ann. N.Y. Acad. Sci.*, 447 (1985) 272.
13 H. Ebrahim and K. Dakshinamurti, *Anal. Biochem.*, 162 (1987) 319.
14 T.M. Suormala, E.R. Baumgartner, J. Bausch, W. Holick and H. Wick, *Clin. Chim. Acta*, 177 (1988) 253.
15 J.L. Chastain, D.M. Bowers-Komro and D.B. McCormick, *J. Chromatogr.*, 330 (1985) 153.
16 T.S. Hudson, S. Subramanian and R.J. Allen, *J. Assoc. Off. Anal. Chem.*, 67 (1984) 994.
17 P.L. Desbene, L. Coustal and F. Frappier, *Anal. Biochem.*, 128 (1983) 359.
18 E. Röder, U. Engelbert and J. Traschütz, *Fresenius' Z. Anal. Chem.*, 319 (1984) 426.
19 J. Stein, A. Hahn, B. Lembcke and G. Rehner, *Anal. Biochem.*, 200 (1992) 89.
20 A. Przyjazny, T.L. Kjellström and L.G. Bachas, *Anal. Chem.*, 62 (1990) 2536.
21 A. Przyjazny and L.G. Bachas, *Anal. Chim. Acta*, 246 (1991) 103.
22 M.S. Barbarakis and L.G. Bachas, *Talanta*, 40 (1993) 1139.
23 M.H.H. Al-Hakiem, J. Landon, D.S. Smith and R.D. Nargessi, *Anal. Biochem.*, 116 (1981) 264.
24 C.M. Selavka, K.-S. Jiao and I.S. Krull, *Anal. Chem.*, 59 (1987) 2221.

Journal of Chromatography A, 654 (1993) 87–91
Elsevier Science Publishers B.V., Amsterdam

CHROM. 25 344

Adsorption of drugs in high-performance liquid chromatography injector loops

Germán C. Fernández Otero, Silvia E. Lucangioli and Clyde N. Carducci*

Department of Analytical Chemistry, Faculty of Pharmacy and Biochemistry, University of Buenos Aires, Junín 956, Buenos Aires (Argentina)

(Received March 22nd, 1993)

ABSTRACT

The effect of solvent injection on the area and peak-height responses of some drugs (ergotamine tartrate, astemizole, terfenadine, bromhexine hydrochloride, caffeine, ambroxol hydrochloride, phenylephrine hydrochloride, enalapril maleate and betamethasone) was evaluated. Reversed-phase chromatographic systems were employed and loops of different sizes and various overfill volumes were assayed. When injection solvents weaker than the mobile phases were used, significant variation in the area responses was observed for astemizole, bromhexine, ergotamine and terfenadine. Adsorption on the internal surface of the injection loops produced this anomalous behaviour depending on the chemical nature of the analyte injected.

INTRODUCTION

Much attention is nowadays focused on the validation of analytical methods for drug determination in complex matrices such as biological fluids and pharmaceutical dosage forms. These analyses require compliance with good laboratory practices (GLPs) and standard operating procedures (SOPs), which dictate in detail the different validation steps of an analytical process. The applicability of HPLC in pharmaceutical analyses is well known and so the procedures used must be fully validated.

A variable to be investigated is the injection system because inaccuracy and lack of reproducibility are often caused by the sample injector. Quantitation problems in measuring peak height or area arising from sample–solvent interaction phenomena [1–9] or adsorption effects onto the injection system [10–13] have been reported. This adsorption is observed particularly when the solvent used is water or weaker than the mobile phase in RP-HPLC.

Taking into account the adsorption effects, Dolan [11] reported different inter-laboratory results obtained in the analysis of an antihistaminic agent because drug adsorption in the injector loop caused increased area responses related to the variable overfill volume. Similar results were found when samples of aqueous nonylphenol ethoxylate surfactant solutions were injected [12]. Inaccuracies and reproducibility problem have also been observed on injection of aqueous solutions of vinblastine and vancomycin, and this has been attributed to their interaction with the injection system [7].

MacLeod *et al.* [10] suggested that the valve rotor caused adsorption of aqueous solutions of an ansiolitic agent, and Simonson and Nelson [13] demonstrated amitriptyline adsorption on the inner wall of the injection loop.

Because of drug regulations, *in vitro* dissolution studies are becoming relevant for testing the bioequivalency of pharmaceutical formulations. These assays use aqueous media and HPLC is

* Corresponding author.

0021-9673/93/$06.00

often the method choice because of its selectivity and sensitivity. Therefore, we considered it of interest to study several drugs with different physicochemical characteristics at present not reported in order to investigate their anomalous response in the injection process.

EXPERIMENTAL

Reagents

Ergotamine tartrate, terfenadine, bromhexine hydrochloride, caffeine, ambroxol hydrochloride, phenylephrine hydrochloride and betamethasone were purchased from Sigma (St. Louis, MO, USA). Astemizole was from Janssen (Denmark) and enalapril maleate was from Merck Sharp & Dohme (USA).

HPLC-grade acetonitrile and methanol were obtained from Merck (Darmstadt, Germany). Heptanesulphonic acid sodium salt was bought from Sigma and potassium dihydrogenphosphate from J.T. Baker (Phillipsburg, NJ, USA). Deionized, double-distilled water was used. Eluents were filtered through a 0.2-μm membrane filter and degassed before use.

Instrumentation

HPLC was carried out with a Varian Model 5020 liquid chromatograph equipped with a Varian UV-100 detector. Data were processed with a Varian 4270 integrator (Varian, Palo Alto, CA, USA). A Rheodyne Model 7125 injector (Cotati, CA, USA) with 20- and 50-μl loops was used. Detection was performed at 276, 254, 246 and 230 nm according to the absorption spectra of the drugs under study and at 0.05 AUFS. The columns used were a 150 × 4.6 mm I.D., 5 μm, MicroPak MCH-5 (Varian) and a 300 × 3.9 mm I.D., 10 μm, μBondapak Phenyl (Waters, Milford, MA, USA).

Solutions

Stock drug solutions of astemizole, terfenadine, caffeine and betamethasone in concentrations ranging from 0.2 to 1.0 mg/ml were prepared in methanol. Stock drug solutions of ergotamine tartrate, phenylephrine hydrochloride, bromhexine hydrochloride, ambroxol hydrochloride and enalapril maleate were prepared in water in concentrations from 0.2 to 1.2 mg/ml.

Working standard solutions were obtained from stock solutions by dilution in water, mobile phase or methanol. The final concentrations were: phenylephrine hydrochloride 19.2 μg/ml, ergotamine tartrate 34.0 μg/ml, bromhexine hydrochloride 20 μg/ml, betamethasone 20 μg/ml, ambroxol hydrochloride 24 μg/ml, enalapril maleate 10 μg/ml, astemizole 20 μg/ml, terfenadine 5 μg/ml and caffeine 30 μg/ml.

Analyses were performed by replicate injections ($n = 4$) of all drug solutions.

RESULTS AND DISCUSSION

In this report we present and discuss the results obtained in the study of the adsorption effects of some drugs on the inner wall of HPLC injector loops. Basic drugs such as phenylephrine hydrochloride, ergotamine tartrate, bromhexine hydrochloride, ambroxol hydrochloride, astemizole and terfenadine were chosen for this study. Caffeine, betamethasone and enalapril maleate were also investigated.

In our experiments a loop of 20 μl was overfilled with 60, 150 and 300 μl of aqueous solutions of the drugs under study. Statistical analysis was performed and a significant increase in the area response ($P < 0.05$) was observed depending on the degree of overfill volume used in the injection (Table I). The results obtained may be attributed to a sample adsorption mecha-

TABLE I

OVERFILL VOLUME EFFECT FOR AQUEOUS SOLUTION INJECTIONS IN A 20-μl LOOP

For chromatographic conditions, see Figs. 1, 2, 3 and 4.

Drug	Area (±S.D.)[a]		
	60 μl	150 μl	300 μl
Astemizole	12155 ± 385	16338 ± 485	17509 ± 418
Bromhexine	19397 ± 623	21725 ± 550	24548 ± 416
Ergotamine	28789 ± 788	31155 ± 584	33802 ± 664
Terfenadine	5118 ± 175	6413 ± 203	7412 ± 213

[a] Mean area (±S.D.) for four injections.

nism and are in agreement with reports of other workers [11–13]. When a strong solvent is used as mobile phase, it flows through the loop, desorbs the retained substance and, consequently, the measured areas increase.

When methanol or mobile phase was used as the injection solvent (Table II) the area response values remained constant and were not affected by the overfill volume because the injection solvents employed are strong enough to prevent drug adsorption (Figs. 1–4). Lack of an adsorption effect might be interpreted in terms of the relative free energies of adsorption and that of solubility. With methanol and mobile phase as injection solvents the free energy of solubility could be favoured [10]. No variations in the mean area responses were obtained with phenylephrine hydrochloride, caffeine, betamethasone, ambroxol hydrochloride and enalapril maleate.

In order to investigate if an adsorption process could be produce on the internal surface of the loop, aqueous solutions of astemizole, bromhexine hydrochloride, ergotamine tartrate and terfenadine were injected in 20- and 50-μl loops with a constant overfill volume of 150 μl of each solution. A comparison of area responses obtained with water and mobile phase is shown in Table III. Differences in the measured areas between the solvents for each loop are evident, and these differences are proportional to the contact surface each injected solution ran through. Our results indicate that adsorption

TABLE II

OVERFILL VOLUME EFFECT FOR MOBILE PHASE SOLUTION INJECTIONS IN A 20-μl LOOP

For chromatographic conditions, see Figs. 1, 2, 3 and 4.

Drug	Area (±S.D.)[a]		
	60 μl	150 μl	300 μl
Astemizole	12768 ± 213	12922 ± 240	12773 ± 204
Bromhexine	19859 ± 189	20003 ± 250	19920 ± 198
Ergotamine	28808 ± 237	28960 ± 207	28911 ± 287
Terfenadine	5072 ± 112	5078 ± 98	5018 ± 124

[a] Mean area (±S.D.) for four injections.

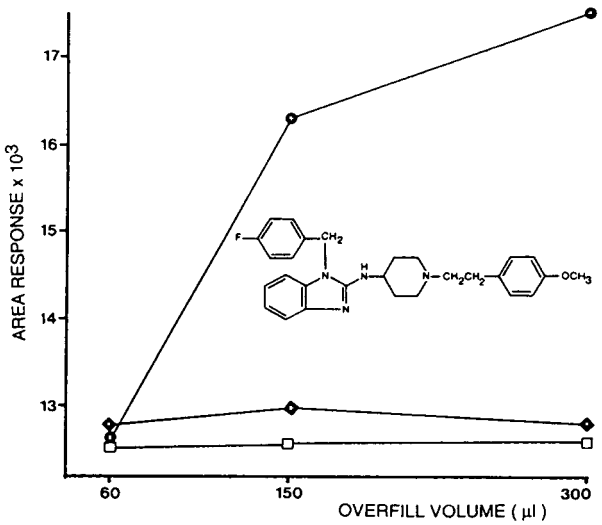

Fig. 1. Astemizole: area response as a function of overfill volume. Injection solvent: ○ = water; ◆ = mobile phase; □ = methanol. Column: MicroPack MCH-5. Mobile phase: methanol–phosphate buffer 0.03 *M*, pH 3.0 (85:15). Flow-rate: 1.5 ml/min. Detection: 276 nm, 0.05 AUFS.

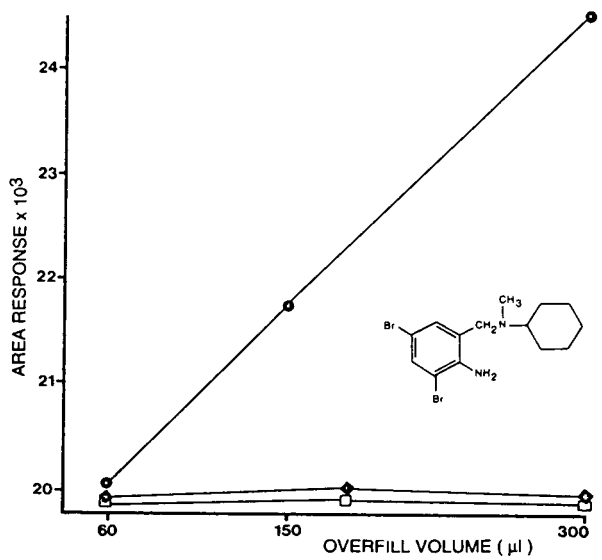

Fig. 2. Bromhexine hydrochloride: area response as a function of overfill volume. Injection solvent: ○ = water; ◆ = mobile phase; □ = methanol. Column: MicroPack MCH-5. Mobile phase: methanol–phosphate buffer 0.03 *M*, pH 3.0 (85:15). Flow-rate: 1.5 ml/min. Detection: 246 nm, 0.05 AUFS.

TABLE III

AREA RESPONSES IN 20- AND 50-μl LOOPS USING WATER AND MOBILE PHASE AS INJECTION SOLVENT FOR A 150-μl OVERFILL VOLUME

For chromatographic conditions, see Figs. 1, 2, 3 and 4.

Drug	Area (±S.D.)[a]			
	Loop 20 μl		Loop 50 μl	
	Water	Mobile phase	Water	Mobile phase
Astemizole	16338 ± 485	12922 ± 240	42806 ± 1229	32305 ± 495
Bromhexine	21725 ± 550	20003 ± 250	53383 ± 990	50010 ± 508
Ergotamine	31155 ± 584	28960 ± 207	75395 ± 1100	72590 ± 475
Terfenadine	6413 ± 203	5078 ± 98	15008 ± 560	12580 ± 209

[a] Mean area (±S.D.) for four injections.

phenomena take place mainly on the inner walls of the injection loops and that drug interaction with the polymeric material of the rotor would not be the only cause of the increased areas observed. If this were the case, at constant overfill volume the area differences between the injections in water and mobile phase would be the same for the two loops used.

Basic drugs that showed adsorption phenomena were slightly soluble in water but more soluble in methanol. Our results are in agreement with those of Zlatkis and Ranatunga [14], who pointed out that the lower the solubility and

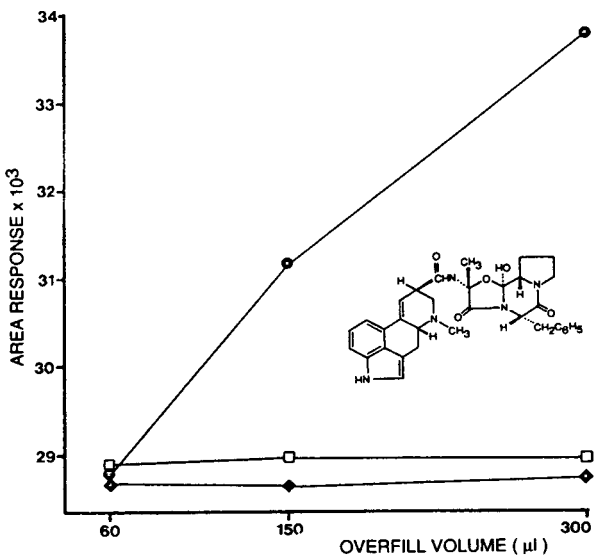

Fig. 3. Ergotamine tartrate: area response as a function of overfill volume. Injection solvent: ○ = water; ◆ = mobile phase; □ = methanol. Column: μBondapak Phenyl. Mobile phase: acetonitrile–heptanesulphonic acid 1.25 m*M* in acetic acid 0.1%, pH 3.25 (65:35). Flow-rate: 1.3 ml/min. Detection: 254 nm, 0.05 AUFS.

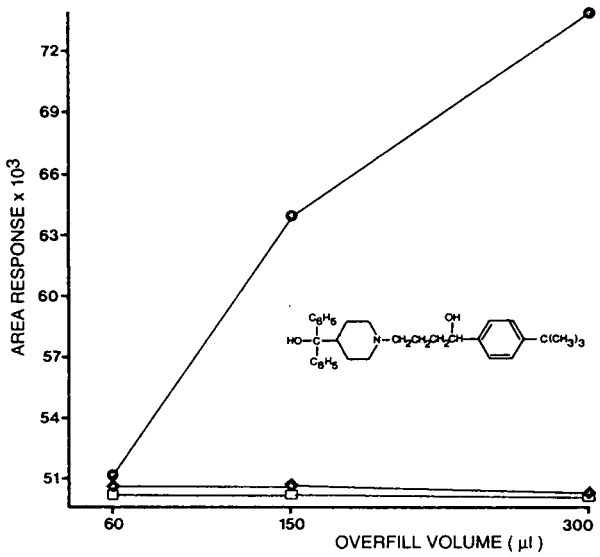

Fig. 4. Terfenadine: area response as a function of overfill volume. Injection solvent: ○ = water; ◆ = mobile phase; □ = methanol. Column: MicroPak MCH-5. Mobile phase: acetonitrile–phosphate buffer 0.03 *M*, pH 3.0 (70:30). Flow-rate: 1.7 ml/min. Detection: 230 nm, 0.05 AUFS.

polarity of a compound the better it is adsorbed on the surface of a capillary tubing.

In brief, inaccuracy and lack of reproducibility in the results of HPLC may be caused by adsorption phenomena in the injector loop. This problem can be overcome if a constant overfill volume or injection solvents that favour the solubility of the drugs are used.

ACKNOWLEDGEMENT

The authors thank Dr. J.O. Muse for his help in the preparation of the manuscript.

REFERENCES

1 M. Tsimidou and R. Macrae, *J. Chromatogr.*, 285 (1984) 178.
2 Ch. Yi, J.L. Fasching and P.R. Brown, *J. Chromatogr.*, 352 (1986) 221.
3 S. Perlman and J.J. Kirschbaum, *J. Chromatogr.*, 357 (1986) 39.
4 J.J. Kirschbaum and S. Perlman, *J. Chromatogr.*, 369 (1986) 269.
5 K.C. Chan and E.S. Yeung, *J. Chromatogr.*, 391 (1987) 465.
6 N.E. Hoffman, S. Pan and A.M. Rusium, *J. Chromatogr.*, 465 (1989) 189.
7 E.L. Inman, A.M. Maloney and E.C. Richard, *J. Chromatogr.*, 465 (1989) 201.
8 N.E. Hoffman and A. Rahman, *J. Chromatogr.*, 473 (1989) 260.
9 N.E. Hoffman and J.H.Y. Chang, *J. Liq. Chromatogr.*, 14 (1991) 651.
10 S.K. MacLeod, D.T. Fagan and J.P. Scholl, *J. Chromatogr.*, 502 (1990) 236.
11 J.W. Dolan, *LC·GC*, 9 (1991) 22.
12 B.B. Sithole, B. Zvilichovsky, C. Lapointe and L.H. Allen, *J. Assoc. Off. Anal. Chem.*, 73 (1990) 322.
13 L. Simonson and K. Nelson, *LC·GC*, 10 (1992) 533.
14 A. Zlatkis and R.P.J. Ranatunga, *Anal. Chem.*, 62 (1990) 2471.

Journal of Chromatography, *A* 654 (1993) 93–104
Elsevier Science Publishers B.V., Amsterdam

CHROM. 25 467

High-performance liquid chromatographic separation and isolation of the methanolic allomerization products of chlorophyll *a*

Pirjo Kuronen, Kristiina Hyvärinen and Paavo H. Hynninen*

Department of Chemistry, Division of Organic Chemistry, P.O. Box 6, University of Helsinki, SF-00014 Helsinki (Finland)

Ilkka Kilpeläinen

Institute of Biotechnology, P.O. Box 45, University of Helsinki, SF-00014 Helsinki (Finland)

(First received March 15th, 1993; revised manuscript received June 22nd, 1993)

ABSTRACT

Isocratic normal-phase HPLC on a silica column with diode-array detection provided a powerful means for the analytical separation and preparative isolation of seven methanolic allomerization products of chlorophyll *a*. Diastereomeric selectivity was achieved for $13^2(R,S)$-hydroxychlorophyll *a*, $13^2(R,S)$-methoxychlorophyll *a* and the Mg complex of $3^1,3^2$-didehydro-15^1-hydroxy-$15^1(R,S)$-methoxyrhodochlorin-15-acetic acid δ-lactone 15^2-methyl 17^3-phytyl ester. The Mg complex of $3^1,3^2$-didehydrorhodochlorin-15-glyoxylic acid $13^1,15^2$-dimethyl 17^3-phytyl ester was also isolated in high purity. Reversed-phase HPLC did not result in an acceptable separation in spite of using several different brands of reversed-phase C_{18} columns and mobile phase compositions. The identification of the allomerization products was based on UV–Vis and ^{1}H NMR spectra, retention times and co-elution with authentic samples. The observed formation of small amounts of numerous side-products is interpreted as further evidence for the free-radical mechanism of the allomerization.

INTRODUCTION

The chlorophylls (Chls) are a group of closely related compounds which play a central role in the photosynthetic conversion of light energy into chemical energy. It is well known that the chlorophylls are extremely susceptible to a number of chemical transformations which can occur during their extraction and separation. Typical reactions are loss of the central magnesium atom (pheophytinization), configurational change at C-13^2 (epimerization), photochemical degradation, transesterification or hydrolysis of the ester groups and oxidation of the isocyclic ring by molecular triplet oxygen (allomerization) [1–5].

The allomerization, first observed by Willstätter and Stoll [1], includes a complicated series of oxidation reactions at C-13^2 by molecular triplet oxygen ($^3O_2$) in alcohol solutions [2–14]. The allomerization reaction, which poses a serious problem in the isolation of chlorophylls from natural sources, may yield several oxidation products depending on the conditions and starting material. Several reaction mechanisms have been proposed for the allomerization of Chl *a* [2–4,6–17]. The free-radical mechanism, where Chl enolate anion is the key intermediate, is supported by ample experimental evidence [4,11], but some details of the reaction are still poorly understood.

* Corresponding author.

A variety of chromatographic procedures, including paper, thin-layer (TLC), conventional column (CC) and high-performance liquid chromatography (HPLC), have been developed and used for analytical and preparative separations of chlorophylls and their derivatives [18–23]. The first published HPLC separation for Chl compounds dates from 1975 [24]. Since then, the trend has been towards increased use of HPLC for the ultimate separation, isolation and analysis of these plant pigments [14,19–23,25–38]. The high resolving power, speed, increased sensitivity and several detection systems now available make modern HPLC superior to other LC techniques. In most studies, reversed-phase (RP) HPLC has been chosen in preference to the normal-phase (NP) separation. Schaber *et al.* [14] were the first to follow the allomerization reaction in methanol by RP-HPLC with tetrahydrofuran (THF)–MeOH–water (36:54:10, v/v/v) as the mobile phase. They obtained good separations for the $13^2(R)$- and $13^2(S)$-epimers of 13^2-hydroxy-Chl *a* and the $15^1(R)$- and $15^1(S)$-epimers of the 15^1-methoxylactone derivative, but they could not detect other allomerization products (see Fig. 1).

In this paper, we report the results of investigations on the allomerization of Chl *a* in methanol, performed under atmospheric oxygen, in darkness and at room temperature. We describe an improved method for the separation, isolation and identification of the main allomerization products and their epimers, using NP-HPLC under isocratic conditions and diode-array detection (DAD) for preliminary identification. The separated compounds were identified more conclusively by NMR spectroscopy.

EXPERIMENTAL

Isolation and purity of chlorophyll a

Chl *a* (Fig. 1) was isolated from clover leaves by the method described previously [41], but since then modified for large-scale preparation. The purity of the Chl *a* was confirmed by UV–Vis spectrophotometry, ^{1}H NMR, TLC and HPLC. The spectroscopic properties of the preparation were identical with those described earlier [42]. The ^{1}H NMR spectrum showed that the only impurity was water (present in a ratio of *ca.* 1:1). TLC on sucrose [43] yielded only one spot, whereas NP-HPLC [Zorbax Sil column (250 × 4.0 mm I.D.), particle size 5 μm (Rockland Technologies, Newport, DE, USA), eluent 1.5% (v/v) 2-PrOH (LiChrosolv; Merck, Darmstadt, Germany) in hexane (LiChrosolv, Merck), flow-rate 1 ml/min, detection at 420 nm] revealed a trace amount of Chl *a'* which may have formed during the analysis.

Allomerization experiments

Experiment 1. An amount of 31.4 mg of solid Chl *a* was dissolved in 15 ml of methanol (J.T. Baker, Denventer, Netherlands, Catalog No. 8045, Absolute, ACS, "Baker analyzed reagent", dried over 3 Å molecular sieves). This solution was continuously stirred magnetically at room temperature in an erlenmeyer flask provided with a loose glass stopper and wrapped with aluminium foil to avoid any effect of light. The course of the reaction was followed by TLC on sucrose [43] employing 1% (w/w) 2-PrOH (analytical-reagent grade, Merck) in light petroleum (analytical-reagent grade, Merck; b.p. 60–80°C, distilled through a Vigreux column) as the eluent. After 3 days, Chl *a* was completely converted into its allomers. Without stirring, the reaction reportedly takes 7 days [10]. The methanolic reaction mixture was poured into a separating funnel containing water–hexane (Extrapure, Merck; distilled through a Vigreux column) (1:1, v/v). The aqueous phase was saturated with sodium chloride and extracted several times with hexane until it was colourless. The combined hexane phases were washed with water and concentrated with a rotary evaporator. An aliquot was taken and evaporated to dryness. The residue was dissolved in diethyl ether and analysed by TLC on sucrose. According to this analysis, the composition of the products had not changed during the extraction process. The allomerization products were studied by RP-HPLC on C_{18} columns and by NP-HPLC on silica columns. The main extract in hexane was evaporated to dryness under an argon stream and the residue was dissolved in a minimum amount of

methanol for RP columns or of 0.5–1.5% (v/v) 2-PrOH in hexane for silica columns.

Experiment 2. The whole allomerization experiment was repeated with the difference that the amounts of Chl *a* and methanol were 304. 5 mg and 150 ml, respectively, and that light petroleum was used instead of hexane as extraction solvent. The mixture of allomerization products obtained was prefractionated on a sucrose column followed by HPLC purification of some fractions for NMR spectroscopy (see below).

Chromatography on a sucrose column

The conventional chromatographic procedure on a sucrose column [43] was employed in the preseparation of the allomerization products from experiment 2. Powdered sugar (Cultor, Kirkkonummi, Finland), passed through a 100-mesh sieve, was used in the separations. The sugar (1500 g) was suspended in 2500 ml of the eluent [light petroleum (analytical-reagent grade, Merck, b.p. 60–80°C) or hexane (Extrapure, Merck), both distilled through a Vigreux column, containing 1% (w/w) of 2-PrOH] to form a slurry, which was then poured into a glass column (6 cm O.D.) to form a sucrose layer, 54 cm high. The mixture of allomerization products was evaporated to dryness and dehydrated by the chloroform co-distillation method [42]. The solvent residues were removed on a vacuum line at room temperature. The dry product was monomerized by dissolving it in 20 ml of diethyl ether [analytical-reagent grade, Merck; dried and stabilized with 2,6-di-*tert.*-butyl-4-methylphenol (BHT)] and evaporating nearly to dryness. The product was dissolved in a minimum amount of the eluent [0.5–1% (w/w) 2-PrOH in distilled hexane or light petroleum] and the solution was introduced on to the top of the sucrose layer. The separation was performed in the dark by wrapping the column with aluminium foil. The flow-rate of the mobile phase was 4–5 ml/min. The collected fractions were analysed using sucrose TLC, UV–Vis spectrophotometry and HPLC. After the analyses, the fractions containing a pure component, were combined, washed several times with distilled water and concentrated to a small volume. Final purification was achieved by NP-HPLC using a semi-preparative Zorbax Sil column.

High-performance liquid chromatography

The HPLC experiments, both analytical and semi-preparative, were performed with a Waters (Milford, MA, USA) liquid chromatograph consisting of two Model 501 pumps controlled by a Model 660 solvent programmer, a Rheodyne (Cotati, CA, USA) Model 7125 injector (10-, 100- and 1000-μl loops) a Waters Model 990 photodiode-array detector, an NEC APC III computer with chromatographic software and a Waters Model 990 recorder. Samples were monitored by absorption at 420 and 430 nm. All HPLC columns were operated under isocratic conditions at ambient temperature. The flow-rate was 3–4 ml/min for the semi-preparative columns and 0.8–1.5 ml/min for the analytical columns.

The reversed-phase separations were performed on five different C_{18}-modified silica columns: Resolve C_{18} (150 × 3.9 mm I.D.), particle size 5 μm (Waters); μBondapak C_{18} (300 × 3.9 mm I.D.), 10 μm (Waters); Novapak C_{18} (150 × 3.9 mm I.D.), 4 μm (Waters); LiChrosorb RP-18 (250 × 4.0 mm I.D.), 5 μm (Merck); and Zorbax ODS (250 × 9.4 mm I.D.), 5–6 μm (semi-preparative column) (DuPont, Wilmington, DE, USA). The mobile phase solvents for RP-HPLC were methanol (MeOH), acetonitrile (ACN) and tetrahydrofuran (THF) (all of LiChrosolv grade, Merck), used in different binary, ternary and quaternary combinations with water (distilled, deionized).

The normal-phase separations were carried out with silica columns: Zorbax Sil (250 × 9.4 mm I.D.), 5–6 μm (semi-preparative column) (DuPont); LiChrospher Si 100 (250 × 4.0 mm I.D.), 10 μm (Merck); LiChroCART HPLC cartridge 250-4 Superspher Si 60 (250 × 4.0 mm I.D.), 4 μm (Merck); and Zorbax Sil (250 × 4.6 mm I.D.), 5 μm (Rockland Technologies). The eluent was usually 2-PrOH (LiChrosolv, Merck) in hexane (LiChrosolv, Merck) with the concentration of the former varying from 0.8 to 2.0% (v/v). In some experiments the mobile phase composition was MeOH–2-PrOH–hexane (0.4:0.8:98.8, v/v/v). The semi-preparative NP

Zorbax Sil column was used both for analytical and preparative purposes.

The HPLC solvents were filtered through a 0.45-μm membrane filter (Millipore, Milford, MA, USA) and thoroughly degassed by application of ultrasound before use. Millex LCR 0.45-μm cartridges (Millipore) were used for the filtration of the HPLC samples and the cartridges were always flushed carefully with the sample solvent. The HPLC columns were thoroughly flushed at the end of each day with a polar solvent; methanol or acetonitrile was used for RP columns and methanol for silica columns.

Component identification was based on UV–Vis and ^{1}H NMR spectra, retention times and co-elution with authentic samples.

Isolation of allomerization products by semi-preparative HPLC

After chromatography on a sucrose column, the fraction (band 4) containing both epimers of the 15^1-MeO-lactone derivative and the other epimer of 13^2-MeO-Chl *a* in addition to numerous minor components (see Fig. 5b) was further fractionated on a semi-preparative Zorbax Sil column. A 1-ml volume of the 2-PrOH–hexane (0.8:99.2, v/v) solution, containing *ca.* 4 mg of the aforementioned mixture, was injected and the column was eluted isocratically with the same solvent. Each component fraction was collected in repeated separations until the amount of the component was sufficient for NMR analyses. The combined fractions, containing a pure component, were washed with water to remove 2-PrOH, hexane was evaporated and the residue was dried by the chloroform co-distillation method. The solids were stored at −18°C.

Thin-layer chromatography

The TLC analyses for separate compounds, mixtures of allomerization products and fractions from the sucrose column were performed on laboratory-prepared sucrose plates, using 1% (w/w) 2-PrOH in light petroleum (analytical-reagent grade, Merck; b.p. 60–80°C, distilled through a Vigreux column) as eluent [43].

UV–visible spectra

Perkin-Elmer Model 550 and 554 spectrophotometers were used for the spectrophotometric characterization of the compounds dissolved in diethyl ether (analytical-reagent grade, Merck; dried) at ambient temperature. In the HPLC separations, the on-line UV–Vis spectra were recorded from 200 to 800 nm with the photodiode-array detector.

Nuclear magnetic resonance spectra

The ^{1}H NMR spectra were recorded on a Varian Gemini-200 instrument and a Varian Unity 500 MHz spectrometer, using 5-mm sample tubes. The NMR samples were dissolved in acetone-d_6 (Aldrich, 99.5, 99.98% ^{2}H, or Merck, 99.8% ^{2}H) to give the concentrations presented in Table I. The ^{1}H chemical shifts (δ) are given in ppm downfield from the internal standard, tetramethylsilane (TMS). The spectra were assigned by comparison with the spectrum of Chl *a* [42] and by using the two-dimensional NMR techniques heteronuclear multiple quantum coherence (HMQC) and heteronuclear multiple bond multiple quantum coherence (HMBC) [44–46].

Preparation of authentic 13^2(R,S)-hydroxy-Chl a

Authentic 13^2(*R*,*S*)-OH-Chl *a* was obtained by further purification of the preparations synthesized earlier in two ways: by horseradish peroxidase-catalysed H_2O_2 oxidation of Chl *a* solubilized with Triton-X 100 [47] and by selenium dioxide oxidation of Chl *a* in pyridine solution under argon [48]. The preparations were re-purified using chromatography on a sucrose column (3 cm O.D., height of the sucrose layer 45 cm). For the chromatography, the preparation was dissolved in 1 ml of diethyl ether plus 4 ml of the eluent. 13^2-Hydroxy-Chl *a* was eluted with 1% (v/v) 2-PrOH–hexane or MeOH–2-PrOH–hexane (0.4:0.8:98.8, v/v/v). The column, wrapped with aluminium foil, was operated in the dark at a flow-rate of 1 ml/min. The collected fractions were analysed by HPLC and the purest fractions were combined, washed with water and dried by the chloroform co-distillation method.

The solvent was evaporated to dryness and the solid was stored at −18°C.

RESULTS AND DISCUSSION

Allomerization reaction of Chl a

Fig. 1 shows the structures and numbering system for Chl *a* (**1a**) and the allomerization products relevant to this study. Except for a trace amount of Chl *a'* (**1b**), no other components could be detected in the original Chl *a* preparation by NP-HPLC. Methanolic solutions of Chl *a* [2.3 m*M*; 31.4 mg in 15 ml (experiment 1) and 304.5 mg in 150 ml (experiment 2)] were found to allomerize completely in 3 days when magnetically stirred under atmospheric oxygen at room temperature in darkness. The seven allomerization products identified were as follows:

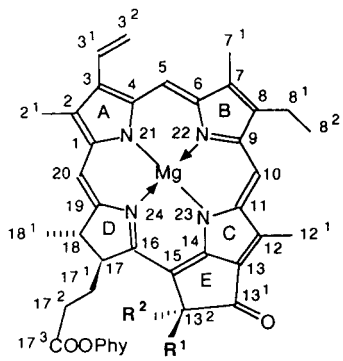

1

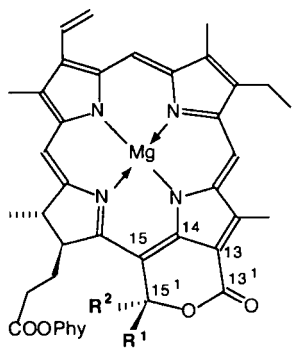

2

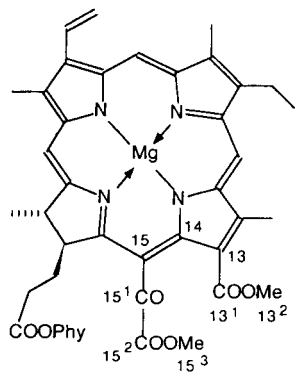

3

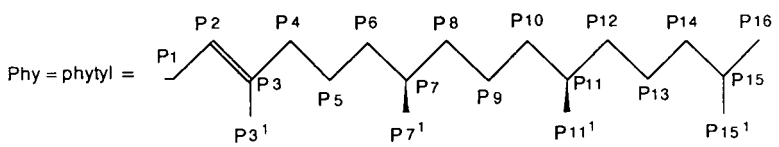

No.	R^1	R^2	Semisystematic name [4,39]	Trivial name [8,40]	Abbreviation
1a	H	$COOCH_3(13^4)$	$13^2(R)$-Chlorophyll *a*	Chlorophyll *a*	Chl *a*
1b	$COOCH_3(13^4)$	H	$13^2(S)$-Chlorophyll *a*	Chlorophyll *a'*	Chl *a'*
1c	$COOCH_3(13^4)$	OH	$13^2(R)$-Hydroxychlorophyll *a*	10(*R*)-Hydroxychlorophyll *a*	$13^2(R)$-HO-Chl *a*
1d	OH	$COOCH_3(13^4)$	$13^2(S)$-Hydroxychlorophyll *a*	10(*S*)-Hydroxychlorophyll *a*	$13^2(S)$-HO-Chl *a*
1e	$COOCH_3(13^4)$	$OCH_3(13^{3'})$	$13^2(R)$-Methoxychlorophyll *a*	10(*R*)-Methoxychlorophyll *a*	$13^2(R)$-MeO-Chl *a*
1f	$OCH_3(13^{3'})$	$COOCH_3(13^4)$	$13^2(S)$-Methoxychlorophyll *a*	10(*S*)-Methoxychlorophyll *a*	$13^2(S)$-MeO-Chl *a*
2a	$COOCH_3(15^3)$	$OCH_3(15^{2'})$	The magnesium complex of $3^1,3^2$-didehydro-15^1-hydroxy-$15^1(R)$-methoxy-rhodochlorin-15-acetic acid δ-lactone 15^2-methyl-17^3-phytyl ester	Mg-10(*R*)-Purpurin 7-lactone methyl ether methylphytyl ester	$15^1(R)$-MeO-lactone-Chl *a*
2b	$OCH_3(15^{2'})$	$COOCH_3(15^3)$	The magnesium complex of $3^1,3^2$-didehydro-15^1-hydroxy-$15^1(S)$-methoxy-rhodochlorin-15-acetic acid δ-lactone 15^2-methyl-17^3-phytyl ester	Mg-10(*S*)-Purpurin 7-lactone methyl ether methylphytyl ester	$15^1(S)$-MeO-lactone-Chl *a*
3			The magnesium complex of $3^1,3^2$-didehydro-rhodochlorin-15-glyoxylic acid $13^1,15^2$-dimethyl-17^3-phytyl ester	Mg-Purpurin 7-dimethyl-phytyl ester	15-Glyox-Chl *a*

Fig. 1. Structures, names and numbering system for Chl *a* and Chl *a'* and their allomerization products.

15^1-MeO-lactone derivative (two epimers, **2a** and **2b**), 13^2-HO-Chl *a* (two epimers, **1c** and **1d**), 13^2-MeO-Chl *a* (two epimers, **1e** and **1f**) and 15-glyox-Chl *a* (**3**). The concentration of Chl *a* has been postulated to affect the number and nature of the products formed in the allomerization reaction [7,12].

Separation and isolation of the allomerization products of Chl a

Column chromatography. The conventional column chromatographic separation of the allomerization products from experiment 2 gave, after eluting with solvents of several polarities, five coloured bands arranged one above another in order of decreasing adsorptivity on sucrose. The order of the bands from the bottom of the sucrose column according to NP-HPLC analysis was (1) pheophytins *a'* and *a*, (2) 15-glyox-Chl *a*, (3) 13^2-MeO-Chl *a* (one epimer), (4) 15^1-MeO-lactone derivative (two epimers), overlapped by the other epimer of 13^2-MeO-Chl *a* (Fig. 2a) and (5) 13^2-HO-CHl *a* (two epimers), overlapped by an unknown impurity and small amounts of 13^2-MeO-lactone epimers and of the other 13^2-MeO-Chl *a* epimer (Fig. 2b). The preparative sucrose column was capable of separating as stereochemically pure compounds 15-glyox-Chl *a* and one epimer of 13^2-MeO-Chl *a*.

Reversed-phase HPLC. Because RP chromatography is used in at least half of all HPLC separations [49], it is always a good first choice for the separation of soluble organic compounds. In addition, Schaber *et al.* [14] used RP-HPLC for following the allomerization reaction. Therefore, also we selected this HPLC method for our first trial. Five C_{18} columns from different manufacturers were tested along with a Zorbax ODS semi-preparative column similar to that used by Schaber *et al.* [14]. Starting with different binary MeOH–water and ACN–water mobile phases, we soon found that the amount of water could be at most 5% (v/v), otherwise the Chl derivatives seemed to form various water adducts that were adsorbed strongly on the RP column and could be washed out only with 100% MeOH. We then tried the Zorbax ODS column using THF–

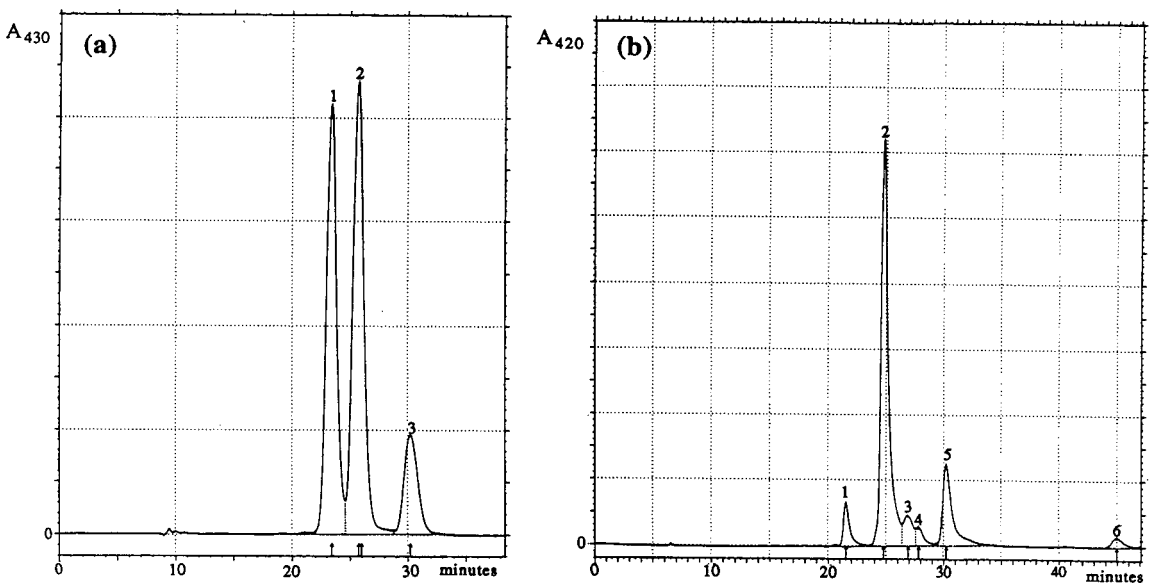

Fig. 2. (a) NP-HPLC of band 4 from the preparative sucrose column (allomerization products from experiment 2). Column, LiChrospher Si 100 (250 × 4.0 mm I.D.), particle size 10 μm; mobile phase, 2-PrOH–MeOH–hexane (0.8:0.4:98.8, v/v/v); flow-rate, 0.8 ml/min. Peaks: 1 and 2 = 15^1-MeO-lactone-Chl *a* epimers; 3 = 13^2-MeO-Chl *a* epimer 2. (b) NP-HPLC of band 5 from the preparative sucrose column (allomerization products from experiment 2). Column, Zorbax Sil (250 × 9.4 mm I.D.), 5–6 μm; mobile phase, 1.25% (v/v) 2-PrOH in hexane; flow-rate, 3 ml/min. Peaks: 1 = unidentified; 2 and 5 = 13^2-HO-Chl *a* epimers; 3 and 4 = 15^1-MeO-lactone-Chl *a* epimers; 6 = 13^2-MeO-Chl *a* epimer 2.

MeOH–water (36:54:10, v/v/v) as the mobile phase, because Schaber *et al.* [14] were able to separate the epimers of 13^2-HO-Chl *a* and those of the 15^1-MeO-lactone derivative with this system. THF coordinates to the fifth and/or sixth coordination position of the central magnesium atom of the allomerization products, thus inhibiting the formation of water adducts. In spite of several attempts under these chromatographic conditions, we were able to resolve only the 15^1-MeO-lactone epimers, the other components, except 15-glyox-Chl *a*, being eluted unresolved (Fig. 3a). 15-Glyox-Chl *a* showed an increased affinity for the RP column, eluting only when the column was flushed with methanol. Attempts were made to improve the separation by varying the proportions of THF, MeOH and water in the ternary mobile phase and some quaternary solvent systems were also tested. The best, but still incomplete, RP-HPLC separation, was achieved by using the Zorbax ODS column and THF–MeOH–water (10:85:5, v/v/v) as the mobile phase (Fig. 3b).

Normal-phase HPLC. The allomerization mixture contains several components, some of which are eluted very close together and hence can be separated only with difficulty. Because we could not achieve the desired separation by the RP-HPLC method, in spite of using several different RP columns and mobile phase combinations, we attempted NP-HPLC on a silica column. This method has often shown a unique capability to resolve isomers, and is also a good choice for preparative-scale HPLC. Watanabe *et al.* [33], for example, achieved a good separation for Chl *a*, *a'*, *b* and *b'* and the corresponding pheophytins using isocratic HPLC on a silica column.

Four silica columns from two manufacturers (Merck and DuPont) were tried in the NP separations. All silica columns afforded better separations than the RP columns. The Zorbax Sil semi-preparative column was the best as it separated all allomers including their epimers (Fig. 4). It is noteworthy that not even the analytical Zorbax Sil column was capable of separating the allomers as effectively as the corresponding semi-preparative column. This demonstrates again that similarity of the chromatographic material does not ensure reproducibility of the retention properties for different batches of the same product, which has been and still is a problem in HPLC. Fig. 4 shows that the elution order of the allomerization products on a silica column did not meet expectations, as the more polar 13^2-HO-Chl *a* epimers were eluted before 13^2-MeO-Chl *a* epimers. For some reason, the latter epimers are retarded more strongly than the former in the polar stationary

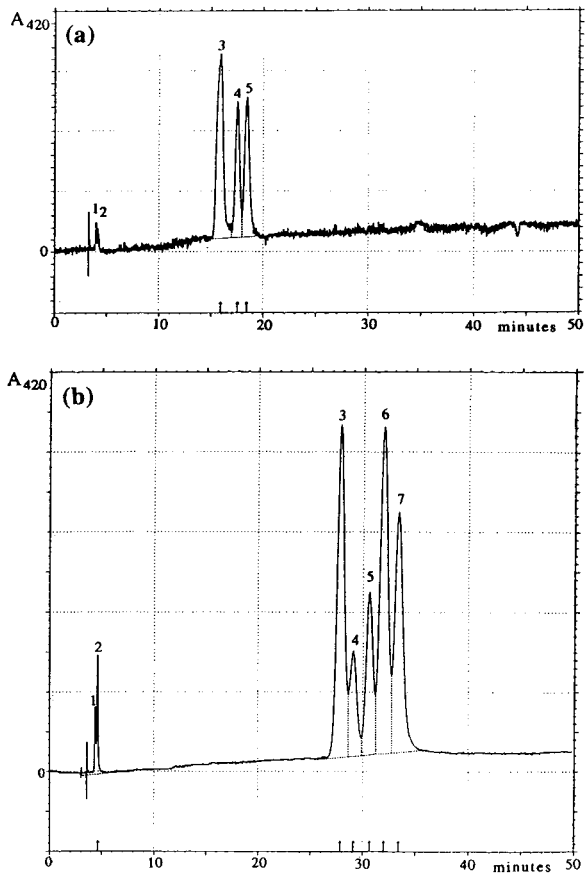

Fig. 3. RP-HPLC separation of the allomerization products on the Zorbax ODS column (250 × 9.4 mm I.D.), 5–6 μm. (a) Mobile phase, THF–MeOH–water (36:54:10, v/v/v); flow-rate, 3 ml/min. Peaks: 1 and 2 = unidentified, possibly pheophytins; 3 = 13^2-MeO-Chl *a* and 13^2-HO-Chl *a* epimers; 4 and 5 = 15^1-MeO-lactone-Chl *a* epimers. (b) Mobile phase, THF–MeOH–water (10:85:5, v/v/v); flow-rate, 3 ml/min. Peaks: 1 and 2 = unidentified, possibly pheophytins; 3, 4 and 5 all have UV–Vis spectra very similar to that of Chl *a* but the components were not identified more precisely; 6 and 7 = 15^1-MeO-lactone-Chl *a* epimers.

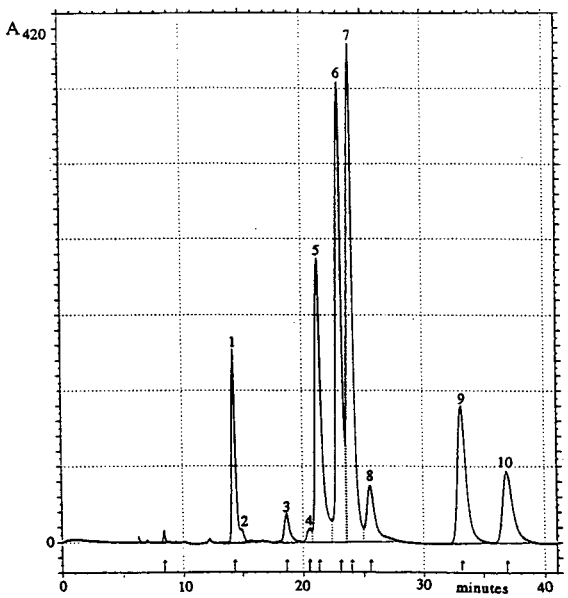

Fig. 4. NP-HPLC separation of the allomerization products on the Zorbax Sil column (250 × 9.4 mm I.D.), 5–6 μm. Mobile phase, 1.5% (v/v) 2-PrOH in hexane; flow-rate, 4 ml/min. Peaks 1 = 15-glyox-Chl *a*; 2, 3 and 4 = unidentified; 5 and 8 = 13^2-HO-Chl *a* epimers; 6 and 7 = 15^1-MeO-lactone-Chl *a* epimers; 9 and 10 = 13^2-MeO-Chl *a* epimers.

phase of silica. The principal allomerization products were the $15^1(R)$- and $15^1(S)$-epimers of the 15^1-MeO-lactone derivative (*ca.* 52% altogether). The amounts of $13^2(R,S)$-HO-Chl *a* and $13^2(R,S)$-MeO-Chl *a* were 21% and 18%, respectively, and the amount of 15-glyox-Chl *a* was 7%. The ratios of epimers 1 and 2, where 1 and 2 denote the elution order of the epimers in NP-HPLC, were 46:54 for the 15^1-MeO-lactone derivative, 79:21 for 13^2-HO-Chl *a* and 62:38 for 13^2-MeO-Chl *a*.

The mobile phase consisted of 0.8–2.0% (v/v) 2-PrOH in hexane or MeOH–2-PrOH–hexane (0.4:0.8:98.8, v/v/v). A very small change (0.1%) in the mobile phase composition affected the NP-HPLC separation results. The addition of MeOH to the mobile phase facilitated the chromatography of the 13^2-HO-Chl *a* epimers. The advantageous effect of MeOH may be attributed to its capability of preventing aggregation of the derivatives. The 13^2-HO-Chl epimers showed a particularly strong and concentration-dependent tendency for aggregation, owing to the presence of the central Mg atom and 13^2-hydroxyl and the 13^1-carbonyl groups in these molecules.

Bands 2 and 3 from the sucrose column (see above) contained pure 15-glyox-Chl *a* and one epimer of 13^2-MeO-Chl *a*, respectively. The chromatogram in Fig. 2a, in contrast, shows that band 4 from the sucrose column contained both epimers of 13^2-MeO-lactone-Chl *a* and the other epimer of 13^2-MeO-Chl *a*. The semi-preparative Zorbax Sil column was used for further purification of band 4. Figs. 5a and b show the analytical and preparative chromatograms, respectively, of band 4 run on the Zorbax Sil semi-preparative column. Fig. 5b shows that the 4-mg sample exhibits a behaviour similar to that of the analytical sample except for the slightly enhanced overlap between peaks 1 and 2 and the change in the retention time of component 4. After repeated separations the amount and purity of collected 13^2-MeO-lactone epimer 1 were 6 mg and 99.9%, respectively, and those of epimer 2 were 10.2 mg and 93–94%. The only impurity in the epimer 2 preparation was epimer 1.

Detection and identification of the allomerization products

Diode-array detection (DAD) has become established as a powerful LC detection method over the last 8 years [50–55]. DAD produces large amounts of multi-wavelength chromatographic and spectroscopic data in a single run. A variety of graphical and numerical strategies have been developed for the presentation of the data [50,53,54]. Most commonly, DAD is used to produce the on-the-fly UV–Vis spectra of the chromatographic peaks. This kind of spectrum was recorded here under isocratic HPLC conditions at the retention time of each allomer peak (Fig. 6) to facilitate its preliminary identification. Chl *a* and the derivatives substituted at C-13^2 have very similar UV–Vis spectra. Consequently, the 13^2-HO-Chl *a* and 13^2-MeO-Chl *a* epimers could not be identified solely on the basis of their UV–Vis spectra. Retention time comparisons and co-elution with authentic compounds and NMR spectroscopy were also needed. Nevertheless, 15-glyox-Chl *a* and the 15^1-MeO-lactone derivatives were distinguish-

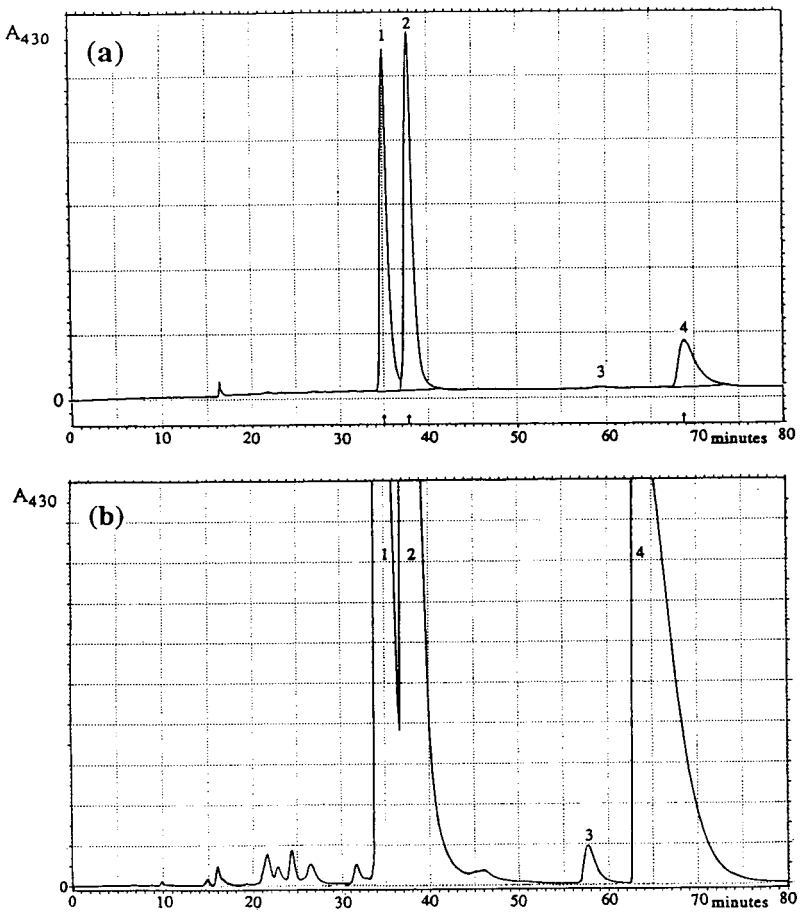

Fig. 5. (a) Analytical and (b) preparative (4 mg) NP-HPLC of the 13^2-MeO-lactone fraction (band 4) from the preparative sucrose column. Column, Zorbax Sil (250 × 9.4 mm I.D.), 5–6 μm; mobile phase, 0.8% (v/v) 2-PrOH in hexane; flow-rate, 4 ml/min. Peaks: 1 and 2 = 15^1-MeO-lactone-Chl *a* epimers; 3 and 4 = 13^2-MeO-Chl *a* epimers.

able by UV–Vis spectra from the other allomerization products.

Although it has been known for a long time that UV–Vis spectra are insufficient for the reliable identification of Chl allomers, NMR spectroscopy has rarely been used for this purpose. The ^{1}H and ^{13}C NMR resonances for the macrocycle of 13^2-HO-Chl *a* have been totally assigned [47,48] and the ^{1}H NMR spectrum of the 13^2-MeO-lactone derivative of Chl *a* has been partly interpreted [12,14]. In this study, the ^{1}H NMR spectra (Table I) were used to identify the allomerization products more conclusively. For about half of the Chl derivatives in Table I, the assignments have already been confirmed using the HMQC and HMBC techniques. For the other derivatives, the mutual order for several assignments is only tentative and requires confirmation by the aforementioned two-dimensional NMR techniques. Such experiments are in progress.

Mechanism of allomerization

Our allomerization results are different from those reported by Schaber *et al.* [14] in that we observed 15-glyox-Chl *a* and $13^2(R)$- and $13^2(S)$-MeO-Chls in addition to the diastereomers of 13^2-HO-Chl *a* and the 15^1-MeO-lactone derivative (major products). Several minor components could also be detected among the allomers (Fig.

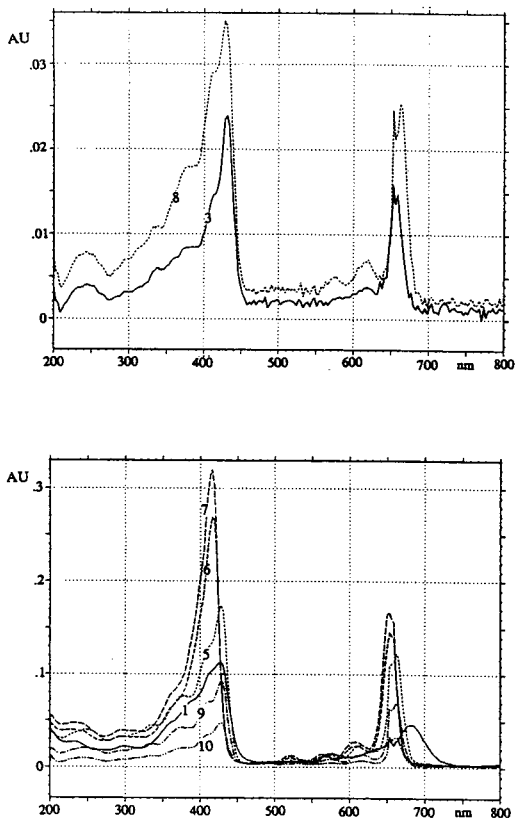

Fig. 6. UV–Vis spectra of the allomerization products of Chl *a* recorded from 200 to 800 nm with the diode-array detector under the chromatographic conditions of Fig. 4. The numbers on the spectra correspond to the numbers of the chromatographic peaks in Fig. 4. The shoulder in the spectra near 650 nm depends on the detector.

5b), but we did not investigate these. According to Schaber *et al.* [14], the 13^2-HO-Chl *a* epimers are major products and are formed in both presence and absence of extraneous nucleophiles (*e.g.*, MeOH), while the epimers of the 15^1-MeO-lactone derivative are formed only when Chl *a* is allowed to allomerize in a polar hydroxylic solvent [14]. They could not detect any 15-glyox-Chl *a* or 13^2-MeO-Chl *a* by RP-HPLC. These differences in results probably arise from differences in the reaction and fractionation conditions used by the two groups. We performed the reactions with continuous stirring and in darkness. Further, the methanol we used was perhaps different from that used by Schaber *et al.* [14] (unfortunately, they did not mention the purity or source of the methanol), and also we used NP-HPLC instead of RP-HPLC.

The free-radical chain mechanism involving triplet oxygen, the Chl C-13^2 radical and the Chl 13^2-hydroperoxide derivative [4,11] can account for the allomerization products formed in this study. Radical reactions are typical of the triplet oxygen. Singlet oxygen cannot be formed in the dark. The large number of the allomerization products (Fig. 5b) supports the radical mechanism. The unexpected ratio of *ca.* 4:1 for the 13^2-HO-Chl *a* epimers can be explained by their formation via two possible routes: (1) the termination reaction of the Chl C-13^2 radical with hydroxyl radical and (2) the homolytic cleavage of the Chl 13^2-hydroperoxide followed by hydrogen atom addition. Moreover, steric reasons may result in unexpected epimeric ratios.

CONCLUSION

The spontaneous allomerization reaction for Chl *a* in methanol (2.3 m*M*) in complete darkness produced as principal products 15^1-MeO-lactone derivatives (52%), consisting of 15^1-diastereomers in a ratio of 46:54. The other products were 13^2-HO-Chl *a* (21%, 13^2-diastereomers in a ratio of 79:21), 13^2-MeO-Chl *a* (18%, 13^2-diastereomers in a ratio of 62:38) and 15-glyox-Cl *a* (7%). In addition, some minor components were detected, but not identified.

The separation, isolation and structural identification of the individual components in the complex mixture of the Chl *a* allomers have posed an analytical problem of practical interest. In this study, the RP-HPLC experiments were carried out with various RP columns and mobile phase compositions, but no RP method resulted in the desired separation. Silica columns proved to have the unique capability of separating all allomerization products and their epimers. Of the silica columns tested in this study, the Zorbax Sil semi-preparative column provided the best separation and a powerful means for the preparative isolation of the allomerization products in milligram amounts. The amounts isolated were sufficient for the characterization of the compounds by NMR techniques. The pre-

TABLE I

^{1}H NMR CHEMICAL SHIFTS (δ^{TMS} IN PPM) FOR CHL *a* AND ITS ALLOMERS IN ACETONE-d_6

Proton[a]	Chl *a* (11.2 m*M*)	15-Glyox-Chl *a* (10.9 m*M*)	15^1-MeO-lactone-Chl *a*		13^2-MeO-Chl *a*		13^2-HO-Chl *a*	
			Epimer 1[b] (8.5 m*M*)	Epimer 2[b] (14.5 m*M*)	Epimer 1[b] (27.0 m*M*)	Epimer 2[b] (2.4 m*M*)	Epimer 1[b] (15.0 m*M*)	Epimer 2[b] (10.0 m*M*)
10-H	9.72	9.52	9.79	9.80	9.78	9.79	9.78	9.79
5-H	9.39	9.28	9.51	9.52	9.42	9.45	9.46	9.46
20-H	8.56	8.39	8.66	8.68	8.61	8.61	8.62	8.61
3^1-H_X	8.12	8.01	8.13	8.13	8.12	8.13	8.14	8.14
3^2-H_B (*trans*)	6.22	6.16	6.23	6.23	6.23	6.24	6.22	6.22
3^2-H_A (*cis*)	6.01	5.96	6.01	6.01	6.02	6.03	6.02	6.02
13^2-OH	–	–	–	–	–	–	6.05	6.02
13^2-H	6.18	–	–	–	–	–	–	–
P2-H	4.95	5.16	5.19	5.14	5.16	5.21	5.14	5.22
17-H	4.16	4.66	4.72	4.85	4.45	4.27	4.68[c]	4.15[c]
18-H	4.55	4.31	4.46	4.45	4.54	4.57	4.55[c]	4.55[c]
P1-CH_2	4.29	4.42	4.45	4.40	4.43	4.48	4.40[c]	4.46[c]
8^1-CH_2	3.80	3.72	3.82	3.83	3.82	3.83	3.83	3.83
13^2-CH_3	–	3.97[c]	–	–	–	–	–	–
13^4-CH_3	3.81	–	–	–	3.62	3.59[c]	3.60[c]	3.58[c]
15$^{2'}$-CH_3	–	–	3.84	3.49	–	–	–	–
15^3-CH_3	–	3.84[c]	3.61	3.65	–	–	–	–
12^1-CH_3	3.59	3.43[c]	3.77	3.77	3.65	3.66[c]	3.64[c]	3.64[c]
2^1-CH_3	3.34	3.23[c]	3.35	3.35	3.35	3.36[c]	3.36[c]	3.36[c]
7^1-CH_3	3.29	3.20[c]	3.31	3.31	3.28	3.31[c]	3.31[c]	3.31[c]
13$^{3'}$-CH_3	–	–	–	–	3.15	3.40[c]	–	–
17^1-CH_2, 17^2-CH_2	2.58–2.12	2.28–1.82	2.47–2.10	2.46–2.24	2.38–1.96	2.70–2.45	2.34–2.22	2.83–2.43
P4-CH_2	1.84	1.90	1.91	1.88	1.89	1.93	1.85	1.79
8^2-CH_3	1.70	1.65	1.70	1.70	1.73	1.72	1.71	1.71
18^1-CH_3	1.76	1.74	1.55	1.69	1.62	1.56	1.65	1.56
P3^1-CH_3	1.51	1.58	1.59	1.55	1.57	1.61	1.56	1.62

[a] See Fig. 1 for numbering of carbon atoms.
[b] Epimer 1 = faster moving epimer and epimer 2 = slower moving epimer in NP-HPLC.
[c] HMQC and HMBC experiments are necessary for the final assignments.

parative-scale isolation of Chl derivatives has formerly relied largely on conventional column chromatography (CC). In this study, however, conventional CC on sucrose had to be complemented by HPLC in order to achieve the separation of all allomerization products including the C-13^2/15^1 epimers. Although conventional CC requires large amounts of column material and solvents, it seems likely to maintain its position as a good preparative preseparation method. The determination of the absolute configuration at C-13^2 or C-15^1 for the isolated allomerization products by NMR is in progress. We should subsequently be able to specify which peaks in the HPLC traces belong to the 13^2/15^1(*R*)-epimers and which to the 13^2/15^1(*S*)-epimers. Additional studies to clarify the allomerization mechanism in further detail are in progress.

REFERENCES

1 R. Willstätter and A. Stoll, *Untersuchungen über Chlorophyll*, Springer, Berlin, 1913, pp. 29 and 147.
2 G.R. Seely, in L.P. Vernon and G.R. Seely (Editors), *The Chlorophylls*, Academic Press, New York, 1966, p. 67.
3 A.H. Jackson, in T.W. Goodwin (Editor), *Chemistry and Biochemistry of Plant Pigments*, Vol. 1, Academic Press, London, 2nd ed., 1975, p. 1.
4 P.H. Hynninen, in H. Scheer (Editor), *Chlorophylls*, CRC Press, Boca Raton, FL, 1991, p. 145.

5 W.A. Svec, in H. Scheer (Editor), *Chlorophylls*, CRC Press, Boca Raton, FL, 1991, p. 89.
6 H. Fischer and H. Pfeiffer, *Justus Liebigs Ann. Chem.*, 555 (1944) 94.
7 L.G. Johnston and W.F. Watson, *J. Chem. Soc.*, (1956) 1203.
8 A.S. Holt, *Can. J. Biochem. Physiol.*, 36 (1958) 439.
9 G.W. Kenner, S.W. McCombie and K.M. Smith, *J. Chem. Soc., Perkin Trans. 1* (1973) 2517.
10 P.H. Hynninen and S. Assandri, *Acta Chem. Scand., Ser. B*, 27 (1973) 1478.
11 P.H. Hynninen, *Z. Naturforsch., Teil B*, 36 (1981) 1010.
12 F.C. Pennington, H.H. Strain, W.A. Svec and J.J. Katz, *J. Am. Chem. Soc.*, 89 (1967) 3875.
13 J.E. Hunt, P.M. Schaber, T.J. Michalski, R.C. Dougherty and J.J. Katz, *Int. J. Mass Spectrom. Ion Phys.*, 59 (1983) 45.
14 P.M. Schaber, J.E. Hunt, R. Fries and J.J. Katz, *J. Chromatogr.*, 316 (1984) 25.
15 D.C. Borg, J. Fajer, R.H. Felton and D. Dolphin, *Proc. Natl. Acad. Sci. U.S.A.*, 67 (1970) 813.
16 M.N. Merzlyak, V.A. Kovrizhnikh, N.S. Kuprianova and I.B. Afanas'ev, *J. Inorg. Biochem.*, 24 (1985) 239.
17 M.N. Merzlyak, V.A. Kovrizhnikh and K.N. Timofeev, *Free Rad. Res. Commun.*, 15 (1991) 197.
18 M. Tswett, *Ber. Dtsch. Bot. Ges.*, 24 (1906) 316, 384.
19 J.A.S. Cavaleiro and K.M. Smith, *Talanta*, 33 (1986) 963.
20 S. Roy, *J. Chromatogr.*, 391 (1987) 19.
21 T.W. Goodwin and G. Britton, in T.W. Goodwin (Editor), *Plant Pigments*, Academic Press, London, 1988, p. 62.
22 Y. Shioi, in H. Scheer (Editor), *Chlorophylls*, CRC Press, Boca Raton, FL, 1991, p. 59.
23 H. Brockmann and N. Risch, in H. Scheer (Editor), *Chlorophylls*, CRC Press, Boca Raton, FL, 1991, p. 103.
24 N. Evans, D.E. Games, A.H. Jackson and S.A. Matlin, *J. Chromatogr.*, 115 (1975) 325.
25 K. Eskins, C.R. Scholfield and H. Dutton, *J. Chromatogr.*, 135 (1977) 217.
26 W.T. Shoaf, *J. Chromatogr.*, 152 (1978) 247.
27 C.A. Rebeiz, M.B. Bazzaz and F. Belanger, *Chromatogr. Rev.*, 4 (1978) 8.
28 K. Iriyama, M. Yoshina and M. Shirak, *J. Chromatogr.*, 154 (1978) 302.
29 S.J. Schwarz, S.L. Woo and J.H. von Elbe, *J. Agric. Food. Chem.*, 29 (1981) 533.
30 J.K. Abaychi and J.P. Riley, *Anal. Chim. Acta*, 107 (1979) 1.
31 T. Braumann and L.H. Grimme, *J. Chromatogr.*, 170 (1979) 264.
32 S.J. Schwartz and J.H. von Elbe, *J. Liq. Chromatogr.*, 5 (1982) 43.
33 T. Watanabe, A. Hongu, K. Honda, M. Nakazato, M. Konno and S. Saitoh, *Anal. Chem.*, 56 (1984) 251.
34 Y. Shioi, M. Doi and T. Sasa, *J. Chromatogr.*, 298 (1984) 141.
35 Y. Shioi, R. Fukae and T. Sasa, *Biochim. Biophys. Acta*, 722 (1983) 72.
36 N. Suzuki, K. Saitho and K. Adachi, *J. Chromatogr.*, 408 (1987) 181.
37 F.L. Canjura and S.J. Schwartz, *J. Agric. Food. Chem.*, 39 (1991) 1102.
38 M.I. Minguez-Mosquera, B. Gandul-Rojas, A. Montano-Asquerino and J. Garrido-Fernandez, *J. Chromatogr.*, 585 (1991) 259.
39 International Union of Pure and Applied Chemistry (IUPAC) and International Union of Biochemistry (IUB), in G.B. Moss (Editor), *Nomenclature of Tetrapyrroles, Pure Appl. Chem.*, 59 (1987) 779.
40 H. Fischer and A. Stern, *Die Chemie des Pyrrols*, Vol. 2, Part 2, Akademische Verlagsgesellschaft, Leipzig, 1940 (reprinted by Johnson Reprint, New York, 1968).
41 P.H. Hynninen, *Acta Chem. Scand., Ser. B*, 31 (1977) 829.
42 P.H. Hynninen and S. Lötjönen, *Synthesis*, 705 (1983).
43 I. Sahlberg and P.H. Hynninen, *J. Chromatogr.*, 291 (1984) 331.
44 A. Bax and S. Subramanian, *J. Magn. Reson.*, 67 (1968) 565.
45 M.F. Summers, L.G. Marzilli and A. Bax, *J. Am. Chem. Soc.*, 108 (1986) 4285.
46 I. Kilpeläinen, S. Kaltia, P. Kuronen, K. Hyvärinen and P.H. Hynninen, *Magn. Reson. Chem.*, submitted for publication.
47 V. Kaartinen, E. Kolehmainen and P.H. Hynninen, in T. Pakkanen (Editor), *9th National NMR Symposium, University of Joensuu, Report Series No. 3*, University of Joensuu, Joensuu, 1985, p. 10.
48 T. Laitalainen, J. Pitkänen and P.H. Hynninen, in K. Wähälä and J.K. Koskimies (Editors), *8th International IUPAC Conference on Organic Synthesis, Helsinki, 1990*, University Press, Helsinki, 1990, p. 246.
49 R.E. Majors, *LC · GC Int.*, 5 (1992) 12.
50 D.G. Jones, *Anal. Chem.*, 57 (1985) 1207A and 1057A.
51 T. Alfredson and T. Sheehan, *J. Chromator. Sci.*, 24 (1986) 473.
52 G.W. Schieffer, *J. Chromatogr.*, 319 (1985) 387.
53 T. Alfredson, T. Sheehan, T. Lenert, S. Aamodt and L. Correia, *J. Chromatogr.*, 385 (1987) 213.
54 S. Ebel and W. Mueck, *Chromatographia*, 25 (1988) 1039.
55 P. Kuronen, *Arch. Environ. Contam. Toxicol.*, 18 (1989) 336.

Journal of Chromatography A, 654 (1993) 105–111
Elsevier Science Publishers B.V., Amsterdam

CHROM. 25 432

Optimization of the anion-exchange separation of metal–oxalate complexes

R.M. Cassidy* and L. Sun

Chemistry Department, University of Saskatchewan, Saskatoon, SK, S7N 0W0 (Canada)

(First received April 26th, 1993; revised manuscript received July 13th, 1993)

ABSTRACT

Anion exchangers, prepared by the sorption of cetylpyridinium chloride onto a reversed phase, have been evaluated for the separation of the transition metal ions Mn^{2+}, Co^{2+}, Ni^{2+}, Cu^{2+}, and Zn^{2+}. Parameters examined included nature of complexing reagent, eluent pH, eluent concentration, speciation of the metal ion in the complexation system, and column capacity. The separations obtained with an oxalate eluent were compared to those obtained with a cation exchanger prepared by the addition of *n*-octanesulfonate to the eluent. Theoretical plate heights were in the range of 0.010 mm to 0.025 mm, and were in many instances, slightly better than those obtained with cation separation systems. Metal ion speciation in the eluent appeared to be a dominant factor determining the efficiency of the anion separation; metal ions with one dominant complexed ion generally gave more efficient separations. Compared to cation separations, analysis times were similar, but separation selectivities were considerably different.

INTRODUCTION

The separation of metal ions on modern high-performance ion exchangers has become an accepted practice in ion chromatography, and many suppliers of chromatographic equipment offer standard methods for such analyses. The majority of the methods available are based on cation-exchange separations with either bonded phases or exchangers formed from the sorption of anionic surfactants onto reversed phases [1,2]. Only a limited number of studies have been reported for the separation of anionic metal ion species [3–9]. The methods reported to date have not been widely adopted, primarily due to poor column efficiency and increased difficulty of detection relative to cation-exchange systems. However, separations based on anionic exchange offer the potential advantages of different selectivity, reduced problems from metal ion hydrolysis, and application to complex sample matrices. The most successful applications reported for anion-exchange separations of metal ions have made use of stable multidentate reagents, such as ethylenediaminetetraacetic acid [4,7]. Other anionic systems [3,5,6,8,9] exhibit separation efficiencies that are much less than normally found for cation exchangers. However, these reported studies suggest that anion exchange offers potential advantages with respect to selectivity and for the analysis of complex samples [3–9].

The diversity of metal species present in the eluent of an anion separation is expected to be greater than that for a cation separation. In cation separations the formation of a small amount of a 1:1 complex with a ligand in the eluent may be sufficient to both effect elution and impart selectivity to the separation. However, for an anion separation, a greater degree of complexation is required to produce the necessary anionic complexes, and if a wider variety of complexed metal species are present, all of these

* Corresponding author.

0021-9673/93/$06.00

species must be in rapid equilibrium for efficient mass transfer between the mobile and stationary phases. Consequently, there is a need to examine anionic systems in more detail in an effort to understand the factors limiting column efficiency in these systems.

In this work the anionic exchange separation of the transition metal ions Mn^{2+}, Co^{2+}, Ni^{2+}, Cu^{2+}, and Zn^{2+} has been evaluated in terms of nature of complexing reagent, eluent pH, eluent concentration, speciation of the metal ion in the complexation system, and column capacity. In addition, detection with postcolumn reaction (PCR) reagents was also briefly examined. Since the complexation reactions of divalent transition metal ions with oxalate have been widely studied, oxalate was the main complexing reagent used in the eluent. Other complexing reagents briefly examined included 2,6-pyridine dicarboxylic acid (PDCA) and tartaric acid. The results obtained with the optimized anion system were then compared to standard cation systems recommended for metal ion separations. Surfactant-modified reversed phases were used in these evaluations to permit the use of the same column for the preparation of a wide variety of exchange capacities, and for application to both anion and cation-exchange separations.

EXPERIMENTAL

Apparatus

The eluent delivery system was a Waters Model 510 HPLC pump (Waters/Millipore, Milford, MA, USA). A Rheodyne Model 7161 injection port (Cotati, CA, USA) with a 20-μl sample loop was used to inject samples onto a 15 cm × 4.6 mm (I.D.) Supelcosil LC-18 (5 μm) column (Supelco, Bellefonte, PA, USA); for some studies self-packed columns with Nucleosil 100-5 C_{18} (5 μm) or 100-10 C_{18} (10 μm) (Macherey-Nagel, Düren, West Germany) were used. The detection system included a screen "T" mixer [10], a reaction coil made from 102 cm long 1/16 in. O.D. × 0.020 in. I.D. (1 in. = 2.54 cm) PTFE tubing knotted into a series of figure-eight knots, and a UV–visible detector set at 520 nm (Waters 484 Tunable Absorbance Detector, Milford, MA, USA). The PCR reagent solution was introduced with helium gas pressure (*ca.* 25 p.s.i.; $1.8 \cdot 10^4$ kg · m^{-2}) at 0.57 ml · min^{-1} with a Matheson Model No. 3473 gas regulator. A small amount of citric acid was placed in a tube between the reagent reservoir and the regulator to prevent diffusion of ammonia into the gas regulator. A Waters BASELINE 810 Chromatography Workstation software (Waters/Millipore) was used to record and analyze the data. Values of height equivalent to a theoretical plate (HETP) were calculated from peak widths measured by the tangent method. Extra-column contribution to band broadening was determined by plots of peak variance as a function of sample volume in the absence of a column. These values of variance were used to correct the values of peak widths used for the calculation of the number of theoretical plates, N, from the common equation, $N = 16(t_R/t_w)^2$ (t_w is peak width).

Chemicals and supplies

Aqueous solutions were prepared with distilled deionized water, and all chemicals were standard analytical grade. Cetylpyridinium chloride (CPCl) (Sigma, St. Louis, MO, USA) in acetonitrile–water (20:80, v/v) solution was used to "permanently" coat reversed-phase columns with CPCl, and thus convert them into anion-exchange columns. Sodium octanesulfonate (SO) (Aldrich, Milwaukee, WI, USA) was used for separations based on ion-interaction exchange mechanisms. Metal ion samples for anion and cation separations were made by dissolving metal salts in the desired eluent, normally at a concentration of 5.0 μg · ml^{-1}. The postcolumn reagents, 4-(2-pyridylazo)resorcinol (PAR) (Aldrich, Milwaukee, WI, USA), and eriochrome black T (EBT) (Aldrich), were used as PCR reagents at a concentration of $2.0 \cdot 10^{-4}$ mol · l^{-1} in a 3.0 mol · l^{-1} NH_3 and 1.0 mol · l^{-1} acetic acid pH 10 buffer. Eluent pH was adjusted with sodium hydroxide. All eluents were filtered through a 0.2-μm filter prior to use.

Column preparation

Self-packed columns were packed with an isooctane–chloroform (1:3, v/v) slurry as described elsewhere [11]. Anion-exchange columns

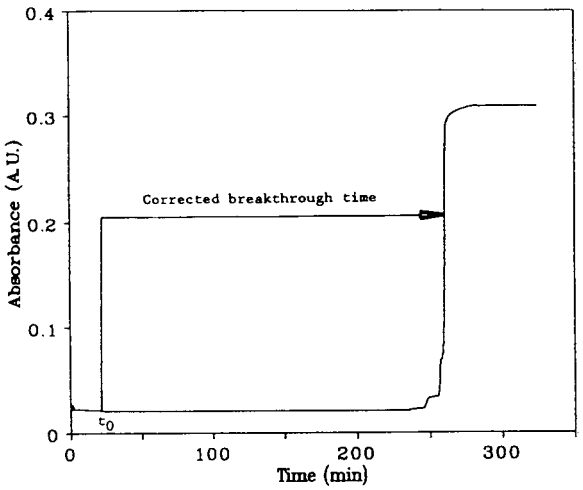

Fig. 1. Breakthrough curve for CPCl adsorption onto a reversed-phase column. Experimental conditions: $1.0 \cdot 10^{-4}$ mol·l^{-1} CPCl in acetonitrile–water (20:80, v/v); 15 cm × 4.6 mm I.D. Supelcosil LC-18 (5 μm) column; CPCl solution flow started at $t = 5.0$ min; the UV absorbance of the eluent was monitored at 254 nm.

were prepared by equilibration of reversed-phase columns with 1-l solutions of CPCl in acetonitrile–water (20:80, v/v) as described elsewhere [2]; concentrations of CPCl in the range of $1.00 \cdot 10^{-2}$ to $1.00 \cdot 10^{-4}$ mol·l^{-1} were used to produce a wide range of exchange capacities. The coating solutions were filtered through 0.2-μm nylon filters and eluted through the reversed-phase

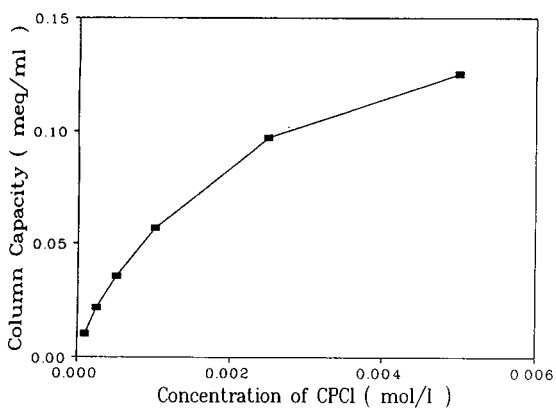

Fig. 2. Anion-exchange capacity as a function of concentration of CPCl in the coating solution. Experimental conditions: 15 cm × 4.6 mm I.D. Supelcosil LC-18 (5 μm) column; CPCl solution, 1 l, was in acetonitrile–water (20:80, v/v).

separation column and a pre-column at a flow-rate of 1.0 ml·min^{-1}. Breakthrough curves [12] were used to determine column capacity, and an example of one of these curves is shown in Fig. 1. The relationship between the concentration of the surfactant in the coating solution and the final effective exchange capacity (per ml of column volume) is shown in Fig. 2.

RESULTS AND DISCUSSION

Detection

Simple metal ions can not be detected with good sensitivity by direct UV–visible absorption. Detection as anionic complexes formed with complexing reagents in the eluent is possible if the complexes exhibit large molar absorptivities at wavelengths different from the free ligand, but this was not the case for any of the eluents used in these studies. Consequently, detection after a PCR was investigated. The main PCR reagents studied were PAR and EBT. PAR is commonly used for the PCR detection of metal ions, and EBT was selected since its conditional stability constants are higher for some metal ions. At pH 10 both PAR and EBT can react with several metal ions, and to maintain a pH value of 10, a 3 mol·l^{-1} ammonia and 1 mol·l^{-1} acetic acid buffer was used in the PCR reaction. Although ammonia can complex metal ions, it did not have an important effect on the formation of PAR or EBT complexes. In spite of the larger conditional formation constants for EBT complexes, experimental results showed that sensitivities with EBT were much worse than those with PAR, possibly due to a slower ligand exchange between metal complexes formed in the eluent and EBT.

Except for Ni^{2+}, good sensitivities were obtained when PAR was used with oxalate eluents. Detection sensitivity for Ni^{2+} decreased with an increase in the concentration of free oxalate in the eluent. Since Ni^{2+} is known to exhibit slow ligand exchange (see below) relative to the other metal ions studied [13], the poor sensitivity with Ni^{2+} was likely a result of a slow reaction with PAR. This conclusion is supported by the fact that with a reaction-delay coil Ni^{2+} was detected with a sensitivity comparable to that for the

other metal ions. With 0.100 mol·l^{-1} PDCA (pH = 5.4) as the eluent, only Co^{2+} and Cu^{2+} were detected without a reaction coil. When the reaction coil was used all metal ions were detected, and detection sensitivities were increased by up to 5-fold for Co^{2+} and Cu^{2+}. However, relative to oxalate eluents, detection limits with PDCA were lower by 2- to 50-fold than those observed for the highest concentration (0.20 mol·l^{-1}) of oxalic acid used as an eluent. The poorer detection limits for PDCA eluents may be a result of the larger conditional formation constants for PDCA complexes (calculated from data in ref. 14). Tartaric acid was also considered as a possible eluent because its conditional formation constants are smaller than those of complexes of oxalate and PDCA [14]. However, detection sensitivities were much lower than with 0.20 mol·l^{-1} oxalic acid as eluent, possibly as a result of a slower reaction between PAR and the tartrate complexes, or the formation of ternary PAR–tartrate–metal complexes, which had smaller molar absorbances, and thus lower detection sensitivity. Consequently, all further studies reported here were obtained with oxalate eluents.

Effect of metal ion speciation on retention

Due to its d^9 structure, Cu^{2+} tends to form primarily 2:1 square planar complexes in the presence of weak-field bidentate ligands [15]. For Mn^{2+}, Co^{2+}, Ni^{2+}, and Zn^{2+}, the difference in crystal-field stabilization energy between the square planar and the octahedral complexes is considerably smaller, and six-coordinated octahedral complexes can form with weak field ligands [15]. Among these cations, Ni^{2+} and Zn^{2+} have been reported to form 1:3 six-coordinated octahedral complexes with oxalate (Ox^{2-}) [14,15]. The fraction of free Ox^{2-} changes from 0.06 to 0.99 in the pH range of 3 to 6, and since the pH value of the eluent can have a pronounced effect on the speciation of the metal ion–oxalate complexes, this pH range was selected for further studies. Values of pH less than 3 were not used because retention times decreased with time due to slow loss of the surfactant from the coated columns.

When the test metal ions were separated on a higher capacity column (*ca.* 0.14 meq·ml^{-1}) at a constant oxalate concentration, significant differences in the pattern of retention order as a function of pH were observed, as shown in Fig. 3. The observed increases in retention can be related to an increase in the anionic character of the metal complexes with increasing pH. Calculations from stability constants [14] showed that the fractions of MOx_2^{2-} for Mn^{2+} and Co^{2+}, and the sum of the fractions of MOx_2^{2-} and MOx_3^{4-} for Ni^{2+} and Zn^{2+} increased over the pH range, and thus retention is expected to increase. The fraction for $CuOx_2^{2-}$ remained almost constant at 1.0 throughout this pH range, and thus the increasing concentration of Ox^{2-} in the eluent caused a decrease in the retention time of Cu^{2+}. This increase in eluent strength with pH would also offset some of the increase in retention time expected for the other metal ions.

Since Ni^{2+} and Zn^{2+} can form small amounts of MOx_3^{4-}, it is not unexpected that these two metal ions are retained longer than Co^{2+} and Mn^{2+} (see Fig. 3). The calculated fraction of $NiOx_3^{4-}$ was larger than that for $ZnOx_3^{4-}$, and this is consistent with the longer retention for Ni^{2+}. It was found that, for any one metal ion, the effect of pH on retention decreased as the exchange capacity of the column was decreased. For example, with an exchange capacity of *ca.* 0.06 meq·ml^{-1} and a 0.1 mol·l^{-1} oxalate eluent

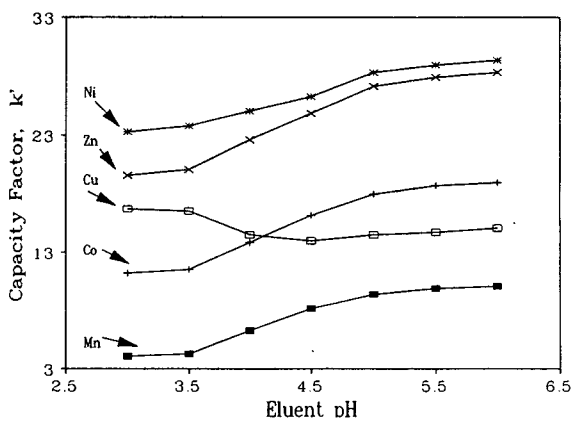

Fig. 3. Variation of capacity factor with eluent pH. Experimental conditions: 0.10 mol·l^{-1} oxalate eluent; 15 cm × 4.6 mm I.D. Supelcosil LC-18 (5 μm) column coated with $1.0 \cdot 10^{-2}$ mol·l^{-1} CPCl solution (*ca.* 0.13 meq·ml^{-1}); sample, 20 μl of 5 μg·ml^{-1} test metal ion.

it was found that the retention times of the metal ions remained relatively constant as a function of pH, except for Cu^{2+} which showed a slight decrease with an increase in eluent pH. The different retention patterns on the lower capacity columns can be attributed to a weaker interaction between the anionic complexes and the lower capacity ion exchanger, resulting in a greater relative effect from the increase in elution strength with pH. With a 0.200 $mol \cdot l^{-1}$ oxalic eluent, a slight increase in the retention time of Cu^{2+} was observed with increased eluent pH. The reason for this is not clear, but may be a result of possible formation of $CuOx_3^{4-}$ at the higher oxalate concentrations.

At pH 4.00, the metal ions could be separated within a relatively short time with good column efficiency (see below). In addition, this pH value is close to $pK_{a,2} = 4.19$ for oxalic acid [14], and thus oxalate is an effective buffer at this pH. Consequently, a pH of 4.00 was selected for further studies.

Metal speciation and column efficiency

In the oxalate eluent system MOx, MOx_2^{2-} and MOx_3^{4-} complexes can be formed, and these different anionic complexes must be in rapid equilibria with one another to maintain fast mass transfer and high separation efficiency. The calculated fractions of the different metal species present at pH 4 as a function of oxalate concentration are shown in Fig. 4. To evaluate if speciation of metal ion and kinetics of ligand exchange influenced column efficiency, a concentration range of $1.50 \cdot 10^{-1}$ to $1.00 \cdot 10^{-3}$ $mol \cdot l^{-1}$ oxalic acid (at pH = 4.00) was evaluated for seven different column capacities over the range of 0.01 to 0.12 $meq \cdot ml^{-1}$. At a constant eluent pH and with increasing concentration of oxalate from 0.001 to 0.15 $mol \cdot l^{-1}$, all metal ions showed a decrease in retention time, and the order of elution was normally $Mn^{2+} < Co^{2+} < Zn^{2+} < Ni^{2+} < Cu^{2+}$. On columns with capacities > 0.1 $meq \cdot ml^{-1}$ and with high oxalate concentrations in the eluent, the order of Cu^{2+} and Ni^{2+} was reversed, possibly due to the ability of Ni^{2+} to form octahedral complexes such as $NiOx_3^{4-}$ (see Fig. 4). The retention order normally observed for the other metal ions was $Ni^{2+} > Zn^{2+} > Co^{2+} > Mn^{2+}$. This order corresponds to what would be expected based on the speciation in Fig. 4. Nickel has the greatest percentage of MOx_3^{4-} species, and the order for the concentration of MOx_2^{2-} species is $Zn^{2+} > Co^{2+} > Mn^{2+}$.

For almost all of the exchange capacities evaluated the HETP values for each metal ion did not show any obvious trend as the concentration of oxalic acid was decreased from $1.50 \cdot 10^{-1}$ to $2.50 \cdot 10^{-2}$ $mol \cdot l^{-1}$. Fig. 5 shows typical results for one of the experimental conditions used in this study. For each metal ion HETP values were generally in the range of 0.010 to 0.025 mm. However, at lower oxalate concen-

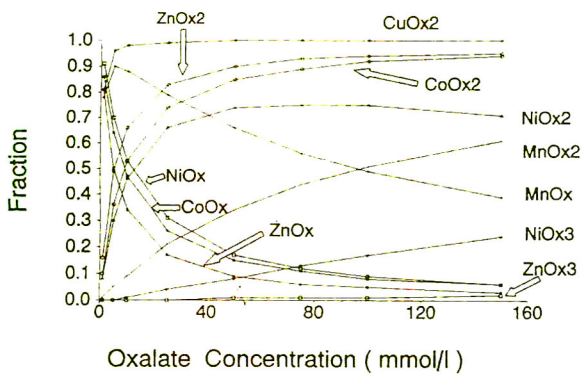

Fig. 4. Fractions of metal oxalate complexes as a function of oxalate concentration at eluent pH of 4.0. Data calculated from constants in ref. 14.

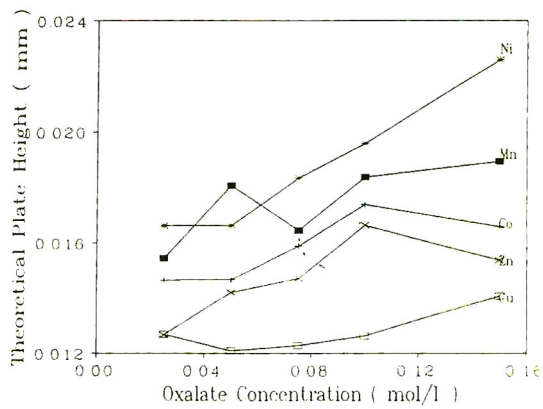

Fig. 5. Column efficiency as a function of oxalate concentration. Experimental conditions: pH 4.0; concentration of CPCl coating solution, $8.0 \cdot 10^{-4}$ $mol \cdot l^{-1}$; 15 cm × 4.6 mm I.D. Supelcosil LC-18 (5 μm) column.

trations with lower capacities columns (coated with $1.00 \cdot 10^{-4}$ and $2.00 \cdot 10^{-4}$ mol·l^{-1} CPCl) the HETP values for Ni^{2+} and Mn^{2+} increased significantly, and the Mn^{2+} peak which had the shortest retention time, began to show obvious tailing. The behaviour of Mn^{2+} may be related to slow exchange between the different manganese species: the fraction of the 2:1 complex, $MnOx_2^{2-}$ was always smaller than that of any of the other metal ions. The behaviour of Ni^{2+} may be related to an inherently slow rate of ligand exchange for Ni^{2+} complexes, as discussed below.

The order of HETP values for the oxalate system was normally in the order, $Ni \geq Mn > Co \approx Zn > Cu$. Since mass transfer should be related to the rate of ligand exchange between the different complex species for any given metal ion, one might expect a relationship between ligand-exchange rates and column efficiency. Exchange rates for all of the metal oxalate systems were not available in the literature, but it is not unreasonable to expect that the general order of rates of exchange for the different metal ions should be related to the exchange rates for coordinated water. This order of water exchange is: Cu $(1 \cdot 10^9) > Zn$ $(5 \cdot 10^7) \approx Mn$ $(2.7 \cdot 10^7) > Co$ $(2 \cdot 10^6) > Ni$ $(3 \cdot 10^4)$ [13]. Except for Ni^{2+} the order of HETP values does not agree with this pattern. An examination of the speciation in Fig. 4 shows that, for any given metal ion, the number and concentration of species other than MOx_2^{2-} increased in the order $Mn > Co \approx Zn > Cu$, which is the same as the order of HETP values. It can be expected that the overall rate of mass transfer would increase with an increase in the number of species in equilibrium with each other. Consequently, although there may be a relationship between the rate of ligand exchange (water exchange rates) and HETP values for the metal ions when the differences between rates are large, the order of the HETP values appears to be primarily determined by the diversity of the speciation.

Comparison of cation and anion separation systems

The performance of the anion separations were compared with separations on a cation exchanger, which was based on an ion-interaction system that used *n*-octanesulfonate to modify the reversed phase. The same column was used for both systems, and this eliminated the influence of variations in the packed bed on the relative performance of the two systems. Fig. 6 shows a comparison of the column efficiencies obtained with a recommended cation procedure [16] and the results obtained with the oxalate anion-exchange separation; also included in Fig. 6 is a cation separation performed with an oxalate eluent. These results show that the anion-exchange system can provide column efficiencies that compare well to that for cation systems. To achieve these efficient anion separations it is necessary to minimize the number of species in equilibrium with one another. Consequently, surfactant-modified reversed phases offer advantages relative to bonded phases because both the capacity and eluent composition can be varied to optimize the speciation of the metal ions. As expected, the order of separation on the anion-exchange system was considerably different from that observed with cation exchange, which could be attractive for certain analytical problems. Both systems were also comparable in terms of total analysis time. Total analysis time for isocratic separations with the anion systems was actually less than that for

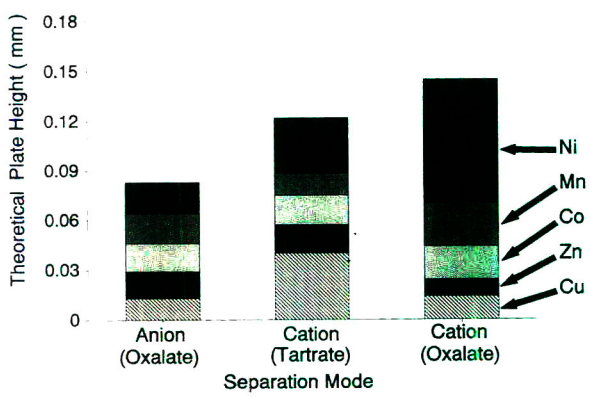

Fig. 6. Comparison of column efficiency for anion- and cation-exchange systems. Experimental conditions: anion system as for Fig. 5; cation systems; 0.0020 mol·l^{-1} sodium octanesulfonate, pH 3.4, and 2% (v/v) acetonitrile in eluent; tartrate concentration, 0.0020 mol·l^{-1}; oxalate concentration, 0.010 mol·l^{-1}; 15 cm × 4.6 mm I.D. Supelcosil LC-18 (5 μm) column.

the cation systems, but this advantage would be reduced if gradient separation conditions were used. Sensitivities, which were also comparable, were generally in the range of 0.3 absorbance units per μg of injected metal ion.

ACKNOWLEDGEMENTS

We would like to acknowledge the financial support of the Natural Science and Engineering Research Council of Canada, and Waters/Millipore.

REFERENCES

1 R.M. Cassidy and S. Elchuk, *Anal. Chem.*, 54 (1982) 1558.
2 R.M. Cassidy and S. Elchuk, *J. Chromatogr.*, 262 (1983) 311.
3 R.D. Rocklin, *Anal. Chem.*, 56 (1984) 1959.
4 T. Tanaka, *Fresenius' Z. Anal. Chem.*, 320 (1985) 125.
5 F.I. Brouchek, R.A. Demetrashvili and O.V. Orlova, *Izv. Akad. Nauk. Gruz. SSR, Ser. Khim.*, 14 (1988) 232.
6 O.N. Obrezkov, V.I. Slyamin and O.A. Shpigun, *Anal. Sci.*, 6 (1990) 617.
7 Z. Lei, S. Tian and J. Chen, *Gaodeng Xuexiao Huaxue Xuebao*, 10 (1989) 156.
8 H. Siren and M.L. Riekkola, *Mikrochim. Acta*, 2 (1989) 77.
9 E.M. Basova, T.A. Bol'shova, E.N. Shapovalova and V.M. Ivanov, *Zh. Anal. Khim.*, 45 (1990) 1947.
10 R.M. Cassidy, S. Elchuk and P.K. Dasgupta, *Anal. Chem.*, 58 (1987) 85.
11 S. Bakalyar, J. Yuen and D. Henry, *Spectra-Physics Chromatography Technical Bulletin*, Spectra-Physics, Santa Clara, CA, 1976.
12 A. Bartha and G. Vigh, *J. Chromatogr.*, 260 (1983) 337.
13 A. Martell, *Coordination Chemistry*, Vol. 2, *ACS Monograph 174*, American Chemical Society, Washington, DC, 1978.
14 D.D. Perrin, *Stability Constants of Metal-Ion Complexes*, Part B, Pergamon, Oxford, 1979.
15 F.A. Cotton and G. Wilkinson, *Advanced Inorganic Chemistry*, Interscience Publishers, New York, 2nd ed., 1966.
16 *Transition Metal Ion Using Postcolumn Derivatization, Waters Ion Chromatography Method M-301,* Waters/Millipore, Milford, MA, USA.

Journal of Chromatography A, 654 (1993) 113–121
Elsevier Science Publishers B.V., Amsterdam

CHROMSYMP. 2873

Ion-chromatographic determination of inorganic anions and cations in some reagents used in the electronics industry☆

Pier Luigi Buldini*, Jawahar Lal Sharma☆☆ and Shikha Sharma☆☆☆

C.N.R.–LAMEL, Laboratorio Analisi Chimica Materiali, Via Idraulico 17/2, I-40138 Bologna (Italy)

(First received September 21st, 1992; revised manuscript received June 10th, 1993)

ABSTRACT

In the electronics industry, wafer cleaning is usually performed by means of hot ammoniacal or acidic hydrogen peroxide solutions, which remove organic surface films by oxidative breakdown and dissolution to expose the substrate surface for concurrent and/or subsequent decontamination reactions. It is difficult to establish the optimum renewal cycle of the cleaning solutions to avoid economic as well as pollution problems. The present work deals with the application of ion chromatography to the determination of anionic as well as cationic impurities in hydrogen peroxide and ammonia, which are extensively used in wafer cleaning technology. As these two reagents cannot be injected directly into the separator column, methods are suggested for the pretreatment of the samples. Hydrogen peroxide was subjected to UV photolysis for about 30 min in an UV digestor at 85 ± 5°C. Though ammonia could also be treated in the same manner, simply heating it at 85 ± 5°C for 45 min in a dust-free cell, to expel most of the ammonia as gas, was found to be satisfactory. The samples were then analysed by ion chromatography and were found to contain chloride, phosphate, sulphate, copper, zinc, iron and manganese as impurities in variable amounts, when analysed at different stages of the wafer cleaning operation (20–1000 μg/l).

INTRODUCTION

Clean surfaces in the fabrication of semiconductor devices are important as a number of processes are highly sensitive to impurities present in the chemicals employed [1]. One of the commonest methods of silicon wafer cleaning and/or photoresist stripping is treatment of the surface with a mixture of hydrogen peroxide and ammonia, followed by a second peroxide treatment at low pH. This is intended to remove any organic surface film by oxidative breakdown and dissolution to expose the silicon or its oxide surface free from organic matter for concurrent or subsequent decontamination reactions. Metallic impurities, whose levels in the bath increase as more wafers are cleaned, are absorbed on the wafer surface and have proved to cause yield and reliability problems in electronic devices [2]. Contrary to this, the modern trend in semiconductor device evolution is to employ very large or ultra-large scale integration (VLSI or ULSI) technology, which in turn emphasizes the requirement for very pure chemicals, resulting in lower defect densities and improved yields [3]. In addition, it is difficult to establish the optimum renewal time of the cleaning solutions with consequent economic as well as pollution prob-

* Corresponding author.

☆ Presented at the *International Ion Chromatography Symposium 1992, Linz, September 21–24, 1992.* The majority of the papers presented at this symposium were published in *J. Chromatogr.*, Vol. 640 (1993).

☆☆ Permanent address: K.M. College, University of Delhi, Delhi 110007, India.

☆☆☆ Permanent address: Satyawatl Sood School, Nizamuddin East, Delhi 110041, India.

0021-9673/93/$06.00

lems, which leads to strict control of impurities in many process steps in order to reduce chemical consumption and waste.

Several techniques, such as flame or flameless atomic absorption spectrometry [4,5], inductively coupled plasma atomic emission spectrometry [6], polarography [7,8], spark source mass spectrometry [9] and inductively coupled plasma mass spectrometry [10], have been suggested for the determination of impurities in ultra-pure reagents. Most of these techniques are based on preconcentration of impurities and/or addition of one or more reagents to the sample prior to analysis, while others require very expensive equipment and highly skilled personnel.

Ion chromatography, introduced by Small *et al.* [11], is one of the simplest and most effective techniques to determine both anionic as well as cationic impurities owing to its high sensitivity, rapidity and ease of operation coupled with the advantage of simultaneous determinations. Dulski [12] determined some anions in hydrofluoric and nitric acids, while Murayama *et al.* [13] determined bromide, nitrate and sulphate in several acids by concentrating these anions on a chromatographic column.

The present work deals with the application of ion chromatography for the determination of fluoride, chloride, phosphate, sulphate, copper(II), cadmium(II), lead(II), zinc(II), iron(III), nickel(II), cobalt(II) and manganese(II) in hydrogen peroxide, ammonia and their mixtures without any preconcentration of the impurities or addition of reagents. The method has been successfully used for monitoring the process media employed for the cleaning of semiconductor wafers.

PRELIMINARY STUDIES

Hydrogen peroxide

The chemistry of hydrogen peroxide has been extensively studied [14–16]. It is a strong oxidizing agent in acidic as well as in alkaline conditions. At room temperature the half-life of acidic (pH 4.5) and alkaline (pH 9.0) hydrogen peroxide is about 50 h and 11 h, respectively. The stability of hydrogen peroxide solutions decreases with an increase in temperature as well as pH. By heating at only 85 ± 5°C, the relative hydrogen peroxide content of the acidic solution (pH 4.5) was found to decrease by 99% in 60 min and by more than 99.9% in 90 min.

When the hydrogen peroxide solution was subjected to UV irradiation at 85 ± 5°C, the relative content of the acidic solution was found to be less than 1% in 15 min and less than 0.1% in 20–25 min. For the alkaline solution (pH 9.0) the corresponding values were found 5 and 11 min, respectively. As hydrogen peroxide cannot be injected directly on the separator column, UV photolysis permits its analysis without any reagent addition.

Recoveries obtained with spiked samples range between 97 and 103% for all the impurities under investigation.

Ammonia

Though ammonia could also be treated in the same manner as hydrogen peroxide, simply heating it at 85 ± 5°C for 45 min in a dust-free cell, to expel most of the ammonia as gas, was found to be satisfactory. Heating was performed in PTFE containers fitted with 29/32 sockets and PTFE heads with 29/32 cones, adapted for passing inert gas through the cell and for water circulation, in order to avoid any eventual loss due to formation of micro-droplets.

By using spiked samples, recoveries of various ions were found to range between 97 and 103%.

EXPERIMENTAL

Reagents and standards

Sodium carbonate, sodium hydrogencarbonate, oxalic acid, lithium hydroxide, 4-(2-pyridylazo)-resorcinol monosodium salt (PAR) and pyridine-2,6-dicarboxylic acid (PDCA) were chromatographic grade (Novachimica, Milan, Italy), hydrogen peroxide (30% m/m, without stabilizer), ammonium hydroxide (30%), sodium hydroxide, glacial acetic acid and nitric acid (70%) were Erbaton electronic grade (Carlo Erba Reagenti, Milan, Italy), and sulphuric acid was analytical grade (Carlo Erba Reagenti). Ammonium acetate (2 *M*, pH 5.5) was chelation grade (Dionex, Sunnyvale, CA, USA). Ultrapure water with conductivity <0.1 μS (DI water)

was obtained from a Milli-Q (Millipore, Bedford, MA USA) four-bowl deionization system.

Working standards were prepared daily by diluting Carlo Erba Reagenti Normex atomic absorption standards (1.000 g/l) or by dissolving the required Carlo Erba Reagenti analytical-grade reagents.

Quartz test tubes and all glassware were cleaned in concentrated nitric acid and carefully washed with DI water. Normal precautions for trace analysis were observed throughout.

Instrumentation

Hydrogen peroxide samples were subjected to UV photolysis in a Metrohm (Herisau, Switzerland) 705 UV digestor equipped with a 500-W high-pressure mercury lamp. The temperature of the sample was maintained at 85 ± 5°C with the aid of a combined air/water cooling system.

Ammonia samples were heated in PTFE tubes fitted with 29/32 sockets, by employing a Berghof (Tübingen, Germany) sample evaporating device equipped with an aluminium heating block (in which the PTFE tubes can be inserted) whose temperature was maintained with the help of a T-P regulator (Berghof). The device was also fitted with PTFE heads with 29/32 cones, adapted for passing inert gas and circulating running water to maintain low temperature to avoid any loss due to the transportation of micro-droplets by the vapour formed.

Chromatographic analyses were performed on a Dionex (Sunnyvale, CA, USA) 2000i ion chromatograph equipped with an EDM eluent degassing module, a GPM gradient pump, an IonPac AG9 guard column and an IonPac AS9 separator column (for anions), an AMMS anion micromembrane suppressor, an IonPac CG5 guard column and an IonPac CS5 separator column (for cations), an IonPac MRAD membrane reactor coupled with a reagent delivery module for post-column reagent addition and a CDM conductivity detector and a VDM2 UV–visible absorbance detector.

All measurements were made at 25 ± 1°C and, in all cases, injection of the sample was done at least in triplicate.

Peak areas were obtained using AI-450 Dionex software and background correction was applied wherever necessary.

All the chromatographic conditions are listed in Table I.

TABLE I

ION CHROMATOGRAPHIC CONDITIONS

	Anions	Cations
Column	IonPac AS9 (+AG9)	IonPac CS5 (+CG5)
Eluent	2.0 m*M* Na_2CO_3 + 0.75 m*M* $NaHCO_3$	50 m*M* $(COOH)_2$ + 95 m*M* LiOH 95 m*M* LiOH (pH 4.8) or [for Fe(III) only] 6 m*M* PDCA + 90 m*M* CH_3COOH + 40 m*M* NaOH (pH 4.6)
Eluent flow-rate	1.5 ml/min	1.0 ml/min
Injection volume	25 μl	25 μl
Detection	Suppressed conductivity	Visible absorbance
Suppressor	AMMS	–
Regenerant	25 m*M* H_2SO_4	–
Regenerant flow-rate	8 ml/min	–
Post-column reagent	–	0.2 m*M* PAR in 3 *M* NH_4OH + 1 *M* CH_3COOH
Post-column reagent flow-rate	–	0.5 ml/min
Wavelength	–	520 nm

During the determination of cations, the eluent flow-rate was maintained at 1.0 ml/min and the post-column reagent flow-rate was 0.5 ml/min, and the total flow-rate (1.5 ml/min) was checked at the exit of the waste line. For optimal signal-to-noise ratio, the output was measured at a wavelength of 520 nm.

Samples preparation

Hydrogen peroxide. Aliquots of 5-ml of hydrogen peroxide or a mixture of hydrogen peroxide and ammonia were placed in quartz tubes and closed with conical PTFE stoppers that tapered to a point. The stoppers acted as cooling fingers, and thus prevented solution losses and also protected samples against contamination. The sample was subjected to UV photolysis at 85 ± 5°C for 30 min. The volume was made up to the original value with DI water, to compensate for the water loss due to evaporation, and analysed by ion chromatography for determining anionic impurities. For the determination of cationic impurities, 10 μl of 2 *M* nitric acid were added to ensure the dissolution of all the metallic oxides, if formed during the course of UV photolysis, followed by the addition of 200 μl of 2 *M* ammonium acetate to maintain the sample pH in the range between 5 and 6, prior to chromatographic analysis. The volume was made up to 5 ml with DI water and analysed.

Ammonia. Aliquots of 5 ml of ammonia were heated at 85 ± 5°C in the sample heating device in an atmosphere of nitrogen for 45 min to reduce the volume to almost half. The volume was made up to the original value with DI water, and analysed for determining anionic impurities. For the determination of cationic impurities, 10 μl of 2 *M* nitric acid were added to ensure the dissolution of all the cationic species. The pH of the sample was maintained in the range 5–6 by adding 200 μl of 2 *M* ammonium acetate. The volume was made up to 5 ml with DI water and analysed by injecting on to the ion chromatograph.

RESULTS AND DISCUSSION

Figs. 1–3 show the chromatograms of a mixture of hydrogen peroxide and ammonia (1:1, v/v) for anion and cation determination.

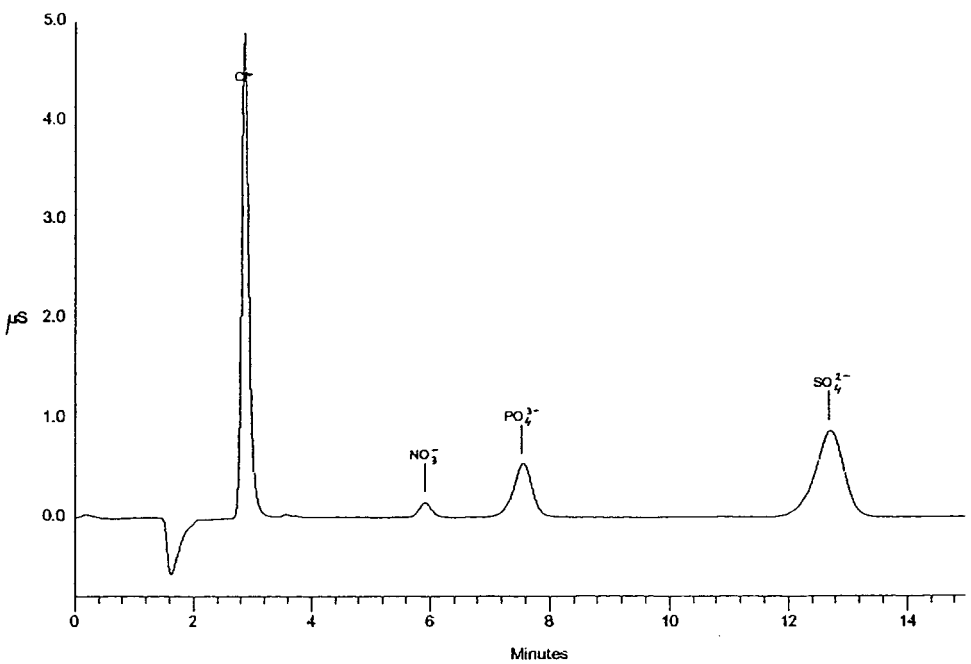

Fig. 1. Determination of anions in a mixture of ammonia and hydrogen peroxide (1:1, v/v) (exhausted batch). Chromatographic conditions as reported in Table I. Chloride 850 μg/l, sulphate 200 μg/l and phosphate 120 μg/l.

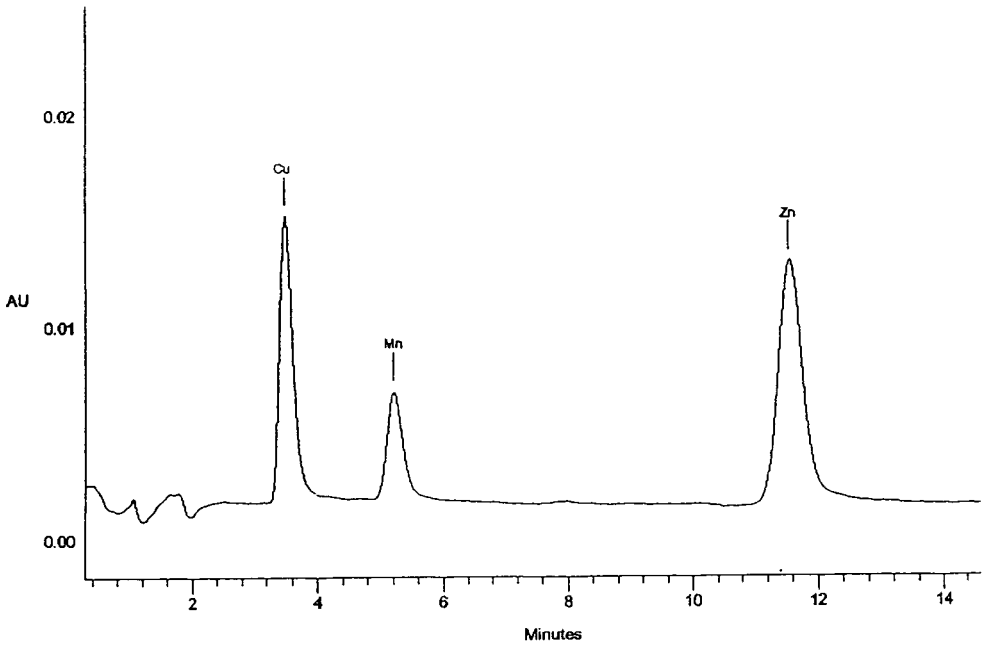

Fig. 2. Determination of cationic impurities in a mixture of ammonia and hydrogen peroxide (1:1, v/v) (exhausted batch). Chromatographic conditions as reported in Table I. Copper(II) 240 μg/l and zinc(II) 380 μg/l.

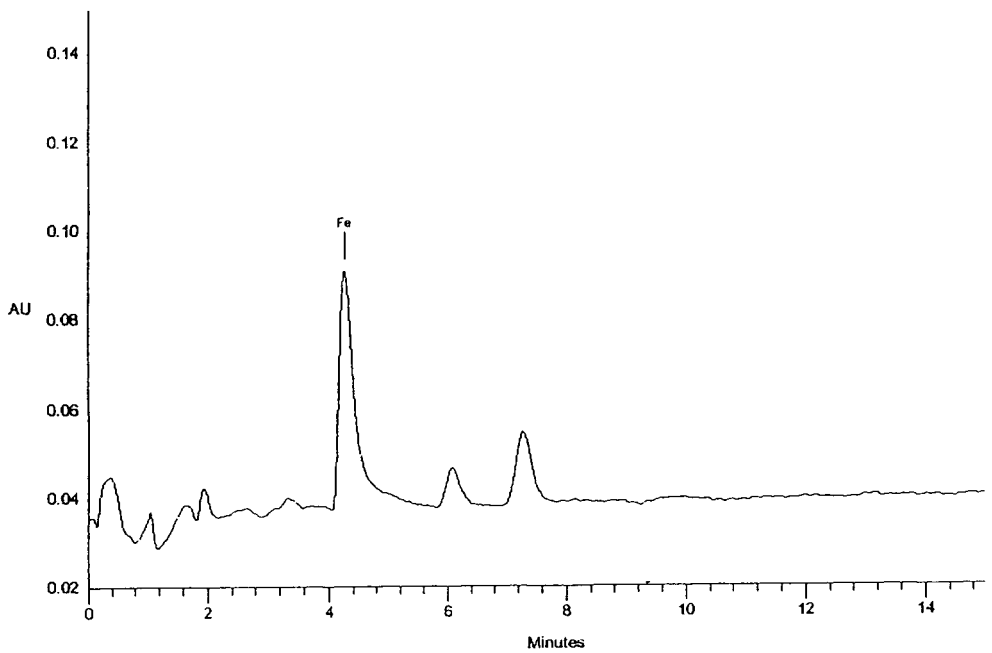

Fig. 3. Determination of iron(III) in a mixture of ammonia and hydrogen peroxide (1:1, v/v) (exhausted batch). Chromatographic conditions as reported in Table I. Iron(III) 950 μg/l.

It is evident that the detection of the various species in these reagents is straightforward. Lead(II) and cadmium(II) cannot be determined with PDCA eluent because these ions are so strongly bound to PDCA that they are not sensitively detected by PAR. Similarly, iron cannot be determined with oxalate eluent, while zinc(II), nickel(II) and cobalt(II) can be determined by either of the two eluents. For convenience, oxalate eluent was used for all the cations except iron, which was determined by PDCA eluent.

In the case of cation determination using oxalate eluent, normally the peak appearing just before lead(II) (at about 2.5 min) becomes larger if the matrix is very rich in various ions, and interferes with its determination. Employing the described sample pretreatment procedure, the size of this peak becomes vanishingly small and lead(II) can be detected in very low amounts, as reported in Table II.

The described ion chromatographic procedure, using the oxalate eluent, suffers from the drawback that cadmium(II) and manganese(II) have retention times very close to each other and therefore coelute with each other, so preventing their simultaneous determination, but the problem is resolved by the use of the PDCA eluent, as this gives a peak only for manganese(II).

The detection limits and concentration ranges in which calibration curves are linear with correlation coefficients greater than 0.99 are shown in Table II.

The effect of UV radiation on various anions and cations in the presence of hydrogen peroxide as well as a mixture of hydrogen peroxide and ammonia was investigated in detail. Deionized water as well as acidic and alkaline hydrogen peroxide samples were spiked with varying amounts of many common anions and heavy/transition metal ions and subjected to UV photolysis for 4 h prior to chromatographic analysis.

As shown in Tables III and IV, it was found that fluoride, chloride, bromide, phosphate and sulphate anions and copper(II), cadmium(II), lead(II), zinc(II), iron(III), nickel(II) and cobalt(II) cations were not affected by UV photolysis and the recovery of these species was between 97 and 103% in deionized water as well as in acidic or alkaline hydrogen peroxide samples. In the case of iodide, nitrite, nitrate and manganese(II) the recoveries were not quantitative. This is because UV photolysis of hydrogen peroxide proceeds via a radical mechanism. The

TABLE II

DETECTION LIMITS AND USEFUL CONCENTRATION RANGES IN HYDROGEN PEROXIDE AND AMMONIA BY ION CHROMATOGRAPHY, AFTER SAMPLE PRETREATMENT

Ion	Eluent	Detection limit (μg/l)	Range (μg/l)
F^-	Carbonate–hydrogencarbonate	5	10–5000
Cl^-	Carbonate–hydrogencarbonate	10	20–4000
Br^-	Carbonate–hydrogencarbonate	15	40–4000
PO_4^{3-}	Carbonate–hydrogencarbonate	25	50–5000
SO_4^{2-}	Carbonate–hydrogencarbonate	25	50–5000
Cu(II)	Oxalate	5	10–1500
Cd(II)	Oxalate	25	50–2500
Pb(II)	Oxalate	10	25–2500
Zn(II)	Oxalate	10	25–2500
Fe(III)	PDCA	5	15–2000
Ni(II)	Oxalate	20	100–1500
Co(II)	Oxalate	10	20–2000
Mn(II)[a]	Oxalate	10	25–1500

[a] Valid for ammonia only.

TABLE III

RECOVERY OF TRACE ANIONS IN 30% (m/m, WITHOUT STABILIZER) HYDROGEN PEROXIDE AND (30%) AMMONIA

Mean of the values obtained for ten samples —triplicate injection each. Chromatographic conditions as previously reported in Table I.

Anion	Added (ppm)	Hydrogen peroxide			Ammonia		
		Found (ppm)	Recovery (%)	R.S.D. (%)	Found (ppm)	Recovery (%)	R.S.D. (%)
Fluoride	0.000	0.000	–	–	0.000	–	–
	0.100	0.103	103	3.0	0.102	102	2.1
	0.500	0.508	101.6	1.9	0.509	101.8	2.0
Chloride	0.000	0.042	–	2.0	0.064	–	1.7
	0.100	0.144	102	2.0	0.166	102	2.0
	0.500	0.548	101.2	1.5	0.572	101.6	1.8
Bromide	0.000	0.000	–	–	0.000	–	–
	0.100	0.102	102	2.0	0.098	98	2.1
	0.500	0.496	99.2	1.1	0.508	101.6	1.9
Nitrite	0.000	0.042	–	15.4	0.017	–	19.6
	0.100	0.096	54	24.9	0.092	75	33.2
	0.500	0.366	65	18.6	0.434	83	22.5
Nitrate	0.000	0.021	–	22.6	0.062	–	37.9
	0.100	0.059	38	31.5	0.157	97	28.9
	0.500	0.328	61.4	37.2	0.555	98.6	33.3
Phosphate	0.000	0.085	–	2.2	0.024	–	1.5
	0.100	0.188	103	3.0	0.122	98.4	1.8
	0.500	0.592	101.2	1.5	0.528	100.7	1.0
Sulphate	0.000	0.034	–	1.5	0.054	–	1.7
	0.100	0.135	101	1.2	0.152	98	2.0
	0.500	0.539	101	1.2	0.561	101.3	1.5

$^{\bullet}$OH radicals formed during the irradiation interact with the mentioned species and give a number of reaction products depending upon the temperature, medium and concentration of the $^{\bullet}$OH radicals [17,18]. Thus, the sample pretreatment employing UV photolysis is not recommended for the determination of iodide, nitrate, nitrite and manganese(II).

CONCLUSIONS

Ion chromatography has been found to be very effective for determining anionic as well as cationic impurities in hydrogen peroxide and ammonia.

These reagents were found to contain chloride, nitrate, phosphate and sulphate as anionic impurities and iron, copper and zinc as cationic impurities. The technique has been successfully applied for determining the impurities in mixtures of hydrogen peroxide and ammonia, and can therefore be used for monitoring trace levels of various anions and cations in baths for semiconductor cleaning.

ACKNOWLEDGEMENT

Two authors (J.L.S. and S.S.) are grateful to the International Centre for Theoretical Physics (Trieste, Italy) for awarding them a fellowship.

TABLE IV

RECOVERY OF TRACE CATIONS IN 30% (m/m, WITHOUT STABILIZER) HYDROGEN PEROXIDE AND (30%) AMMONIA

Mean of the values obtained for ten samples —triplicate injection each. Chromatographic conditions as reported in Table I.

Cation	Added (μg/l)	Hydrogen peroxide			Ammonia		
		Found (ppm)	Recovery (%)	R.S.D. (%)	Found (ppm)	Recovery (%)	R.S.D. (%)
Pb(II)	0.000	0.000	–	–	0.000	–	–
	0.050	0.051	102	2.1	0.051	102	2.0
	0.100	0.101	101	1.7	0.102	102	2.2
Cd(II)[a]	0.000	0.000	–	–	0.000	–	–
	0.050	0.051	102	2.0	0.051	102	2.0
	0.100	0.101	101	1.3	0.102	102	2.1
Fe(III)	0.000	<0.010	–	–	<0.010	–	–
	0.050	0.059	100	0.5	0.060	101	1.6
	0.100	0.110	100	0.5	0.112	102	2.1
Cu(II)	0.000	0.012	–	1.6	0.017	–	1.9
	0.050	0.063	102	2.0	0.068	102	2.1
	0.100	0.114	102	2.2	0.119	102	2.0
Ni(II)	0.000	0.000	–	–	0.000	–	–
	0.100	0.098	98	2.0	0.98	98	2.0
	0.500	0.510	102	2.0	0.500	100	1.5
Zn(II)	0.000	<0.020	–	–	<0.020	–	–
	0.050	0.068	100	1.3	0.065	100	1.5
	0.100	0.119	100	1.5	0.118	101	2.0
Co(II)	0.000	0.000	–	–	0.000	–	–
	0.050	0.049	98	2.0	0.051	102	2.0
	0.100	0.100	10	1.0	0.101	101	1.5
Mn(II)[a]	0.000	0.000	–	–	<0.025	–	–
	0.050	0.042	84	3.5	0.075	100	1.0
	0.100	0.088	88	4.8	0.125	100	1.0

[a] Cadmium(II) and manganese(II) not determined simultaneously.

REFERENCES

1 G. Gould and E.A. Irene, *J. Electrochem. Soc.*, 134 (1987) 1031.
2 M. Heyns, *Microcontamination*, 9 (1991) 29.
3 H.J. Rath and R. Neuteufel, in B.O. Kolbesen, D.V. McCaughan and W. Vandervorst (Editors), *Analytical Techniques for Semiconductor Materials and Process Characterization*, The Electrochemical Society, Pennington, NJ, 1990, p. 335.
4 E. Ivanova, I. Havezov, N. Vracheva and N. Jordanov, *Fresenius' Z. Anal. Chem.*, 320 (1985) 133.
5 F.J. Langmyhr and J.T. Haekedal, *Anal. Chim. Acta*, 83 (1976) 127.
6 R.N.P. Farrow, *Anal. Proc.*, 24 (1987) 178.
7 P.L. Buldini and D. Ferri, *Microchim. Acta*, I (1980) 423.
8 V.A. Stenger, J.D. McLean and R.M. Van Effen, *Anal. Chem.*, 57 (1985) 27A.
9 T.A. Chanysheva, I.R. Shelpakova, A.I. Saprykin, L.M. Yankovskaya and I.G. Yudelevich, *Zh. Anal. Khim.*, 38 (1983) 979.
10 P.J. Paulsen, E.S. Beary, D.S. Bushee and J.R. Moody, *Anal. Chem.*, 60 (1988) 971.
11 H. Small, T.S. Stevens and W.C. Bauman, *Anal. Chem.*, 47 (1975) 1801.
12 T.R. Dulski, *Anal. Chem.*, 51 (1979) 1439.
13 M. Murayama, M. Suzuki and S. Takitani, *J. Chromatogr.*, 466 (1989) 355.

14 W.C. Schumb, C.N. Satterfield and R.L. Wentworth, *Hydrogen Peroxide*, Reinhold., New York, 1955.
15 J.W. Faust Jr., in H.C. Gatos (Editor), *Surface Chemistry of Metals and Semiconductors*, Wiley, New York, 1960, p. 151.
16 R.P.S. Black and A.T. Hawkinson, *Symposium on Cleanness and Materials Processing for Electronic and Space Applications* (*ASTM STP*, No. 342), American Society for Testing and Materials, Philadelphia, PA, 1962, p. 87.
17 R.W. Glass and T.W. Martin, *J. Am. Chem. Soc.*, 92 (1970) 5084.
18 A. Farkas and L. Farkas, *Trans. Faraday Soc.*, 34 (1938) 1113, 1120.

Journal of Chromatography A, 654 (1993) 123–128
Elsevier Science Publishers B.V., Amsterdam

CHROMSYMP. 2875

Determination of inorganic ions in carboxylic acids by ion chromatography☆

Pier Luigi Buldini*, Jawahar Lal Sharma☆☆

C.N.R.–LAMEL, Laboratorio Analisi Chimica Materiali, Via Idraulico 17/2, I-40138 Bologna (Italy)

Anna Mevoli

Centro Nazionale per la Ricerca e lo Sviluppo dei Materiali, S.S. 7, km. 7, I-72100 Brindisi (Italy)

(First received September 21st, 1992; revised manuscript received June 10th, 1993)

ABSTRACT

A method has been developed for the quantitative determination of various inorganic impurities present in carboxylic acids. The spiked as well as unspiked analytes were subjected to oxidative UV photolysis prior to ion chromatographic analysis. This procedure has definite advantages compared with other sample pretreatment methods: it is a simple procedure and the reagent requirement is minimal. Inorganic cations and anions, except nitrite, nitrate, iodine, sulphite and manganese(II), are unaffected by UV radiation. Depending upon the nature of impurity to be analysed and the amount of carboxylic acid, the UV photolysis time can be adjusted as required. The method was tested on several aliphatic as well as aromatic acids and found to be satisfactory for the determination of chloride, bromide, phosphate, sulphate, iron(III), lead(II), copper(II), zinc(II), nickel(II) and cobalt(II). Detection limits of the proposed method are between 5 and 25 ng/ml and calibration curves were found to be linear up to 1–2 μg/ml.

INTRODUCTION

Carboxylic acids play a vital role in the modern industrial world and find numerous applications. They are widely used in the food, pharmaceutical and electronics industries. The determination of trace inorganic constituents in carboxylic acids is desirable in a number of industrial processes, as in many industries the requirements for lower impurity levels are exceeding the limits of current analytical methods. In many instances, new specifications are being set with impurities at μg/l levels.

The determination of trace inorganic impurities in organic matrices including carboxylic acid is generally based on classical analytical techniques such as volumetric and gravimetric analysis and/or turbidimetry and colorimetry [1]. These techniques require sample preparation aimed at destroying the organic matrix, which is usually done by dry ashing, involving complete destruction of all organic matter at very high temperatures, or by wet digestion with mixed acids.

Ion chromatography is a well-established and quite sensitive technique for the simultaneous determination of many ionic impurities in various matrices [2,3], as it is flexible in terms of operation and optimization. However, in many cases this technique, too, needs to be sup-

* Corresponding author.

☆ Presented at the *International Ion Chromatography Symposium 1992, Linz, September 21–24, 1992.* The majority of the papers presented at this symposium were published in *J. Chromatogr.*, Vol. 640 (1993).

☆☆ Permanent address: K.M. College, University of Delhi, Delhi 110007, India.

0021-9673/93/$06.00

plemented with sample pretreatment to overcome the problems related to matrix interferences.

PRELIMINARY STUDIES

The chromatographic behaviour of many carboxylic acids was examined using an AS9 anion separator column and different eluents containing varying proportions of sodium carbonate and sodium hydrogencarbonate at different flow-rates. Many carboxylate ions were found to have retention times close to those of the inorganic anions to be analysed as impurities, *i.e.*, chloride, bromide, nitrite, nitrate, phosphate, arsenate, sulphite and sulphate. In most cases it was found that the large peak due to the carboxylate ion masked the smaller peaks due to the spiked inorganic impurity anions. Attempts to analyse the cationic impurities, *viz.*, lead, copper, iron, manganese, cobalt, zinc and nickel, without sample pretreatment also failed, as most of the carboxylate ions formed complexes with the metals, thereby making their quantitation almost impossible. In order to reduce the matrix effect, the dilution of the matrix was not preferred, because this led to the dilution of the impurities to below the detection limits for the various ions under investigation. It was therefore necessary to modify the sample in a manner that avoids dilution and permits quantitation without interferences resulting from the matrix. For this purpose UV photolysis of carboxylic acids was utilized as it is quite effective for the destruction of the organic matrix, without affecting most of the inorganic ions.

UV photolysis optimization

A 50-mg aliquot of each carboxylic acid sample was mixed with 1 ml of H_2O_2 (30%) and subjected to UV photolysis at 85 ± 5°C. Later, it was cooled, diluted to 5 ml and analysed by ion chromatography. It was found that the photolysis time for the destruction of the carboxylic acid depend upon the quantity and the nature/type of the acid. In most cases 2 h of UV photolysis was sufficient for the complete decarboxylation/destruction of the matrix. The carboxylic acids, having a strong electron-attracting group (–I substituent, where I = inductive effect) on the α-carbon atom, were decarboxylated in less time. On the other hand, decarboxylation of formic and acetic acid required much time, because in the presence of hydrogen peroxide these acids form stable peroxy acids and thus prevent the formation of free $^{\bullet}OH$ radicals. The findings related to the decarboxylation and UV photolysis time are summarized in Table I.

To make the present sample pretreatment amenable for the widest range of applications, the procedure was optimized by making investigations with "synthetic solution 1", comprising 1000 mg/l each of formic, acetic, lactic, citric, tartaric, oxalic, malonic, succinic, fumaric, benzoic, phenylacetic, phthalic and salicylic acids. A 1-ml volume of "synthetic solution 1" was subjected to UV photolysis in the presence of hydrogen peroxide, as described earlier. Investigations revealed that 1 ml of this solution requires 1 ml of hydrogen peroxide for the complete disappearance of all the peaks due to carboxylate ions in 2 h, thus permitting the determination of inorganic anions. However, the

TABLE I

PHOTOLYSIS TIME FOR DECARBOXYLATION OF DIFFERENT AMOUNTS OF ACIDS

Acid	Photolysis time for complete destruction (min)		
	50 mg	100 mg	200 mg
Formic	100	120	150
Acetic	200	240	360
Propanoic	80	110	125
Butyric	80	120	125
Benzoic	60	60	60
Lactic	60	75	90
Glutamic	90	120	150
Oxalic	90	120	150
Malonic	60	60	60
Succinic	60	100	100
Citric	80	120	180
Tartaric	60	100	150
Phthalic	60	60	75
Phenylacetic	60	75	100
Salicylic	60	75	90
Caprilic	100	150	200
Ascorbic	60	80	100

UV photolysis time can be reduced, if desired, by increasing the amount of hydrogen peroxide.

For the determination of cationic impurities, *viz.*, iron(III), lead(II), copper(II), cobalt(II), manganese(II), zinc(II) and nickel(II), complete destruction of all types of carboxylic acids was found to be unnecessary. Carboxylic acids (L) forming weaker complexes with the metal ions (M), than the metal–oxalate (Ox) complex formed by the eluent do not require destruction/decarboxylation of the acid by UV photolysis, as the oxalate ion of the eluent is capable of displacing the weak carboxylate ion from the M–L complex, *i.e.*, $M–L + Ox \rightarrow M–Ox + L$, and thereby separating various metal ions, which further complex with 4-(2-pyridylazo)-resorcinol monosodium salt and are detected and quantitated. This has been found to be true in the case of aliphatic monocarboxylic acids of low molecular mass, especially formic, acetic, propanoic and butyric acids. On the other hand, di-, poly- and/or hydroxy-substituted carboxylic acids capable of forming stronger M–L complexes (compared with M–Ox complexes) require matrix destruction prior to ion chromatographic analysis. Detailed investigations were made on "synthetic solution 2" consisting of 1000 ppm each of malonic, oxalic, tartaric, citric, salicylic and phthalic acids. A 1-ml volume of this solution was spiked with 50 μg/l each of Fe(III), Cu(II), Pb(II), Mn(II), Co(II), Zn(II), and Ni(II), treated with 1 ml of H_2O_2 and subjected to UV photolysis at 85 ± 5°C. A 20-μl aliquot of HNO_3 (5 *M*) was added after 30 min to ensure the dissolution of the oxides or other insoluble metallic species formed during the course of sample pretreatment and the samples were analysed after different periods of photolysis. The recovery of Fe(III), Pb(II), Cu(II) and Zn(II) was quantitative within 1 h of photolysis, while Co(II) and Ni(II) require at least $1\frac{1}{2}$ h for their complete recovery. The recovery of Mn(II) could not be ascertained, as it is probably oxidized to a higher oxidation state. These findings are summarized in Table II.

In all subsequent studies, carboxylic acids were subjected to 2 h of UV photolysis, to ensure the complete recovery of all the cationic impurities under investigation.

Effect of UV photolysis on impurity ions

The effect of hydrogen peroxide and UV radiation on various anions and cations was investigated in detail. "Synthetic solutions 1 and 2" were spiked with 1 mg/l of many common anions and cations, respectively, and subjected to UV photolysis for 4 h, followed by ion chromatographic analysis.

It was found that the recovery of chloride, bromide, phosphate, sulphate, iron(III), lead(II), copper(II), zinc(II), nickel(II) and cobalt(II) ranged between 97% and 102%, while iodide, nitrite, nitrate and sulphite were lost owing to the influence of UV radiation. It was also found that manganese(II) was oxidized to a higher oxidation state. Hence the present meth-

TABLE II

RECOVERY OF VARIOUS METAL IONS AFTER DIFFERENT UV PHOTOLYSIS TIMES

Metal ion	Recovery (%) after					
	30 min	45 min	60 min	75 min	90 min	120 min
Pb(II)	78	92	102	101	102	100
Cu(II)	84	95	102	100	101	101
Mn(II)	44	58	69	62	56	51
Co(II)	51	61	72	89	101	101
Zn(II)	67	83	101	100	102	101
Ni(II)	37	48	63	77	102	98
Fe(III)	39	86	102	101	102	102

od of sample pretreatment is not recommended for the determination of manganese(II) and the above-mentioned anions, if present, in carboxylic acids.

EXPERIMENTAL

Reagents and standards

Sodium carbonate, sodium hydrogencarbonate, oxalic acid, lithium hydroxide, 4-(2-pyridylazo)-resorcinol monosodium salt (PAR) and pyridine-2,6-dicarboxylic acid (PDCA) were chromatographic grade (Novachimica, Milan, Italy), hydrogen peroxide (30% m/m, without stabilizer), ammonium hydroxide (30%), sodium hydroxide, glacial acetic acid and nitric acid (70%) were Elbatron electronic grade (Carlo Erba Reagenti, Milan, Italy), and sulphuric acid was analytical grade (Carlo Erba Reagenti). Ammonium acetate (2 *M*, pH 5.5) was chelation grade (Dionex, Sunnyvale, CA, USA). Ultrapure water with conductivity <0.1 μS (DI water) was obtained from a Milli-Q (Millipore, Bedford, MA, USA) four-bowl deionization system.

Working standards were prepared daily by diluting Carlo Erba Reagenti Normex atomic absorption standards (1.000 g/l) or by dissolving the required Carlo Erba Reagenti analytical-grade reagents.

Quartz test tubes and all glassware were cleaned in concentrated nitric acid and carefully washed with DI water. Normal precautions for trace analysis were observed throughout.

Eluent, regenerant and post-column reagent solutions

A 2.0 m*M* sodium carbonate–0.75 m*M* sodium hydrogencarbonate solution was used as chromatographic eluent for anions.

A 2.5 m*M* sulphuric acid solution was used as regenerant for the anion micromembrane suppressor at 8 ml/min flow-rate.

For the analysis of lead(II), copper(II), manganese(II), cobalt(II), zinc(II) and nickel(II), a mixture of 50 m*M* oxalic acid and 95 m*M* lithium hydroxide (pH 4.8) was used as the eluent. While a mixture of 6 m*M* PDCA, 90 m*M* acetic acid and 40 m*M* sodium hydroxide (pH 4.6) was employed for the determination of iron(III). 0.2 m*M* PAR dissolved in 3 *M* ammonium hydroxide and 1 *M* acetic acid was used as the post-column reagent for cationic analysis with both the eluents.

Instrumentation

Carboxylic acid samples were subjected to UV photolysis in a Metrohm (Herisau, Switzerland) 705 UV digestor equipped with a 500-W high-pressure mercury lamp. The temperature of the sample was maintained at 85 ± 5°C with the help of a combined air/water cooling system.

Chromatographic analysis were performed on a Dionex (Sunnyvale, CA, USA) 2000i ion chromatograph equipped with an EDM eluent degassing module, a GPM gradient pump, an IonPac AG9 guard column and an IonPac AS9 separator column (for anions), an AMMS anion micromembrane suppressor, an IonPac CG5 guard column and an IonPac CS5 separator column (for cations), an IonPac MRAD membrane reactor coupled with a reagent delivery module for post-column reagent addition and a CDM conductivity detector and a VDM2 UV–visible absorbance detector.

Injections of 25 μl of sample were performed.

All measurements were made at 25 ± 1°C, and in all cases injection of the sample was done at least in triplicate.

Precautions were taken to ensure that the analyte did not remain either on the column or on the injection loop overnight. At the end of the analysis, the membrane reactor device was washed with 0.1 *M* ammonium hydroxide. The injection loop was washed with DI water prior to each analysis.

Peak areas were obtained using Al-450 Dionex software, and background correction was applied wherever necessary.

During the determination of anions, the eluent flow-rate was maintained at 1.5 ml/min, while for cations the eluent flow-rate was 1.0 ml/min and that of the post-column reagent was 0.5 ml/min; the total flow-rate (1.5 ml/min) was checked at the exit of the waste line. For optimal signal-to-noise ratio, the output was measured at a wavelength of 520 nm.

Sample preparation

A amount of 50–100 mg of carboxylic acid was weighed into a quartz tube and 2 ml of hydrogen peroxide were added. The quartz tube was closed with its proper conical PTFE stopper, which tapered to a point. The stopper acted as a cooling finger, prevented solution losses and also protected samples against contamination. The sample was subjected to UV photolysis at 85 ± 5°C for 120 min. The volume was made up to 5 ml and analysed by ion chromatography for determining anionic impurities. For the determination of cationic impurities, 10 μl of 2 *M* nitric acid were added to ensure the dissolution of all the metallic oxides, if formed during the course of UV photolysis, followed by the addition of 200 μl of 2 *M* ammonium acetate to maintain the sample pH in the range 5–6, prior to chromatographic analysis. The volume was made up to 5 ml with DI water.

RESULTS AND DISCUSSION

The detection limits of various anions and cations were determined by spiking "synthetic solutions 1 and 2" with varying amounts of different anions and cations, and subjecting them to UV photolysis for 2 h, followed by ion chromatographic analysis. The linearity range and limits of detection for the anions and cations determined are summarized in Table III.

As evident from Table III, the present method is highly suitable for the determination of very low amounts of iron(III), lead(II), copper(II), zinc(II), nickel(II) and cobalt(II), but suffers from the drawback that cadmium(II) and manganese(II) coelute. Further, the retention times of lead(II) (2.8 min) and copper(II) (3.4 min) are very close to each other; hence, only if these two ions are present in amounts less than 2 μg/ml each, the peaks are well separated.

Sodium, potassium, ammonium, calcium and magnesium at levels higher than 1:1000 do not interfere in the determination of iron(III), lead(II), copper(II), zinc(II), nickel(II) and cobalt(II).

Since many carboxylate ions elute very close to the common inorganic anions, *viz.*, chloride, phosphate and sulphate, interferences due to the simultaneous presence of common inorganic and carboxylate anions were investigated in detail.

It was found that citrate interferes in the determination of chloride, succinate interferes in the determination of phosphate and malonate interferes with the determination of sulphate, if present in amounts greater than those reported in Table IV. Interestingly, the above-mentioned

TABLE III

DETECTION LIMITS AND LINEARITY RANGE FOR VARIOUS IONS DETERMINED IN CARBOXYLIC ACIDS AFTER SAMPLE PRETREATMENT

Ion	Detection limit (μg/l)	Range of linearity (μg/l)
Cl^-	10	20–2000
Br^-	20	40–2000
PO_4^{3-}	25	50–1500
SO_4^{2-}	25	50–2000
Cu(II)	5	50–2000
Pb(II)	10	20–1000
Zn(II)	10	25–1500
Fe(III)	5	15–2000
Ni(II)	25	50–2000
Co(II)	10	20–2000

TABLE IV

TOLERANCE LIMITS (IN mg/l) OF THE VARIOUS CARBOXYLATE IONS DURING THE DETERMINATION OF 1 mg/l OF EACH OF CHLORIDE, PHOSPHATE AND SULPHATE

Carboxylate ion	Chloride	Phosphate	Sulphate
Formate	5	50	1000
Acetate	5	50	1000
Citrate	0.5	30	1000
Benzoate	5	20	800
Succinate	–	5	10
Malonate	–	100	15
Salicylate	–	800	200
Oxalate	–	800	200
Phthalate	–	400	100
Tartrate	20	50	500
Ascorbate	5	150	500
Lactate	5	150	500

interferences during the determination of anions were overcome by the sample pretreatment involving UV photolysis.

The present sample pretreatment method coupled with ion chromatography was applied to determine the impurities in different commercial carboxylic acids. Most of the carboxylic acids were found to contain chloride, sulphate and phosphate as the anionic impurities, while common cationic impurities were found to be iron(III), lead(II), copper(II) and zinc(II).

CONCLUSIONS

UV photolysis of the carboxylic acids followed by ion chromatography was found to be very effective for the simultaneous determination of many inorganic anionic as well as cationic impurities in carboxylic acids. The various ions can be very well determined in the range between 0.6 μM and 1 μM as the present method has excellent resolution, sufficient precision and is more convenient than traditional methods.

ACKNOWLEDGEMENT

One of the authors (J.L.S.) acknowledges financial support from the International Centre for Theoretical Physics (Trieste, Italy).

REFERENCES

1 Prolabo, *Normes Analytiques des Réactifs*, Rhone-Poulenc, Paris, 1980.
2 J.G. Tarter, *Ion Chromatography*, Marcel Dekker, New York, 1987.
3 H. Small, *Ion Chromatography*, Plenum Press, New York, 1989.

Journal of Chromatography A, 654 (1993) 129–134
Elsevier Science Publishers B.V., Amsterdam

CHROMSYMP. 2874

Determination of total phosphorus in soaps/detergents by ion chromatography☆

Pier Luigi Buldini* and Jawahar Lal Sharma☆☆

C.N.R.–LAMEL, Laboratorio Analisi Chimica Materiali, Via Idraulico 17/2, I-40138 Bologna (Italy)

Donatella Ferri

U.S.L. 28, Presidio Multizonale Prevenzione, Via Triachini 17, I-40138 Bologna (Italy)

(First received September 21st, 1992; revised manuscript received June 10th, 1993)

ABSTRACT

The quantitative determination of phosphorus in soaps and detergents is a classical analytical problem owing to the complexity of the matrix containing a variety of chemical species (*i.e.*, surfactants, complexones and/or zeolites, optical whiteners, perfumes, etc.). A new method has been developed for the analysis of total phosphorus in soaps and detergents which employs UV photolysis of the analyte. It has the advantages that it is a simple procedure and has very low blank values because of the small amount of reagent required for the sample pretreatment. Different types of soaps and detergents were subjected to oxidative UV photolysis. It was found that the organic matrix was degraded in about 60 min, thereby permitting the quantitative analysis of various inorganic species, especially the phosphate ion. Soaps and detergents of different "types and brands" were found to contain phosphate from a few mg/l or mg/kg to the 1% level. The results were compared with those obtained by conventional alkaline fusion followed by reduction to molybdenum blue, and were found to be in good agreement.

INTRODUCTION

The determination of total phosphorus in soaps, detergents and other cleaning agents has gained much importance because of legislation in many parts of the world that limits their use as they are one of the causes of eutrophication. This, in turn, has resulted in demand for sensitive and rapid instrumental analytical techniques for a precise control of the phosphorus content, not only in the inorganic form, but also present as combined organic derivatives in various forms.

Different techniques are routinely used for the determination of phosphate in detergents. These include gravimetry [1], spectrophotometry [2,3], voltammetry [4] and flow injection analysis [5], but these methods suffer from various drawbacks, such as cumbersome sample preparation and long analysis time.

The remarkable developments in high-efficiency liquid chromatography, in particular ion chromatography, have provided the opportunity to explore a new approach to analyse the total phosphorus content in detergent products. High-performance liquid chromatography with flame photometric detection has been used [6] for the determination of inorganic phosphate in de-

* Corresponding author.

☆ Presented at the *International Ion Chromatography Symposium 1992, Linz, September 21–24, 1992.* The majority of the papers presented at this symposium were published in *J. Chromatogr.*, Vol. 640 (1993).

☆☆ Permanent address: K.M. College, University of Delhi, Delhi 110007, India.

0021-9673/93/$06.00

tergents, but the method is not recommended for the determination of the phosphorus present as organic derivatives.

The present work deals with the development of a new sample treatment method for the analysis of total phosphorus in soaps and detergents which employs oxidative UV photolysis of the analyte to destroy organic matter prior to the ion chromatographic analysis. It has the advantages that it is a simple procedure and has very low blank values because of the small amount of reagent required for sample pretreatment.

When the proposed method was compared with the conventional alkaline fusion method followed by spectrophotometric molybdenum blue detection the results were found to be in good agreement.

PRELIMINARY STUDIES

Investigations were performed on a large number of commercially available soaps, detergents and cleaning agents and revealed that the composition of these products varies not only in terms of the total phosphorus content, but also in terms of total chlorine, nitrogen and sulphur content. After UV photolysis, some of the products show a very large peak for chloride, nitrite, nitrate and/or sulphate ions. In some cases the partially photolysed samples were also found to contain one or more carboxylate ions as photolysis products. Some of these ions have retention times very close to that of orthophosphate, and can be confused with the presence of phosphate, even if it is not present in the product. It therefore becomes necessary to study the effect of various ions on the retention behaviour and quantitation of phosphate. Chloride, nitrite, nitrate, sulphate and a number of carboxylate ions were chosen to study the interferences because one or more of these ions are formed after UV photolysis of the commercially available products. Borate and silicate were also included in the list of possible interferents in the determination of phosphate as these are, or might be, present as one of the constituents of soaps and detergents. For this study, a series of solutions containing 1 mg/l phosphate and varying amounts of possible interferents were prepared. The pH of all the solutions was adjusted to 7.5 by adding dilute ammonia solution and the solutions were then analysed by ion chromatography following the procedure described in the Experimental section. In most cases, a sufficiently high concentration of the added anion did not interfere with the quantitation of phosphate. These findings are summarized in Table I.

Effect of pH

The retention time and the peak area of phosphate are very much influenced by the change in pH of the eluent as well as the analyte. This is largely because phosphate undergoes protonation/deprotonation and is present in different forms. The free orthophosphate form is predominant in alkaline conditions, while at acidic pH the protonated form dominates. The carbonate–hydrogencarbonate eluent used for the present chromatographic analysis has a pH of 9.7, at which the divalent form (HPO_4^{2-}) predominates. However, if the sample is too acidic to be neutralized by the eluent, the initial retention of the analyte is disturbed, probably because its valence is continuously changing as the buffer takes effect, and thus its retention time as well as the peak area changes. Experiments revealed that for a sample injection volume of 25 μl the area of the phosphate peak is not affected if the pH of the analyte is in the range 4.5–10.

TABLE I

TOLERANCE LIMITS FOR VARIOUS ANIONS FOR THE DETERMINATION OF 1 mg/l PHOSPHATE (AT pH 7.5)

Ion	Tolerance limit (mg/l)	Ion	Tolerance limit (mg/l)
Oxalate	1000	Palmitate	500
Formate	1000	Oleate	500
Acetate	1000	Laurate	1000
Benzoate	1000	Chloride	1000
Succinate	1000	Nitrite	1000
Salicylate	400	Nitrate	100
Phthalate	250	Sulphate	1000
Malonate	200	Silicate	5000
Stearate	500	Borate	5000

EXPERIMENTAL

Reagents and standards

Sodium carbonate and sodium hydrogencarbonate were chromatographic grade (Novachimica, Milan, Italy), hydrogen peroxide (30% m/m, without stabilizer), hydrochloric acid (37%), ammonia solution (30%) and sodium hydroxide were Erbatron electronic grade (Carlo Erba, Milan, Italy), sulphuric acid, ammonium molybdate, sodium nitrate, sodium sulphite and N-*p*-methylaminophenol sulphate were analytical grade (Carlo Erba), and sodium hydrogensulphite was analytical grade (Janssen Pharmaceutica, Geel, Belgium). Ultrapure water with conductivity <0.1 μS (DI water) was obtained from a Milli-Q (Millipore, Bedford, MA, USA) four-bowl deionization system.

Working standards were prepared daily by dissolving pH standard-grade potassium dihydrogenphosphate and reagent-grade potassium pyrophosphate (Carlo Erba).

Quartz test tubes and all glassware were cleaned in concentrated nitric acid and carefully washed with DI water. Normal precautions for trace analysis were observed throughout.

Eluent and regenerant solutions

A solution of 2.0 m*M* sodium carbonate and 0.90 m*M* sodium hydrogencarbonate (pH 9.7) was prepared by dissolving the requisite amounts in DI water and used as chromatographic eluent at a flow-rate of 1.5 ml/min. The regenerant solution for the anion micromembrane suppressor was 125 m*M* sulphuric acid at a flow-rate of 8 ml/min.

Spectrophotometric solutions

Reducing solution. A 250-g amount of N-*p*-methylaminophenol sulphate, 1.25 g of sodium sulphite and 37.5 sodium hydrogen sulphite were dissolved in DI water and make up to 500 ml. Since this solution deteriorates in contact with air, it was prepared freshly when needed.

Ammonium molybdate solution. A 12.5-g amount of ammonium molybdate was dissolved in 125 ml of 10 *M* sulphuric acid and diluted to 500 ml.

Instrumentation

Samples were subjected to UV photolysis in a Metrohm (Herisau, Switzerland) 705 UV digestor equipped with a 500-W high-pressure mercury lamp. The temperature of the sample was maintained at 85 ± 5°C with the aid of a combined air–water cooling system.

Chromatographic analyses were performed on a Dionex (Sunnyvale, CA, USA) 2000i ion chromatograph equipped with an EDM eluent degassing module, a GPM gradient pump, a 25-μl injection loop, an IonPac AG9 guard column and an IonPak AS9 separator column, an AMMS anion micro-membrane suppressor and a CDM conductivity detector.

All measurements were made at 25 ± 1°C and, in all cases, injection of the sample was done at least in triplicate.

Precautions were taken to ensure that the analyte did not remain either on the column or on the injection loop overnight. The injection loop was washed with DI water prior to every analysis.

Peak areas were obtained using Al-450 Dionex software and background correction was applied wherever necessary.

Spectrophotometric analyses were performed on a Baush & Lomb (Rochester, NY, USA) Spectronic 21 UV-D spectrophotometer.

Sampling

An appropriate sampling procedure is essential to ensure that the sample taken represents all the characteristics/properties of the bulk material, because only a small amount is required for the analysis.

The sampling of commercially available soaps, detergents and cleaning agents was done on the basis of their physical form. Transparent liquid detergents free from deposit and suspensions were used directly without any sampling treatment. But the liquid products containing insoluble deposit or suspended matter were heated to 40°C with constant stirring to homogenize all the components present in the product. Powdered products were sampled using a conical divider such as the Pascall Rotary Cascade Sample Divider. Products in the form of cakes were homogenized by warming with water at 40°C.

Ion chromatographic procedure

A 0.05-g amount of sample was mixed with 0.5 ml of hydrogen perioxide in a quartz tube, which was closed with conical PTFE stoppers that tapered to a point. The stoppers acted as cooling fingers, and thus prevented solution losses and also protected the sample from contamination. The sample was subjected to UV photolysis at 85 ± 5°C for 60 min, then it was diluted to 25 ml (100 ml in case of samples containing a relatively large amount of phosphate) and analysed by ion chromatography. Under the present chromatographic conditions, the retention time for phosphate was found to be 7.7 min.

Spectrophotometric procedure

For comparison purposes, the spectrophotometric method for the determination of phosphate, as proposed by Longman [7], was used: 0.5 g of the detergent/soap sample were mixed with an equal amount of sodium nitrate, and heated gently in a platinum cap to oxidize the organic matter. When cold, the fuse was treated with 10 ml of hydrochloric acid (25%) and evaporated to dryness. The addition of hydrochloric acid was repeated and the mixture again evaporated to dryness. The residue was dissolved in 5 ml of hydrochloric acid (25%) and filtered into a 500-ml flask. The cap and filter were washed with hydrochloric acid, and the washings were added to the flask. The solution was neutralized with 10% sodium hydroxide solution (using phenolphthalein as indicator) and diluted to 500 ml. A 45-ml aliquot of this solution was transferred to a 100-ml flask and mixed with 10 ml of ammonium molybdate solution and 20 ml of the reducing solution. This mixture was diluted to 100 ml with DI water and its optical density was measured at 720 nm, employing DI water as the blank.

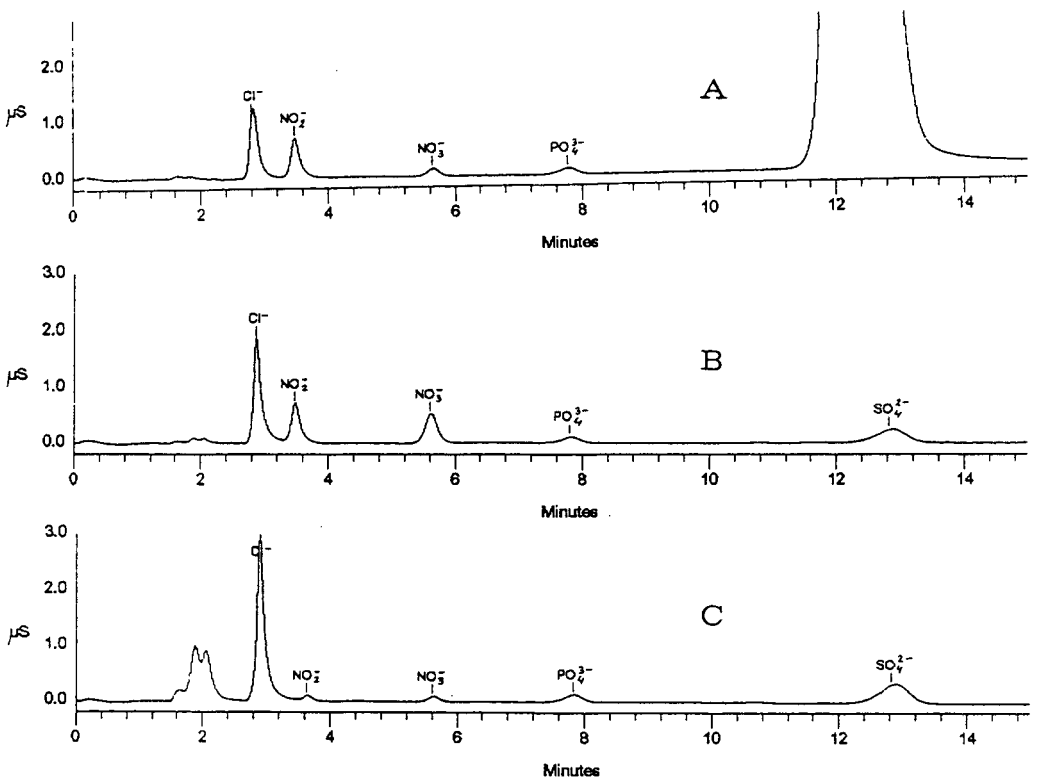

Fig. 1. Determination of phosphorus (as PO_4^{3-}) in detergent (A), soap (B) and shampoo (C). Eluent: 2.0 m*M* Na_2CO_3 + 0.9 m*M* $NaHCO_3$.

RESULTS AND DISCUSSION

Fig. 1 shows typical chromatograms obtained for three different detergent samples, which had been subjected to UV photolysis prior to chromatographic analysis.

The commercially available soaps, detergents and other cleaning agents contain phosphorus in a variety of chemical forms, including simple phosphates, pyro- and polyphosphates, alkyl or phenyl phosphates and their derivatives, imidophosphates, alkylphosphonates, etc. These chemicals are hydrolysed during the course of UV photolysis in the presence of hydrogen peroxide. Experiments were performed by analysing a mixture of potassium dihydrogenphosphate and potassium pyrophosphate, after it had been subjected to UV photolysis. The chromatogram of this solution gave only one peak at 7.7 min and the peak area was in agreement with the area that would be obtained with the equivalent amount of orthophosphate. Similar studies could not be made on organic derivatives of phosphorus, since the compounds were not available in pure form.

At the same time, it is interesting to note that for different soaps, detergents and cleaning agents analysed after 1 h of UV photolysis, at pH

TABLE II

THE PHOSPHORUS CONTENT OF VARIOUS COMMERCIALLY AVAILABLE SOAPS, DETERGENTS AND CLEANING AGENTS

Category	Determined by	
	Ion chromatography (ppm)[a]	Spectrophotometry (ppm)[a]
Toilet		
(A) Cake	260	257
(B) Liquid emulsion	275	277
Shampoo		
(A) Liquid clear	174	180
(B) Liquid emulsion	202	207
Laundry soap		
(A) Cake, white	0	0
(B) Cake, yellow	9	9
(C) Flakes	44	45
Detergent		
(A1) Liquid, wool	0	0
(A2) Liquid, wool	0	0
(B1) Liquid, hand washing	72	71
(B2) Liquid, hand washing	259	257
(B3) Liquid, hand washing	631	628
(C1) Powder, machine washing	181	175
(C2) Powder, machine washing	197	191
(C3) Powder, machine washing	919	920
Fabric softener		
(A) Liquid emulsion	0	0
Fabric whitener		
(A) Powder	7495	7500
Dishwasher detergent		
(A) Liquid, hand washing	74	70
(B) Powder, machine washing	2813	2850

[a] Liquid detergents, ppm = mg/l; solid detergents, ppm = mg/kg.

greater than 7, the retention time for phosphate changed by only 5%, thus suggesting that phosphorus present in different forms (inorganic as well as organic) is converted to orthophosphate after UV photolysis.

Apart from the determination of phosphate, the present method can be successfully used to determine the total chlorine and sulphur content of detergents in the form of chloride and sulphate ions, as good separation of their peaks is achieved. The method is not recommended for the determination of the nitrogen content of soaps and detergents, as nitrogen is oxidized to nitrite and nitrate, which are broken down during UV photolysis.

The reproducibility, working range and sensitivity of the present method were evaluated by spiking one phosphate-free detergent sample with different amounts of standard phosphate and pyrophosphate solutions, and subjecting it to UV photolysis prior to analysis. The reproducibility of the successive injections of the same sample solution was better than 2% R.S.D. In the concentration range 0.2–100 mg/l phosphate. Peak area was found to be linearly related to phosphate concentration for the spiked solutions covering the entire working range of 0.2–100 mg/l.

The total phosphorus content as determined for different "types and brands" of soaps and detergents varies from product to product. Most of the toilet soaps and a few shampoos were found to contain phosphate in low amounts (<1000 mg/l or mg/kg). Interestingly, dishwasher detergents were found to contain very large amounts of phosphate compared with other types of detergents, while the detergents for cleaning woollen clothes were free from phosphate. The comparison of the proposed ion chromatographic method with the conventional spectrophotometric procedure has shown good results. These results are reported in Table II.

ACKNOWLEDGEMENT

One of the authors (J.L.S.) is grateful to the International Centre for Theoretical Physics (Trieste, Italy) for awarding with a fellowship.

REFERENCES

1 *British standard, BS 3762:* Section 3.19:1983 (ISO 4313-1976), British Standard Institution, Milton Keynes.
2 V. Ramasubramanian and K.S. Narayan, *Indian J. Technol.*, 17 (1979) 355.
3 G. Graffmann, W. Schneider and L. Dinkioh, *Fresenius' Z. Anal. Chem.*, 301 (1980) 364.
4 A.G. Fogg, G.C. Cripps and B.J. Birch, *Analyst*, 108 (1983) 1485.
5 P.W. Alexander and J. Koopetngarm, *Anal. Chim. Acta*, 197 (1987) 353.
6 T.L. Chester, C.A. Smith and S. Culshaw, *J. Chromatogr.*, 287 (1984) 447.
7 G.F. Longman, *The Analysis of Detergents and Detergent Products*, Wiley, New York, 1978, p. 457.

Journal of Chromatography A, 654 (1993) 135–141
Elsevier Science Publishers B.V., Amsterdam

CHROM. 25 385

Inverse gas chromatography in characterization of surfactants

Determination of binary parameter

A. Voelkel* and J. Janas

Poznań Technical University, Institute of Chemical Technology and Engineering, Poznań, Pl. M. Skłodowskiej-Curie 2, 60-965 Poznań (Poland)

J.A. Garcia-Dominguez

CSIC, Instituto de Quimica Fisica "Rocasolano", Serrano 119, 28006 Madrid (Spain)

(First received April 19th, 1993; revised manuscript received June 23rd, 1993)

ABSTRACT

Binary parameters corresponding to hydrogen bonding ($I_{12\,h}$) and polar ($I_{12\,p}$) interactions were determined by inverse gas chromatography. The influence of the structures of broad-range and narrow-range distributed oxyethylene derivatives of 1-hexadecanol on the binary parameters was studied. The relationship between the binary parameters ($I_{12\,h}$ and $I_{12\,p}$) and the polarity of the compounds used as stationary phases is presented and discussed, in addition to the effect of the solubility parameter and its increments on the values of the two binary parameters.

INTRODUCTION

Inverse gas chromatography (IGC) is widely used in the characterization of the physico-chemical properties of a variety of liquid and solid materials. The term "inverse" indicates that the material of interest is placed in a chromatographic column (as the stationary phase) and that the retention data for the test solutes are measured. Physico-chemical parameters calculated from retention data described intermolecular solute–examined material interactions, which are influenced by the properties of the liquid or solid used as the stationary phase [1] in the chromatographic system.

The properties of polymers and their blends can be determined relatively easily and accurately by IGC parameters. The Flory–Huggins solute–polymer interaction parameter is given as

$$\chi_{1,2}^{\infty} = \ln\left(\frac{273.15R}{p_1^0 V_g^0 M_1}\right) - \frac{p_1^0}{RT}(B_{11} - V_1^0) + \ln\left(\frac{\rho_1}{\rho_2}r\right) - \left(1 - \frac{V_1^0}{V_2^0}\right) \quad (1)$$

where M_1, p_1^0, B_{11}, V_1^0, ρ_1 and V_g^0 are the molecular mass, saturated vapour pressure, second virial coefficient, molar volume and specific retention volume of the solute, respectively; ρ_2

* Corresponding author.

0021-9673/93/$06.00

and V_2^0 are the density and molar volume of the polymer, respectively, T is the column temperature and R is the gas constant. In the evaluation of eqn. 1, the value of V_1^0/V_2^0 is normally taken as zero. The parameter χ^∞ exhibits high values for poor solvents [2–6] whereas low values indicate good solubility.

The cohesive energy, E_{coh}, of a substance in a condensed state is defined as the increase in internal energy, U, per mole of substance if all intermolecular forces are eliminated. The square root of the cohesive energy density is called the solubility parameter, δ, and is defined as $\delta_1 = (E_{coh}/V)^{1/2}$ $(J/m^3)^{1/2}$. The units of solubility parameter are $(cal/cm^3)^{1/2}$, $(J/m^3)^{1/2}$ or $(MPa)^{1/2}$.

The solubility parameter of a volatile compound can be calculated from the basic equation

$$\delta = \left(\frac{\Delta H_v - RT}{V_1^0}\right)^{1/2} \quad (2)$$

where ΔH_v is the enthalpy of vaporization, R in the gas constant, T is the absolute temperature and V_1^0 is the molar volume of the compound.

For low-volatile or non-volatile species, the use of eqn. 2 is not possible. Guillet and DiPaola-Baranyi [7,8] presented a procedure for the evaluation of the solubility parameter for polymeric substances with the use of the solute–solvent interaction parameter χ^∞. They applied the Hildebrand–Scatchard expression of χ^∞ in the form

$$\chi^\infty = \frac{V_1^0(\delta_1 - \delta_2)^2}{RT} + \chi_s^\infty \quad (3)$$

where V_1^0 is the solute molar volume, δ_1 and δ_2 are solubility parameters of the solute and solvent, respectively, and χ_s^∞ is the entropic factor of the interaction parameter. This led to the equation

$$\frac{\delta_1^2}{RT} - \frac{\chi^\infty}{V_1^0} = \frac{2\delta_2}{RT} \cdot \delta_1 - \left(\frac{\delta_2^2}{RT} + \frac{\chi_s^\infty}{V_1^0}\right) \quad (4)$$

which allowed the calculation of the solubility parameter, δ_2, of the substance used as the stationary phase in the chromatographic system.

The application this procedure has been reported in several papers [7,9–19]. Most often, excellent linearity is obtained when using eqn. 4 [1]. However, Price [13] reported the significant deviations from linearity for compounds (stationary phases) having relatively low molecular mass. Price determined the contributions to the solubility parameter attributed to dispersive (δ_d) and polar (δ_p) solute–solvent interactions. Recently, Voelkel and Janas [20,21] followed up this idea. They examined oligooxyethylene derivatives of 1-hexadecanol and oligooxyethylene surfactants having perfluoroalkane groups in their hydrophobic parts. They separated three contributions corresponding to the dispersive, polar and hydrogen bonding interactions. This allowed the determination of the total, corrected solubility parameter from the equation earlier proposed by Hansen [22,23] for cohesive energy contributions:

$$\delta_T^2 = \delta_d^2 + \delta_p^2 + \delta_h^2 \quad (5)$$

However, the Hildebrand–Scatchard theory [24,25] and eqn. 3 are valid under the assumptions that the volume change of mixing is zero and the segment interactions are binary, and these assumptions are valid only for non-polar systems, where the only molecular forces are London or dispersive forces. It is possible that deviations observed by Price *et al.* [13], Becerra *et al.* [14] and Voelkel and Janas [20,21] are caused by Debye, Keesom or hydrogen bonding interactions negligible for high-molecular-mass polymer–solute systems.

As was shown by Mikos and Peppas [26], the enthalpic component of the solute–solvent interaction parameter should be modified as follows:

$$\chi_h^\infty = \frac{V_1^0}{RT}[(\delta_1 - \delta_2)^2 + 2I_{12}\delta_1\delta_2] \quad (6)$$

where I_{12} is a binary parameter. Binary parameters depend on the molecular size and the chemical nature of the interacting species, and may be positive or negative depending on molecular interactions [24,25]. For the applicability of the Hildebrand–Scatchard theory, $I_{12} = 0$.

Rearranging eqn. 6, we obtain

$$\frac{\delta_1^2}{RT} - \frac{\chi^\infty}{V_1^0} = \frac{2\delta_2(1 - I_{12})}{RT} \cdot \delta_1 - \left(\frac{\delta_2^2}{RT} + \frac{\chi_s^\infty}{V_1^0}\right) \quad (7)$$

where the slope of hypothetical straight line depends on the value of I_{12}.

Plotting the left-hand side of eqn. 7 *versus* δ_1, it is possible to obtain straight lines of different slopes [20,21] if only solutes of one of the following three groups are used, each group representing different types of intermolecular interactions, *i.e.*, dispersive, polar and hydrogen bonding interactions:

(a) The first group is *n*-alkanes. Here the slope of the straight line would be the same as that obtained with eqn. 4, as it may be assumed that no specific intermolecular interactions exist between the examined material and this type of test probe (*i.e.*, $I_{12} = 0$).

(b) A second group of probes represent polar interactions, for which the slope of the line obtained on application of eqn. 7 would be

$$\text{slope}_{\text{polar}} = \frac{2\delta_2}{RT}(1 - I_{12p}) \quad (8)$$

where I_{12p} denotes a binary parameter for polar interactions.

(c) The third group of probes represent hydrogen bonding properties. Here,

$$\text{slope}_{\text{H-bond}} = \frac{2\delta_2}{RT}(1 - I_{12h}) \quad (9)$$

where I_{12h} represents a binary parameter for hydrogen bonding interactions.

The aim of this work was to evaluate binary parameters for the set of oligooxyethylene derivatives of 1-hexadecanol, evaluate and discuss the relationships between polarity parameters, solubility parameters and derived binary parameters, discuss the effect of the structures of the compounds examined on the binary parameters and examine the temperature dependence of both binary parameters.

EXPERIMENTAL

Materials

1-Hexadecanol of 94.5% purity was used to obtain conventional products with a broad-range distribution (BRD) of homologues and narrow-range distributed ethoxylates (NRD) having an average ethoxylation number from 3 to 11. NRD products are characterized by a lower content of homologues with a number of oxyethylene units significantly different from the average. Moreover, comparison of the homologue distribution in NRD products indicates a slight shift of the maximum towards a higher content of oxyethylene groups. Conventional products were obtained using sodium hydroxide as a catalyst, whereas a proprietary catalyst was utilized to produce NRD ethoxylates. All products were synthesized at the Institute of Heavy Organic Synthesis "Blachownia". Kędzierzyn-Koźle, Poland. Other data on these products were presented in previous papers [20,27].

IGC experiments

The examined oxyethylate was placed in a GC column as liquid stationary phase coated on an inert support of Celite (80–120 mesh) (25%, w/w). The use of such a high content of liquid phase is suggested to eliminate adsorption effects. Other conditions for the GC experiments were as follows: chromatograph CHROM 5 (Kovo, Prague, Czech Republic) equipped with a flame ionization detector; column, 1 m × 3 mm I.D.; column temperatures (isothermal), 70, 90 and 110°C; injector temperature, 150°C; detector temperature, 200°C; and carrier gas (helium) flow-rate, 40 ml/min. The testing probes were *n*-alkanes from *n*-pentane to *n*-decane, benzene, toluene, xylene, ethylbenzene, *n*-alkanols from methanol to 1-butanol, 2-butanone, 2-pentanone, nitropropane and pyridine. Their adjusted retention times were determined as described [28–30].

RESULTS AND DISCUSSION

We assumed that the values of I_{12} are similar within each of the three selected groups of test solutes, *i.e.*, alkanes, hydrogen-bonding probes and polar probes. This assumption is justified by the occurrence of straight lines for each group. If the I_{12} values within a group were significantly different for each solute–solvent pair, application of eqn. 7 would not produce a straight line. Moreover, we also assumed that the value of I_{12} for an alkane–stationary phase pair is zero, although Preston and Prausnitz [31] reported I_{12} values for carbon dioxide–alkanes mixtures dif-

ferent from but very close to zero. In other words, one should treat our values of binary parameters $I_{12\,p}$ and $I_{12\,h}$ as a measure of the deviation from the stationary phase–alkane system.

The values of the binary parameters are presented in Tables I and II. We should discuss the dependence of I_{12} on the type of stationary phase–BRD and NRD series of oxyethylates examined, the length of the oxyethylene chain, the series of test solutes and the temperature of the chromatographic column. Almost all reported values are negative and lie, with a few exceptions, in the range 0 to −0.5. The values of $I_{12\,h}$ for donor–acceptor series of solutes decrease with increase in oxyethylation ratio for both the BRD and NRD series of oxyethylates. The lowest values are observed for "homologues" containing 7 (BRD) or 6–8 (NRD) oxyethylene units. For products having more than 8–9 oxyethylene units $I_{12\,h}$ increases. For NRD products one may observe a wide minimum for both $I_{12\,h}$ and $I_{12\,p}$ (Fig. 1). $I_{12\,p}$ is always higher and for $C_{16}E_3$ (BRD) it is even positive. The influence of the oxyethylation ratio on $I_{12\,p}$ is similar to that on $I_{12\,h}$. The difference between $I_{12\,h}$ and $I_{12\,p}$ for BRD oxyethylates decreases with increasing oxyethlation ratio whereas for NRD products this difference is approximately constant and equal to 0.2 (Fig. 2). The type of distribution of oxyethylene products significantly influences the range of changes in the $I_{12\,h}$ and $I_{12\,p}$ binary parameters. The difference between their highest and lowest values is much larger for BRD products, *e.g.*, at 70°C the maximum $\Delta I_{12\,h}$ (BRD) = 0.573 whereas the maximum $\Delta I_{12\,h}$ (NRD) = 0.212.

The effect of temperature on the values of $I_{12\,h}$ and $I_{12\,p}$ can be given various interpretations. Both $I_{12\,h}$ and $I_{12\,p}$ increase or decrease in value depending on the particular stationary phase used. In several extreme cases deviations were observed at 90°C. No general rule can be formulated for the temperature dependence of the binary parameters determined by an IGC method.

TABLE I

BINARY PARAMETER $I_{12\,h}$ FOR HYDROGEN BONDING INTERACTIONS IN PROBE–STATIONARY PHASE SYSTEMS

Type	Average number of EO units	$I_{12\,h}$		
		70°C	90°C	110°C
BRD	3	−0.063	0.087	−0.082
	4	−0.237	−0.252	−0.174
	5	−0.375	−0.385	−0.349
	6	−0.410	−0.458	−0.446
	7	−0.636	−0.650	−0.672
	8	−0.547	−0.596	−0.579
	9	−0.435	−0.385	−0.475
	10	−0.283	−0.337	−0.405
	11	−0.292	−0.286	−0.233
NRD	3	−0.315	−0.300	−0.321
	4	−0.322	−0.330	−0.347
	5	−0.440	−0.430	−0.461
	6	−0.489	−0.477	−0.542
	7	−0.480	−0.420	−0.461
	8	−0.485	−0.424	−0.428
	9	−0.358	−0.380	−0.417
	10	−0.273	−0.335	−0.344
	11	−0.282	−0.323	−0.335

TABLE II

BINARY PARAMETER $I_{12\,p}$ FOR POLAR INTERACTIONS IN PROBE–STATIONARY PHASE SYSTEMS

Type	Average number of EO units	$I_{12\,p}$		
		70°C	90°C	110°C
BRD	3	0.026	0.001	−0.010
	4	−0.110	−0.125	−0.062
	5	−0.126	−0.170	−0.255
	6	−0.159	−0.166	−0.173
	7	−0.404	−0.418	−0.428
	8	−0.342	−0.368	−0.388
	9	−0.272	−0.275	−0.282
	10	−0.253	−0.292	−0.356
	11	−0.312	−0.307	−0.365
NRD	3	−0.089	−0.079	−0.108
	4	−0.146	−0.183	−0.206
	5	−0.276	−0.258	−0.278
	6	−0.310	−0.290	−0.335
	7	−0.321	−0.264	−0.268
	8	−0.382	−0.351	−0.406
	9	−0.203	−0.230	−0.261
	10	−0.140	−0.208	−0.224
	11	−0.112	−0.107	−0.165

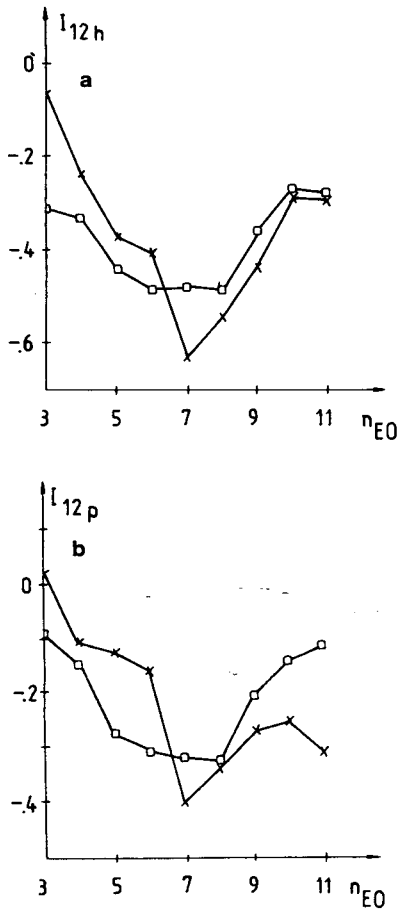

Fig. 1. Influence of the number of oxyethylene units and the type of their distribution on binary parameters at 70°C. × = BRD oxyethylates; □ = NRD oxyethylates.

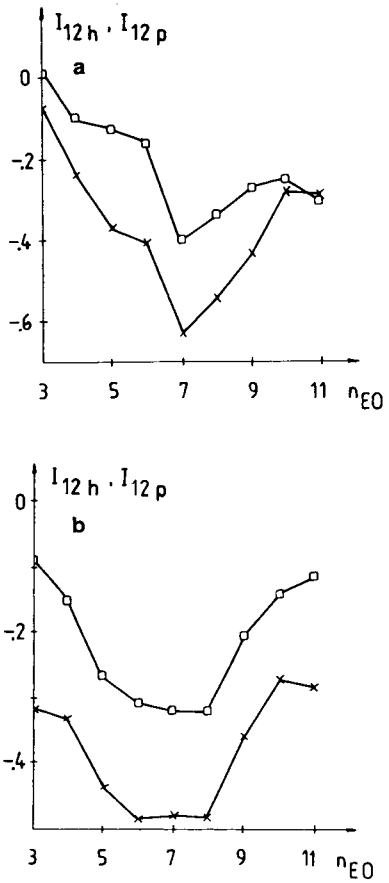

Fig. 2. Comparison of binary parameters for (a) BRD oxyethylates and (b) NRD oxyethylates at 70°C. × = $I_{12\,h}$; □ = $I_{12\,p}$.

Oligooxyethylene derivatives of 1-hexadecanol were previously characterized by polarity parameters [27] and also by the solubility parameter δ_2 and its increments corresponding to dispersive, polar and hydrogen bonding interactions. $I_{12\,h}$ and $I_{12\,p}$ decrease with increasing polarity of the stationary phase as measured by the sum of the first five McReynolds constants [32] $\Sigma_{i=1}^{5} \Delta I_i$ and/or the polarity index *PI* (Fig. 3). A narrow minimum is observed for an $\Sigma_{i=1}^{5} \Delta I_i$ value of *ca.* 1100 i.u. for BRD products, whereas for NRD analogues minimum I_{12} values are observed over a fairly wide range of $\Sigma_{i=1}^{5} \Delta I_i$ values (1000–1200).

A strong relationship exists between the binary parameters discussed here and the increments of the solubility parameters corresponding to interactions of the hydrogen bonding (δ_h) and polar (δ_p) types determined earlier by Voelkel and Janas [20]. The respective linear relationships are as follows:

$$I_{12\,h} = -9.944\delta_h + 1.604 \quad R = 0.960 \tag{10}$$

$$I_{12\,p} = -11.563\delta_p + 0.702 \quad R = 0.976 \tag{11}$$

Both $I_{12\,h}$ and $I_{12\,p}$ decrease with increase in the corresponding component of the solubility parameter (Fig. 4). The deviations from a regular solution (as measured by I_{12}) increase with increasing contribution of hydrogen bonding and

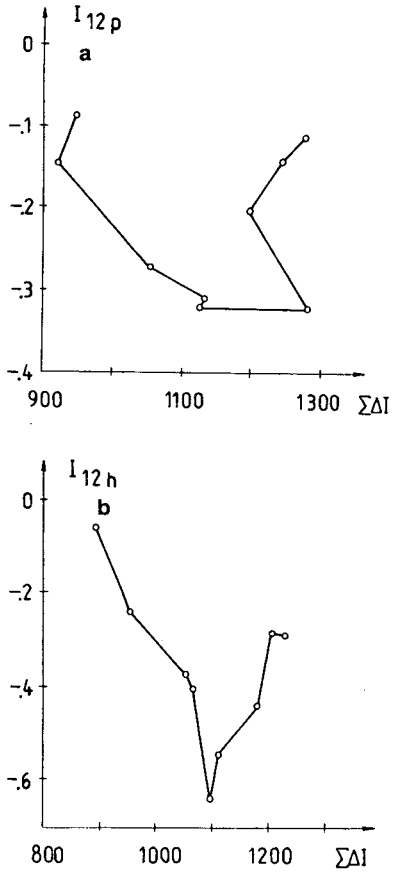

Fig. 3. Influence of the polarity of the stationary phase on its binary parameters at 70°C: (a) $I_{12\,h}$ *vs.* $\Sigma_{i=1}^{5} \Delta I_i$ for BRD oxyethylates; (b) $I_{12\,p}$ *vs.* $\Sigma_{i=1}^{5} \Delta I_i$ for NRD oxyethylates.

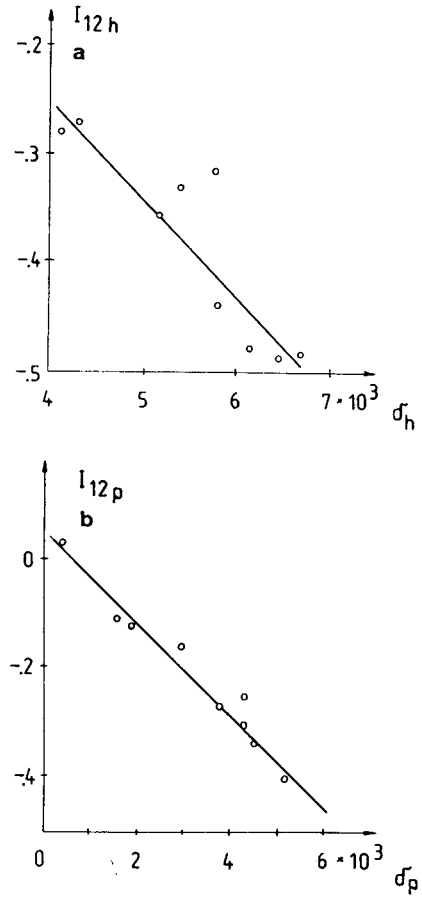

Fig. 4. Relationship between binary parameters and increments of solubility parameter at 70°C: (a) $I_{12\,h}$ *vs.* δ_h for NRD oxyethylates; (b) $I_{12\,p}$ *vs.* δ_p for BRD oxyethylates.

polar binary parameters to the total solute–solvent interactions.

CONCLUSIONS

It has been shown that the binary parameters $I_{12\,h}$ and $I_{12\,p}$ can be calculated from GC data. The values of the binary parameters were determined not for single species but for two groups of test solutes representing hydrogen bonding and polar solute–solvent interactions. This means that a given value of a binary parameter (*e.g.*, $I_{12\,h}$) is characteristic of solutes that can interact with the solvent (stationary phase) by hydrogen bonding interactions. As the sets of test solutes were the same for each oxyethylate examined, the changes in the hydrogen bonding $I_{12\,h}$ and polar $I_{12\,p}$ binary parameters may be attributed to changes in the structure of the stationary phase and to the temperature of the chromatographic column. $I_{12\,h}$ and $I_{12\,p}$ are a measure of the deviations from a regular solution for a given solute–solvent system. No general relationship was found between $I_{12\,h}$ and $I_{12\,p}$ and the temperature of the chromatographic column.

The relationships between the binary parameters and polarity parameters exhibit minima of different character depending on the type of oxyethylate (BRD or NRD). The significant relationship between $I_{12\,h}$ and $I_{12\,p}$ and the corresponding increments of the solubility parameter indicates that an increasing contribution

of hydrogen bonding and polar interactions increases the deviations from a regular solution.

REFERENCES

1 A. Voelkel, *CRC Crit. Rev. Anal. Chem.*, 22 (1991) 411.
2 J.I. Irribaren, M. Iriarte, C. Uriarte and J.J. Iruin, *J. Appl. Polym. Sci.*, 37 (1989) 3459.
3 C. Uriarte, M.J. Fernandez-Berridi, J.M. Elorza, J.J. Iruin and L. Kleintkens, *Polymer*, 30 (1989) 1493.
4 A. Edelman and A. Fradet, *Polymer*, 30 (1989) 317.
5 A. Edelman and A. Fradet, *Polymer*, 30 (1989) 324.
6 E. Fernandez-Sanchez, A. Fernandez-Torres, J.A. Garcia-Dominguez and J.M. Santiuste, *J. Chromatogr.*, 457 (1988) 55.
7 G. DiPaola-Baranyi and J.E. Guillet, *Macromolecules*, 11 (1978) 228.
8 J.E. Guillet, *J. Macromol. Sci. Chem.*, 4 (1970) 1669.
9 Y. Ren and P. Zhu, *J. Chromatogr.*, 457 (1988) 354.
10 M.R. Becerra, E. Fernandez-Sanchez, A. Fernandez-Torres, J.A. Garcia-Dominguez and J.M. Santiuste, *J. Chromatogr.*, 547 (1991) 269.
11 E. Fernandez-Sanchez, A. Fernandez-Torres, J.A. Garcia-Dominguez and M.D. Salvador-Moya, *J. Chromatogr.*, 556 (1991) 485.
12 G.J. Price, in D.R. Lloyd, T.C. Ward and H.P. Schreiber (Editors), *Inverse Gas Chromatographic Characterization of Polymers and Other Materials* (*ACS Symposium Series* No. 391), American Chemical Society, Washington, DC, 1989, Ch. 5, pp. 48–58.
13 G.J. Price, J.E. Guillet and J.H. Purnell, *J. Chromatogr.*, 369 (1986) 273.
14 M.R. Becerra, E. Fernandez-Sanchez, A. Fernandez-Torres, J.A. Garcia-Dominguez and J.M. Santiuste, *Macromolecules*, 25 (1992) 4665.
15 O. Humpa, J. Uhdeova and M. Roth, *Macromolecules*, 24 (1991) 2514.
16 Z.H. Shi and H.P. Schreiber, *Macromolecules*, 24 (1991) 3522.
17 Z.Y. Al-Saigh, *Polym. Commun.*, 32 (1991) 459.
18 A. Etxeberria, J. Alfageme, C. Uriarte and J.I. Iruin, *J. Chromatogr.*, 607 (1992) 227.
19 E. Fernandez-Sanchez, A. Fernandez-Torres, J.A. Garcia-Dominguez and E. Lopez de Blas, *J. Chromatogr. A*, 655 (1993) in press.
20 A. Voelkel and J. Janas, *J. Chromatogr.*, 645 (1993) 141.
21 A. Voelkel and J. Janas, *J. Fluorine Chem.*, in press.
22 C.M. Hansen, *Ind. Eng. Chem., Prod. Res. Dev.*, 8 (1969) 104 and 13 (1974) 218.
23 C.M. Hansen, *J. Paint Technol.*, 39 (1967) 104 and 39 (1967) 505.
24 J.M. Prausnitz, R.N. Lichtenthaler and E.G. de Azevedo, *Molecular Thermodynamics of Liquid Phase Equilibria*, Prentice-Hall, New York, 2nd. ed., 1986.
25 R.S. Reid, J.M. Prausnitz and T.K. Sherwood, *The Properties of Gases and Liquids*, McGraw-Hill, New York, 3rd ed. 1977.
26 A.G. Mikos and N.A. Peppas, *Biomaterials*, 9 (1988) 419.
27 A. Voelkel, J. Szymanowski and W. Hreczuch, *J. Am. Oil. Chem. Soc.*, in press.
28 J. Szymanowski, *CRC Crit. Rev. Anal. Chem.*, 21 (1990) 407.
29 A. Voelkel, *J. Chromatogr.*, 450 (1988) 291.
30 A. Voelkel, *Wiad. Chem.*, 41 (1987) 671.
31 G.T. Preston and J.M. Prausnitz, *Ind. Eng. Chem., Process Des. Dev.*, 9 (1970) 264.
32 W.O. McReynolds, *J. Chromatogr. Sci.*, 8 (1970) 685.

Journal of Chromatography A, 654 (1993) 143–149
Elsevier Science Publishers B.V., Amsterdam

CHROM. 25 425

Least-squares analysis of gas chromatographic data for polychlorinated biphenyl mixtures

Jordan L. Spencer*

Department of Chemical Engineering, Materials Science and Mining Engineering, Columbia University, New York, NY 10027 (USA)

James P. Hendricks and D. Kerr

Astoria General Laboratories, Consolidated Edison Company of New York, 31-01 20th Avenue, Long Island City, NY 11105 (USA)

(First received July 14th, 1993; revised manuscript received July 9th, 1993)

ABSTRACT

A method for processing the peak area *vs.* retention time data obtained in the gas chromatographic analysis of polychlorinated biphenyl (PCB) mixtures is described. The method is based on a least-squares procedure for representing the chromatogram of the unknown (sample) as a linear combination of the chromatograms of the base PCB mixtures of which the sample is assumed to be composed. A factor used to adjust for minor variations in retention times is also determined by an optimization procedure.

INTRODUCTION

In laboratories responsible for analyzing samples containing polychlorinated biphenyls (PCBs), it is often necessary to process samples made up of PCBs from several sources. (In the following we will call a mixture of polychlorinated biphenyl congeners of fixed composition a PCB, e.g. Arochlor 1260 is a PCB. A combination of PCBs will be called a blend.) A given PCB may contain 10 to 30 or more distinct chemical species, since 209 PCB congeners exist [1]. Thus a PCB or a blend, when analyzed using a suitable column and chromatographic procedure, produces a chromatogram made up of multiple peaks, each with a corresponding area and retention time.

Methods for separating PCB congeners by gas chromatography are well developed and have been used for many years [1–6]. If each PCB shows one or more large peaks which do not occur in any of the others, it is easy to calculate the amount of each PCB in a blend. However this is not always the case, because each PCB is in fact made up of the same distinct chemical species (congeners). Thus a more sophisticated method for processing the peak area *vs.* retention time data is needed. In this paper we report the development and testing of such a method, and show that it performs well in analyzing PCB blends.

THEORY

The data analysis involves two stages. In the first, the peak area *vs.* retention time data are used to reconstruct a continuous function of time that approximates the original signal obtained from the chromatograph detector as the sample is eluted from the column. This continuous function is then sampled at evenly spaced times to produce a discrete-time function, or vector.

* Corresponding author.

0021-9673/93/$06.00

We denote the value of the kth function at the jth time as C_j^k.

Assuming that the chromatograph operates in the linear range, the signal produced when analyzing a PCB mixture is a linear combination of the signals produced when running each of the pure PCB samples. The coefficients of the linear combination are proportional to the amounts of pure PCB which make up the sample being analyzed. In the second phase of the processing these coefficients are determined by requiring that they produce a least-squares fit to the experimental chromatogram. This method has the advantage that all of the data are used, rather than limiting the analysis to a small number of peaks. If, however, data corresponding to certain ranges of retention times are known to be especially reliable (or unreliable), these data can be weighted more (or less) heavily in determining the coefficients.

Elution curve reconstruction

The reconstructed chromatogram, $C(t)$, is the sum of Gaussian functions, each Gaussian centered at the corresponding retention time and having an area proportional to the area of the peak occurring at that time. Thus

$$C(t) = \sum_{i=1}^{L} p_i \, e^{-[(t-t_i)/a]^2}$$

Here p_i is the area of the ith peak, t is time, t_i is the retention time for the ith peak, a is the peak width, and L is the number of peaks. Note that, in the absence of other information, each peak is assumed to have the same width.

The peak width a can be chosen arbitrarily. If, however, a is too small, slight variations in the retention time of a peak will have a major effect on the coefficients, and thus on the results. On the other hand, if a is too large, peaks located close to each other will appear to coalesce and accuracy will be compromised. In practice, a is easily chosen so as to reproduce reasonably well the experimental spectra.

Finally, the discrete-time version of the chromatogram, C_j, is determined by sampling the continuous function $C(t)$ at M evenly spaced points, *e.g.*

$$C_j = C(j\,\Delta t)$$

where j indexes the time ($j = 1, 2, \ldots, M$) and Δt is the time increment between points.

Parameter estimation

The problem now becomes that of expressing the chromatogram of the sample, corresponding to the M-dimensional vector V, as a linear combination of the K M-dimensional chromatogram vectors C^k exactly. That is, we want

$$V = \sum_{k=1}^{K} b_k C^k$$

where the K parameters b_k are to be determined. Note that on physical grounds the parameters b_k must be non-negative, since it is not possible to use a negative amount of a mixture in preparing a sample. We choose, however, not to impose an inequality constraint on the parameters. Instead the occurrence of a significantly negative parameter value will be taken as the sign of a problem in fitting the data.

Since V and C^k are M-dimensional vectors, with M greater than K, this problem cannot in general be solved exactly. Thus we employ the widely used method of least-squares, *i.e.* we determine the parameters b_k by minimizing the objective function J, with

$$J = r^{\mathrm{T}} r$$

The residual vector r is given by

$$r_j = V_j - \sum_{k=1}^{M} b_k C_j^k$$

If we define the $M \times M$ matrix B as

$$B_{jk} = C_j^k$$

the minimum of J is found by solving the K linear equations (often called the normal equations)

$$B^{\mathrm{T}} B b = B^{\mathrm{T}} r$$

for the parameter vector b. Here superscript T denotes transposition.

The standard error, s_k, of the kth parameter can be found as

$$s_k = \sqrt{s_{\mathrm{m}}^2 [(B^{\mathrm{T}} B)^{-1}]_{kk}}$$

where s_m^2 is the variance of the measured data, which can be estimated by running the same sample a number of times and determining the run-to-run variation in the chromatogram.

The parameter correlation matrix P is found from the matrix $W = (B^T B)^{-1}$ as follows:

$$P_{jk} = W_{jk}/(\sqrt{W_{jj}}\sqrt{W_{kk}})$$

In general, when all the off-diagonal elements of P (which are necessarily less than or equal to 1 in absolute value) are smaller than, say, 0.9, the parameters will be accurately determined. This occurs when the standards (PCBs) differ widely from each other in their congeneric content, and thus exhibit very different chromatograms. If, on the other hand, one of the standards is very close to being a mixture of the other standards, one of the off-diagonal elements of P will approach unity in absolute value, and the parameters corresponding to the row and column of this element will not be well-determined. This situation will reveal itself also in large parameter standard errors.

In the actual practice of chromatography, the retention time of a given species depends inversely on the flow rate of the eluting gas and also on the temperature of the column, both of which are subject to variations which are in general small, but not exactly zero. When the peaks are narrow and well separated, even a small shift in the retention time can lead to errors in the estimation of the composition of the sample using the above algorithm. Thus we have added as a parameter to be determined a factor, denoted f, which multiplies the observed retention times of the sample. This factor was de-

TABLE I

RETENTION TIMES AND PEAK AREAS FOR AROCHLOR STANDARDS

Peak number	Arochlor 1242		Arochlor 1254		Arochlor 1260	
	Time	Area	Time	Area	Time	Area
1	1.27	0.140	1.40	0.299	1.40	0.141
2	1.44	4.247	1.69	0.064	1.69	0.034
3	1.70	6.605	2.09	0.209	2.09	0.093
4	1.89	2.409	2.44	2.509	2.45	0.163
5	2.09	18.359	2.93	1.776	3.55	1.095
6	2.31	5.748	3.27	0.497	3.73	1.622
7	2.47	12.975	3.55	6.790	4.30	0.089
8	2.69	0.345	3.73	7.553	4.87	4.036
9	2.94	6.238	4.32	2.202	5.34	5.531
10	3.06	6.006	4.52	2.148	5.92	9.551
11	3.27	4.430	4.83	6.875	6.30	1.371
12	3.56	14.717	5.20	12.476	6.89	6.213
13	4.25	8.035	5.85	16.808	7.64	18.509
14	4.83	1.956	6.92	5.492	8.51	1.930
15	5.20	2.320	7.68	16.875	9.35	5.221
16	5.85	3.317	8.39	1.290	9.83	4.557
17	6.89	0.148	9.29	1.630	11.10	18.201
18	7.55	1.781	10.14	3.260	13.26	7.439
19	18.21	0.105	11.18	5.165	14.59	7.713
20	25.30	0.122	13.21	0.552	17.75	1.658
21	–	–	14.59	1.681	21.00	3.664
22	–	–	17.80	0.202	23.63	1.168
23	–	–	21.03	0.390	–	–
24	–	–	23.68	0.109	–	–
25	–	–	27.96	0.064	–	–

termined by calculating the RMS residual for three values of f, namely 0.990, 1.000, and 1.010. Then a quadratic was fitted to these points and the next f, denoted f^*, was calculated as that value which minimized the quadratic. Repeating this procedure for $f^* - 0.002$, f^*, and $f^* + 0.002$ gave the final value of f, which minimized almost exactly the RMS residual. In the results reported below, this procedure was used. A search over a range of values of f close to 1.000 gave essentially the same results, but was somewhat slower.

EXPERIMENTAL

The analyses were carried out using Perkin-Elmer 8400 Series gas chromatographs, according to a procedure described previously [2]. These chromatographs are temperature-programmed single channel units using Ni^{63} electron capture detectors. The conditions were as follows: column packing, Chromosorb W HP; column load, 4% OV-225; mesh size, 180–250 μm; column size, 1.8 m × 4 mm I.D.; carrier gas, argon–methane (95:5, v/v); carrier gas flow, 30 ml/min; oven temperature, 225°C; auxiliary temperature, 375°C.

Table I contains the retention times and peak areas for the three standards used, namely Arochlor 1242, Arochlor 1254, and Arochlor 1260. The samples were made up from these standards. Note that in all cases the solvent peak, which occurs at less that 1 min, has been removed.

While Arochlor 1242 has large peaks at lower retention times, the other two standards show peaks over a wide range of retention times.

Samples used to test the method were prepared by accurately weighing specified amounts

TABLE II

RETENTION TIMES AND PEAK AREAS FOR SAMPLES 1, 2, AND 3

Peak number	Sample 1		Sample 2		Sample 3	
	Time	Area	Time	Area	Time	Area
1	1.42	0.530	1.42	0.297	1.39	0.158
2	1.70	0.411	1.70	0.278	1.69	0.062
3	1.89	0.109	1.89	0.078	2.09	0.125
4	2.10	1.185	2.10	0.796	2.45	0.344
5	2.45	3.333	2.31	0.231	2.93	0.243
6	2.94	2.203	2.47	0.620	3.29	0.063
7	3.28	0.680	2.94	0.255	3.55	1.551
8	3.56	7.260	3.07	0.272	3.74	2.115
9	3.74	7.306	3.28	0.151	4.31	0.319
10	4.33	2.492	3.56	1.575	4.54	0.204
11	4.53	2.076	3.74	1.625	4.87	4.201
12	4.84	6.743	4.28	0.256	5.34	6.162
13	5.21	12.196	4.88	3.843	5.93	10.075
14	5.87	16.468	5.35	5.457	6.30	1.355
15	6.93	5.329	5.94	9.396	6.90	6.202
16	7.70	16.524	6.31	1.262	7.65	18.430
17	8.40	1.263	6.91	5.942	8.53	1.930
18	9.30	1.529	7.66	18.222	9.36	4.976
19	10.16	3.357	8.54	1.702	9.85	4.461
20	11.21	5.526	9.38	4.953	11.12	17.303
21	13.26	0.876	9.86	4.373	13.26	6.730
22	14.64	1.813	11.14	17.809	14.62	6.969
23	17.79	0.230	13.29	6.989	17.76	1.480
24	21.06	0.394	14.64	7.219	21.05	3.450
25	23.65	0.103	17.78	1.613	23.72	1.090
26	27.12	0.063	21.07	3.632	–	–

of the standards, which were supplied as 1000 ppm (w/w) solutions in isooctane by Supelco, Bellefonte, PA (USA). Table II shows the retention times and peak areas obtained by analyzing the first three of these samples.

RESULTS AND DISCUSSION

In order to demonstrate the effect of the peak width parameter, denoted a, that is used in reconstructing the chromatograms, the peak area *vs.* retention time data for Arochlor 1260 (Table I) were used. Peak width values of 0.100 min, 0.250 min, and 1.000 min were employed to generate the chromatograms (for Arochlor 1260) shown in Fig. 1. It is evident that $a = 0.100$ min produces very sharp and well separated peaks, such that the value of the chromatogram at a given time can be extremely sensitive to the retention time of the peak. In contrast, for $a = 1.000$ the peaks are much broader and tend to overlap strongly. In fact the nine peaks with retention times between 4 and 10 min coalesce into a single peak with one shoulder. When a peak width of 0.250 min is used the peaks are somewhat less sharp, but remain well separated except for the coalescence of a few peaks between 5 and 8 min. Thus a peak width of 0.250 was chosen for the cases discussed below. This is also justified by the good qualitative agreement between the original chromatogram (Fig. 2, in which the detector signal in arbitrary units is plotted for 660 values of the retention time) and the reconstructed chromatogram, for $a = 0.250$, in Fig. 1. Note that in the original chromatogram

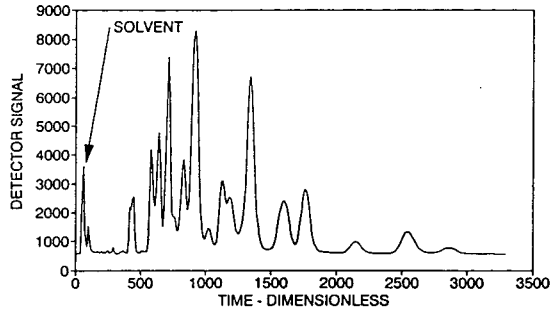

Fig. 2. Original chromatogram for Arochlor 1260, with every fifth of 3300 original points plotted.

the solvent peak at a retention time of about 1 min has been retained, while the solvent peak has been removed in the reconstructed chromatograms.

Fig. 3 shows the reconstructed chromatograms for the three PCB mixtures from which the samples were prepared. Note that they all overlap to some extent, particularly Arochlors 1254 and 1260. Nevertheless they differ sufficiently that it is reasonable to assume that a given blend can be accurately resolved into its components. This in fact is true, as the results below show.

The data in Table II were used to reconstruct discrete-time chromatogram vectors of dimension 501, *i.e.* vectors corresponding to 501 evenly-spaced points 0.050 min apart and thus covering a 25-min interval. From these vectors the composition of each sample was calculated by setting up and solving the normal equations. In Table III the calculated compositions (in mass percent) are compared with the compositions of

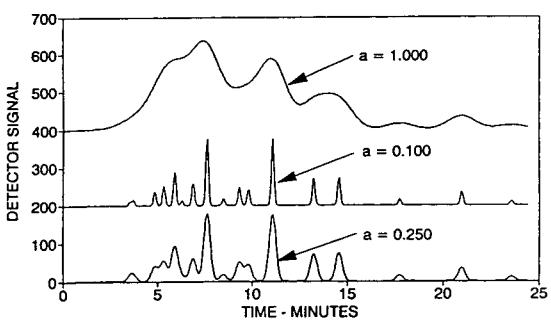

Fig. 1. Reconstructed chromatograms for Arochlor 1260 for various values of peak width parameter: $a = 0.100$, $a = 0.250$, and $a = 1.000$. Solvent peaks have been removed.

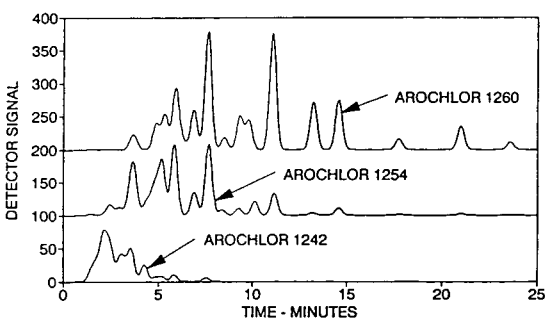

Fig. 3. Reconstructed chromatograms for Arochlors 1242, 1254, and 1260. Peak width parameter $a = 0.250$. Chromatograms shifted upward to avoid overlap.

TABLE III

CALCULATED AND KNOWN COMPOSITIONS IN MASS PERCENT FOR SAMPLES 1–9

Sample	Known Arochlor			Calculated Arochlor		
	1242	1254	1260	1242	1254	1260
1	10.00	0.00	90.00	11.14	−1.01	88.38
2	0.00	10.00	90.00	0.95	10.50	90.44
3	0.00	90.00	10.00	−0.23	91.86	11.09
4	10.00	90.00	0.00	9.48	88.11	1.57
5	1.00	99.00	0.00	0.39	97.92	−0.31
6	0.00	1.00	99.00	0.11	1.48	99.25
7	0.00	99.00	1.00	−0.20	98.62	0.49
8	0.00	1.00	99.00	0.80	1.05	97.94
9	99.00	0.00	1.00	98.70	0.59	1.43

the samples produced by accurate volumetric mixing of the standards.

In general the agreement is excellent. The maximum difference between the known and calculated mass percents is 1.89%, and the average difference is 0.26%. Note also that in only four cases was a negative mass percent calculated, even though the estimated parameters were not constrained to be non-negative. And the largest negative mass percent was −0.26%, the other three being −0.11, −0.09, and −0.02%.

The variance–covariance matrix was used to estimate the standard error of the parameter estimates, based on the RMS residuals. In all cases the standard errors lay between 0.10 and 0.40% (w/w), which is consistent with the observed differences. The parameter correlation matrix P,

$$P = \begin{bmatrix} 1.0000 & -0.5736 & 0.3891 \\ -0.5736 & 1.0000 & -0.8133 \\ 0.3891 & -0.8133 & 1.0000 \end{bmatrix}$$

shows that the standards are sufficiently different in congener content to give relatively low parameter correlation, and thus permit accurate estimates of the parameters. Note that parameters 2 and 3 are the most strongly correlated, corresponding to the occurrence of peaks (see Fig. 3) with retention times between 3 and 12 min in the chromatograms of Arochlors 1254 and 1260.

As another indication of the results, Fig. 4a–c shows the reconstructed and best-fit chromatograms for samples 1, 2 and 3, respectively. Also shown are the residuals. These are quite small, indicating again that the best-fit chromatograms fit the reconstructed experimental chromatograms well.

As a further test, new standards were prepared and run, and four samples with Arochlor ratios of 1:1:0, 1:0:1, 0:1:1 and 1:1:1 were run

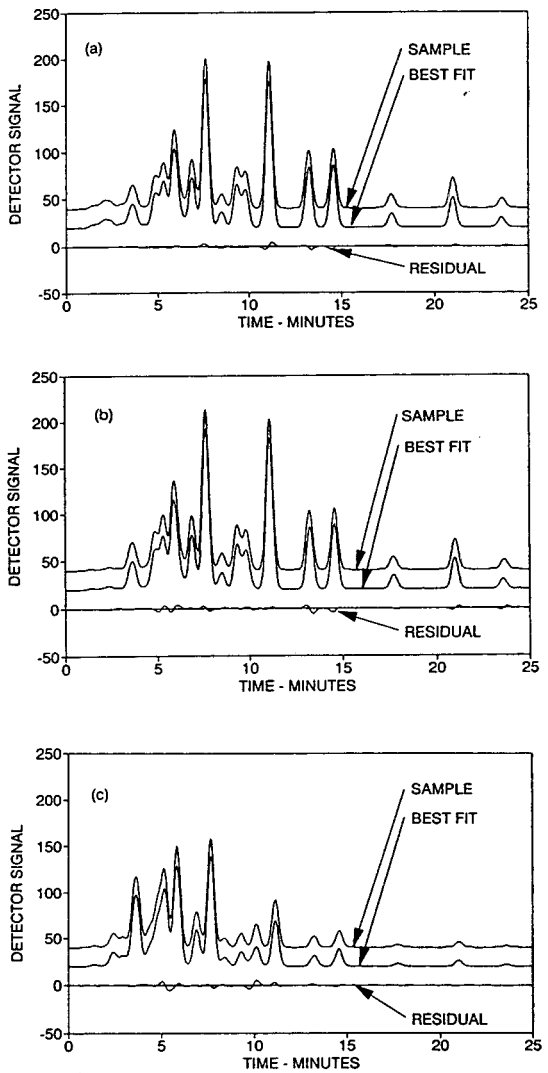

Fig. 4. Reconstructed and best-fit chromatograms for samples 1, 2 and 3, and the corresponding residuals. (a) Sample 1; (b) sample 2; (c) sample 3.

TABLE IV

CALCULATED AND KNOWN COMPOSITIONS IN MASS PERCENT FOR ADDITIONAL SAMPLES

Sample	Known Arochlor			Calculated Arochlor		
	1242	1254	1260	1242	1254	1260
1	50.00	50.00	0.00	50.21	49.78	0.00
2	50.00	0.00	50.00	50.33	0.98	48.69
3	0.00	50.00	50.00	0.52	47.80	51.69
4	33.33	33.33	33.33	34.39	32.79	32.82

using the data from the standards. The results are shown in Table IV. Negative mass percents (one value only, −0.78%) were set to zero, and the rest were scaled to bring the sum of the mass percents to 100. Again agreement was good, with a maximum absolute error of 2.2% (w/w), and an average error of 1.06%.

In summary, the least-squares procedure, as applied to 13 known blends each made up from three PCBs (Arochlors 1242, 1254, and 1260), worked well. The results were quite close to the known compositions of the samples. The use of an optimization method to determine a best value for the retention time factor also contributed to the accuracy of the method, and produced good agreement between chromatograms reconstructed from peak area *vs.* retention time data and the best-fit chromatogram as determined by the least-squares calculation.

REFERENCES

1 D.E. Schulz, G. Petrick and J.C. Duiker, *Environ. Sci. Tech.*, 23 (1989) 852–858.
2 S.I. Lerman, H. Gordon and J.P. Hendricks, *Amer. Lab.*, 42 (1981) 176–181.
3 C. Strang, S.P. Levine, B.P. Orlan, T.A. Gouda and W.A. Saner, *J. Chromatogr.*, 314 (1984) 482–487.
4 R.P. Kozloski, *J. Chromatogr.*, 318 (1985) 211–219.
5 S. Sabbah and M.L. Bouguerra, *J. Chromatogr.*, 552 (1991) 206–212.
6 M.R. Driss, S. Sabbah and M.L. Bouguerra, *J. Chromatogr.*, 552 (1991) 213–222.

Journal of Chromatography A, 654 (1993) 151–158
Elsevier Science Publishers B.V., Amsterdam

CHROM. 25 389

Affinity gel electrophoresis of nucleic acids

Nucleobase-selective separation of DNA and RNA on agarose-poly(9-vinyladenine) conjugated gel

Eiji Yashima[☆], Natsumi Suehiro, Noriyuki Miyauchi and Mitsuru Akashi*

Department of Applied Chemistry and Chemical Engineering, Faculty of Engineering, Kagoshima University, Korimoto, Kagoshima 890 (Japan)

(First received April 6th, 1993; revised manuscript received June 29th, 1993)

ABSTRACT

Poly(9-vinyladenine) (PVAd) was immobilized within an agarose gel matrix to produce a novel affinity gel for the base-specific separation of nucleic acids by electrophoresis. The shape (single- or double-stranded) and base content of nucleic acids were specifically recognized by the affinity gel. Only single stranded DNA, of which the sequence is not regular enough to form a stable duplex hairpin structure, was selectively adsorbed over double-stranded DNA. Among five polynucleotides having different bases such as poly(A), poly(G), poly(C), poly(U) and poly(I), poly(U) and poly(I) were base-specifically adsorbed by PVAd, probably by hydrogen bond formation. The effect of the molecular mass and size of poly(9-vinyladenine) was also examined.

INTRODUCTION

The separation and purification of nucleic acids on the basis of size, shape, base composition and base sequence are very important in gene technology and related fields. The most commonly used techniques for this purpose are standard agarose or polyacrylamide gel electrophoresis [1] and high-performance liquid chromatography (HPLC) [2,3], which mainly offer separation based on differences in size or chain length; a smaller molecule migrates through the matrices faster than a larger molecule. On the other hand, affinity gel electrophoresis (AGE) [4] and high-performance affinity chromatography (HPAC) [5] are attractive techniques for the specific base and sequence recognition of nucleic acids, and affinity ligands such as poly(uridylic acid) [poly(U)], one strand of polynucleotides, and oligonucleotides are immobilized on supports such as cellulose, agarose and silica gel for the specific separation of the complementary strand in mixtures of polynucleotides [6–8]. These affinity materials will resolve nucleic acids with high specificity, but there is a defect in the stability of nucleic acids immobilized on a support. Nucleic acids are decomposed by enzyme-catalysed hydrolysis and are not suitable as affinity ligands for electrophoresis because of their anionic character. Therefore, synthetic neutral analogues having nucleic acid bases such as vinyl polymer analogues of nucleic acids [9,10] will be promising as affinity ligands for specific base recognition by HPAC and AGE.

The concept of base recognition by the analogues is based on the idea that analogues having

* Corresponding author.
☆ Present address: Department of Applied Chemistry, Faculty of Engineering, Nagoya University, Chikusa-ku, Nagoya 464-01, Japan.

0021-9673/93/$06.00

bases will interact with nucleic acids via complementary hydrogen bonding and/or stacking interaction, which will result in retardation of the mobility of nucleic acids having complementary bases. We selected poly(9-vinyladenine) (PVAd) as one of the fully synthetic vinyl polymer analogues of nucleic acids because it possesses advantages of ease of preparation, high solubility in aqueous media and stability against chemical- and enzyme-catalysed hydrolysis over natural polynucleotides and additionally in electrophoresis PVAd does not undergo electroosmotic flow because of its neutral character. Moreover, PVAd forms a complex with poly(U) by complementary hydrogen bonding, as established by UV and NMR spectroscopy [11,12].

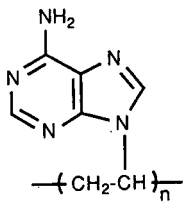

PVAd

We have demonstrated the validity of PVAd as an affinity ligand for the nucleobase-selective separation of nucleic acids in HPAC [13,14], AGE [15] and capillary affinity gel electrophoresis (CAGE) [16–20]. PVAd was chemically bonded to silica gel to separate oligonucleotides differing in length from mixtures of oligoadenylic and oligouridylic acids with base selectivity. Agarose–PVAd conjugated gel separated poly(adenylic acid) [poly(A)] and poly(U) of similar size in affinity gel electrophoresis. Further, we have developed a capillary filled with polyacrylamide–PVAd conjugated gel, which selectively separated oligothymidylic acids from mixtures of oligothymidylic and oligodeoxyadenylic acids with high resolution and high speed. The effects of urea, temperature and molecular mass and concentration of PVAd in a gel filled with polyacrylamide were examined to develop high-sensitivity and high-speed base recognition of oligonucleotides.

In this paper, a more detailed investigation and the efficiency of PVAd as an affinity ligand in AGE are described. This approach will also serve to elucidate the interaction of PVAd with nucleic acids which may not be detectable by usual spectroscopic methods.

EXPERIMENTAL

Materials

Boric acid, ethylenediaminetetraacetic acid (EDTA), bromophenol blue, xylene cyanol, ethidium bromide and methylene blue were of analytical-reagent grade from Nacalai Tesque (Kyoto, Japan). Tris(hydroxymethyl)aminomethane (Tris), agarose and ΦX174 Hae III and λ Hind III restriction enzyme fragments were obtained from Sigma (St. Louis, MO, USA), Takara (Kyoto, Japan) and Toyobo (Osaka, Japan), respectively. Poly(guanylic acid) [poly(G)] was purchased from Pharmacia–LKB (Uppsala, Sweden). Poly(A), poly(inosinic acid) [poly(I)], poly(cytidylic acid) [poly(C)], triple-stranded [poly(A)–poly(U)–poly(U)], double-stranded [poly(deoxyadenylic acid)–poly(deoxythymidylic acid)] [poly(dA)–poly(dT)], [poly(dA–dT)–poly(dA–dT)], [poly(dG–dC)–poly(dG–dC)], single-stranded M13 mp8 phage DNA and calf thymus DNA were purchased from Sigma. pUC18 plasmid DNA was a gift of Professor Higashi and Dr. Uchiumi of the Department of Biology, Kagoshima University.

PVAd was prepared by the polymerization of vinyladenine according to the literature [16,21]. The PVAd obtained was fractionated using an ultrafiltration technique (Amicon 8200 standard cell) with Amicon membranes (molecular mass cut-offs 10 000, 30 000 and 50 000) under nitrogen pressure (2.0 kg/cm^2). Three PVAd samples having molecular mass ranges of <10 000, 10 000–30 000 and 30 000–50 000 were obtained.

Sonication

As most commercially available nucleic acids have high molecular masses and a very broad range of distribution of molecular mass and are not suitable for affinity gel electrophoresis, they were sonicated in TE buffer (10 m*M* Tris–1 m*M* EDTA, pH 7.5) containing 0.5 *M* NaCl. Sonication was conducted under nitrogen or helium at 0–8°C using a Tomy Seiko sonicator (Model

UR-200P) with a high gain and a 25% pulse cycle using a programmable timer (Kagaku Kyoeisha, Osaka, Japan) to prevent heating. After sonication, the solution was filtered through a 0.45-μm Millipore filter and then dialysed in a solution of 0.1 *M* NaCl and 1 m*M* EDTA using a Spectra Por membrane (molecular mass cut off 6000–8000) that had been pretreated twice with a boiling solution of EDTA (2 m*M*) for 15 min. The dialysed solution was lyophilized and the sample obtained was stored at −20°C until used. The relative size of the sonicated nucleic acid was estimated against λ Hind III restriction enzyme fragments by agarose (0.7%) gel electrophoresis. The sizes of the sonicated nucleic acids were in the range 200–400 base pairs (bp) except for poly(A) (300–700 bp). Double-stranded poly(A)–poly(U), poly(G)–poly(C) and poly(I)–poly(C) were prepared by mixing equimolar amounts of the sonicated single-stranded polynucleotides.

Gel electrophoresis

Gel electrophoresis was performed according to a protocol [22] using a submarine-type gel apparatus (Bio-Rad DNA SUB CELL) at a constant voltage (100 V) on an ATTO AE-8350 power supply usually for 2 h using TBE buffer (89 m*M* Tris–89 m*M* boric acid–2 m*M* EDTA, pH 8). Agarose gel (0.7 or 1.4%) was prepared in the usual manner using a Mupid Gel Maker Set (Cosmo Bio, Tokyo, Japan) and agarose-PVAd conjugated gel was prepared by dissolving agarose and the desired amount of PVAd in buffer. Nucleic acids were dissolved in TE buffer (10 m*M* tris–1 m*M* EDTA) and the solution (10–20 m*M*) was mixed with glycerol containing bromophenol and xylene cyanol. Denaturation of nucleic acids was done by heating the solution of nucleic acids to 95 or 100°C, followed by cooling quickly to 0°C.

After electrophoresis, the gels were placed on a TLC sheet (20 × 20 cm) (Merck, Art. 5735) containing fluorescence agents, and the positions of the nucleic acids loaded were recorded under UV light. The gels were first stained with the intercalating dye ethidium bromide to reveal DNA and double-stranded RNA by fluorescence under UV light (312 nm; Cosmo-Bio, CSF-20B transilluminator). Because ethidium bromide was not satisfactory as a stain for a single-stranded RNA, the gels were rinsed for 15 min in 1.0 *M* acetic acid to lower the pH of the gels and were then stained with 0.2 wt.% methylene blue dissolved in an acetate buffer for 1–2 h. The excess stain was removed from the gels using a continuous flow of fresh water for about 12 h. The blue bands of single-stranded RNA in the gel were clearly observed. It has been reported that methylene blue had a high affinity for binding to RNA, but the binding of ethidium bromide to poly(A) and poly(U) was negligibly small [23]. The electrophoresis experiments were repeated several times and the reproducibility was satisfactory.

Photographs were taken with a Polaroid ACMEL CRT camera (M-0851) with Polaroid Type 665 P/N film.

Polyacrylamide gel (5%) (acrylamide: bisacrylamide = 19:1) was prepared in a similar manner to agarose gel under a nitrogen atmosphere.

Measurements

UV spectra and "melting temperature" (T_m) corresponding to a 50% transition of complexes were obtained with a Hitachi Model 200-20 spectrophotometer in a 1.0-cm path-length quartz cell equipped with a temperature controller (Tanson TC 3). Hypochromicity was obtained by continuous variation mixing curves in 0.1 *M* phosphate buffer (pH 7.0) containing 50 m*M* NaCl at 25°C by monitoring the absorbance at 253 and 290 nm for PVAd or the poly(A) and poly(I) systems. Melting curves were obtained by monitoring the absorbance change at 253 and 290 nm with slow heating at a rate below 0.5°C/min.

RESULTS AND DISCUSSION

Electrophoresis of DNA

We first examined the effects of molecular mass and concentration of PVAd on the mobility of double-stranded DNA in agarose gel (0.7%) electrophoresis. It should be noted that the elution of PVAd from the gel is negligible. The double-stranded DNA interacts weakly with

PVAd as determined by UV spectroscopic analysis. The hyperchromicity of calf thymus DNA to PVAd was about 5% based on the continuous variation mixing curve. Therefore, double-stranded DNA was suitable as a standard to calibrate the mobilities of other nucleic acids in AGE containing PVAd. Three PVAds having molecular mass ranges of <10 000, 10 000–30 000 and 30 000–50 000 and a vinyladenine monomer were used as affinity ligands. The numbers of adenine bases of these PVAd were <60, 60–180 and 180–310, respectively.

The results of the mobilities of DNAs including covalently closed circular (ccc) and open circular (oc) pUC 18 plasmid in agarose gel electrophoresis in the absence and presence of different PVAds with respect to molecular mass and concentration are illustrated in Fig. 1.

Fig. 1a demonstrates that the mobilities of linear and circular DNAs decreased as the molecular mass of PVAd increased. The retardation of DNA mobility was not much different when the molecular mass of PVAd ranged from 10 000 to 50 000. In these electrophoreses, the concentration of PVAd was held constant at 10% (w/w) relative to agarose. The concentration of PVAd also affects the mobility of DNA. An increase in the concentration of PVAd resulted in a decrease in the migration of DNA, but the retardation was almost constant at more than 10% (w/w) PVAd. Although the interaction between equimolar PVAd and double-stranded DNA was weak based on UV spectroscopy, excess of PVAd entrapped within the gel matrix will cause retardation of the mobility in electrophoresis. Consequently, we employed PVAd having a molecular mass of >30 000 for affinity gel electrophoresis, and the concentration was held constant at 10% (w/w) relative to agarose throughout.

A dramatic decrease in mobility of DNA was found when the double-stranded DNA was denatured by heating at 95°C for 3 min (Fig. 2, lane 2). We thought that this was due to hydrogen bonding or base pairing of PVAd with the denatured, probably, single-stranded DNA. In order to elucidate this, the single-stranded (+)-M13mp8 was loaded on to the same gel. As shown in lanes 3 and 4, the DNA was almost completely trapped at the upper part of the gel by PVAd. This may be applicable to selective

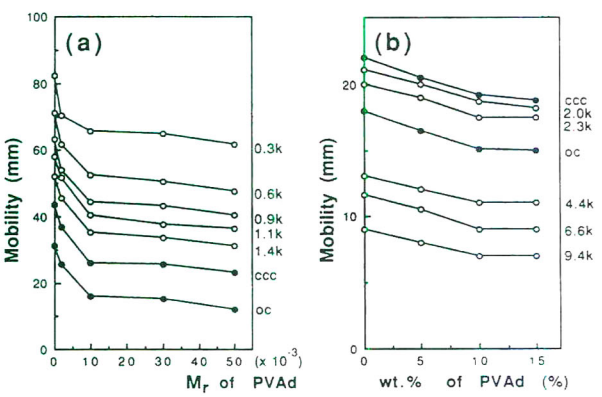

Fig. 1. (a) Effect of the molecular mass of PVAd on the mobility of ΦX174 Hae III fragments and (b) effect of the concentration of PVAd on the mobility of λ Hind III fragments. (a) The gel contained 0.7% agarose and 10% (w/w) PVAd and (b) the molecular mass of PVAd in the gel was 30 000–50 000. Gel electrophoresis was performed using TBE buffer (89 m*M* Tris–89 m*M* boric acid–2 m*M* EDTA, pH 8). The abbreviations ccc, oc and k mean covalently closed circular, open circular and 10^3 (base pairs), respectively.

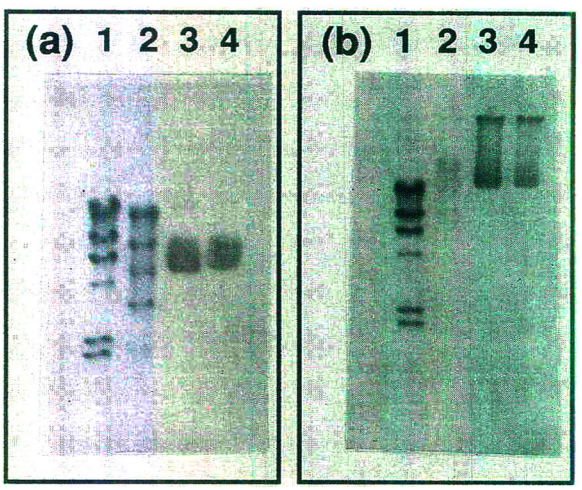

Fig. 2. Electrophoresis of DNA on (a) agarose gel (0.7%) and (b) agarose–PVAd gel. The concentration and molecular mass of PVAd in the gel were 10% (w/w) and 30 000–50 000, respectively. Lanes: 1 = Hind III restriction enzyme digests of λ DNA; 2 = sample 1 heated at 95°C for 3 min; 3 = single-stranded M13 mp8 phage DNA; 4 = sample 3 heated at 95°C for 3 min. Gel electrophoresis was performed using TBE buffer (89 m*M* Tris–89 m*M* boric acid–2 m*M* EDTA, pH 8). The gels were stained with ethidium bromide.

separation of double-stranded DNA in mixtures of single- and double-stranded DNAs [24].

The ability of PVAd for specific base recognition of DNA was examined using several DNAs with different base sequences and dT content such as poly(dA–dT)$_2$, poly(dG–dC)$_2$, calf thymus DNA (dT content *ca.* 30%) and poly(dA)–poly(dT) in agarose–PVAd conjugated gel electrophoresis (Fig. 3, lanes 1–13, and Fig. 4, lanes 1 and 2). All double-stranded DNAs were denatured by heating them at 95 or 100°C to give single-stranded DNAs. It was found that only the denatured calf thymus DNA was trapped by PVAd (lanes 7 and 9 in Fig. 3), and other DNAs migrated rapidly in both the gels. We first expected that the single-stranded poly(dA–dT) and poly(dT) may be adsorbed most strongly in the agarose–PVAd conjugated gel owing to complementary hydrogen bond formation between dT bases of poly(dA–dT) and poly(dT) and adenyl moieties of PVAd. However, the differences in the mobility of the denatured poly(dA–dT)$_2$ and poly(dA)–poly(dT) with and without PVAd were not regarded as significant. This may be due to rapid intramolecular renaturation of the resulting single-stranded poly(dA–dT) and intermolecular renaturation of the poly(dA) and poly(dT). In the former instance, when a sequence of bases is a complementary sequence in the same chain as in poly(dA–dT), the chain will fold back to form a duplex hairpin by base pairing between complementary sequences. Therefore, the poly(dA–dT) having a duplex hairpin, which was expected to retain its original half size, migrated faster than the poly(dA–dT)$_2$ without interacting with PVAd. In the latter instance, the poly(dT) will renature with the poly(dA) before it interacts with the immobilized PVAd in the gel, and then the resulting double-stranded poly(dA)–poly(dT) may migrate like the untreated substance. The interaction of poly(dT) with PVAd might be strong because the migration of oligo(dT)$_{12-18}$ in a capillary filled with polyacrylamide gel containing only 0.05% (w/w) PVAd was strongly retarded by PVAd even in the presence of an excess of urea such as 7 *M*, as reported previously [16].

The single-stranded calf thymus DNA, of which the base sequence may not be regular enough to form a stable duplex hairpin, easily interacted with PVAd by base pairing to result in electrophoretic retardation.

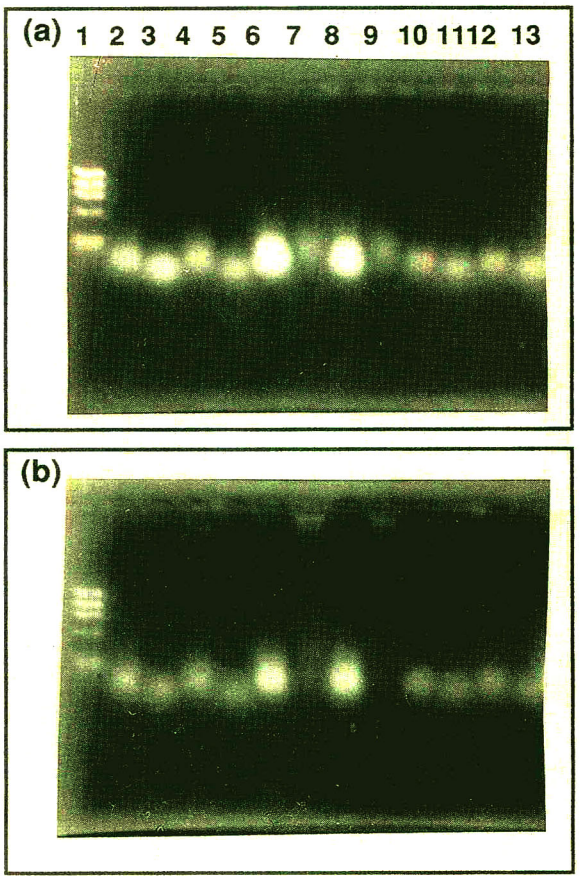

Fig. 3. Electrophoresis of DNA on (a) agarose gel and (b) agarose–PVAd gel. Conditions as in Fig. 2. Lanes: 1 = Hae III restriction enzyme digests of ΦX174 DNA; 2 = poly(dG–dC)$_2$; 3 = sample 2 heated at 100°C for 10 min; 4 = poly(dG–dC)$_2$–PVAd [1:1 (mol/mol)]; 5 = sample 4 heated at 100°C for 10 min; 6 = calf thymus DNA; 7 = sample 6 heated at 100°C for 10 min; 8 = calf thymus DNA–PVAd [1:1 (mol/mol)]; 9 = sample 8 heated at 100°C for 10 min; 10 = poly(dA–dT)$_2$; 11 = sample 10 heated at 100°C for 10 min; 12 = poly(dA–dT)$_2$–PVAd [1:1 (mol/mol)]; 13 = sample 12 heated at 100°C for 10 min. The gels were stained with ethidium bromide.

Electrophoresis of polynucleotides

Based on imino ^{1}H and ^{31}P NMR, UV and circular dichroism spectroscopy, PVAd was found to form a complex with poly(U) by com-

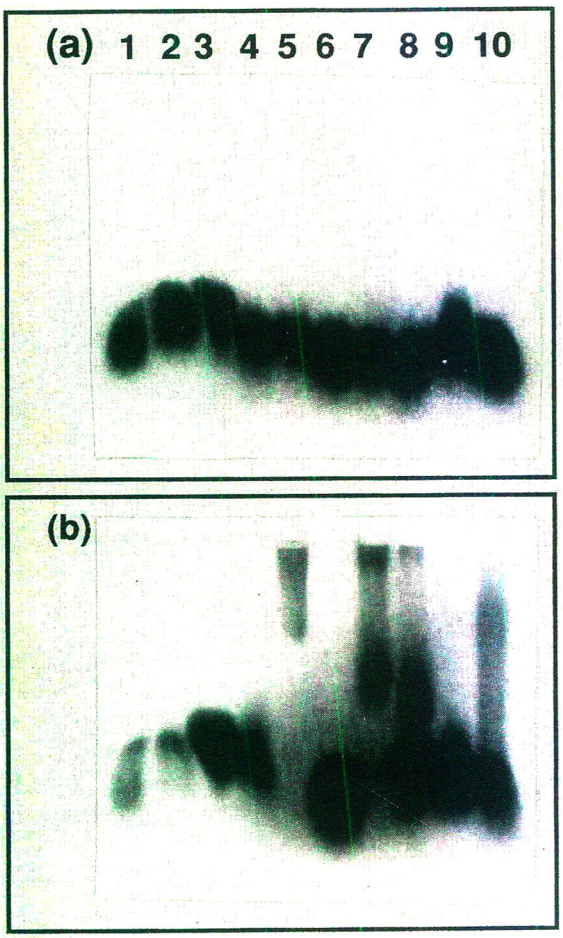

Fig. 4. Electrophoresis of DNA and polynucleotides on (a) agarose gel and (b) agarose–PVAd gel. Conditions as in Fig. 2. Lanes: 1 = poly(dA)–poly(dT); 2 = sample 2 heated at 95°C for 3 min; 3 = poly(A); 4 = poly(G); 5 = poly(I); 6 = poly(C); 7 = poly(U); 8 = poly(A)–poly(U); 9 = poly(G)–poly(C); 10 = poly(I)–poly(C). The gels were stained with methylene blue.

plementary hydrogen bonding [12]. The complex formation was also established in agarose–PVAd conjugated gel electrophoresis [15,25]. The mobility of poly(U) was considerably retarded by PVAd, but that of poly(A) was not significantly affected by PVAd. Such base recognition ability of PVAd can be utilized for the base-specific separation of oligonucleotides and oligodeoxynucleotides in HPLC [14] and in capillary gel electrophoresis [16–20]. Here, we employed five polynucleotides having different bases to investigate the more detailed base-specific recognition ability of PVAd in agarose–PVAd conjugated gel. The results serve to elucidate the characteristics of complex formation of PVAd with nucleic acids, which may not easily be detectable by the usual spectroscopic methods.

Fig. 4 shows the electrophoretic patterns of single- and double-stranded polynucleotides on agarose and agarose–PVAd conjugated gels. Among the five single-stranded polynucleotides with different base composition, poly(U) and poly(I) were base-specifically recognized by PVAd (lanes 5 and 7) and those electrophoretic mobilities were significantly diminished, but other polynucleotides exhibited almost the same electrophoretic mobility in both gels. Base pairing between poly(U) and PVAd, which is established by NMR and UV spectroscopy, will lead to the retardation of migration of poly(U). The situation seems to be very similar with poly(I), as it forms a double helix with poly(A) by hydrogen bonding between the bases. Similarly, PVAd will be expected to interact with poly(I). However, no clear spectroscopic variations in base pairing between PVAd and poly(I) were observed in UV spectroscopy. Hypochromicity and melting between them were not regarded as significant, whereas those for a mixture of poly(A) and poly(I) were clearly observed with *ca.* 25% of hypochromicity, *ca.* 60% of hyperchromicity and a T_m of 33°C. The exact nature of the interaction between PVAd and poly(I) cannot be explained. Weak hydrogen bonding interactions or hydrophobic interactions between them, which will be small enough to escape detection by UV spectroscopy, should be considered.

Lanes 8, 9 and 10 in Fig. 4 demonstrate that the duplexes of poly(A)–poly(U) and poly(I)–poly(C) are resolved into two bands even without heat treatment (b), but the bands are single in agarose gel (a). Band broadening occurred especially with poly(I)–poly(C), probably owing to strong binding to the immobilized PVAd as shown in Fig. 4b. Poly(G)–poly(C) migrated similarly in both gels. These results suggest that the immobilized PVAd interacted with the duplexes of poly(A)–poly(U) and poly(I)–poly(C), then pulled off the poly(U) and poly(I) strands

from the duplexes and complexed with them to give the PVAd–poly(U) and PVAd–poly(I) complexes, respectively. Therefore, the upper broad bands may be assigned to the PVAd–poly(U) and PVAd–poly(I) complexes and the lower sharp bands to the free poly(A) and poly(C), respectively. The base-pairing ability of PVAd to poly(U) and poly(I) seems to be superior to that of poly(A) under these conditions.

Next, in order to investigate the interaction between PVAd and multi-stranded polynucleotides, double- and triple-stranded polynucleotides were loaded and the gels were stained with ethidium bromide and methylene blue.

Fig. 5 shows the electrophoretic patterns of double- and triple-stranded polynucleotides and/or DNA in agarose gel with (b and d) and without (a and c) PVAd. The patterns observed in Fig. 5b and d were complicated. When ethidium bromide was used as a stain, only single bands appeared at around 1.4 kbp of DNA size marker (Fig. 5b, lanes 4–7). On the other hand, staining with methylene blue gave additional bands smaller in size than the former bands (Fig. 5d). Ethidium bromide can stain multi-stranded nucleic acids but is not suitable for single-stranded nucleic acids. Methylene blue can stain both single- and multi-stranded nucleic acids. Therefore, the lower bands, stained only with methylene blue should be the free poly(A) and the upper bands, stained with two dyes, will be the PVAd–poly(U) complex, to which ethidium bromide will intercalate and fluoresce. The strong interaction of PVAd with the Hoogstein-paired poly(U) of the triple-stranded poly(A)–2poly(U) was established by UV and ^{31}P NMR spectroscopy [12]. However, a significant interaction between PVAd and the Watson–Crick-paired poly(U) could not be detected by these methods. Therefore, a weak interaction between PVAd and the Watson–Crick-paired poly(U) of the double-stranded poly(A)–poly(U) may be amplified throughout the affinity gel electrophoresis, which will cause retardation of the mobility of the poly(U).

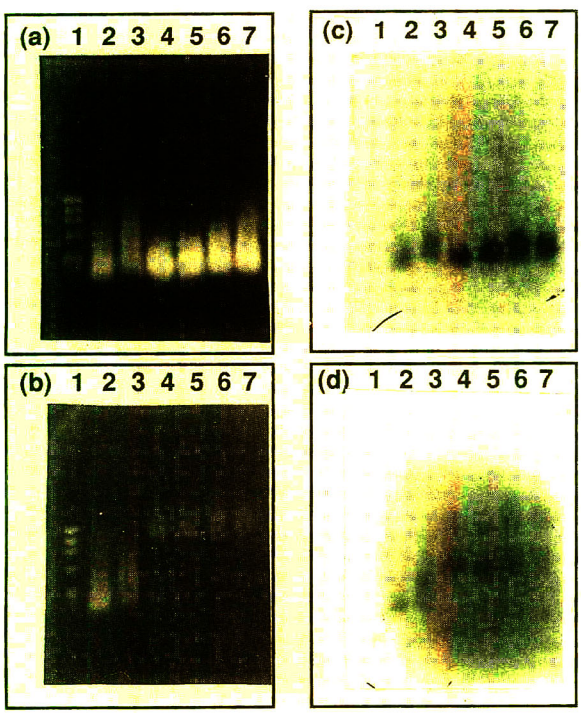

Fig. 5. Electrophoresis of DNA and polynucleotides on (a) agarose gel and (b) agarose–PVAd gel. Conditions as in Fig. 2. The gels were stained with (a and b) ethidium bromide and (c and d) methylene blue. Lanes: 1 = Hae III restriction enzyme digests of ΦX174 DNA; 2 = poly(dA)–poly(dT); 3 = sample 2 heated at 95°C for 3 min; 4 = poly(A)–poly(U); 5 = sample 4 heated at 95°C for 3 min; 6 = poly(A)–2poly(U); 7 = sample 6 heated at 95°C for 3 min.

In conclusion, PVAd was found to be effective as an affinity ligand in affinity gel electrophoresis. PVAd specifically recognizes not only poly(U) but also poly(I), probably by hydrogen bond formation, and does not interact with poly(A), poly(G) and poly(C) in agarose gel. PVAd interacts only with a single-stranded DNA, the sequence of which is not regular enough to form a stable duplex hairpin structure. As many synthetic nucleic acid analogous have been prepared [10], most of them should be utilized as affinity ligands in affinity gel electrophoresis, and our approach developed here will be valuable for the base and shape recognition of nucleic acids.

ACKNOWLEDGEMENTS

The authors thank Professor Higashi and Dr. Uchiumi of the Department of Biology, Kagoshima University, for supplying pUC 18

plasmid and for useful suggestions and encouragement.

REFERENCES

1 D. Rickwood and B.D. Hames (Editors), *Gel Electrophoresis of Nucleic Acids—a Practical Approach*, IPL Press, Oxford, 2nd ed., 1990.
2 H. Schott, in A. Henschen, K.-P. Hupe, F. Lottspeich and W. Voelter (Editors), *High Performance Liquid Chromatography in Biochemistry*, VCH, Weinheim, 1985, p. 413.
3 A.M. Krstulovic (Editor), *CRC Handbook of Chromatography, Nucleic Acids and Related Compounds*, Vol. 1, Parts A and B, CRC Press, Boca Raton, FL, 1987.
4 K. Takeo, *Adv. Electrophoresis*, 1 (1987) 229.
5 G. Fassina and I.M. Chaiken, *Adv. Chromatogr.*, 27 (1987) 247.
6 W.B. Jakoby and M. Wilchek, *Methods Enzymol.*, 34 (1974).
7 P.-O. Larsson, M. Glad, L. Hansson, M.-O. Mansson, S. Ohlson and K. Mosbach, *Adv. Chromatogr.*, 21 (1983) 41.
8 T.A. Goss, M. Bard and H.W. Jarrett, *J. Chromatogr.*, 508 (1990) 279.
9 J. Pitha, M. Akashi and M. Draminski, in E.P. Goldberg and A. Nakajima (Editors), *Biomedical Polymers: Polymeric Materials and Pharmaceuticals for Biomedical Use*, Academic Press, New York, 1980, pp. 271–297.
10 K. Takemoto, Y. Inaki and R.M. Ottembrite (Editors), *Functional Monomers and Polymers*, Marcel Dekker, New York, 1987, p. 413.
11 H. Kaye, *J. Am. Chem. Soc.*, 92 (1970) 5777.
12 E. Yashima, T. Tajima, N. Miyauchi and M. Akashi, *Biopolymers*, 32 (1992) 811.
13 M. Akashi, M. Yamaguchi, H. Miyata, M. Hayashi, E. Yashima and N. Miyauchi, *Chem. Lett.*, (1988) 1093.
14 E. Yashima, T. Shiiba, T. Sawa, N. Miyauchi and M. Akashi, *J. Chromatogr.*, 603 (1992) 111.
15 E. Yashima, N. Suehiro, M. Akashi and N. Miyauchi, *Chem. Lett.*, (1990) 1113.
16 Y. Baba, M. Tsuhako, T. Sawa, M. Akashi and E. Yashima, *Anal. Chem.*, 64 (1992) 1920.
17 M. Akashi, T. Sawa, Y. Baba and M. Tsuhako, *J. High. Resolut. Chromatogr.*, 15 (1992) 625.
18 T. Sawa, M. Akashi, Y. Baba and M. Tsuhako, *Nucleic Acids Symp. Ser.*, 27 (1992) 51.
19 T. Sawa, E. Yashima, M. Akashi, Y. Baba and M. Tsuhako, *J. High. Resolut. Chromatogr.*, submitted for publication.
20 Y. Baba, M. Tsuhako, T. Sawa and M. Akashi, *J. Chromatogr.*, 632 (1993) 137.
21 M. Akashi, H. Iwasaki, N. Miyauchi, T. Sato, J. Sunamoto and K. Takemoto, *J. Bioact. Compatible Polym.*, 4 (1989) 124.
22 J.W. Zyskind and S.I. Bernstein, *Recombinant DNA Laboratory Manual*, Academic Press, San Diego, 1989.
23 A.C. Peacock and C.W. Dingman, *Biochemistry*, 6 (1967) 1818.
24 E. Yashima, N. Suehiro, N. Miyauchi and M. Akashi, *J. Chromatogr. A*, 654 (1993) 159.
25 J. Pitha, *Anal. Biochem.*, 65 (1975) 422.

Journal of Chromatography A, 654 (1993) 159–166
Elsevier Science Publishers B.V., Amsterdam

CHROM. 25 390

Affinity gel electrophoresis of nucleic acids

Specific base- and shape-selective separation of DNA and RNA on polyacrylamide–nucleobase conjugated gel

Eiji Yashima[☆], Natsumi Suehiro, Noriyuki Miyauchi and Mitsuru Akashi*

Department of Applied Chemistry and Chemical Engineering, Faculty of Engineering, Kagoshima University, Korimoto, Kagoshima 890 (Japan)

(First received April 6th, 1993; revised manuscript received June 29th, 1993)

ABSTRACT

Two types of affinity gels consisting of cross-linked polyacrylamide and affinity ligands possessing nucleic acid bases were prepared. One type of gel was polyacrylamide–poly(vinylnucleobase) conjugated gel, where the poly(vinylnucleobase) such as poly(9-vinyladenine) (PVAd) bearing a nucleobase in the side-chain was entrapped in the gel matrix. The other type of gel, in which a nucleobase such as adenine is chemically bonded to polyacrylamide gel, was prepared by copolymerization of acrylamide, cross-linker and 9-vinyladenine. These affinity gels, especially the former, demonstrated characteristic nucleobase- and shape-selective separation of nucleic acids. The gels showed high affinity for single-stranded DNA and both single- and double-stranded polynucleotides and could separate a double-stranded DNA in mixtures of double-stranded DNA and polynucleotides. The electrophoretic mobilities of poly(uridylic acid) and poly(inosinic acid) were selectively retarded even in the presence of 7 *M* urea. The electrophoretic behaviours of nucleic acids on the polyacrylamide–PVAd conjugated gels were compared with those on the agarose–PVAd conjugated gel. The effects of urea, temperature and concentration of PVAd were also examined. The polyacrylamide–PVAd conjugated gel served to elucidate interactions between PVAd and nucleic acids that could not be detected by usual spectroscopic methods.

INTRODUCTION

Gel electrophoresis, a most commonly used technique for the separation and purification of nucleic acids, has been developed into an essential tool in gene technology and related fields and separates nucleic acids mainly on the basis of size [1]. On the other hand, affinity gel electrophoresis (AGE) [2] may separate nucleic acids with specific base or sequence recognition. However, specific base recognition of nucleic acids has not been realized in gel electrophoresis. Several intercalator dyes [3,4] and phenylboronate [5] have been introduced in a polyacrylamide gel matrix for specific base-sequence or base-content separation and isolation of RNA in electrophoresis, respectively.

One strand of natural or synthetic polynucleotide can recognize the complementary strand in mixtures of polynucleotides but will not be suitable for an affinity ligand in electrophoresis because of electroosmotic flow due to its anionic character. Fully synthetic neutral vinylpolymer analogues of nucleic acids having nucleic acid

* Corresponding author.
☆ Present address: Department of Applied Chemistry, Faculty of Engineering, Nagoya University, Chikusa-ku, Nagoya 464-01, Japan.

0021-9673/93/$06.00

bases in the side-chain should be promising affinity ligands for base-specific separation of nucleic acids in electrophoresis [6–13] and chromatography [14–16]. Poly(9-vinyladenine) (PVAd), a novel water-soluble neutral vinyl polymer analogue [17,18], has been demonstrated to be an excellent affinity ligand for the base-specific separation of oligonucleotides in high-performance liquid chromatography (HPLC) [14,15] and capillary gel electrophoresis [9–13] using PVAd-immobilized silica gel and a capillary filled with cross-linked polyacrylamide gel conjugated with PVAd, respectively. PVAd is also valuable in conventional affinity gel electrophoresis for the base- and shape (single- or double-stranded)-selective separation of DNA and RNA [6–8]. Only single-stranded DNA was selectively adsorbed over double-stranded DNA, and poly(uridylic acid) [poly(U)] and poly(inosinic acid) [poly(I)] were base-specifically recognized by PVAd entrapped in agarose gel among five polynucleotides having different bases [8].

In this study, we prepared two types of affinity gels consisting of polyacrylamide and affinity ligands having nucleic acid bases as illustrated in Fig. 1. One was a polyacrylamide–poly(vinylnucleobase) conjugated gel (type I), in which the vinyl polymer analogues having nucleobases were entrapped within the gel matrix. PVAd, poly[N-(2-uracylethyl)acrylamide] and poly(vinylhypoxanthine) were used as such a macroligand. In the second affinity gel (type II), nucleobases as affinity ligands were chemically bonded to the polyacrylamide gel matrix by the

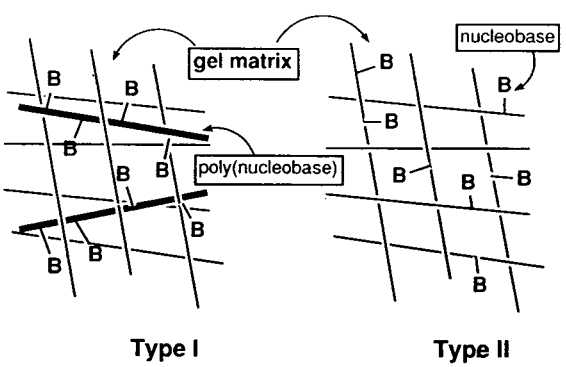

Fig. 1. Schematic representation of affinity gels.

copolymerization of acrylamide, a cross-linker and vinylnucleobases such as vinyladenine and N-(9-adenylethyl)acrylamide. These affinity gels were expected to exhibit different base-recognition abilities for nucleic acids depending on the kinds of immobilized bases, and the electrophoretic behaviours of nucleic acids on the gels were compared with those on the agarose–PVAd conjugated gel [8]. The effects of urea, temperature and concentration of PVAd on the electrophoretic mobility of nucleic acids in affinity gel electrophoresis were also examined. Affinity gel electrophoresis using the polymeric analogues serves to elucidate the interaction of the analogues and nucleic acids, which is too weak to detect by common spectroscopic methods.

EXPERIMENTAL

Materials

Boric acid, ethylenediaminetetraacetate (EDTA), bromophenol blue, xylene cyanol, ethidium bromide, methylene blue, ammonium peroxodisulphate, potassium peroxodisulphate and urea were of analytical-reagent grade from Nacalai Tesque (Kyoto, Japan). Acrylamide, N,N′-methylenebis(acrylamide) (Bis), and N,N,N′,N′-tetramethylethylenediamine (TEMED) were of electrophoretic grade from Nacalai Tesque. Tris(hydroxymethyl)aminomethane (Tris) and ΦX174 Hae III restriction enzyme fragments were obtained from Sigma (St. Louis, MO, USA) and Toyobo (Osaka, Japan), respectively. Poly(adenylic acid) [poly(A)] and poly(U) were obtained from Yamasa (Chiba, Japan) and Sigma. Poly(I), poly(cytidylic acid) [poly(C)], double-stranded poly(deoxyadenylic acid)–poly(deoxythymidylic acid)] [poly(dA)–poly(dT)], calf thymus DNA, and RNA (Type III from bakers' yeast) were purchased from Sigma, and poly(guanylic acid) [poly(G)] from Pharmacia–LKB (Uppsala, Sweden).

The preparation and polymerization of 9-vinyladenine have been described previously [9,19]. N-(9-Adenylethyl)acrylamide, N-(2-uracylethyl)-acrylamide and vinylhypoxanthine were prepared according to reported methods [20–23]. The polymerization was carried out in water or dimethylformamide with ammonium peroxodi-

sulphate or potassium peroxodisulphate as a radical initiator. Poly(9-vinyladenine) (PVAd) was fractionated using an ultrafiltration technique [24] and PVAd with molecular mass >30 000 was used as an affinity ligand in electrophoresis throughout [8].

Sonication and gel electrophoresis

Sonication and gel electrophoresis were performed in a similar manner to that reported previously [8,24]. RNA from bakers' yeast was small enough and used without sonication. The relative size of the sonicated nucleic acids was estimated against ΦX174 Hae III restriction enzyme fragments by polyacrylamide (5%) gel electrophoresis. The sizes of the sonicated nucleic acids were in the range 60–200 base pairs (bp) except for poly(A) (80–450 bp) and poly(G) (40–300 bp). Double-stranded poly(A)–poly(U), poly(G)–poly(C) and poly(I)–poly(C) were prepared by mixing equimolar amounts of the sonicated single-stranded polynucleotides.

Gel electrophoresis was performed according to the method reported previously [8] using a submarine-type gel apparatus (Bio-Rad DNA SUB CELL) at a constant voltage (100 V) on an ATTO AE-8350 power supply usually for 2 h in TBE buffer (89 m*M* Tris–89 m*M* boric acid–2 m*M* EDTA, pH 8). Polyacrylamide gel (5.0%; acrylamide:Bis = 19:1) was prepared using a Mupid Gel Maker Set (Cosmo-Bio, Tokyo, Japan) under a nitrogen atmosphere and polyacrylamide–PVAd conjugated gel was prepared by copolymerization of acrylamide and Bis (19:1) in the presence of the desired amount of PVAd (0.05–15%, w/w). N-(9-Adenylethyl)-acrylamide and vinyladenine were covalently immobilized to the gel matrix by copolymerization with acrylamide and Bis under a nitrogen atmosphere. Ammonium peroxodisulphate was used as a radical initiator. Unreacted monomers were removed by immersing the gels in TBE buffer for more than 1 h.

After electrophoresis, the gels were first stained with the intercalating dye ethidium bromide to reveal DNA and double-stranded polynucleotides by fluorescence under UV light (312 nm; Cosmo-Bio, CSF-20B transilluminator). As ethidium bromide was not suitable for staining a single-stranded RNA, the gel was then stained with 0.2 wt.% methylene blue. The electrophoretic experiments were repeated several times and the reproducibility was satisfactory.

Photographs were taken with a Polaroid ACMEL CRT camera (M-0851) with Polaroid Type 665 P/N film.

Measurements

UV spectra and "melting temperature" (T_m) corresponding to a 50% transition of complexes were obtained with a Hitachi Model 200-20 spectrophotometer in a 1.0-cm path-length quartz cell equipped with a temperature controller (Tanson TC 3). Hypochromicity and hyperchromicity were obtained by continuous variation mixing curves in 0.1 *M* phosphate buffer (pH 7.0) containing 50 m*M* NaCl at 25°C. Melting curves were obtained by monitoring the absorbance change with slow heating at a rate below 0.5°C/min.

RESULTS AND DISCUSSION

Preparation of affinity gel with nucleobase

Some water-soluble synthetic vinyl polymer analogues of nucleic acids can interact with nucleic acids through specific interactions, *i.e.*, complementary hydrogen bonding (base pairing) and hydrophobic interaction or stacking depending on the degree of the polymerization [17–19,24]. Such specific interactions can be applicable to affinity chromatography and affinity electrophoresis in which the analogues serve as an effective affinity ligand for base-specific recognition of nucleic acids having complementary bases.

We prepared two types of affinity gels consisting of polyacrylamide and affinity ligands having nucleic acid bases as illustrated in Fig. 1. One was a polyacrylamide–poly(vinylnucleobase) conjugated gel, in which the vinyl polymer analogues having nucleobases in the side-chain were entrapped within the gel matrix (type I) by polymerization of acrylamide and Bis in the presence of poly(vinylnucleobase). PVAd, poly[N-(2-uracylethyl)acrylamide] and poly(vinylhypoxanthine) were chosen and prepared for use as affinity macroligands because they

possess advantages of ease of preparation and stability against enzyme-catalysed hydrolysis over natural polynucleotides and additionally in electrophoresis they will not undergo electro-osmotic flow because of their neutral character. PVAd was found to show almost no electrophoretic mobility in slab gel electrophoresis [6,7]. Among the analogues, PVAd was fairly soluble in water, but the others were less soluble.

In the second type of affinity gel, nucleobases were chemically bonded to the polyacrylamide gel matrix by the copolymerization of acrylamide, Bis and vinylnucleobases such as vinyladenine and N-(9-adenylethyl)acrylamide (type II). This is a very convenient method of immobilizing nucleobases within the gel matrix by covalent bonding. Another type of affinity gel would be possible using a low molecular mass nucleobase monomer as a mobile carrier. However, the mobile ligand will interact very weakly with nucleic acids and is not suitable as an affinity ligand for the specific separation of nucleic acids. Therefore, the two methods described above were employed for the immobilization of affinity ligands.

We first evaluated the specific base- and shape-recognition ability of the polyacrylamide–PVAd conjugated gel in electrophoresis and the electrophoretic migration behaviour of nucleic acids on the gel was compared with that on agarose–PVAd conjugated gel [8]. Nucleic acids displayed different electrophoretic migrations on the polyacrylamide–PVAd conjugated gel. The effects of the concentrations of PVAd and urea and temperature were also examined.

Electrophoresis of DNA and RNA on polyacrylamide–PVAd conjugated gel

Fig. 2 demonstrates the effect of the polyacrylamide gel matrix on the electrophoretic migration of typical single- and double-stranded DNA and polynucleotides in (b) the presence and (a) the absence of PVAd. The retardation of the mobility of double-stranded DNA was not much affected by PVAd (lane 1). A dramatic decrease in mobility of DNA was observed when the double-stranded DNA was denatured by heating at 95°C for 3 min (lane 2), as seen with

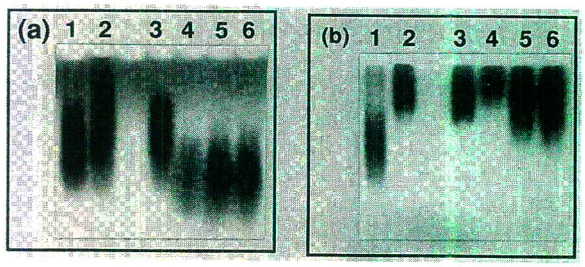

Fig. 2. Electrophoresis of nucleic acids on (a) polyacrylamide gel (5.0%; acrylamide:Bis = 19:1) and (b) polyacrylamide–PVAd (1%, w/w) gel. Gel electrophoresis was performed using TBE buffer (89 m*M* Tris–89 m*M* boric acid–2 m*M* EDTA, pH 8). The gels were stained with methylene blue. Lanes: 1 = calf thymus DNA; 2 = sample 1 heated at 95°C for 3 min; 3 = poly(A); 4 = poly(U); 5 = poly(A)–poly(U); 6 = sample 5 heated at 95°C for 3 min.

the agarose–PVAd conjugated gel [7,8]. This might be due to base pairing of PVAd with the denatured single-stranded DNA, since the electrophoretic migration of single-stranded (+)-M13mp8 DNA was almost completely retarded by PVAd immobilized in agarose gel [8].

The most different electrophoretic behaviour was found with polynucleotides including poly(A), poly(U) and the double-stranded poly(A)–poly(U), all of which were electrophoretically retarded in spite of the kind of base and shape (single- or double-stranded) (lanes 3–6). Complementary hydrogen bonding between poly(U) and PVAd, established by spectroscopic methods [24,25], reasonably leads to retardation of the migration of poly(U). However, no clear spectroscopic variations in interaction between PVAd and poly(A) were observed from UV and ^{31}P NMR spectroscopy, indicating that the interaction was so weak that the usual spectroscopic methods could not detect it. Hypochromicity and melting between them were not regarded as significant. The same observation was reported by Pitha [6], who claimed that very weak co-stacking between them caused retardation of the mobility of poly(A) in the presence of PVAd in polyacrylamide gel, although the mobility of poly(A) was not affected even in the presence of 10% (w/w) PVAd in agarose gel electrophoresis [7,8]. These results suggest that the mobility retardation of poly(A) in the polyacrylamide–PVAd conjugated gel may be related to the size

of gel porosity of polyacrylamide other than hydrophobic or stacking interaction between PVAd and poly(A). The relatively small pores of the polyacrylamide (5%) compared with those of agarose (0.7%), in which PVAd was entrapped, will make it possible to associate with nucleic acids effectively.

Interestingly, the migration of the double-stranded poly(A)–poly(U) was also strongly retarded without heat treatment in the polyacrylamide–PVAd system (lane 5 in Fig. 2). In the agarose–PVAd conjugated gel, the duplex was separated into two bands; poly(U) migrated slowly and poly(A) migrated rapidly [7,8]. Therefore, in the polyacrylamide–PVAd system, the following complex interaction may be occurring: the duplex first interacts with the immobilized PVAd, and then the PVAd pulls off the poly(U) to complex with it. The resulting single-stranded poly(A) also interacted with PVAd as seen in lane 3. Consequently, both strands were trapped in the gel.

The results clearly indicate that the polyacrylamide–PVAd conjugated gel electrophoresis will be applicable to the separation of double-stranded DNA in mixtures of single- and double-stranded DNA and RNA. An example is demonstrated in Fig. 3. Only double-stranded DNA migrated, but polynucleotides were trapped in the slot.

Next, the effect of the concentration of PVAd on the mobility of single- and double-stranded polynucleotides was examined. The electropherograms are shown in Fig. 4. The detectable retardation of the migration of all polynucleotides occurred only with 0.05% (w/w) PVAd, and the mobility was greatly decreased as the concentration of PVAd increased. A similar concentration effect was also observed in capillary gel electrophoresis of oligo(dT)$_{12-18}$ using polyacrylamide–PVAd conjugated gel [9]. The migration of oligo(dT)$_{12-18}$ in a capillary filled with polyacrylamide gel containing only 0.05% (w/w) PVAd was strongly retarded even in the presence of excess of urea.

From the band broadening in Fig. 4 it was found that poly(U) binds to PVAd more strongly than poly(A).

To examine the more detailed base-specific

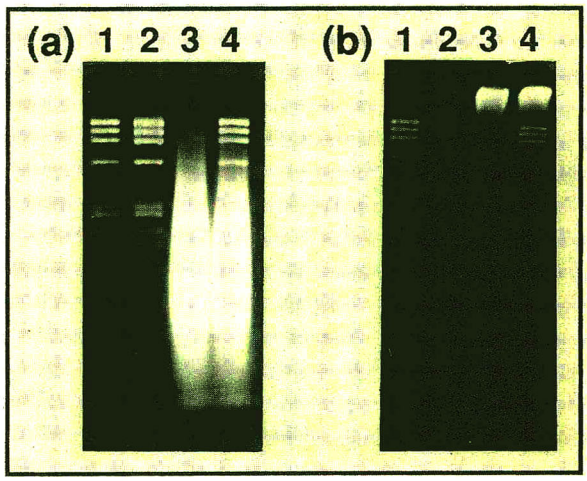

Fig. 3. Electrophoresis of DNA and polynucleotides on (a) polyacrylamide gel and (b) polyacrylamide–PVAd (10%, w/w). Conditions as in Fig. 2. The gels were stained with ethidium bromide. Lanes: 1 = Hae III restriction enzyme digests of ΦX174 DNA; 2 = sample 1 heated at 95°C for 3 min; 3 = poly(A)–poly(U); 4 = mixtures of Hae III restriction enzyme digests of ΦX174 DNA and poly(A)–poly(U).

recognition ability of PVAd in polyacrylamide gel, RNA from bakers' yeast, five polynucleotides having different bases and double-stranded poly(dT)–poly(dA) were electrophoresed. Among the five polynucleotides, only poly(I) and poly(U) were electrophoretically retarded in the agarose–PVAd gel [8]. The

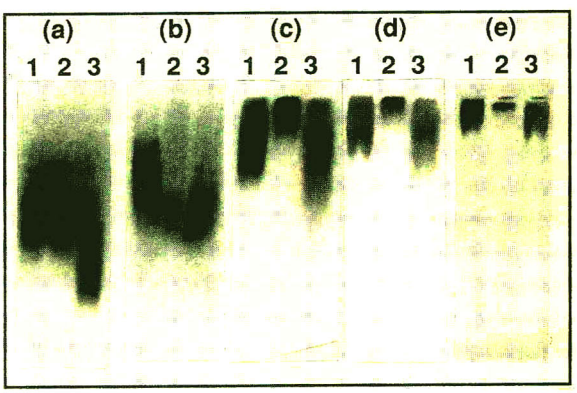

Fig. 4. Effect of the concentration of PVAd on the migration of single- and double-stranded polynucleotides. Concentration of PVAd: (a) 0, (b) 0.05, (c) 0.5, (d) 1 and (e) 5%. Other conditions as in Fig. 2. The gels were stained with methylene blue. Lanes: 1 = poly(A); 2 = poly(U); 3 = poly(A)–poly(U).

electrophoretic patterns of these DNA and RNA are shown in Fig. 5. All single-stranded polynucleotides except poly(C) were strongly adsorbed by PVAd (lanes 4–8). The retardation of the mobilities of poly(U) and poly(I) was due to base pairing, since poly(I) and poly(U) were strongly adsorbed by PVAd in agarose gel and those of poly(A) and poly(G) may be due to a weak hydrophobic interaction. Poly(C), which may not interact with PVAd either by base pairing or by hydrophobic interaction, migrated rapidly in both gels.

The double-stranded poly(G)–poly(C) and poly(I)–poly(C) migrated to afford a very broad band and two bands, respectively (lanes 10 and 11). The upper band in lane 11 was assigned to poly(I) and the band broadening of the poly(G)–poly(C) may be due to strong interaction of poly(G) with PVAd in comparison with the migration behaviour of the corresponding single-stranded poly(G) and poly(C) in the presence of PVAd (lanes 5 and 7). The poly(dA)–poly(dT) duplex was also separated into two broad bands, and the upper band should be poly(dT) which binds to PVAd by complementary hydrogen bonding. The migration of oligo(dT)$_{12-18}$ in a capillary filled with polyacrylamide gel containing only 0.05% (w/w) PVAd was strongly retarded even in the presence of excess urea, but the migration of oligo(dA)$_{12-18}$ was not affected by PVAd. The reason for different migration behaviour of single-stranded poly(dA) and poly(A) (lanes 3 and 4) in the presence of PVAd is not clear.

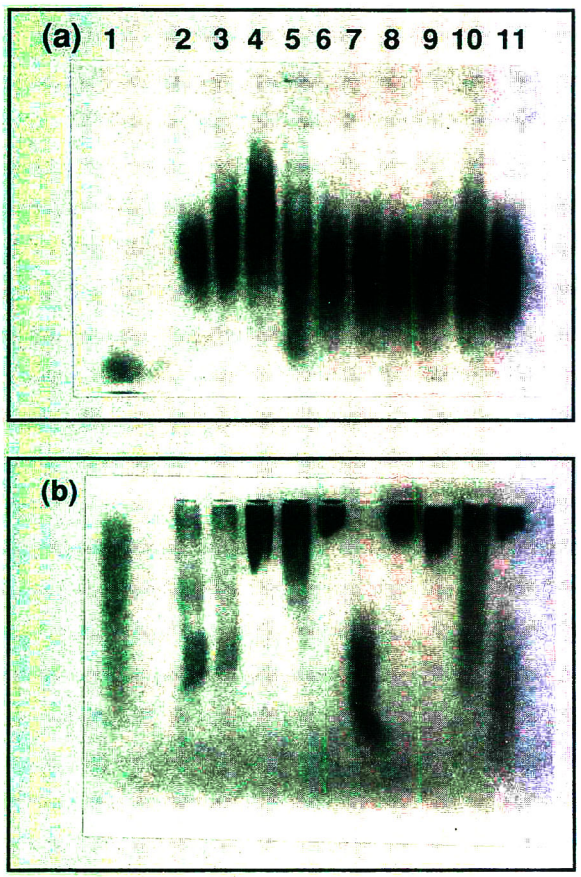

Fig. 5. Electrophoresis of nucleic acids on (a) polyacrylamide gel and (b) polyacrylamide–PVAd (5%, w/w) gel. Other conditions as in Fig. 2. The gels were stained with methylene blue. Lanes: 1 = RNA from bakers' yeast; 2 = poly(dA)–poly(dT); 3 = sample 2 heated at 95°C for 3 min; 4 = poly(A); 5 = poly(G); 6 = poly(I); 7 = poly(C); 8 = poly(U); 9 = poly(A)–poly(U); 10 = poly(G)–poly(C); 11 = poly(I)–poly(C).

We further examined the effect of urea to elucidate the interaction mechanism of PVAd with polynucleotides in polyacrylamide gel electrophoresis (Fig. 6). Urea is usually used as a denaturing agent to avoid a secondary structure formation of DNA and polynucleotides in gel electrophoresis. Surprisingly, the electrophoretic migration behaviour of most nucleic acids did not change even in the presence of 2 *M* urea but slightly changed at 7 *M* urea. RNA from bakers' yeast migrated rapidly using 7 *M* urea, probably because urea breaks the hydrogen bonds of the base-paired complex of RNA and PVAd. The migrations of poly(A), poly(G) and poly(G)–poly(C) were also affected by urea (lanes 4, 5 and 10 in Fig. 6). We first thought that the mobilities of these polynucleotides would be insensitive to changes in the concentration of urea, because the interaction of poly(A) and poly(G) with PVAd was considered to be caused by weak hydrophobic or stacking interactions. However, the present results indicate the existence of hydrogen bonding interactions between them. Again, the size of the gel porosity of polyacrylamide should be considered in explaining this unusual behaviour, because these polynucleotides migrated rapidly in agarose gel even in the presence of 10% (w/w) PVAd [8].

Poly(U) and poly(I) did not migrate even in

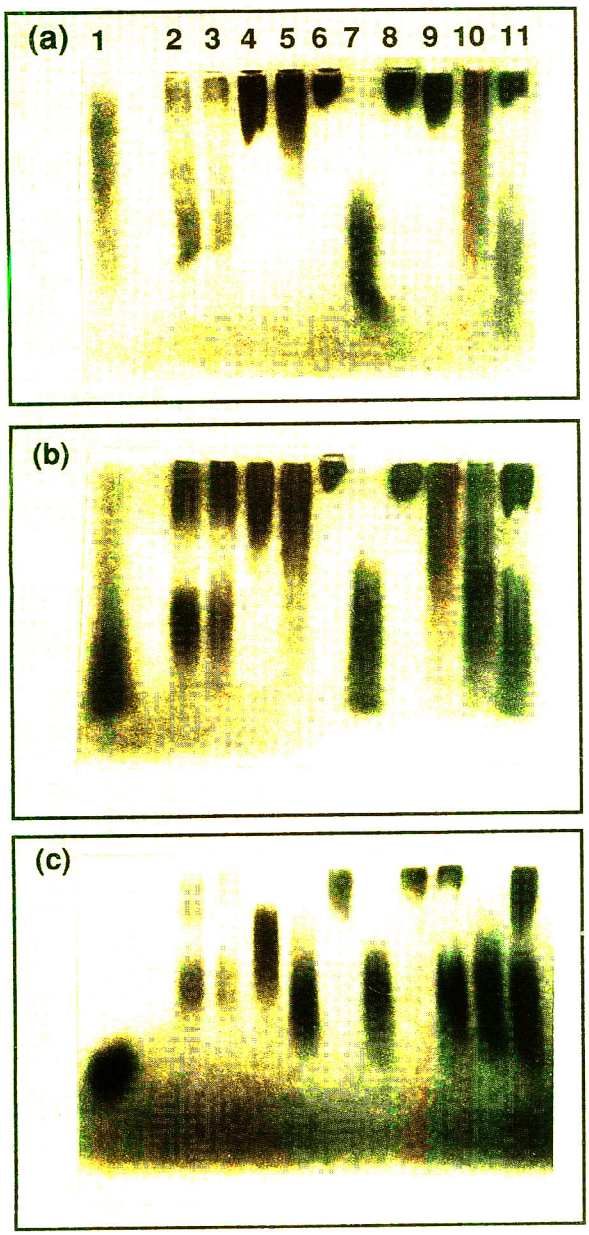

Fig. 6. Effect of the concentration of urea on the migration of nucleic acids on polyacrylamide–PVAd (5%, w/w) gel. Concentration of urea: (a) 0, (b) 2.0 and (c) 7.0 *M*. Other conditions as in Fig. 2. The gels were stained with methylene blue. Lanes: 1 = RNA from bakers' yeast; 2 = poly(dA)–poly(dT); 3 = sample 2 heated at 95°C for 3 min; 4 = poly(A); 5 = poly(G); 6 = poly(I); 7 = poly(C); 8 = poly(U); 9 = poly(A)–poly(U); 10 = poly(G)–poly(C); 11 = poly(I)–poly(C).

the presence of 7 *M* urea (lanes 6 and 8) but migrated at 10 *M* urea in polyacrylamide–PVAd (0.5%, w/w) gel electrophoresis. Base pairing of poly(U)–PVAd and poly(I)–PVAd was so strong that it could not be broken even in the presence of excess urea. To evaluate the base-pairing ability of poly(I) and poly(U) with PVAd, the polynucleotides were electrophoresed on polyacrylamide–PVAd (0.5%, w/w) gel at different temperatures (29 ± 1, 55 ± 1 and 77 ± 1°C). Poly(U) migrated at 55 ± 1°C but poly(I) did not and the band was broadened considerably even at 77 ± 1°C, probably owing to very strong binding to PVAd. The results suggest that the binding ability of poly(I) to PVAd is superior to that of poly(U).

From these results, the order of the binding ability of polynucleotides with PVAd was assumed to be poly(I) > poly(U) > poly(G) ≈ poly(A) ≫ poly(C).

Poly[N-(2-uracylethyl)acrylamide] and poly(vinylhypoxanthine) were also used as macroligands for the base-specific separation of nucleic acids. However, significant nucleobase recognition could not be observed in AGE, because the polymers were not soluble in a running buffer; therefore, the conjugated gel became turbid, which gave rise to normal electrophoretic migration of nucleic acids even in the presence of the macroligands.

Electrophoresis of polynucleotides on polyacrylamide–nucleobase immobilized gel

A type II affinity gel was prepared by copolymerization of acrylamide, Bis and a vinyl monomer bearing a nucleobase in the side-chain such as 9-vinyladenine and N-(9-adenylethyl)-acrylamide. The electrophoreses of poly(A), poly(U) and the poly(A)–poly(U) duplex using the affinity gel are shown in Fig. 7. The concentration of the vinyl monomers was held constant at 10% (w/w). Fig. 7 demonstrates that the base-specific separation of poly(U) was achieved only by using 9-vinyladenine as a comonomer; the migration of poly(U) was retarded, but that of poly(A) was not changed in the electrophoresis. In contrast, the electrophoretic migrations of polynucleotides were not influenced by introduction of N-(9-adenylethyl)acrylamide (Fig. 7c). The copolymerizability of the monomers

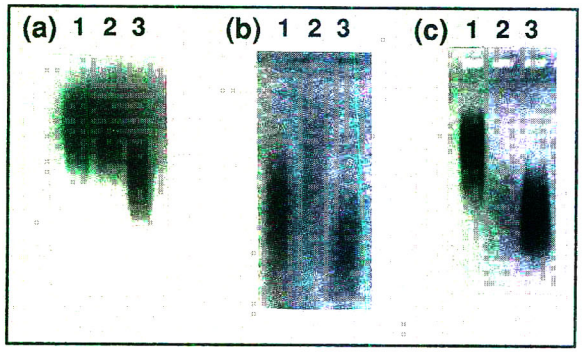

Fig. 7. Electrophoresis of polynucleotides on (a) polyacrylamide, (b) poly[acrylamide–co-10% (w/w) vinyladenine] and (c) poly[acrylamide–co-10% (w/w) adenylethylacrylamide]. Other conditions as in Fig. 2. The gels were stained with methylene blue. Lanes: 1 = poly(A); 2 = poly(U); 3 = poly(A)–poly(U).

with acrylamide in water might affect the electrophoretic migration behaviour. N-(9-Adenylethyl)acrylamide, which has an ethylene group as a spacer between the adenine and vinyl groups, will be easily copolymerized with acrylamide in a random fashion. However, 9-vinyladenine will copolymerize with acrylamide to afford a block-like copolymer, because 9-vinyladenine aggregates in water as a result of hydrophobic interactions [19]. Therefore, the 9-vinyladenine gel, in which nucleic acid bases localized in the gel matrix, can weakly interact with poly(U) to result in the retardation of electrophoretic migration. To achieve effective nucleobase recognition, at least three or more continuous 9-vinyladenine sequences should be necessary in the gel matrix [15].

In conclusion, we have found that poly(9-vinyladenine) was a useful affinity ligand for affinity polyacrylamide gel electrophoresis to achieve the shape-selective separation of DNA and RNA and the nucleobase-selective separation of polynucleotides could be possible using urea gels. The polyacrylamide–PVAd gel served to elucidate interactions between PVAd and nucleic acids that could not be detected by the usual spectroscopic methods.

REFERENCES

1 D. Rickwood and B.D. Hames (Editors), *Gel Electrophoresis of Nucleic Acids —a Practical Approach*, IPL Press, Oxford, 2nd ed., 1990.
2 K. Takeo, *Adv. Electrophoresis*, 1 (1987) 229.
3 H. Bunemann and W. Muller, *Nucleic Acids Res.*, 5 (1978) 1059.
4 S. Takenaka, K. Dohtsu, N. Nakashima and M. Takagi, *Anal. Sci.*, 3 (1987) 557.
5 G.L. Igloi and H. Kossel, *Nucleic Acids Res.*, 19 (1985) 6881.
6 J. Pitha, *Anal. Biochem.*, 65 (1975) 422.
7 E. Yashima, N. Suehiro, M. Akashi and N. Miyauchi, *Chem. Lett.*, (1990) 1113.
8 E. Yashima, N. Suehiro, N. Miyauchi and M. Akashi, *J. Chromatogr. A*, 654 (1993) 151.
9 Y. Baba, M. Tsuhako, T. Sawa, E. Yashima and M. Akashi, *Anal. Chem.*, 64 (1992) 1920.
10 M. Akashi, T. Sawa, Y. Baba and M. Tsuhako, *J. High Resolut. Chromatogr.*, 15 (1992) 625.
11 T. Sawa, M. Akashi, Y. Baba and M. Tsuhako, *Nucleic Acids Symp. Ser.*, 27 (1992) 51.
12 T. Sawa, E. Yashima, M. Akashi, Y. Baba and M. Tsuhako, *J. High. Resolut. Chromatogr.*, submitted for publication.
13 Y. Baba, M. Tsuhako, T. Sawa and M. Akashi, *J. Chromatogr.*, 632 (1993) 137.
14 M. Akashi, M. Yamaguchi, H. Miyata, M. Hayashi, E. Yashima and N. Miyauchi, *Chem. Lett.*, (1988) 1093.
15 E. Yashima, T. Shiiba, T. Sawa, N. Miyauchi and M. Akashi, *J. Chromatogr.*, 603 (1992) 111.
16 S. Nagae, Y. Suda, Y. Inaki and K. Takemoto, *J. Polym. Sci., Polym. Chem. Ed.*, 27 (1989) 2593.
17 J. Pitha, *Polymers*, 18 (1977) 425.
18 J. Pitha, M. Akashi and M. Draminski, in E.P. Goldberg and A. Nakajima (Editors), *Biomedical Polymers: Polymeric Materials and Pharmaceuticals for Biomedical Use*, Academic Press, New York, 1980, pp. 271–297.
19 M. Akashi, H. Iwasaki, N. Miyauchi, T. Sato, J. Sunamoto and K. Takemoto, *J. Bioact. Compatible Polym.*, 4 (1989) 124.
20 N.N. Leonard and R.F. Lambert, *J. Org. Chem.*, 34 (1969) 3240.
21 Y. Inaki, S. Sugita, T. Takahara and K. Takemoto, *J. Polym. Sci., Polym. Chem. Ed.*, 24 (1986) 3201.
22 K. Kondo, S. Tanioku and K. Takemoto, *Makromol. Chem. Rapid Commun.*, 1 (1980) 303.
23 K. Kondo, H. Iwasaki, N. Ueda, K. Takemoto and M. Imoto, *Makromol. Chem.*, 125 (1969) 42.
24 E. Yashima, T. Tajima, N. Miyauchi and M. Akashi, *Biopolymers*, 32 (1992) 811.
25 H. Kaye, *J. Am. Chem. Soc.*, 92 (1970) 5777.

Journal of Chromatography A, 654 (1993) 167–176
Elsevier Science Publishers B.V., Amsterdam

CHROM. 25 462

Capillary electrophoretic analysis of inorganic cations

Role of complexing agent and buffer pH

T.-I. Lin*, Y.-H. Lee and Y.-C. Chen

Department of Chemistry, National Taiwan University, Taipei 106 (Taiwan)

(First received May 4th, 1993; revised manuscript received July 28th, 1993)

ABSTRACT

Capillary electrophoresis for the determination of inorganic metal cations in the presence of various complexing agents was investigated. The complexing agents studied were acetic, glycolic, lactic, hydroxyisobutyric, oxalic, malonic, malic, tartaric, succinic and citric acid. They were all suitable as complexing agents for separating a mixture of six alkali and alkaline earth metal ions (lithium, sodium, potassium, magnesium, calcium and barium) using indirect UV detection with imidazole as a carrier buffer and background absorbance provider. The pH of the carrier buffer affected the electrophoretic separation in a complex but predictable way. The optimum pH for separating these ions in the presence of the complexing agent was around the pK_1 of the acid. When di- and triprotic acids were used, electrophoresis carried out above the second acid dissociation constant resulted in a significant decrease in the mobility of divalent ions and a decrease in number of theoretical plates, N, due to complex formation. In most of the cases reported here one could obtain, typically, a migration time span from 1 to 2 min, a minimum and a maximum resolution of 1 and 15, respectively, and N from 16 000 to 750 000 per metre. Of the ten complexing agents studied, lactic, succinic, hydroxyisobutyric and malonic acid seemed to give the best overall performance.

INTRODUCTION

Capillary electrophoresis (CE) has rapidly developed into a reliable microanalytical separation technique for a variety of applications [1,2]. Inorganic ion analysis, however, has received relatively little attention. This is due, in part, to the existence of other sensitive techniques and the lack of a direct detection method. The latter problem has been solved recently by the introduction of indirect UV absorption method [3–7], which is readily available with all commercial capillary electrophoresis systems.

Foret *et al.* [3] utilized indirect UV detection to demonstrate the separation of fourteen lanthanide cations by CE. Highly efficient separation was obtained within 5 min with the aid of hydroxyisobutyric acid (HIBA) as a complexing agent and creatinine as a UV-absorbing co-ion. Wildman *et al.* [4] and Weston and co-workers [5–7] investigated the factors that affect the separation of metal cations and optimized the detection sensitivity for metal cations using indirect photometric detection. They showed that a mixture of nineteen alkali, alkaline earth and lanthanide metal cations can be resolved at the baseline level within less than 2 min. Beck and Engelhardt [8] investigated several background electrolytes for indirect UV detection and found imidazole to be suitable for separation of metal ions, amines and amino alcohols. Gross and Yeung [9] employed indirect fluorescence detection for the CE of several metal cations. Bachmann *et al.* [10] utilized Ce(III) as a fluorescent carrier electrolyte and reported indirect fluores-

* Corresponding author.

0021-9673/93/$06.00

cence detection for the CE of ammonium and alkali and alkaline earth metal ions. Swaile and Sepaniak [11] described the separation of three divalent cations with a chelating and fluorescent agent, 8-hydroxyquinoline-5-sulphonic acid (HQS). Timerbaev *et al.* [12] used HQS for the CE of transition and alkaline earth metals as precolumn-formed chelates with direct UV detection. Aguilar *et al.* [13] presented a detection scheme for iron, copper and zinc cations in electroplating solution using cyanide complexes with direct UV detection.

In this study, we investigated the use of mono-, di- and triprotic carboxylic and hydroxycarboxylic acids as complexing agents in the separation of metal ions using the alkali and alkaline earth metal ions Li, Na, K, Mg, Ca and Ba as examples (charges are omitted for brevity). We have also studied how the pH of the carrier buffer affected the separation of these metal ions. These complexing agents can selectively modulate the mobility of metal cations by forming metal chelates with varying degrees of stability. It appears that the complexing agent and the pH of the carrier electrolyte influence the separation of these cations in a very intricate manner. They affect the electrophoretic mobility and the migration order of these ions, the separation efficiency as measured by the number of theoretical plates and the resolution.

EXPERIMENTAL

Chemicals

All metal ion solutions were prepared from chloride salts. They were prepared as stock solutions of 100 ppm, mixed and diluted to 10 ppm (metal ion concentration). Unless specified otherwise, all six ions shown in Figs. 1–6 were present at a concentration of 10 ppm each. The corresponding ion molar equivalent concentrations were Li 1.43, Na 0.44, Mg 0.41, K 0.26, Ca 0.25 and Ba 0.073 mequiv. Imidazole was used both as the background carrier electrolyte (providing strong UV absorption at 215 nm) and buffer ($pK_a = 6.95$). Ten carboxylic and hydroxycarboxylic acids were used (see Table I). They include monoprotic acetic, glycolic, lactic and hydroxyisobutyric acid, diprotic oxalic, malonic, succinic, malic and tartaric acid and triprotic citric acid. These acids and metal chloride salts and imidazole all were of analytical-reagent or reagent grade from various vendors. Doubly deionized water prepared with a Milli-Q system (Millipore, Bedford, MA, USA) or doubly deionized, distilled water was used exclusively for all solutions. The water blank was routinely checked for contamination with traces of alkali and alkali earth metal ions.

Buffers and pH adjustment

The running buffer contained 5 m*M* imidazole, which served as both the carrier electrolyte and background absorber for indirect UV detection. The pH was varied as specified in the figures, being adjusted by adding a 1 *M* stock solution of complexing agent to the desired pH in the range 3–6 depending on the experiments. The concentration of the complexing acid was varied from 0.1 to 6.4 m*M* (calculated by the volume added) as specified in the figures. For each acid studied, typically CE for each sample was carried out at 0.5 pH increments. When a fixed concentration of the complexing agent was desired, the pH of the solution was adjusted with aliquots of 1 *M* HCl (adjustment with sulphuric acid gave very different migration orders; see Results and Discussion).

Apparatus

CE experiments were carried out in a fully automated Spectra Phoresis Model 1000 instrument (Spectra Physics Analytical, San Jose, CA, USA). The system was equipped with a rapid-scanning UV–Vis detector with 5-nm wavelength resolution. In most of the cases reported here, however, the detector wavelength was fixed at 215 nm to obtain a more stable and less noisy baseline. The instrument was also equipped with autosamplers, a capillary cartridge and a solid-state Peltier temperature control unit. A personal computer (486 IBM AT-compatible PC) was used to control the instrument settings, data acquisition and analysis with the vendor-provided software. The separation capillaries (bare fused silica) from Polymicro Technologies (Phoenix, AZ, USA) were 42 cm (35 cm to the detector) × 50 μm I.D. × 375 μm O.D. UV–Vis

absorption spectra of the background electrolytes and complexing agents were measured with a Hitachi (Tokyo, Japan) U-2000 double-beam scanning spectrophotometer.

Electrophoretic procedures

Prior to first use, a new capillary was subjected to a wash cycle of 10 min each with the following steps: (a) 1 *M* NaOH, (b) 0.1 *M* NaOH and (c) deionized water at 60°C, (d) the running buffer at the running temperature and (e) the running buffer at the running voltage and temperature. Subsequent runs were carried out with the following standard cycle: (a) prefilled running buffer for 5 min, (b) sample injection, (c) separation run at the indicated voltage and temperature and (d) deionized water post-wash for 3 min. Sample injection was carried out in the electrokinetic mode at +5 kV for 2 s. The separation run was at +25 kV constant voltage at 25°C constant temperature and with a current of 2–10 μA. The capillary was also washed with 0.1 *M* NaOH and deionized water as a daily routine. All buffer solutions were freshly prepared using deionized, distilled or doubly deionized water, filtered through 0.20-μm membranes and degassed under vacuum for 10 min.

RESULTS AND DISCUSSION

Influence of complexing agents on migration time and order

As reported previously [8], the separation was most efficient if CE was carried out when the mobility of the analytes matched well that of the carrier electrolyte. Imidazole has been found to be satisfactory for this purpose. However, in the absence of a complexing agent, only five peaks were found (Fig. 1a); Na and Mg could not be resolved. Changing the pH of the buffer changed only the migration time span [the separation time was shorter at higher pH owing to the increase in the electroosmotic flow (EOF)]; it could not resolve the Na–Mg peak or alter the migration order. In general, the migration time was shorter in the absence of a complexing agent at the same pH. We also noted that the acid added to adjust the buffer pH affected the resolution and the migration order of the ions, in particular for Ba, Mg and Ca. If HCl was used to adjust the pH, Na and Mg could not be resolved. If H_2SO_4 was used instead, then all six ions could be separated in the absence of a complexing agent; the migration order was Na < Ba < Ca, as found previously [8].

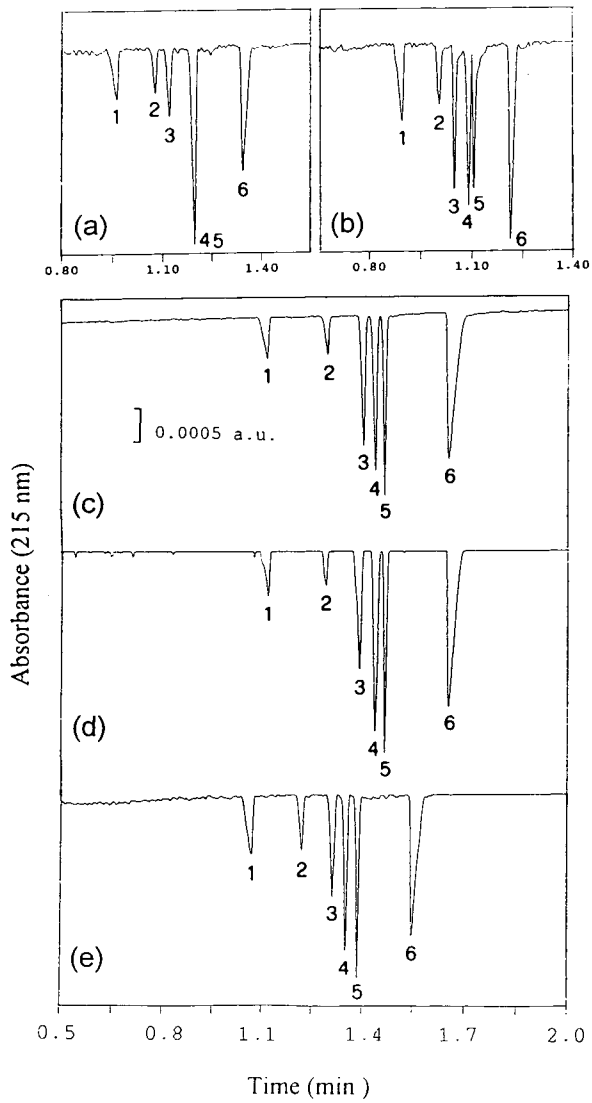

Fig. 1. Comparison of electropherograms (a) in the absence of complexing agent (pH 4.0) and (b) in the presence of 2.1 m*M* acetic acid (pH 6.0), (c) 4.55 m*M* glycolic acid (pH 4.0), (d) 5.0 m*M* lactic acid (pH 4.0) and (e) 6.4 m*M* HIBA (pH 4.0). Peaks K, Ba, Ca, Na, Mg and Li in that order in all figures. The pH was adjusted with (a) 1 *M* HCl and (b)–(e) a 1 *M* solution of the complexing acids.

Monoprotic acids. The four monoprotic complexing agents, acetic, glycolic and lactic acid and HIBA, affected the separation of the six metal ions in a similar way. The pK_a values for these four acids are given in Table I. Note that the hydroxy group lowers the pK_a of comparable carboxylic acids. As with HIBA reported previously [6–8], separation into six peaks could be readily seen in the presence of any of the other three monoprotic acids. The migration order of the six ions, K < Ba < Ca < Na < Mg < Li, was the same in these four acids. The electropherograms in the absence of complexing agent and in the presence of these four monoprotic acids are compared in Fig. 1a–e. The migration order was not altered significantly by the pH but the resolution at the baseline level was influenced by the pH. The pH range where the migration order was not affected by the pH and a good separation could be obtained was 3.5–6.0 for lactic acid, 3.5–5.0 for glycolic acid, 3.5–5.5 for HIBA and 6.0–6.5 for acetic acid. Note that in acetic acid a baseline separation of all ions was possible only at pH > 6.0. The migration time and its span were shorter at higher pH owing to the increase in EOF, as expected. All four monoprotic acids are suitable as complexing agents in the pH range indicated above. As the pK_a of the carrier electrolyte imidazole is about 6.9, the CE operating pH is restricted to about 6.0. However, as noted above, adjustment of the pH with H_2SO_4 should be avoided. In HIBA, we found that if the pH was adjusted to 4.5 with H_2SO_4, the Ca and Na peaks could not be resolved (Fig. 2a). However, lowering the pH to 4.0 (Fig. 2b) restored the migration profile as in HIBA without H_2SO_4 (Fig. 1e). Adjusting the pH down to 3.0 with H_2SO_4 changed the migration order completely; all three divalent ions (peaks 2, 3 and 5) migrated more slowly and were between Na and Li (peaks 4 and 6, Fig. 2c). All six peaks seemed to be broadened considerably. It seems that sulphate anion behaves similarly to a complexing agent and affects the migration of divalent ions even more than HIBA.

TABLE I

pK_a VALUES OF THE VARIOUS COMPLEXING AGENTS

Value for HIBA from ref. 14, all others from ref. 15.

Acid	pK_a	Acid	pK_a
Acetic	4.75	Malonic	2.83, 5.69
Glycolic	3.83	Succinic	4.16, 5.61
Lactic	3.86	Malic	3.40, 5.11
HIBA	3.97	Tartaric	2.98, 4.34
Oxalic	1.23, 4.19	Citrate	3.14, 4.77, 6.39

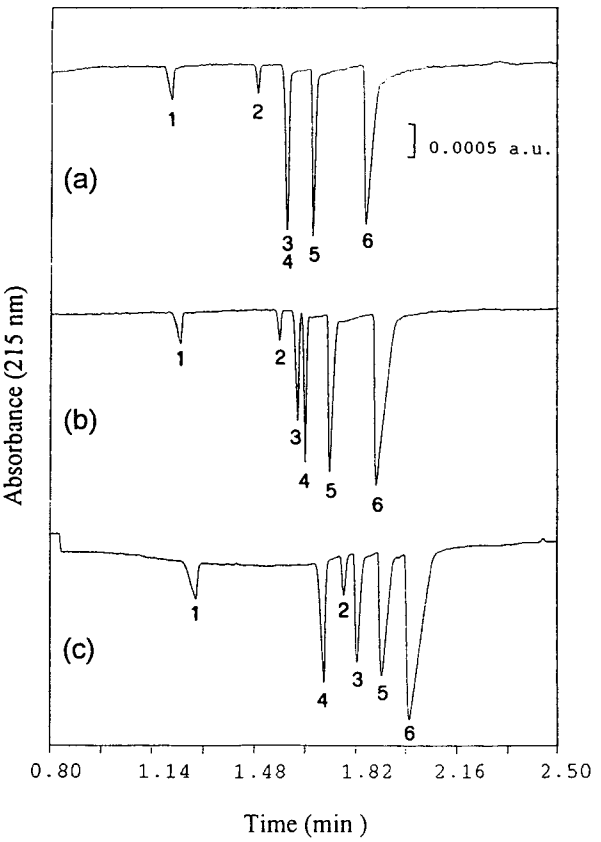

Fig. 2. Effect of pH adjusted with sulphuric acid on the electropherograms in the presence of 3 m*M* HIBA at pH (a) 4.5, (b) 4.0 and (c) 3.0. Peaks as in Fig. 1.

Diprotic acids. The effects of diprotic oxalic, malonic, succinic, malic and tartaric acid on the separation of metal ions were more complex, depending also on the pH. The acid dissociation constants, pK_1 and pK_2, of these acids are also given in Table I. A dicarboxylic acid with a longer carbon chain has higher acid dissociation constants. A hydroxyl group lowers the first and

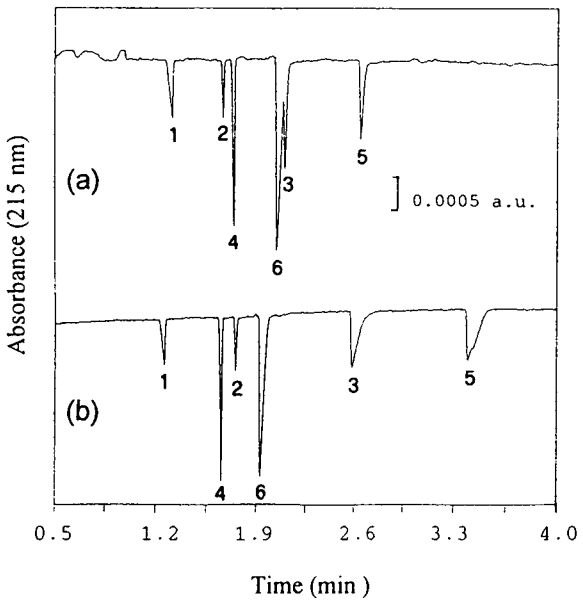

Fig. 3. Comparison of electropherograms in the presence of oxalic acid at (a) 3.4 m*M* (pH 3.0) and (b) 1.9 m*M* (pH 4.0). The pH was adjusted with 1 *M* oxalic acid. Peaks as in Fig. 1.

second acid constants by about 0.5–0.6 p*K* unit. In oxalic acid at pH 3.0 (Fig. 3a), the resolution of Li and Ca was poor. The migration order of the six ions was considerably different from that in the monoprotic acids. The pH affected the migration time and order and also the resolution substantially. At pH 4.0 (Fig. 3b), all ions were well separated. The mobilities of all three divalent ions decreased greatly, resulting in a much larger time span. The migration order also changed; Ba migrated behind Na, and Ca and Mg both moved far behind Li. Apparently, this was due to the complex formation of divalent ions with the anionic conjugated base. Using oxalic acid as the complexing agent, the pH range suitable for the CE is 4.0–6.0.

The best separation in the presence of malonic acid was obtained at pH 4.0 (Fig. 4a). All six ions were well separated at the baseline level and the migration order was the same as with the monoprotic acids. At higher pH, the degree of complexing of the divalent cations with malonic acid seemed to increase, resulted in overlap of the Ba peak (at pH 5.5, Fig. 4b) or the Ca peak (pH 5.0, data not shown) with the Na peak. In

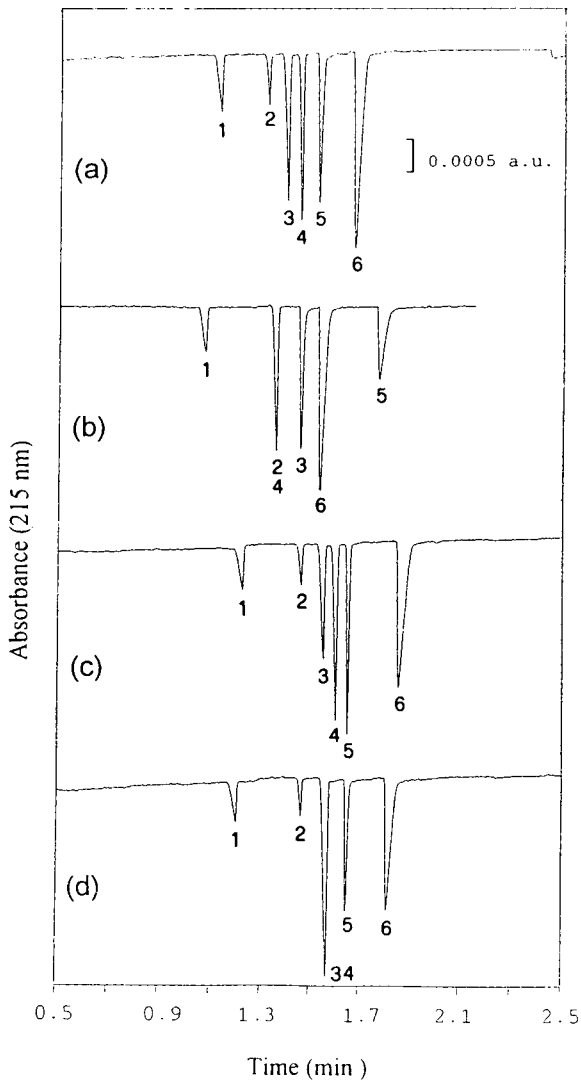

Fig. 4. Comparison of electropherograms in the presence of malonic acid at (a) 4.0 m*M* (pH 4.0) and (b) 2.2 m*M* (pH 5.5) and in the presence of succinic acid at (c) 3.0 m*M* (pH 4.5) and (d) 2.1 m*M* (pH 5.0). The pH was adjusted with a 1 *M* solution of the complexing acid. Peaks as in Fig. 1.

succinic acid, the effect of pH on the separation of the ions was similar to that in malonic acid. The best separation was obtained at pH 4.5 with the same migration order as in malonic acid (Fig. 4c). The pH affected the migration profile in a similar way. As the pH increased, Ca migrated more slowly and overlapped the Na peak at pH 5.0 (Fig. 4d) but moved apart again at pH 5.5 (thus the Ca peak moved behind the Na peak;

data not shown). Comparing the electrophoretic profiles in these three acids, the separation of ions in malonic and succinic acid was more equally spaced and in a narrower time span than in oxalic acid. As the divalent cations formed a more stable ring–chelate complex with oxalate than with malonate or succinate, the complexing effect in oxalic acid seemed to be more pronounced. Also the effect of pH, which affected the degree of ionization of the complexing acid (and thus the stability of the metal chelate), on the separation of the ions seemed to be more sensitive with oxalate.

In malic acid, a baseline-resolved separation into six peaks was possible only at pH ≈ 3.7 (Fig. 5a). At higher pH, all three divalent cations seemed to form complexes with malate anion and migrated more slowly (Fig. 5b). The migration order depended greatly on the pH, which affected mostly the mobilities of the three divalent ions. Similarly, in tartaric acid baseline separation into six peaks could be obtained only at pH 4.0 (Fig. 5c). Also similarly to malic acid, as the pH was raised to 5.0 all three divalent ions migrated more slowly, the Ba and Ca peaks merged and moved closer to the Li peak and the Mg peak appeared further away from the Li peak (Fig. 5d). The two hydroxy diprotic acids behaved differently to the above three diprotic acids. The pH effect in the two hydroxy acids seemed to be more sensitive and pronounced, resulting in a very limited pH range where all six ions could be baseline resolved.

Triprotic acid. The effect of triprotic citric acid on the separation of divalent ions was even greater than that of diprotic acids. As expected, the influence was dependent on the pH, which determined the charge carried by the metal chelate complex. The stability constants of citrate with all three alkali earth metal ions are high [14]. Hence the experiments were carried out at different citrate concentrations. A baseline separation of all six ions could be obtained at pH 4.5 (adjusted with citric acid to 2.4 m*M*). All three divalent ions trailed behind the alkali metal ions (Fig. 6a) with a large time span. Both Ca and Mg, which migrated far behind the Ba peak, showed a considerable triangular trailing shape. If the concentration of

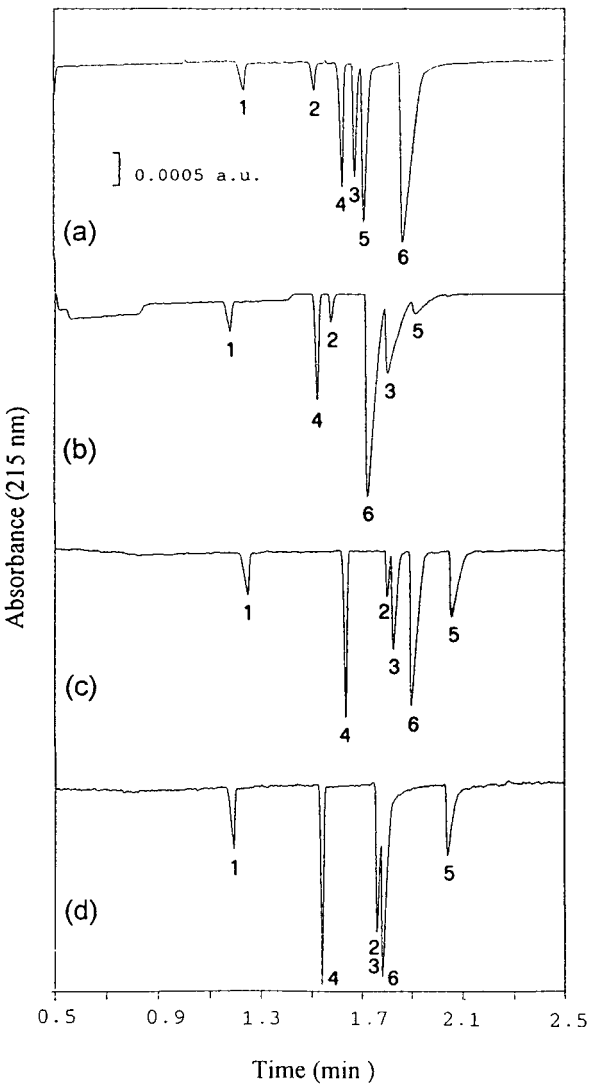

Fig. 5. Comparison of electropherograms in the presence of malic acid at (a) 3.6 m*M* (pH 3.7) and (b) 1.8 m*M* (pH 5.0) and in the presence of tartaric acid at (c) 1.9 m*M* (pH 4.0) and (d) 1.4 m*M* (pH 5.0). The pH was adjusted with a 1 *M* solution of the complexing acid. Peaks as in Fig. 1.

citric acid was kept at 1 m*M* and the pH was adjusted to 3.0–4.0 with 1 *M* HCl, the migration order was very different (Fig. 6b). At pH 3.0 hardly any complexes seemed to be formed and Ba and Ca migrated ahead of Na, which co-migrated with Mg. At pH 3.5 Ca co-migrated with Na but Mg was separated (data not shown). However, no complete separation of all six ions

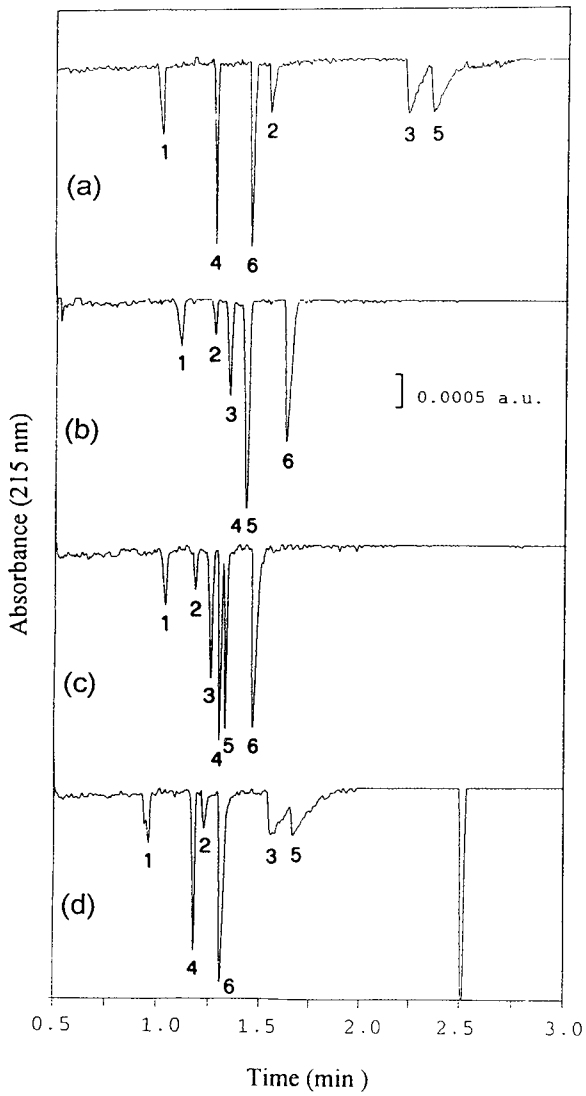

Fig. 6. Effect of citrate concentration and pH on the electropherograms. Citrate concentration: (a) 2.4; (b) 1.0; (c) and (d) 0.1 m*M*. pH: (a) 4.5; (b) 3.0; (c) 4.0; (d) 5.5. The pH was adjusted with (a) 1 *M* citric acid and (b)–(d) 1 *M* HCl. Peaks as in Fig. 1.

could be obtained under these conditions. When the citrate concentration was lowered further to 0.1 m*M*, a marginal separation of all six ions could be obtained at pH 4.0 (Fig. 6c) with six sharp peaks similar to those observed in mono- or diprotic acids. As the pH increased, Ba, Ca and Mg ions all moved more slowly. Their peaks overlapped with the Na and Li peaks, depending on the pH used. At pH 5.5 the electrophoretic profile became very similar to that at higher citrate concentration (Fig. 6d). Thus, in citric acid, the separation was affected both by the concentration of the complexing agent and the pH. Fig. 7 shows a comparison of migration time and order for the six ions in these ten acids at the pH were optimum separation can be obtained. While critic and oxalic acid have a larger separation time span, all eight other acids provide faster separation with reasonable to excellent baseline separation. Further, the first four acids provide a wider operating pH range.

Resolution and number of theoretical plates

The resolution was judged by the number of theoretical plates, N, and maximum and minimum peak separation, R_s. These parameters, analogous to those used in the liquid chromatography, are calculated by the following equation for each ion:

$$N = 5.54(t_m / W_{1/2})^2$$

$$R_s = 2[(t_m)_2 - (t_m)_1]/(W_1 + W_2)$$

where t_m, $W_{1/2}$ and W are the migration time, the width of the peak of the ion at half-height and

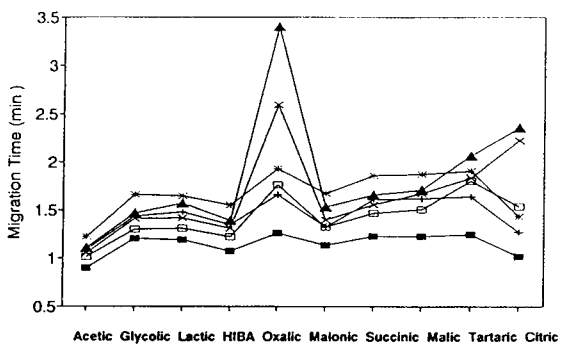

Fig. 7. Comparison of migration times for the six ions in the presence of different complexing agents in the pH range where optimum separation could be obtained: in acetic acid at pH 6.0, in succinic and citric acid at pH 4.5, in malic acid at pH 3.7 and in all other acids at pH 4.0. The pH was adjusted with a 1 *M* solution of the complexing acid. ◘ = K; + = Na, * = Li; □ = Ba; × = Ca; ▲ = Mg.

the width of the peak of the ion at the baseline in the electrophortogram, respectively; subscripts 1 and 2 refer to the peak number. The influence of complexing agents on the resolution of electropherograms is compared in Fig. 8. In general, the ions that co-migrate closer to the carrier imidazole have better N values. Thus, the fronting K and the trailing Li both have poorer N values than the other ions and are affected less by the type of acid present. The N values for Ca and Mg varied most significantly; they are particularly low in oxalic and critic acid, in which the stability constants of the complexing agent with these two ions is high. In citric acid, Na has the best N, but all other divalent ions have the poorest N. In glycolic acid, Mg has the highest N of all, reaching 760 000/m.

The ion pair with the largest peak separation distance is K–Li with the maximum R_s of 8.4–15.9 in most of the complexing agents except tartaric, oxalic and citric acid. In these three acids, K–Mg has the maximum R_s of 12.3–22.9. The minimum R_s varies in different acids; the Na–Ca pair ($R_s = 0.7$–1.2) is usually more difficult to separate than any other ion pairs.

Reproducibility, quantification, linearity and detection limit

The reproducibility of the CE method was studied by making five consecutive runs with all six ions present at 10 ppm in 3.0 mM succinic acid–5 mM imidazole. All other electrophoretic conditions were the same except that hydrodynamic (HD) sample injection for 2 s was also studied in addition to the standard electrokinetic injection (EK) mode (+5 kV for 2 s). The precisions in terms of relative standard deviations (R.S.D.) for the EK and ED modes are compared in Table II. Both injection modes provided excellent precision for the migration time but not as good for the peak area. The better peak-area precision for Li could be attributed to the higher molar equivalent concentration of Li ions present in the mixture. For quantitative purpose, it may be better to use peak height, which offered a slightly better precision. On the other hand the calculated percentage peak-area ratio for K:Ba:Ca:Na:Mg:Li, being 4.1:2.5:9.9:10.5:20:53, is more consistent with the molar equivalent concentration ratio of these ions present in the standard solution. The peak-height ratio is not in the correct proportion to the molar equivalent concentration for Mg and Li, as is apparent in all the figures shown. This is due in part to the broader peak width and more significant trailing of the Li peak.

The calibration graphs expressed as peak area *vs.* concentration in the concentration range 0.0145–1.45 mequiv. (0.1–10 ppm for Li) are compared in Fig. 9. All five ions (K was not

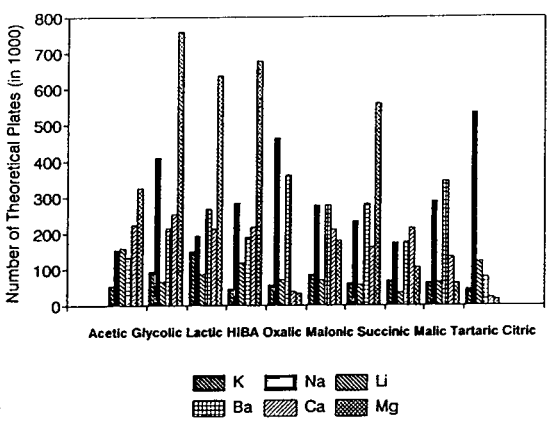

Fig. 8. Comparison of number of theoretical plates in different complexing agents. Conditions as in Fig. 7.

TABLE II

COMPARISON OF PRECISIONS WITH THE TWO INJECTION MODES

t = Migration time; A = peak area; H = peak height.

Ion	R.S.D. (%)[a]					
	EK mode			HD mode		
	t	A	H	t	A	H
K	0.73	5.8	3.5	0.80	6.5	3.6
Ba	0.83	3.3	2.7	0.63	5.5	1.8
Ca	1.02	3.8	2.8	0.59	4.8	2.2
Na	1.02	5.2	1.9	0.58	4.9	2.8
Mg	1.02	2.7	0.9	0.47	2.6	1.2
Li	1.30	1.2	1.0	0.69	2.2	1.3

[a] $n = 5$.

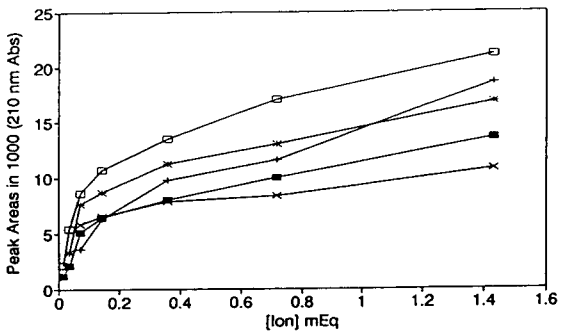

Fig. 9. Comparison of calibration graphs for the various ions in the presence of 3.0 m*M* succinic acid (pH 4.5). The pH was adjusted with 1 *M* succinic acid: × = Na; ■ = Li; + = Ba; * = Ca; □ = Mg.

included in this analysis) exhibit hyperbola-shaped curves. It is apparent that the calibration sensitivity is much better in the lower concentration range. Therefore, for quantitative analysis, the sample should be diluted serially such that the concentration of the analyte will fall into the range where the calibration graph is linear. The non-linearity problem in the indirect detection method has been noted previously [8]. Weston *et al.* [5] reported a good linearity in the low concentration range (2–160 ppb) over only 1.5 orders of magnitude. Beck and Engelhardt [8] reported that whereas a linear correlation with peak area exists for ion concentrations between 2 and 10 ppm, signal saturation with peak height occurs above 4 ppm. We found that the linearity and sensitivity are indeed better at the sub-ppm and tens of ppb level. The detection limit in this study is conservatively estimated to be at the tens of ppb to sub-ppm level and in good agreement with those reported by Weston *et al.* [5]. We are currently investigating methods for improving the precision, linearity and detection limit.

CONCLUSIONS

CE of alkali and alkaline earth metal ions using indirect UV detection with imidazole as background carrier buffer in conjunction with a complexing agent can be performed efficiently. When choosing a complexing agent, the pH of the carrier buffer should be around the pK_a of the complexing acid. If a diprotic acid is used, the pH must be between pK_1 and pK_2 value of the complexing acid. If sulphuric acid is used instead of HCl to adjust the pH, it will compete with the complexing agent and produce results different to those in its absence.

Monoprotic HIBA and lactic acid, offering a wider applicable pH range with good separation, migration time span and plate number, are good complexing agents for analyses for inorganic metal cations. Use of acetic acid is more limited (pH range 6.0–6.5) owing to its higher pK_a value, being closer to the operating range of imidazole buffer. The separation in glycolic acid is more sensitive to pH and the operating pH range is narrower than in HIBA or lactic acid (pH 3.5–5.5 *vs.* pH 3.5–6.0).

Diprotic oxalic, malonic and succinic acid, which provide a wider migration time span with a wider peak-to-peak separation time, are also good choices if manipulation of the migration times of divalent ions is desired. The migration time and order of Ba, Ca and Mg ions in these three acids are particularly sensitive to pH changes. Hydroxy diprotic malic and tartaric acid have a narrower operating pH range because the difference in pK_1 and pK_2 values is smaller than for the former two diprotic acids (1.3 *vs.* 3.0 pH unit difference). They are suitable for analysis at pH near 4.0.

Triprotic citric acid has a higher stability constant toward Group IIA metal ions. It provides a unique way to manipulate the mobility of divalent ions by varying the pH. Its drawbacks are a poorer plate number, slower migration time for the divalent ions and a limited pH operating range.

The migration order of monovalent ions, $K < Na < Li$, is always the same, independent of the type of complexing agent present. The migration order of divalent ions, $Ba < Ca < Mg$, is also the same and independent of the complexing acid used, but the migration times overlap with those of Na and Li. Hence the overall migration order and time span depend strongly on the running pH and the kind of complexing acid used. They are little affected by the monoprotic acids but are affects substantially by the complexing agent with the highest stability constant.

For routine determinations of these metal ions in real samples, we recommend CE running conditions as specified under Experimental. In addition, the following situations with regard to the complexing agent employed should be considered. (a) When the concentrations of all ions are comparable (and diluted to 0.1–1.0 mequiv.), using malonic acid (pH 4.0) or succinic acid (pH 4.5) will give the best separation. Using glycolic or lactic acid or HIBA at pH 4.0 will also provide good separation. (b) When the concentration of one ion species in the sample is particularly high (*e.g.*, in serum the Na concentration is approximately 40–50 times higher than those of K, Mg, or Ca), using oxalic acid (pH 4.0) or citric acid (pH 4.5) will avoid the problem of overlap of the large Na peak with the small peaks of the other three ions. As the ion concentration in real samples can vary greatly from sample to sample, the above conditions can only be regarded as a starting point and fine tuning is required for each individual circumstance.

ACKNOWLEDGEMENT

This work was supported in part by grants (NSC81-0208-M002-535 and NSC81-0512-L205E-01) from the National Science Council, Republic of China (Taiwan).

REFERENCES

1 W.G. Kuhr and C.A. Monnig, *Anal. Chem.*, 64 (1992) 389R.
2 W.G. Kuhr, *Anal. Chem.*, 62 (1990) 403R.
3 F. Foret, S. Fanali, A. Nardi and P. Bocek, *Electrophoresis*, 11 (1990) 780.
4 W.J. Wildman, P.E. Jackson, W.R. Jones and P.G. Alden, *J. Chromatogr.*, 546 (1991) 495.
5 A. Weston, P.R. Brown, P. Jandik, A.L. Heckenberg and W.R. Jones, *J. Chromatogr.*, 608 (1992) 395.
6 A. Weston, P.R. Brown, P. Jandik, W.R. Jones and A.L. Heckenberg, *J. Chromatogr.*, 593 (1992) 289.
7 A. Weston, P.R. Brown, P. Jandik, A.L. Heckenberg and W.R. Jones, *J. Chromatogr.*, 602 (1992) 249.
8 W. Beck and H. Engelhardt, *Chromatographia*, 33 (1992) 313.
9 L. Gross and E.S. Yeung, *Anal. Chem.*, 62 (1990) 427.
10 K. Bachmann, J. Boden and I. Haumann, *J. Chromatogr.*, 626 (1992) 259.
11 D.F. Swaile and M.J. Sepaniak, *Anal. Chem.*, 63 (1991) 179.
12 A.R. Timerbaev, W. Buchberger, O.P. Semenova and G.K. Bonn, *J. Chromatogr.*, 630 (1993) 379.
13 M. Aguilar, X. Huang and R.N. Zare, *J. Chromatogr.*, 480 (1989) 427.
14 J. Pospichal, P. Gerbauer and P. Bocek, *Chem. Rev.*, 89 (1989) 419.
15 R.C. Weast, M.J. Astle and W.H. Beyer (Editors), *Handbook of Chemistry and Physics*, CRC Press, Boca Raton, 69th ed., 1988.

Journal of Chromatography A, 654 (1993) 177–182
Elsevier Science Publishers B.V., Amsterdam

CHROM. 25 466

Short Communication

Determination of organic ionic lead and mercury species with high-performance liquid chromatography using sulphur reagents

Jörg Bettmer, Karl Cammann* and Marlene Robecke

Institut für Chemo- und Biosensorik e.V., Anorganisch-Chemisches Institut der Westfälischen Wilhelms-Universität Münster, Lehrstuhl für Analytische Chemie, Wilhelm-Klemm-Str. 8, D-48149 Münster (Germany)

(First received June 1st, 1993; revised manuscript received July 27th, 1993)

ABSTRACT

We have verified the suitability of different sulphur-containing complexing reagents for the HPLC separation of ionic lead and mercury compounds with subsequent photometric detection. For the optimization of the separations, different parameters, *e.g.* the pH value of the mobile phase, were varied and their influence on the retention of the species determined. For the first time on-column derivatization with mercaptoethanol was used for the separation of lead compounds. Based on the optimized chromatographic conditions, an on-line enrichment system was developed with recoveries between 75 and 88%. The use of methyl thioglycolate as the second complexing reagent made it possible to determine all analytes, organolead and organomercury compounds, simultaneously. Finally, both methods are compared briefly.

INTRODUCTION

In recent years the importance of speciation analysis in the field of trace element analysis has grown enormously. Because of several disasters, the organometal compounds of the elements lead and mercury have become of particular interest [1–4]. First, the ionic di- and trialkyllead and monoalkylmercury compounds [dimethyllead (DiML), diethyllead (DiEL), trimethyllead (TriML), triethyllead (TriEL), methylmercury (MMM) and ethylmercury (MEM)] are the subjects of analytical research because of their high toxicity and bioavailability compared with the inorganic ions [2,5]. In addition to GC, liquid chromatography has often been employed for the determination and separation of the analytes [6–8]. A disadvantage of separating these compounds by GC is the need to perform a derivatization step, such as propylation or butylation, to form volatile compounds. It is not necessary, though it may be easily accomplished, to perform a derivatization step for the HPLC separation. Table I summarizes the methods using different sulphur compounds which are often used for the derivatization and separation.

The possibility of separating mercury compounds using on-column derivatization with mercaptoethanol led us to apply a similar system for the determination of organolead compounds. Separation was carried out on an RP-18 column

* Corresponding author.

0021-9673/93/$06.00

TABLE I

METHODS USING SULPHUR COMPOUNDS FOR THE SEPARATION OF LEAD AND MERCURY COMPOUNDS WITH HPLC

Analytes	Sulphur compound	Detector[a]	References
Pb^{2+}, DiML, DiEL, TriML, TriEL	Dithizone	QTAAS	7, 9
Hg^{2+}, MMM, MEM	Dithizone	UV–VIS	10, 11
Pb^{2+}, DiML, DiEL, TriML, TriEL	Alkyldithiocarbamate	QTAAS	7, 9
Hg^{2+}, MMM, MEM	Alkyldithiocarbamate	UV–VIS	12
Hg^{2+}, MMM, MEM	Mercaptoethanol	ED	13
Hg^{2+}, MMM, MEM	Mercaptoethanol	GFAAS	14
Hg^{2+}, MMM, MEM	Mercaptoethanol	UV–VIS	15, 16
Hg^{2+}, MMM, MEM	Mercaptoethanol	MIP–AES	16
Hg^{2+}, MMM, MEM	Mercaptoethanol	ICP–MS	17
Hg^{2+}, MMM, MEM	Cysteine	CVAAS	18

[a] QTAAS = quartz tube atomic absorption spectrometry; UV–VIS = ultraviolet/visible; ED = electrochemical detector; GFAAS = graphite furnace atomic absorption spectrometry; MIP–AES = microwave-induced plasma atomic emission spectrometry; ICP–MS = inductively coupled plasma mass spectrometry; CVAAS = cold vapour atomic absorption spectrometry.

and with a methanolic citric acid buffer as mobile phase; for detection at UV–VIS detector at 235 nm was used. Chromatographic separation of dialkyllead compounds and trimethyllead was achieved by systematically varying mobile phase parameters; for the elution of triethyllead a gradient had to be established. Furthermore, the separation was completed by developing an on-line enrichment method involving the preconcentration of mercaptoethanol complexes of the lead compounds on an RP-18 precolumn.

Methyl thioglycolate was employed as a second sulphur compound for the complexation of the ionic lead and mercury species and allowed us to determine simultaneously all the organometal compounds mentioned above in a 40-min isocratic run.

EXPERIMENTAL

Reagents

For the preparation of the mobile phases methanol AR, trisodium citrate dihydrate AR (both obtained from Merck, Darmstadt, Germany) and twice-distilled water were used. The pH was adjusted with hydrochloric acid AR (Baker, Deventer, Netherlands) and sodium hydroxide AR (Merck). For the derivatization mercaptoethanol AR (Merck) and methyl thioglycolate 98% (Riedel de Haën, Seelze, Germany) were used. Trialkyllead and organomercury compounds were obtained from Alfa Products (Karlsruhe, Germany) as their chlorides. Dialkyllead species were self-prepared [19]. All analytes were stored at 4°C and dried in the desiccator ($CaCl_2$) prior to use.

HPLC equipment

The HPLC system consisted of the following set-up: a consta Metric 4100 gradient pumping system (LDC Analytical, Gelnhausen, Germany), an HPLC pump 64 and a UV–VIS detector variable-wavelength monitor (both obtained from Knauer, Bad Homburg, Germany), a six-way injection valve with 20-μl sample loop and the same injection valve (Knauer) with a precolumn (Nucleosil C_{18} 120-5, 30 mm × 4 mm I.D.). The analytical columns were RP-18 columns (Hypersil ODS, 100-5, 250 mm × 4 mm I.D., and Nucleosil C_{18} 120-5, 250 mm × 4 mm I.D.), and for their protection precolumns (5 mm) with the same filling were used. The chromatograms were evaluated by a C-R6A integrator (Shimadzu, Duisburg, Germany). The mobile phases and the sample solutions were

degassed in a Sonorex TK 52 ultrasonic bath (Bandelin, Berlin, Germany).

Sample preparation

The concentrations of the prepared stock solutions (analytes in methanol/twice-distilled water; 50/50, v/v) were about 1 mg/ml. This solutions were diluted daily with twice-distilled water to concentrations from 0.5–100 μg/ml. For the injections methanolic solutions of the derivatization reagent (0.08%, v/v) were added because of the need for pre-column complexation. The concentrations were about 0.02% (v/v).

RESULTS AND DISCUSSION

Mercaptoethanol as complexing reagent

Mercaptoethanol is widely used in the complexation and chromatographic separation of mercury compounds, as shown in Table I. Lead and its organo compounds also show a high affinity for sulphur compounds, and mercaptoethanol was tested for its usefulness in the separation of ionic lead compounds. The primary reactions during the pre- and on-column derivatization are summarized in eqn. 1.

$$R_{4-n}PbCl_n + nHSCH_2CH_2OH \rightleftharpoons R_{4-n}Pb(SCH_2CH_2OH)_n + nH^+ + nCl^- \quad n = 1, 2 \qquad (1)$$

The UV spectra of the resulting complexes showed characteristic peaks of absorption between 225 and 240 nm [20]. Further measurements were carried out at a wavelength of 235 nm.

The first parameter varied for the optimization of the chromatographic separation was the concentration of mercaptoethanol. High concentrations of mercaptoethanol displace the formation equilibrium (eqn. 1) to the right with the effect of increasing the capacity factors. For all subsequent investigations the concentration of mercaptoethanol was held constant at 0.02% (v/v).

The influence of the concentration of citric acid in the range 0.05–0.15 mol/l is negligible, but at 0.2 mol/l citric acid a decrease in the capacity factors could be observed. Owing to the limited solubility of citric acid in the methanol–water mixture used, it was not possible to investigate higher concentrations. A concentration of 0.2 mol/l was chosen for the separations. The next parameter to be varied in order to optimize the separation conditions was pH value (Fig. 1). Particularly in the pH range 6.7–7.0, the capacity factors increase enormously with pH. This phenomenon is based on two effects: (1) with increasing pH the formation equilibrium (eqn. 1) is displaced to the right and (2) the deprotonation of mercaptoethanol is favoured by decreasing concentration of protons.

For separation a pH value of 6.7 was suitable. If the composition of the mobile phase was held constant, it was possible to separate the three organolead compounds (DiML, DiEL and TriML) on the reversed-phase column. For the elution of triethyllead it was necessary to increase the concentration of methanol up to 55% (v/v). The gradient conditions are given in Table II. A chromatogram recorded at the conditions described is shown in Fig. 2.

Calibrations, detection limits

During the calibration experiments we found that the standard solutions were light sensitive. Further examinations were carried out to explain this phenomenon by storing the solutions in daylight for a defined period. The influence on the stability of the complexes is shown in Fig. 3.

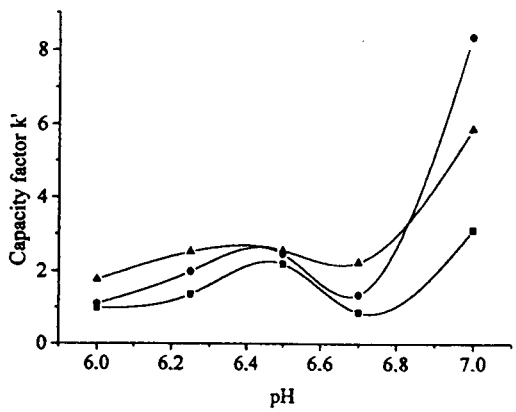

Fig. 1. Influence of the pH value on the capacity factors. □ = DiML; ○ = TriML; ▲ = DiEL.

TABLE II

GRADIENT FOR THE ELUTION OF THE LEAD COMPOUNDS

Stationary phase, Nucleosil C_{18} 120-5, 250 mm × 4 mm; Mobile phase A, methanol–0.2 mol/l citric acid (20/80, v/v), adjusted to pH 6.7, 0.02% (v/v) mercaptoethanol; mobile phase B, methanol–0.2 mol/l citric acid (55/45, v/v); adjusted to pH 6.7, 0.02% (v/v) mercaptoethanol; flow, 1.0 ml/min.

Time (min)	Mobile phase A (%)	Mobile phase B (%)
0	100	0
10	100	0
12	0	100
22	0	100
24	100	0

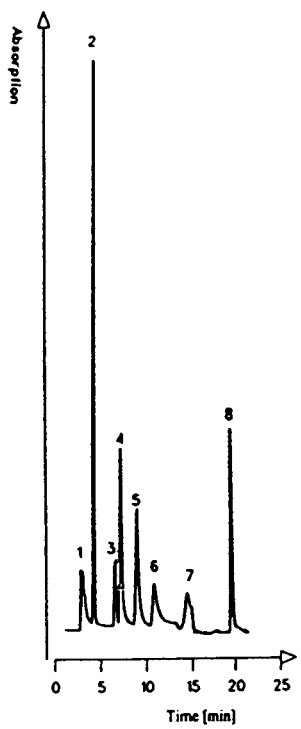

Fig. 2. Chromatogram of the lead compounds. For chromatographic conditions see Table II. UV detection: 235 nm; 0.04 a.u.f.s. Peak 1 = 620 ng of Pb^{2+}; peak 2 = mercaptoethanol; peak 3 = impurity from mercaptoethanol; peak 4 = 321 ng of DiML; peak 5 = 493 ng of TriML; peak 6 = 982 ng of DiEL; peak 7 = system peak; peak 8 = 756 ng of TriEL.

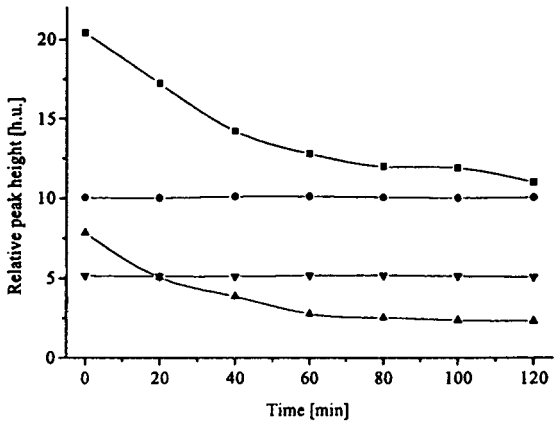

Fig. 3. Influence of daylight on the stability of mercaptoethanol complexes. □ = DiML; ○ = TriML; △ = DiEL; ▽ = TriEL.

Only the complexes of the dialkyllead compounds and not those of the trialkyllead species decomposed in daylight. Additional investigations proved that it was the mercaptoethanol complexes and not the metal ions themselves that were sensitive to light. Consequently, the samples were stored in the dark before injection.

The chromatographic conditions used for the calibrations are summarized in Table II.

Linearity with correlation coefficients between 0.997 and 0.999 was obtained for each analyte in the range between approximately 50 and 1500 ng (the specifications refer to the organometallic compounds and not to the elements). The detection limits ($S/N = 3:1$; $n = 10$) were from 18 ng for DiML to 61 ng for TriEL (see also Table III).

For the determination of trace amounts an enrichment system had to be tested, and is described below.

Enrichment from water samples

For enrichment the HPLC system used was enlarged by installing a second injection valve with an RP-18 precolumn (30 mm). An HPLC pump delivered the solutions onto the precolumn and then the analytes were loaded into the chromatographic system by switching the injection valve. The chromatographic conditions for the enrichment from water samples are summarized as follows: flow, 5.0 ml/min; pH, 7.0; citric

acid concentration, 0.1 mol/l; mercaptoethanol, 0.02% (v/v).

The recoveries were 75.2 ± 7.9% for DiML, 87.4 ± 4.2% for TriML, 77.9 ± 9.9% for DiEL and 88.2 ± 5.1% for TriEL. The results obtained were not satisfactory, so further investigations should improve the recoveries and their reproducibility.

Methyl thioglycolate as complexing reagent

Mercaptoethanol was used to obtain a simultaneous determination of the organolead and organomercury species. Because of peak overlaps and co-elutions methyl thioglycolate, another sulphur compound, was preferred to solve this analytical problem. Its reactions with the analytes were similar to those shown in eqn. 1. The complexes could be determined photometrically at 235 nm [21]. For the separation a methanolic citric acid buffer was again used. The concentration of methanol was kept at 40% (v/v) and the concentration of citric acid buffer at 0.1 mol/l. The effects of pH and concentration of methyl thioglycolate were similar to the effects on mercaptoethanol. With increasing proton concentration and decreasing concentration of the complexing reagent in the mobile phase, the capacity factors decreased for the lead compounds. On the other hand, mercury compounds were not affected. For the separation, a pH of 5.8 and 0.02% (v/v) methyl thioglycolate proved to be suitable. A chromatogram recorded under these conditions is shown in Fig. 4.

To prevent the decomposition of the complexed analytes the solutions were stored in the dark before the injections. Calibration graphs were linear in the range between approximately 50 and 600 ng for each analyte with correlation coefficients between 0.993 and 0.998. A comparison of the detection limits with both complexing reagents is demonstrated in Table III. However, the complexation with methyl thioglycolate resulted in lower detection limits for the trialkyllead compounds.

Following the enrichment procedure described above, the lead and mercury compounds could be preconcentrated in the same way. The recoveries for all the analytes were between 70 and 80%, thus there was no improvement compared with the recoveries obtained with mercaptoethanol.

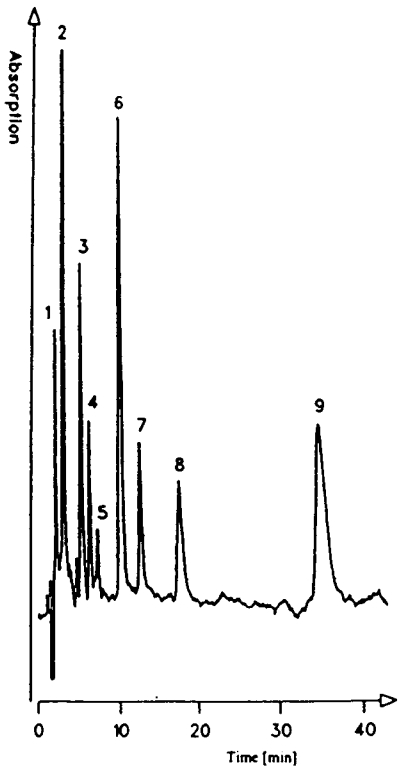

Fig. 4. Chromatogram of the lead and mercury compounds. Stationary phase: Hypersil ODS 100-5, 250 mm × 4 mm. Mobile phase; methanol–0.1 mol/l citric acid (40/60, v/v), adjusted to pH 5.8, 0.02% (v/v) methyl thioglycolate. UV detection: 235 nm; 0.04 a.u.f.s. Peak 1 = methanol; peak 2 = methyl thioglycolate; peak 3 = 181 ng of TriML; peak 4 = 226 ng of MMM; peak 5 = impurity from methyl thioglycolate; peak 6 = 129 ng of DiML; peak 7 = 208 ng of MEM; peak 8 = 238 ng of DiEL; peak 9 = 246 ng of TriEL.

CONCLUSIONS

Two methods for the enrichment and determination of lead compounds are presented. New methods of complexation of the analytes using sulphur compounds were considered, and proved to be alternative methods of separation and determination. The use of methyl thioglycolate made it possible to determine simultaneously organolead and organomercury compounds in a 40-min isocratic run. For the enrichment an on-line method was tested but the recoveries ob-

TABLE III

DETECTION LIMITS OF THE ANALYTES, COMPLEXED WITH METHYL THIOGLYCOLATE AND MERCAPTOETHANOL

$S/N = 3/1$; $n = 10$.

Analytes	Detection limits in ng absolute	
	Methyl thioglycolate	Mercaptoethanol
DiML	12	18
TriML	17	35
DiEL	31	30
TriEL	32	61
MMM	25	–
MEM	19	–

tained for both complexing reagents were unsatisfactory.

ACKNOWLEDGEMENTS

The authors kindly acknowledge the financial support of the Deutsche Forschungsgemeinschaft.

REFERENCES

1 G. Tölg and I. Lorenz, *Chemie in unserer Zeit*, 5 (1977) 150.
2 E. Merian, *Metals and Their Compounds in the Environment*, VCH Verlagsgesellschaft, Weinheim, 1991.
3 W. Wirth and C.H. Gloxhuber, *Toxikologie*, Thieme, Stuttgart, 1985.
4 World Health Organization, *Environmental Health Criteria I, Mercury*, Geneva, 1976.
5 W.R.A. De Jonghe and F.C. Adams, *Talanta*, 29 (1982) 1057.
6 R.-D. Wilken and H. Hintelmann, in J.A.C. Brockaert, S. Guçer and F.C. Adams (Editors), *Metal Speciation in the Environment*, Springer, Berlin, 1990.
7 J.S. Blais, W.D. Marshall and F.C. Adams, in J.A.C. Brockaert, S. Guçer and F.C. Adams (Editors), *Metal Speciation in the Environment*, Springer, Berlin, 1990.
8 B. Neidhart, M. Blaskewicz, U. Backes and G. Dieckmann, in J.A.C. Brockaert, S. Guçer and F.C. Adams (Editors), *Metal Speciation in the Environment*, Springer, Berlin, 1990.
9 J.S. Blais and W.D. Marshall, *J. Anal. Atom. Spectrom.*, 4 (1989) 271.
10 K. Cammann and M. Robecke, *Chem. Industrie*, 6 (1990) 32.
11 W. Langseth, *Anal. Chim. Acta*, 185 (1986) 249.
12 W. Langseth, *Fresenius' Z. Anal. Chem.*, 325 (1986) 267.
13 W.A. MacCrehan, *Anal. Chem.*, 53 (1981) 74.
14 F.E. Brinckman, W.R. Blair, K.L. Jewett and W.P. Iverson, *J. Chromatogr. Sci.*, 15 (1977) 393.
15 R.-D. Wilken, *Fresenius' Z. Anal. Chem.*, 342 (1992) 795.
16 D. Kollotzek, D. Oechsle, G. Kaiser, P. Tschöpel and G. Tölg, *Fresenius' Z. Anal. Chem.*, 318 (1984) 485.
17 D.S. Bushee, *Analyst*, 113 (1988) 1167.
18 M. Fujita and E. Takabatake, *Anal. Chem.*, 55 (1983) 454.
19 R. Heap, B.C. Saunders and G.J. Stacey, *J. Chem. Soc.*, I (1951) 658.
20 M. Robecke, *Doctoral dissertation*, Münster, 1992.
21 J. Bettmer, *Diploma Thesis*, Münster, 1992.

Journal of Chromatography A, 654 (1993) 183–189
Elsevier Science Publishers B.V., Amsterdam

CHROM. 25 482

Short Communication

Correlation between gas chromatographic retention indices of linear alkylbenzene isomers and molecular connectivity indices

Vilma E.F. Heinzen and Rosendo A. Yunes*

Departamento de Química, Universidade Federal de Santa Catarina, 88040-900, Florianópolis, Santa Catarina (Brazil)

(First received April 20th, 1993; revised manuscript received July 13th, 1993)

ABSTRACT

The gas chromatographic retention indices of linear alkylbenzene isomers (LABs), with C_{10}–C_{14} linear alkyl chains were correlated using different molecular connectivity indices. The single linear correlations showed that these do not explain the chromatographic retention of the isomeric structures. Corrected molecular connectivity indices, searching to consider the steric effects produced by the phenyl group on the alkyl chain, showed a good correlation with the retention indices of LABs and a correct elution sequence. Multiple linear correlation with connectivity indices that encode complementary information gives good correlation coefficients and the correct elution sequence of most of the compounds.

INTRODUCTION

The existence of a quantitative structure–retention index relationship (QSRR) makes possible the prediction of retention indices of compounds through their chemical structures, or permits the prediction of structures from retention indices [1–3]. Structural information based on the use of topological (graph–theoretical) indices characterizes the molecule by a simple number. In spite of the molecule being described by a one-dimensional parameter (topological index), it is surprising how much relevant structural information is retained in a given topological number index. Many topological indices have been proposed [4–6]. One of the most useful is the molecular connectivity index introduced by Randic [7] and developed extensively by Kier [8] because of its important applications [9,10]. According to Mihalic and Trinajstic [11], one of the weakest points of these kinds of indices is the lack of discrimination of positional isomers.

The aim of this study was to evaluate the ability of molecular connectivity indices to predict the retention indices of linear alkylbenzene isomers (LABs). The importance of LABs with alkyl carbon numbers of 10–14 is that they are found as residues from incomplete sulphonation and are carried with linear alkylbenzenesulphonates (LAS) in detergents. Recent reviews [12,13] on the presence of LABs in river waters and estuarine sediment cores show that LAB pollution starts from the depth corresponding to the time when LAS detergents began being used

* Corresponding author.

0021-9673/93/$06.00

in the catchment area [13]. LABs consist of isomers that differ in the position of the phenyl group on the alkyl side-chain. For detergents and untreated domestic wastes the relative abundances of isomers with a given alkyl chain length are nearly equal. For river and coastal sediments, however, internal isomers (those having the phenyl attachment toward the middle of the alkyl chain, *e.g.*, 6-C10) dominate over external isomers (those having the phenyl attachment near the end of the alkyl chain, *e.g.*, 2-C10; *n*-C*m*, where *n* indicates the position of the benzene ring in the alkyl chain and *m* indicates the number of carbon atoms of the alkyl chain). This difference in isomeric composition has been considered to be caused by selective biodegradation of external isomers relative to internal isomers [13]. In this form, the composition of LABs may provide information on the extent of its biodegradation and it can be used as a molecular tracer of domestic wastes in the environment.

EXPERIMENTAL

The chromatographic retention indices (I) of linear alkylbenzene isomers with C_{10}–C_{14} alkyl chains (LABs) were reported by Takad and Ishiwatari [12] and Peng *et al.* [3].

The molecular connectivity index path (X_p) and cluster (X_c, X_{pc}) of different orders were calculated by the method of Kier [8] utilizing the Molconn-X computer program for molecular topology analysis [14].

The connectivity indices (^1X, ^2X, ..., ^hX) were calculated according to the Kier's [8] equation:

$$^hX = \sum_{s=1}^{t} (\delta_i \cdot \delta_j \cdots \delta_{n+1}) \quad (1)$$

where s refers to a single path or subgraph of length h, t is the total number of paths h in a graph, δ_i, δ_j, ..., δ_{n+1} represent values attributed to the adjacent atoms i and j in the hydrogen-supressed molecular graph and the superscript h on X denotes the so-called order of connectivity index. The path connectivity index (X_p) with one order conveys more information about the number of atoms in a molecule and with higher order (2–7) encodes also information about branching.

X^* values are obtained, for example, by taking the difference between the x intercept values of the straight lines corresponding to the homologous series (2C10–2C14, 3C10–3C14, 4C10–4C14, 5C10–5C14 and 6C11–6C14) and the x intercept values of homologous series (1C10–1C14), decreasing these values of the ^4X_p index.

All calculations of single and multiple linear regression analyses were carried out on an IBM AT/486 computer. To test the quality of the regression equation, the correlation coefficient (r), the coefficient of determination (r^2) and the test of null hypothesis (F-test) were utilized as statistical parameters.

RESULTS AND DISCUSSION

The values of chromatographic retention indices (I) of isomers of LABs with C_{10}–C_{14} linear alkyl chains [3,12] and their connectivity indices ^1X, ^2X, ^3X_p, ^4X_p, ^5X_p, ^6X_p and ^7X_p are given in Table I.

The connectivity indices of lower orders, ^1X, ^2X and ^3X_p, do not distinguish the positional isomers of the aromatic ring; the distinction only occurs from ^4X_p. Considering the unsaturation in the aromatic ring, the valence connectivity indices were applied, but did not improve the distinction of the same isomers.

Although the cluster connectivity indices (^3X_c and $^4X_{pc}$) encode more information about branching, they do not distinguish the positional isomers 3C, 4C, 5C and 6C of the aromatic ring; the distinction only occurs when the aromatic ring is in the position 1C and 2C of the alkyl chain. It is important to note that the $I_{SE\text{-}54}$ and $I_{DB\text{-}1}$ values decrease when the position of the aromatic ring go from C1 to Cn (n = 2, 3, 4, 5 and 6) in the same isomeric series. When the position of the aromatic ring is more internal in the molecule, it interposes between the alkyl chain and the stationary phase and the molecule becomes more symmetrical and more compact, decreasing the interaction surface, and so its chromatographic retention index decreases

TABLE I

MOLECULAR CONNECTIVITY INDICES AND OBSERVED RETENTION INDICES OF LINEAR ALKYLBENZENES WITH C_{10}–C_{14} LINEAR ALKYL CHAINS ON SE-54 AND DB-1 STATIONARY PHASES

Compound	I_{SE-54} [a]	I_{DB-1} [b]	^1X_p	^2X_p	^3X_p	^4X_p	^5X_p	^6X_p	^7X_p
1C10	100.00	1664	7.9319	5.7676	4.1907	3.0427	2.2077	1.1840	0.7747
2C10	92.84	1588	7.8425	5.9318	4.4676	3.1855	2.2710	1.2025	0.7878
3C10	89.37	1553	7.8805	5.7693	4.5193	3.3888	2.4150	1.3041	0.8549
4C10	87.54	1534	7.8805	5.7962	4.4044	3.4254	2.5587	1.3990	0.9555
5C10	86.70	1526	7.8805	5.7962	4.4233	3.3442	2.5751	1.5413	1.0144
1C11	110.00	1771	8.4319	6.1211	4.4407	3.2195	2.3327	1.2724	0.8372
2C11	102.71	1692	8.3425	6.2854	4.7176	3.3623	2.3963	1.2909	0.8503
3C11	99.15	1656	8.3805	6.1229	4.7693	3.5656	2.5400	1.3925	0.9221
4C11	97.15	1636	8.3805	6.1497	4.6544	3.6022	2.6837	1.4941	0.9893
5C11	96.20	1626	8.3805	6.1497	4.6734	3.5209	2.7096	1.5890	1.0898
6C11	95.92	1620	8.3805	6.1497	4.6734	3.5344	2.6426	1.6480	1.1488
1C12	120.00	1870	8.9319	6.4747	4.6907	3.3963	2.4577	1.3608	0.8997
2C12	112.63	1791	8.8425	6.6389	4.9676	3.5391	2.5213	1.3792	0.9128
3C12	108.95	1755	8.8805	6.4764	5.0193	3.7424	2.6650	1.4809	0.9846
4C12	106.09	1735	8.8805	6.5033	4.9044	3.7790	2.8087	1.5825	1.0565
5C12	105.76	1723	8.8805	6.5033	4.9234	3.6977	2.8346	1.6841	1.1236
6C12	105.31	1719	8.8805	6.5033	4.9234	3.7111	2.7771	1.6957	1.2242
IC13	130.00	1978	9.4319	6.8282	4.9407	3.5730	2.5827	1.4492	0.9622
2C13	122.52	1894	9.3425	6.9925	5.2176	3.7159	2.6463	1.4676	0.9753
3C13	118.81	1854	9.3805	6.8300	5.2693	3.9191	2.7900	1.5693	1.0471
4C13	116.59	1833	9.3805	6.8568	5.1544	3.9557	2.9337	1.6709	1.1190
5C13	115.42	1821	9.3805	6.8568	5.1734	3.8745	2.9596	1.7725	1.1909
6C13	114.75	1814	9.3805	6.8568	5.1734	3.8879	2.9021	1.7908	1.2580
1C14	140.00		9.9319	7.1818	5.1907	3.7498	2.7077	1.5376	1.0247
2C14	132.46		9.8425	7.3460	5.4676	3.8927	2.7713	1.5560	1.0378
3C14	128.67		9.8805	7.1835	5.5193	4.0959	2.9150	1.6577	1.1096
4C14	126.37		9.8805	7.2104	5.4044	4.1325	3.0587	1.7593	1.1815
5C14	125.01		9.8805	7.2104	5.4234	4.0513	3.0846	1.8609	1.2534
6C14	124.20		9.8805	7.2104	5.4234	4.0647	3.0271	1.8792	1.3252

[a] From ref. 12.
[b] From ref. 3.

owing to the steric and conformational effects. It has been indicated that steric and polar rather than hydrophobic interactions take place in GLC separations [15].

The behaviour of the values of the connectivity indices differs. The ^6X_p and ^7X_p indices increase when the phenyl group changes from C1 to C6 because the number of subgraphs for their calculation also increases. A possible interpretation is that not all the subgraphs must be considered to contribute to the retention, taking into account the steric and conformational effects. For this reason, ^4X_p, ^5X_p, ^6X_p and ^7X_p do not give good information about these isomers and a simple linear correlation with I is not acceptable. Nevertheless, this linear correlation for SE-54 and DB-1 shows a good correlation between the retention indices and connectivity indices for each homologous series (1C10–1C14, . . .). Fig. 1 shows the correlation with ^7X_p. The same results were obtained with ^1X, ^2X, ^3X_p with the number of carbon atoms and molecular mass.

However, the difference in the x intercept values (when $I = 112$ for SE-54 and $I = 1740$ for DB-1) may be considered as a measure of the steric or conformational effects on the connectivity indices corresponding to the distinct position of the aromatic ring in the alkyl chains. This

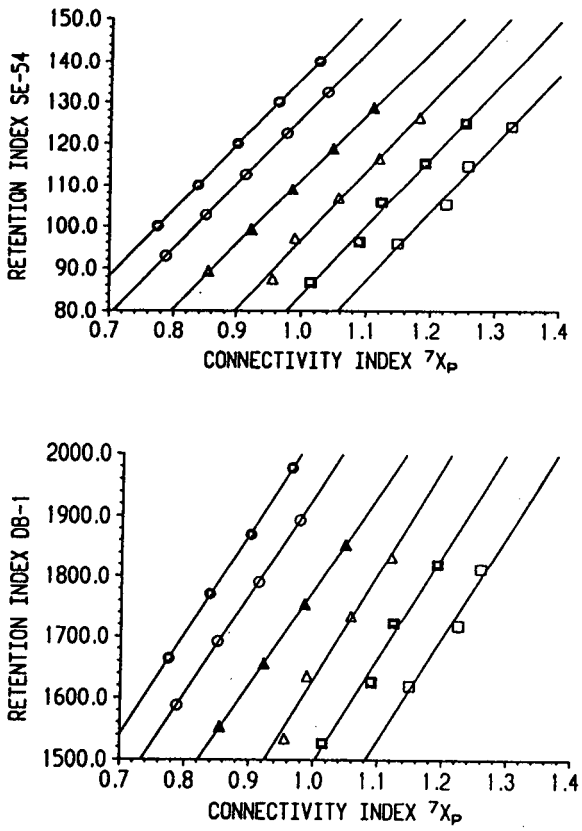

Fig. 1. Correlation between experimental retention indices and molecular connectivity index, ^7X_p, for homologous series of linear alkylbenzene isomers: SE-54: ● = 1C10–1C14; ○ = 2C10–2C14; ▲ = 3C10–3C14; △ = 4C10–4C14; ■ = 5C10–5C14; □ = 6C11–6C14. DB-1: ● = 1C10–1C13; ○ = 2C10–2C13; ▲ = 3C10–3C13; △ = 4C10–4C13; ■ = 5C10–5C13; □ = 6C11–6C13.

consideration does not have any sense with respect to the number of carbon atoms, the molecular mass, etc.

With the purpose of correcting for these effects and to obtain an equation that is able to predict the retention and the elution sequence of LABs, a method is proposed. The values of the slopes of the straight lines, for each homologous series, are slightly different. As the steric and conformational effects much be the same, the median slope is utilized, and new x intercept values can be obtained for each straight line. Taking the difference between the x intercept values corresponding to the different straight lines and the x intercept value of 1C10–1C14, on decreasing these values of the ^7X_p index new corrected values, $^7X_p^*$, are obtained. These new values $^7X_p^*$ correlate in an excellent way with $I_{SE\text{-}54}$ ($r = 0.9975$) and with $I_{DB\text{-}1}$ ($r = 0.9954$) and give the correct elution sequence for most of the compounds (Fig. 2). The same results are obtained with the other indices that distinguish the positional isomers such as ^4X_p, ^5X_p and ^6X_p (Table II).

This method was also applied to the retention indices [16] on a squalane stationary phase for 24 methylalkane isomers with C_{10}–C_{14} alkyl chains. The results were almost the same as those for alkylbenzene isomers. The correlation of $I_{squalane}$ with $^7X_p^*$ is excellent ($r = 0.9999$). Hence it seems that this method can be used in a general way.

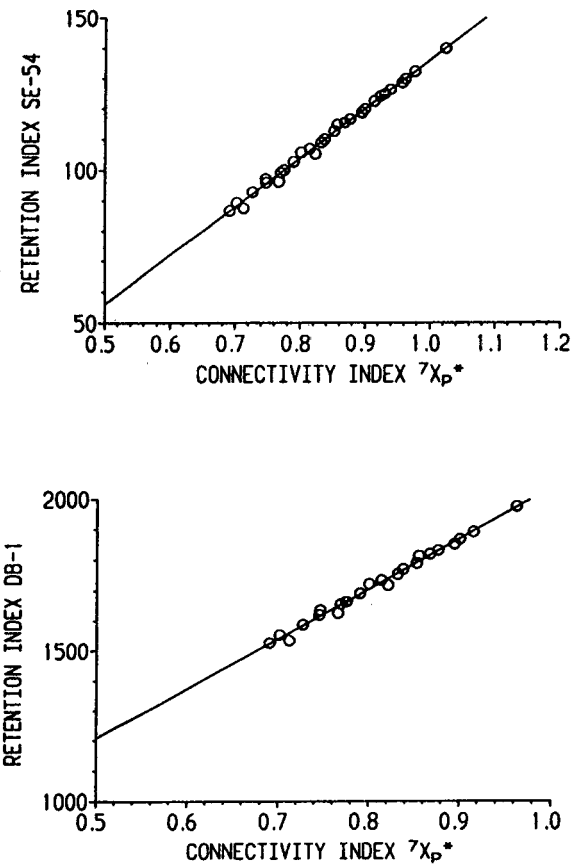

Fig. 2. Correlation between experimental retention indices (SE-54 and DB-1) and corrected molecular connectivity index $^7X_p^*$ of linear alkylbenzene isomers.

TABLE II

CORRECTED VALUES OF MOLECULAR CONNECTIVITY INDICES OF LINEAR ALKYLBENZENES WITH C_{10}–C_{14} LINEAR ALKYL CHAINS

Compound	$^4X_p^{*\,a}$	$^5X_p^{*\,a}$	$^6X_p^{*\,a}$	$^7X_p^{*\,a}$	$^4X_p^{*\,b}$	$^5X_p^{*\,b}$	$^6X_p^{*\,b}$	$^7X_p^{*\,b}$
1C10	3.0427	2.2077	1.1840	0.7747	3.0427	2.2077	1.1840	0.7747
2C10	2.9090	2.1115	1.1189	0.7268	2.9023	2.1073	1.1168	0.7271
3C10	2.8429	2.0656	1.0865	0.7026	2.8375	2.0612	1.0861	0.7015
4C10	2.8052	2.0387	1.0627	0.7131	2.8022	2.0359	1.0637	0.7123
5C10	2.7854	2.0170	1.0869	0.6916	2.7837	2.0156	1.0870	0.6903
1C11	3.2195	2.3327	1.2724	0.8372	3.2195	2.3327	1.2724	0.8372
2C11	3.0858	2.2368	1.2072	0.7893	3.0791	2.2326	1.2052	0.7896
3C11	3.0197	2.1906	1.1749	0.7698	3.0143	2.1862	1.1745	0.7687
4C11	2.9820	2.1637	1.1578	0.7469	2.9790	2.1609	1.1580	0.7461
5C11	2.9621	2.1515	1.1346	0.7670	2.9604	2.1501	1.1347	0.7657
6C11	2.9505	2.1346	1.1672	0.7476	2.9492	2.1339	1.1659	0.7452
1C12	3.3963	2.4577	1.3608	0.8997	3.3963	2.4577	1.3608	0.8997
2C12	3.2626	2.3618	1.2955	0.8518	3.2559	2.3576	1.2935	0.8521
3C12	3.1965	2.3156	1.2633	0.8323	3.1911	2.3112	1.2629	0.8312
4C12	3.1588	2.2887	1.2462	0.8141	3.1558	2.2859	1.2472	0.8133
5C12	3.1389	2.2765	1.2297	0.8008	3.1372	2.2751	1.2298	0.7995
6C12	3.1272	2.2691	1.2149	0.8230	3.1259	2.2684	1.2136	0.8206
1C13	3.5730	2.5827	1.4492	0.9622	3.5730	2.5827	1.4492	0.9622
2C13	3.4394	2.4868	1.3839	0.9143	3.4327	2.4826	1.3819	0.9146
3C13	3.3732	2.4406	1.3517	0.8948	3.3678	2.4362	1.3513	0.8937
4C13	3.3355	2.4137	1.3346	0.8766	3.3325	2.4109	1.3356	0.8758
5C13	3.3157	2.4015	1.3181	0.8681	3.3140	2.4001	1.3182	0.8668
6C13	3.3040	2.3941	1.3100	0.8568	3.3027	2.3934	1.3087	0.8544
1C14	3.7498	2.7077	1.5376	1.0247				
2C14	3.6162	2.6118	1.4723	0.9768				
3C14	3.5500	2.5656	1.4401	0.9573				
4C14	3.5123	2.5387	1.4230	0.9391				
5C14	3.4925	2.5265	1.4065	0.9306				
6C14	3.4808	2.5191	1.3984	0.9240				

[a] $I_{SE\text{-}54}$ from ref. 12.
[b] $I_{DB\text{-}1}$ from ref. 3.

Multiple linear correlation

The analysis by the single linear regression method demonstrates that the correlation with only one connectivity index without correction is not sufficient to give a good correlation or a correct elution sequence. This led us to test multi-variable regression equations with indices that were able to give a better representation of the molecules. To select the connectivity indices, a correlation matrix between them was applied, and to define the type of function that relates the retention indices with each connectivity index the scatter plot method was used.

The best correlation with two connectivity indices was obtained with ^1X and ^5X_p (eqns. 2 and 3):

$$I_{SE\text{-}54} = 27.5536\,{}^1X - 32.1700\,{}^5X_p - 48.6688 \quad (2)$$

$n = 29$; $r = 0.9955$; $F(^1X) = 2110.96$ ($P > 0.0001$);

$r^2 = 0.9911$; $F(^5X_p) = 317.00$ ($P > 0.0001$)

$$I_{DB\text{-}1} = 283.0253\,{}^1X - 329.4509\,{}^5X_p + 133.9781 \quad (3)$$

$n = 23$; $r = 0.9923$; $F(^1X) = 1133.88$

($P > 0.0001$);

$r^2 = 0.9847$; $F(^5X_p) = 212.88$ ($P > 0.0001$)

The ^1X index conveys more information about the number of atoms in a molecule and the ^5X_p index encodes more information about branching. The ^1X index decreases with displacement of the phenyl group from the end to the middle of the alkyl chain of an isomeric series according to the I values, but it does not distinguish the isomers 3C, 4C, 5C and 6C. The ^5X_p index increases with displacement of the phenyl group from the end to the middle of the alkyl chain and distinguishes all the compounds.

In spite of the good correlation coefficient that eqn. 2 shows, the elution sequence is not correct for eight compounds and eqn. 3 for six compounds. A better correlation is obtained with three connectivity indices ^1X, ^3X_p and ^5X_p (eqns. 4 and 5):

$$I_{SE\text{-}54} = 31.8111\,^1X - 10.5633\,^3X_p - 28.3486\,^5X_p - 4.9117 \quad (4)$$

$n = 29$; $r = 0.9985$; $F(^1X) = 1996.83$ ($P > 0.0001$);

$r^2 = 0.9969$; $F(^3X_p) = 47.89$ ($P > 0.0001$);

$F(^5X_p) = 546.91$ ($P > 0.0001$)

$$I_{DB\text{-}1} = 331.3419\,^1X - 121.1496\,^3X_p - 285.4131\,^5X + 180.7905 \quad (5)$$

$n = 23$; $r = 0.9979$; $F(^1X) = 1622.25$ ($P > 0.0001$);

$r^2 = 0.9958$; $F(^3X_p) = 49.59$ ($P > 0.0001$);

$F(^5X_p) = 433.82$ ($P > 0.0001$)

Surprisingly, the ^3X_p index, which gives more information about branching in simpler molecules, permits the elution sequence of more compounds to be determined (the sequence given by eqn. 4 is wrong for only four compounds, 6C11–6C14, and that given by eqn. 5 for three compounds, 6C11–6C13).

These correlations show that the combination of different connectivity indices that encode complementary information permits the structures of the positional isomers to be distinguished and the correct elution sequence of most of them to be determined.

CONCLUSIONS

LAB isomers with the phenyl group attached at the extremity of the alkyl chains, have a larger surface for interaction with the stationary phase, thus showing larger I values than when the phenyl group is attached in a more internal position because the molecule becomes more compact and symmetrical. While the retention index decreases with displacement of the phenyl group from the end to the middle of the alkyl chain, the connectivity indices ^4X_p, ^5X_p, ^6X_p and ^7X_p, which distinguish the isomers, in general increase owing to the increase in the number of subgraphs.

Thus, a single connectivity index does not show a good correlation with the retention index of positional isomers for both sets of retention indices determined with different standards, different constants assigned for each carbon atom increment and different stationary phases. Steric and conformational effects are not considered by these indices. However, compounds with a phenyl group attached in the same position of the alkyl chain of the homologous series (C10–C14) give a good correlation.

Considering the difference between the values of the intercepts on the abscissa for different homologous series, as a measure of steric effects that are not considered by the subgraphs used to calculate the connectivity indices, and assuming that all the straight lines should have the same slope, it is possible to correct the connectivity indices. Taking the difference between the x intercept of each straight line and the x intercept of the straight line for 1C10–1C14, and decreasing the values of the respective ^7X_p, new values are obtained, $^7X_p^*$.

The new corrected molecular connectivity index was also applied to isomers of methylalkanes (with C_{10}–C_{14} alkyl chains) and correlated in an excellent way with the retention index

having a correct elution sequence, showing that this method could be extended to all the positional isomers of alkanes.

Multiple regression equations with different connectivity indices (^1X, ^3X_p and ^5X_p) gave very good results, showing that also using indices that encode complementary information it is possible to distinguish the structures of positional isomers and to determine the elution sequence of most of them.

ACKNOWLEDGEMENT

The authors thank CNPq (Brazil) for financial support.

REFERENCES

1 C.T. Peng, S.F. Ding, R.L. Hua and Z.C. Yang, *J. Chromatogr.*, 436 (1988) 137.
2 C.T. Peng, Z.C. Yang and S.F. Ding, *J. Chromatogr.*, 586 (1991) 85.
3 C.T. Peng, R.L. Hua and D. Maltby, *J. Chromatogr.*, 589 (1992) 231.
4 R. Kaliszan, *Quantitative Structure Chromatographic Retention Relationships*, Wiley, New York, 1987, Ch. 8, p. 138.
5 R. Kaliszan, *CRC Crit. Rev. Anal. Chem.*, 16 (1986) 323.
6 N. Dimov and M. Moskovkina, *J. Chromatogr.*, 552 (1991) 59.
7 M. Randic, *J. Am. Chem. Soc.*, 97 (1975) 6609.
8 L.B. Kier, in S.H. Yalkowsky, A. Sinkula and S.C. Valvani (Editors), *Physical Chemical Properties of Drugs*, Marcel Dekker, New York, 1980 Ch. 9, p. 277.
9 V.A. Gerasimenko and V.M. Nabivach, *J. Chromatogr.*, 498 (1990) 357.
10 V.E.F. Heinzen and R.A. Yunes, *J. Chromatogr.*, 598 (1992) 243.
11 Z. Mihalic and N. Trinajstic, *J. Chem. Educ.*, 69 (1992) 701.
12 H. Takad and R. Ishiwatari, *J. Chromatogr.*, 346 (1985) 281.
13 H. Takad and R. Ishiwatari, *Environ. Sci. Technol.*, 24 (1990) 86.
14 L.H. Hall and L.B. Kier, *Molconn-X, a Program for Molecular Topology Analysis, User's Guide*, Quincy, MA 1991.
15 R. Kaliszan, *J. Chromatogr.*, 220 (1981) 71.
16 F. Khorasheh, M.R. Gray and M. Selucky, *J. Chromatogr.*, 481 (1989) 1.

Journal of Chromatography A, 654 (1993) 190–195
Elsevier Science Publishers B.V., Amsterdam

CHROM. 25 490

Short Communication

Rapid capillary gel electrophoresis of proteins

R. Lausch and T. Scheper*

Westfälische Wilhelms-Universität Münster, Institut für Biochemie, Wilhelm Klemm Strasse 2, W-48149 Münster (Germany)

O.-W. Reif, J. Schlösser, J. Fleischer and R. Freitag

Universität Hannover, Institut für Technische Chemie, Callinstrasse 3, W-30167 Hannover (Germany)

(First received June 14th, 1993; revised manuscript received August 5th, 1993)

ABSTRACT

The rapid separation of sodium dodecyl sulphate–protein complexes according to their molecular masses (M_r) by capillary gel electrophoresis is described. Using commercial equipment, standard proteins with M_r in the range 29 000–97 400 were resolved to the baseline in less than 2 min by utilizing a separation distance of 7 cm. A linear relationship between migration time and log M_r was found and rapid determination of the molecular mass of light and heavy chains of human immunoglobulin G is reported. The results are compared with applications using longer separation distances, showing that rapid and efficient analysis and adequate resolution can be obtained by using short separation distances.

INTRODUCTION

Capillary gel electrophoresis of proteins has made tremendous advance in recent years. The first separations were performed in cross-linked polyacrylamide matrices which were covalently attached to the capillary inner wall [1]. Excellent resolution was achieved owing to the anticonvective effect of the gel and the method was applied to protein standards and to complex natural mixtures of proteins [2,3]. However, the production of these gel-filled capillaries turned out to be time consuming and the lifetime was limited to a few experiments owing to bubble formation and deterioration of the gel structure. While improvements in production and in increasing the lifetime of gel-filled columns [4–7] were made, the application of columns, filled with linear, non-cross-linked polyacrylamide, was examined. These columns were easier to produce and they had a longer lifetime. Successful approaches were made with both gels formed in the capillary [4,8] and gels that were introduced into the capillary after polymerization [9,10]. The advantage of introducing the gels after formation is that the capillary can easily be emptied and refilled, leading to flexible, easy-to-use systems. However, the UV absorption of polyacrylamide at 200 and 214 nm is significant, causing relatively high detection limits [10]. Thus, UV-transparent liquid polymers such as

* Corresponding author.

0021-9673/93/$06.00

dextran, poly(ethylene glycol) (PEG) or poly(ethylene oxide) (PEO) were used for the separations of proteins based on molecular mass (M_r). Further, they have the advantage of low viscosity, which made introduction and removal of these gels easier to perform [9,11].

However, one of the main advantages of capillary electrophoresis, the speed of analysis, has not yet been fully employed in the capillary gel electrophoresis of proteins, although approaches have been made with oligonucleotides [12]. This paper describes high-speed separations of proteins according to their molecular mass.

EXPERIMENTAL

Chemicals

With two exceptions all reagents were bought from Sigma (St. Louis, MO, USA) and were of the following qualities.

Proteins. Carbonic anhydrase (M_r 29 000), ovalbumin (M_r 45 000), bovine serum albumin (M_r 69 000) and phosphorylase *b* (rabbit muscle; subunit M_r 97 400) were of electrophoresis reagent grade and human immunoglobulin G (IgG), purified, was of reagent grade.

Buffers. Tris(hydroxymethyl)aminomethane (Tris), crystalline 99%, and 2-(N-cyclohexylamino)ethanesulphonic acid (CHES) were of analytical-reagent grade, 2-mercaptoethanol, 98%, of electrophoresis reagent grade and sodium dodecyl sulphate (SDS), crystalline (Serva, Heidelberg, Germany) of research grade.

Coatings. γ-(Glycidoxypropyl)trimethoxysilane was of analytical-reagent grade and N,N,N,-N-tetraethylmethylethylendiamine (TEMED), 99%, acrylamide, 99%, and ammonium peroxodisulphate (APS) (Biometra, Göttingen, Germany) were of electrophoresis reagent grade.

Gel. Dextran (M_r 2 000 000) was of analytical-reagent grade.

Instrumentation

In all experiments a P/ACE 2000 system (Beckman, Palo Alto, CA, USA) was used with P/ACE system software controlled by an IBM PS/2 computer. Fused-silica capillaries were obtained from CS-Chromatographie Service (Langerwehe, Germany) with 27 cm total length and 50 or 100 μm I.D. The distance from the detector was either 7 or 20 cm. The capillary was thermostated at 25°C and the samples were injected on the cathodic side by electromigration for 10 s at 10 kV. Detection was performed by measuring UV absorption at 200 nm.

Procedures

Columns. The capillaries were coated as described by Hjerten [13] using γ-(glycidoxypropyl)trimethoxysilane and 4% linear polyacrylamide. Prior to this coating procedure a detection window 2 mm long was made by removing the outer polyimide coating at a distance of 7 cm from one end of the capillary.

Buffer. Tris (0.1 *M*) containing 0.1% SDS was titrated to pH 8.6 with 0.1 *M* CHES which also contained 0.1% SDS. All buffer solutions were filtered through a 0.45-μm filter (Sartorius, Göttingen, Germany).

Gel. A 1-g amount of dextran was mixed with 10 ml of the buffer solution described above and stirred for about 10 min. The clear liquid polymer solution was degassed prior to use. The gel was then filled in one of the buffer vials and introduced into the capillary by pressure.

Samples. The proteins were dissolved in 0.05 *M* Tris–CHES buffer (pH 8.6) containing 1% SDS and 5% 2-mercaptoethanol and then heated for 15 min at 95°C.

RESULTS AND DISCUSSION

Fig. 1 shows the separation of the SDS–protein complexes of carbonic anhydrase (M_r 29 000), ovalbumin (M_r 45 000), bovine serum albumin (M_r 69 000) and phosphorylase *b* (M_r 97 400) in the 20-cm long part of the capillary. Baseline resolution of the four standard proteins was achieved and the migration time obviously depends on the molecular mass. For phosphorylase *b* two peaks can clearly be distinguished, indicating a degradation product of the protein with $M_r = 87\,000$. Using a field of 370 V/cm in the capillary of 100 μm I.D. the analysis was completed within 12 min.

In order to reduce the migration time of the

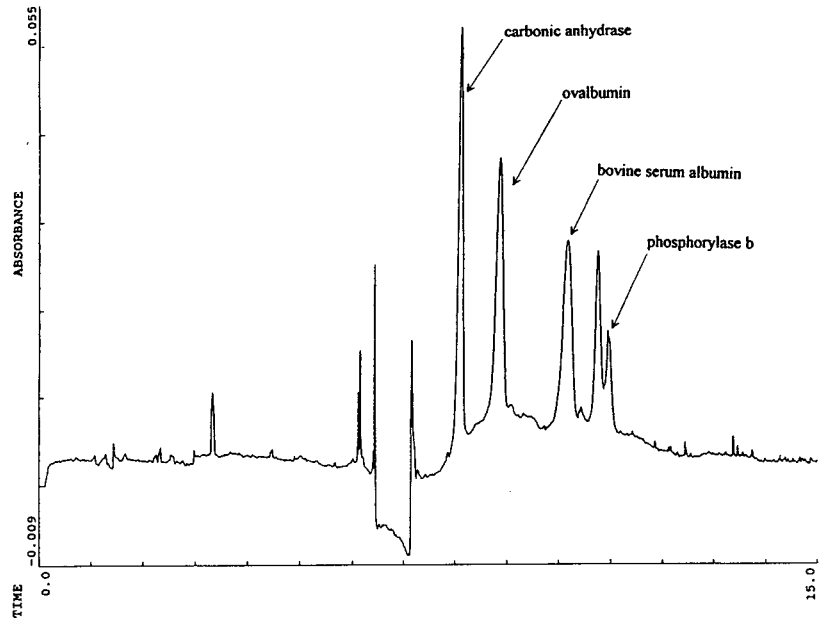

Fig. 1. Electropherogram of the SDS complexes of four standard proteins using the 20-cm long part of a 27 cm × 100 μm I.D. capillary. The proteins are separated according to their molecular masses. Other conditions: buffer, 0.1 *M* Tris–CHES containing 0.1% SDS and 10% (w/v) dextran (pH 8.6); applied field, 370 V/cm; UV detection at 200 nm, 0.025 a.u.f.s.; injection, electromigration, 10 s, 10 kV. Time in min.

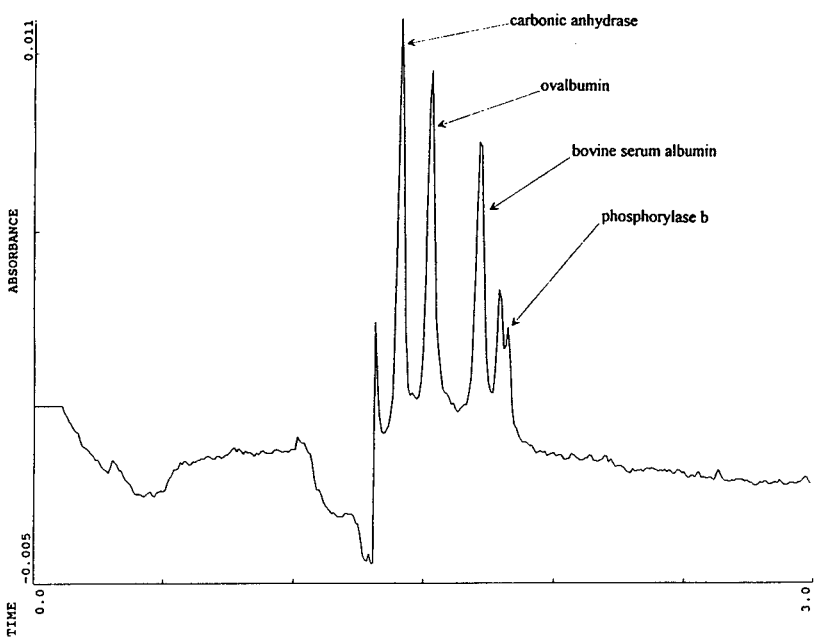

Fig. 2. Rapid separation of SDS complexes of four standard proteins according to their molecular masses using the 7-cm long part of a 27 cm × 50 μm I.D. capillary. Other conditions as in Fig. 1 except applied field, 740 V/cm. Time in min.

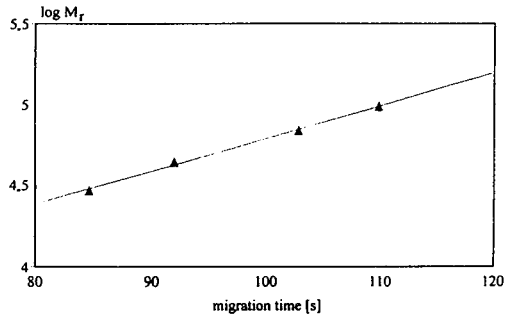

Fig. 3. Linear dependence of the migration time of the SDS–protein complexes on log M_r with $r = 0.998$. Data from Fig. 2.

proteins, higher field strengths of 740 V/cm were applied to the capillary. Baseline separation was achieved within 6 min, but the resolution was 7% lower than that obtained with the lower field. For a further decrease in migration time, the short, 7-cm long end of the capillary was used for the separation. Further, a field of 740 V/cm was applied to the column, which of course led to enhanced generation of Joule heat in the capillaries. For better heat dissipation capillaries of 50 μm I.D. were used, which have the additional advantage that the electrical resistance increases with decreasing inner diameter and thus less heat is generated in the electrophoresis process. However, the decrease in optical path length leads to poorer detection limits.

In Fig. 2 the rapid separation of the four standard SDS–protein complexes is demonstrated. All four proteins are resolved to the baseline in less than 2 min, although the resolution decreases under these conditions to 72% of that achieved with a 20-cm separation distance and 370 V/cm field strength. This decrease in resolution might be a drawback when dealing with very complex mixtures, which might contain several hundred proteins. In such cases longer separation distances will certainly be advantageous. However, the impurity in the phosphorylase *b* can still be distinguished from the protein, which means that proteins with differences of 11% in molecular mass can be resolved. Moreover, the correlation between migration time and

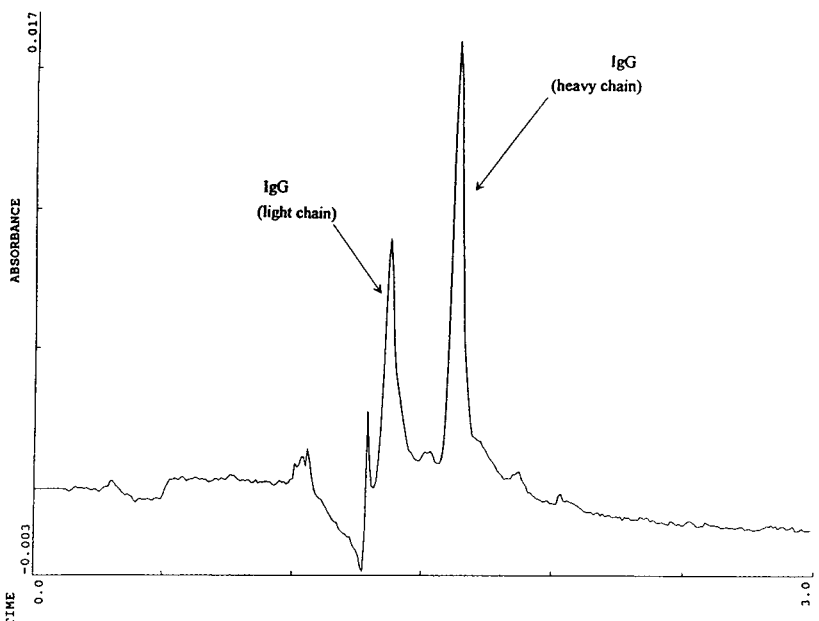

Fig. 4. Rapid separation of the SDS complexes of light and heavy chains of human IgG in the short, 7-cm end of the 27 cm × 50 μm I.D. capillary. Other conditions as in Fig. 2. Time in min.

log M_r is excellent ($r = 0.998$), as can be seen from Fig. 3. Hence this method can be used for high-speed molecular mass determinations of proteins.

In Fig. 4, the analysis of a commercial human IgG using rapid capillary gel electrophoresis is shown. Owing to the use of the reducing agent, the immunoglobulin is fractionated into its light and heavy chains, which are clearly separated according to their molecular masses. From the linear calibration graph of migration time *versus* log M_r, molecular masses of 25 600 for the light chain and 55 100 for the heavy chain of IgG were calculated. As a control experiment, the same determination was carried out, using the long end of the capillary. The differences in the molecular masses were less than 1%. In repetitive analysis the migration times proved to be highly reproducible, as can be seen in Table I. For twenty consecutive runs the SDS complexes of the standard proteins and the IgG were analysed by capillary gel electrophoresis. Between the runs the column was emptied and refilled with the dextran gel. The reproducibility of the migration times was excellent, with a relative standard deviation of 0.77%. Hence this method can be routinely used for rapid determinations of molecular masses of proteins.

CONCLUSIONS

Rapid separations of proteins according to their molecular mass can be performed by using a short separation distance of 7 cm and high electric field strengths. Baseline resolution of protein standards can be achieved in less than 2 min with a relative standard deviation of 0.77% in repetitive analyses. The capillary gel system

TABLE I

MIGRATION TIMES OF THE SDS COMPLEXES OF FOUR STANDARD PROTEINS MEASURED IN ALTERNATING ORDER WITH HUMAN IgG FOR 20 SUBSEQUENT RUNS

Run no.	Migration time (s)					
	Carbonic anhydrase	Ovalbumin	Bovine serum albumin	Phosphorylase *b*	IgG (light chain)	IgG (heavy chain)
1	85.7	94.5	104.8	111.4		
2					84.2	99.6
3	86.5	94.3	105.2	111.8		
4					83.9	100.9
5	85.3	92.3	103.4	109.7		
6					83.0	99.4
7	85.1	92.9	104.4	110.6		
8					84.6	99.7
9	86.5	93.6	104.4	111.4		
10					83.8	100.1
11	86.1	92.3	103.3	109.5		
12					82.8	98.6
13	85.7	92.9	103.4	109.5		
14					83.2	98.6
15	86.4	92.9	104.0	110.8		
16					84.0	98.6
17	85.7	92.9	104.0	110.7		
18					85.7	100.1
19	85.7	92.0	102.9	109.5		
20					83.8	98.6
R.S.D. (%)	0.60	0.85	0.67	0.76	0.95	0.77

using the UV-transparent dextran gel as a matrix is easy to handle and offers the possibility of high-speed molecular mass determinations.

REFERENCES

1 S. Hjertén, *J. Chromatogr.*, 270 (1983) 409.
2 A.S. Cohen and B.L. Karger, *J. Chromatogr.*, 397 (1987) 409.
3 O.-W. Reif, K. Hebenbrock and K. Schügerl, presented at the *4th International Symposium on Capillary Electrophoresis, Amsterdam, 1991.*
4 H.F. Yin, J.A. Lux and G. Schomburg, *J. High Resolut. Chromatogr.*, 13 (1990) 624.
5 J.A. Lux, H.F. Yin and G. Schomburg, *J. High Resolut. Chromatogr.*, 13 (1990) 436.
6 A.S. Cohen, D.N. Heiger and B.L. Karger, *Eur. Pat. Appl.*, EP 417925 A2 (1991).
7 K. Tsuji, *J. Chromatogr.*, 550 (1991) 823.
8 D. Wu and F.E. Regnier, *J. Chromatogr.*, 608 (1992) 349.
9 K. Ganzler, K.S. Greve, A.S. Cohen, B.L. Karger, A. Guttman and N. Cooke, *Anal. Chem.*, 64 (1992) 2665.
10 A. Widhalm, C. Schwer, D. Blaas and E. Kenndler, *J. Chromatogr.*, 549 (1991) 446.
11 A. Guttman, J. Horvath and N. Cooke, *Anal. Chem.*, 65 (1993) 199.
12 A. Guttman and N. Cooke, *Am. Biotechnol. Lab.*, 9, No. 4 (1991) 10.
13 S. Hjertén and M.J. Kiesling-Johansson, *J. Chromatogr.*, 550 (1991) 811.

Chromatography of Mycotoxins

Techniques and Applications

edited by **V. Betina**

Journal of Chromatography Library Volume 54

This work comprises two parts, Part A: Techniques and Part B: Applications. In Part A the most important principles of sample preparation, extraction, clean-up, and of established and prospective chromatographic techniques are discussed in relation to mycotoxins. In Part B the most important data, scattered in the literature, on thin-layer, liquid, and gas chromatography of mycotoxins have been compiled. Mycotoxins are mostly arranged according to families, such as aflatoxins, trichothecenes, lactones etc. Chromatography of individual important mycotoxins and multi-mycotoxin chromatographic analyses are also included. Applications are presented in three chapters devoted to thin-layer, liquid, and gas chromatography of mycotoxins.

Contents:

1993 xiv + 440 pages
Price: US $ 180.00 / Dfl. 315.00
ISBN 0-444-81521-X

ORDER INFORMATION

For USA and Canada
ELSEVIER SCIENCE PUBLISHERS
Judy Weislogel,
P.O. Box 945
Madison Square Station,
New York, NY 10160-0757
Fax: (212) 633 3880

In all other countries
ELSEVIER SCIENCE PUBLISHERS
P.O. Box 211,
1000 AE Amsterdam
The Netherlands
Fax: (+31-20) 5803 705

US$ prices are valid only for the USA & Canada and are subject to exchange rate fluctuations; in all other countries the Dutch guilder price (Dfl.) is definitive. Customers in the European Community should add the appropriate VAT rate applicable in their country to the price(s). Books are sent postfree if prepaid.

ELSEVIER
SCIENCE PUBLISHERS

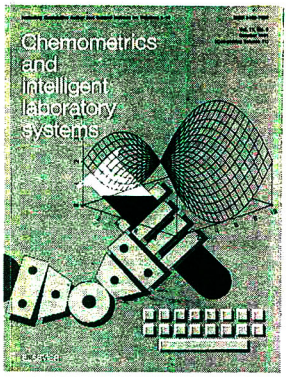

CHEMOMETRICS AND INTELLIGENT LABORATORY SYSTEMS

An International Journal Sponsored by the Chemometrics Society

With the Chemometric Newsletter, official bulletin of the Chemometrics Society and including "Laboratory Information Management"

AIMS AND SCOPE

This international journal publishes articles about new developments on laboratory techniques in chemistry and related disciplines which are characterized by the application of statistical and computer methods. Special attention is given to emerging new technologies and techniques for the building of intelligent laboratory systems, i.e. artificial intelligence and robotics. The journal aims to be interdisciplinary; more particularly it intends to bridge the gap between chemists and scientists from related fields, statisticians, and designers of laboratory systems. In order to promote understanding between scientists from different fields the journal features a special section containing tutorial articles.

The journal deals with the following topics: Chemometrics; Computerized acquisition, processing and evaluation of data; Robotics; Developments in statistical theory and mathematics with application to chemistry; Intelligent laboratory systems; Application (case studies) of statistical and computational methods; New software; Imaging techniques and graphical software applied in chemistry. The research papers and tutorials are complemented by the Monitor Section which contains news, a calendar of forthcoming meetings, reports on meetings, software reviews, book reviews, news on societies and announcements of courses and meetings.

ABSTRACTED/INDEXED IN: ASCA, Analytical Abstracts, BioSciences Information Service, Cambridge Scientific Abstracts, Chemical Abstracts, Chromatography Abstracts, Current Contents, Current Index to Statistics, Excerpta Medica, INSPEC, SCISEARCH.

1993 SUBSCRIPTION INFORMATION
Volumes 18-21 (in 12 issues)
Dfl. 1444.00 / US $ 825.00 (including postage) ISSN 0169-7439

CHROM

I would like
- ☐ a free sample copy of Chemometrics and Intelligent Laboratory Systems.
- ☐ Instructions to Authors.
- ☐ to enter a subscription for 1993. Please send me a Proforma Invoice.

Name _____

Address _____

_____

_____

Audience

Chemists and physical and life scientists as well as statisticians and information specialists working in a variety of fields of chemistry, including analytical chemistry, organic chemistry and synthesis, environmental chemistry, food chemistry, industrial chemistry, pharmaceutical chemistry and pharmacy.

Elsevier Science Publishers
Attn. Carla G.C. Stokman
P.O. Box 330, 1000 AH Amsterdam
The Netherlands
Fax: (+31-20) 5862 845
In the USA & Canada
Attn. Judy Weislogel
P.O. Box 945, Madison Square Station
New York, NY 10160-0757, USA
Fax: (212) 633 3880

PUBLICATION SCHEDULE FOR THE 1994 SUBSCRIPTION

Journal of Chromatography A and *Journal of Chromatography B: Biomedical Applications*

MONTH	O 1993	N 1993	D 1993	
Journal of Chromatography A	652/1 652/2 653/1	653/2 654/1 654/2 655/1	655/2 656/1 + 2 657/1 657/2	The publication schedule for further issues will be published later.
Bibliography Section				
Journal of Chromatography B: Biomedical Applications				

INFORMATION FOR AUTHORS

(Detailed *Instructions to Authors* were published in Vol. 609, pp. 437–443. A free reprint can be obtained by application to the publisher, Elsevier Science Publishers B.V., P.O. Box 330, 1000 AH Amsterdam, Netherlands.)

Types of Contributions. The following types of papers are published: Regular research papers (Full-length papers), Review articles, Short Communications and Discussions. Short Communications are usually descriptions of short investigations, or they can report minor technical improvements of previously published procedures; they reflect the same quality of research as Full-length papers, but should preferably not exceed five printed pages. Discussions (one or two pages) should explain, amplify, correct or otherwise comment substantively upon an article recently published in the journal. For Review articles, see inside front cover under Submission of Papers.

Submission. Every paper must be accompanied by a letter from the senior author, stating that he/she is submitting the paper for publication in the *Journal of Chromatography A* or *B*.

Manuscripts. Manuscripts should be typed in **double spacing** on consecutively numbered pages of uniform size. The manuscript should be preceded by a sheet of manuscript paper carrying the title of the paper and the name and full postal address of the person to whom the proofs are to be sent. As a rule, papers should be divided into sections, headed by a caption (*e.g.*, Abstract, Introduction, Experimental, Results, Discussion, etc.) All illustrations, photographs, tables, etc., should be on separate sheets.

Abstract. All articles should have an abstract of 50–100 words which clearly and briefly indicates what is new, different and significant. No references should be given.

Introduction. Every paper must have a concise introduction mentioning what has been done before on the topic described, and stating clearly what is new in the paper now submitted.

Experimental conditions should preferably be given on a *separate* sheet, headed "Conditions". These conditions will, if appropriate, be printed in a block, directly following the heading "Experimental".

Illustrations. The figures should be submitted in a form suitable for reproduction, drawn in Indian ink on drawing or tracing paper. Each illustration should have a legend, all the *legends* being typed (with double spacing) together on a *separate sheet*. If structures are given in the text, the original drawings should be supplied. Coloured illustrations are reproduced at the author's expense, the cost being determined by the number of pages and by the number of colours needed. The written permission of the author and publisher must be obtained for the use of any figure already published. Its source must be indicated in the legend.

References. References should be numbered in the order in which they are cited in the text, and listed in numerical sequence on a separate sheet at the end of the article. Please check a recent issue for the layout of the reference list. Abbreviations for the titles of journals should follow the system used by *Chemical Abstracts*. Articles not yet published should be given as "in press" (journal should be specified), "submitted for publication" (journal should be specified), "in preparation" or "personal communication".

Vols. 1–651 of the *Journal of Chromatography*; *Journal of Chromatography, Biomedical Applications* and *Journal of Chromatography, Symposium Volumes* should be cited as *J. Chromatogr.* From Vol. 652 on, *Journal of Chromatography A* (incl. Symposium Volumes) should be cited as *J. Chromatogr. A* and *Journal of Chromatography B: Biomedical Applications* as *J. Chromatogr. B*.

Dispatch. Before sending the manuscript to the Editor please check that the envelope contains four copies of the paper complete with references, legends and figures. One of the sets of figures must be the originals suitable for direct reproduction. Please also ensure that permission to publish has been obtained from your institute.

Proofs. One set of proofs will be sent to the author to be carefully checked for printer's errors. Corrections must be restricted to instances in which the proof is at variance with the manuscript. "Extra corrections" will be inserted at the author's expense.

Reprints. Fifty reprints will be supplied free of charge. Additional reprints can be ordered by the authors. An order form containing price quotations will be sent to the authors together with the proofs of their article.

Advertisements. The Editors of the journal accept no responsibility for the contents of the advertisements. Advertisement rates are available on request. Advertising orders and enquiries can be sent to the Advertising Manager, Elsevier Science Publishers B.V., Advertising Department, P.O. Box 211, 1000 AE Amsterdam, Netherlands; courier shipments to: Van de Sande Bakhuyzenstraat 4, 1061 AG Amsterdam, Netherlands; Tel. (+31-20) 515 3220/515 3222, Telefax (+31-20) 6833 041, Telex 16479 els vi nl. *UK*: T.G. Scott & Son Ltd., Tim Blake, Portland House, 21 Narborough Road, Cosby, Leics. LE9 5TA, UK; Tel. (+44-533) 753 333, Telefax (+44-533) 750 522. *USA and Canada*: Weston Media Associates, Daniel S. Lipner, P.O. Box 1110, Greens Farms, CT 06436-1110, USA; Tel. (+1-203) 261 2500, Telefax (+1-203) 261 0101.